UNIVERSITAT DE BARCELONA

Development of Analytical Methodologies for Rapid Determination of Alpha and Beta Emitters by Liquid Scintillation Spectrometry in Water Samples

Jordi Fons Castells

UNIVERSITAT DE BARCELONA

Development of analytical methodologies for rapid determination of alpha and beta emitters by liquid scintillation spectrometry in water samples

Jordi Fons Castells

Jordi Fons Castells

Tesi Doctoral

2017

UNIVERSITAT DE BARCELONA

Jordi Fons Castells

Development of analytical methodologies for rapid determination of alpha and beta emitters by liquid scintillation spectrometry in water samples

UNIVERSITAT DE BARCELONA

Tesis Doctoral

Development of analytical methodologies for rapid determination of alpha and beta emitters by liquid scintillation spectrometry in water samples

Jordi Fons Castells

2017

Programa de Doctorat

"Química Analítica del Medi Ambient i la Pol·lució"

Development of Analytical Methodologies for Rapid Determination of Alpha and Beta Emitters by Liquid Scintillation Spectrometry in Water Samples

Jordi Fons Castells

TESI DOCTORAL

Dirigida per

Dra. Montserrat Llauradó Tarragó

Professora titular del Departament d'Enginyeria Química i Química Analítica de la Universitat de Barcelona

UNIVERSITAT DE BARCELONA

La Dra. Montserrat Llauradó Tarragó, Professora Titular del Departament d'Enginyeria Química i Química Analítica, Secció de Química Analítica, de la Universitat de Barcelona,

FA CONSTAR

que la present que el present treball d'investigació que porta per títol:

Development of Analytical Methodologies for Rapid Determination of Alpha and Beta Emitters by Liquid Scintillation Spectrometry in Water Samples

ha estat realitzat sota la seva direcció per Jordi Fons Castells, per optar al Títol de Doctor per la Universitat de Barcelona.

Barcelona, 18 abril del 2017

Dra. Montserrat Llauradó Tarragó

"Cuando tomas un fruto
con espinas por fuera
y te pinchas la mano,
te pinchas en vano.
Tomar espinas con la mano es malo
en vez de la mano, se usa siempre un palo."

Baloo (El Libro de la Selva)

Acknowledgements

En primer lloc vull agrair a la Dra. Montserrat Llauradó l'haver-me donat la oportunitat de realitzar aquesta tesi doctoral sota la seva direcció, i haver-me fet partícip en tot moment de tots els àmbits que la recerca implica. A la Joana qui, a banda de estar sempre disposada a donar un cop de mà en el que faci falta, especialment la espectrometria gamma, m'ha inculcat la forma de treball rigorosa que requereix un laboratori de radiologia ambiental.

També als companys de laboratori als d'abans i als d'ara als grans i als petits, de qui a vegades aprens molt més del que pensaries, especialment a la Clarimma, l'Eva, la Raquel i l'Oriol, que han passat de ser *Arbeitskollegen*—es una mica gratuït, però m'ha semblat que uns agraïments en només quatre idiomes quedarien pobres—a ser amics.

I also wish to acknowledge the contribution of my mentors at SCK·CEN, Dr. Mirela Vasile and Dr. Michele Bruggeman, as well as my lab mates specially Hilde and Benny with whom I did the most surrealistic sampling of my life.

Sense un fort tronc, les fulles verdes i plenes d'energia no tenen suport on créixer. Agraeixo als meus pares, el tronc de la meva vida, l'haver despertat en mi la curiositat de conèixer, fet que m'ha portat a tenir la necessitat d'aprendre contínuament i en definitiva a ser qui sóc. Agraeixo al tronc i agraeixo a les arrels que ho sustenten tot, han nodrit el tronc i les fulles i que ho continuen fent.

A la fulla de ma germana, que encara que la teva rama hagi crescut cap una altra banda, sempre formarem part del mateix arbre.

A Saroa, a quien me he encontrado en el trascurso y gracias a esta tesis y de quien espero no separarme, cuando definitivamente podamos estar juntos, *eskerrik asko maitia*.

Development of Analytical Methodologies for Rapid Determination of Alpha and Beta Emitters by Liquid Scintillation Spectrometry in Water Samples

Acronyms and contractions

cpm	counts per minute	**PLS**	Partial least squares
CSN	Consejo de Seguridad Nuclear, Nuclear Safety Council	**PMT**	Photomultiplier tube
DHC	Dihydrogen ammonium citrate	**POPOP**	1,4-bis(5-phenyloxazol-2-yl) benzene
DIN	Diisopropyl naphthalene	**PPO**	2,5-diphenyloxazole
EDTA	Ethylenediamine tetraacetic acid	**PSA**	Pulse shape analyser
ENAC	Entidad Nacional de Acreditación, national accreditation body	**PSD**	Pulse shape discriminator
ID	Indicative dose	**PVRA**	Plan de Vigilancia Radiológica Ambiental, environmental radiological surveillance program
LV	Latent variable	**PVRAIN**	Plan de Vigilancia Radiológica Ambiental Independiente, environmental radiological surveillance independant program
MCA	Multichannel analyser	**RMSE**	Root mean squares error
MDA	Minimum detectable activity	**ROI**	Region of interest
NPP	Nuclear power plant	**SPE**	Solid phase extraction
PC	Principal component	**SQP[E]**	Standard quenching parameter of an external source
LSS	Liquid scintillation spectrometry	**RN**	Radionuclide
PCA	Principal component analysis	**TOT-DOT**	three over two fitting and digital overlay technique
PCR	Principal component regression		

TABLE OF CONTENTS

1. THESIS STRUCTURE

1.1.Thesis structure

This thesis has eight chapters. Chapter 1 describes the structure of the thesis and the scientific papers it considers. Chapter 2 introduces the topic of radioactivity in the environment and radiation protection directives, specifically regarding human drinking water and the state of the art in LSS deconvolution. The results of this thesis are presented in the next three chapters as a compendium of scientific papers. The fourth chapter describes the optimization and validation of gross alpha and beta determination by LSS. Chapter 5 includes two papers regarding the development and validation of the direct measurement of ^{226}Ra, ^{228}Ra and ^{210}Pb in drinking water by extraction with a 3M Empore Radium RAD disk. Chapter 6 includes a paper on the feasibility study of PLS applied to LS spectra deconvolution and a study of chemical and colour quenching, which is a critical aspect in LS spectra quantification. Chapter 7 globally discusses the results obtained. Furthermore, a strategy for the rapid determination of alpha and beta emitters via the procedures validated in the thesis is described and the results obtained are discussed. Finally, Chapter 8 contains the conclusion of the present thesis.

1.2.List of scientific papers presented in this thesis

1- ***Simultaneous determination of gross alpha, gross beta and ^{226}Ra in natural water by liquid scintillation counting.***

Authors: J. Fons, D. Zapata-García, J. Tent, M. Llauradó

Journal: Journal of Environmental Radioactivity 125 (2013). pp. 56-60.

2- ***A comparative experimental study of gross alpha methods on natural waters.***

Authors: Montaña, M.; Fons, J.; Corbacho, J.A.; Camacho, A.; Zapata-García, D.; Guillén, J.; Serrano, I.; Tent, J.; Baeza, A.; Llauradó, M.; Vallés, I.

Journal: Journal of Environmental Radioactivity 118 (2013). pp. 1-8.

3- ***On the direct measurement of ^{226}Ra and ^{228}Ra using 3M Empore™ RAD disk by liquids scintillation spectrometry.***

Authors: J. Fons-Castells, M. Vasile, H. Loots, M. Bruggeman, M. Llauradó, F. Verrezen

Journal: Journal of Radioanalytical and Nuclear Chemistry 309 (2016). pp. 1123-1131.

4- Simultaneous determination of ^{226}Ra, ^{228}Ra and ^{210}Pb in drinking water using 3M Empore™ RAD disk by LSC-PLS.

Authors: J. Fons-Castells, J. Oliva, J. Tent-Petrus, M. Llauradó

Journal: Applied Radiation and Isotopes 124 (2017). pp. 83-89.

5- Simultaneous determination of specific alpha and beta emitters by LSC-PLS in water samples.

Authors: J. Fons-Castells, J. Tent-Petrus, M. Llauradó

Journal: Journal of Environmental Radioactivity 166 (2017). pp. 195-201.

6- Effect quenching on efficiency, spectra shape and alpha-beta discrimination in liquid scintillation spectrometry.

Authors: J. Fons-Castells, V. Díaz, A. Badía, J. Tent-Petrus, M. Llauradó

Accepted for publication in *Applied Radiation and Isotopes.*

2. INTRODUCTION

2.1. Radioactivity

Radioactivity is the process by which an unstable nucleus decays to a more stable nucleus by losing energy spontaneously and emitting radiation. This liberation of energy is the result of a reorganization of the internal nuclear structure caused by an unstable ratio of protons and neutrons. The emitted radiation can be classified as alpha, beta, gamma or neutrons.

Alpha radiation occurs when an atom undergoes radioactive decay by giving off a particle that consist of two protons and two neutrons (essentially a nucleus of ^{4}He). The energy of the alpha particle is characteristic of the emitter. Due to their large charge and mass, alpha particles interact strongly with matter to cause ionization, and travel only a few centimetres in air. Alpha particles are unable to penetrate the outer layer of skin cells, but are capable, if an alpha-emitting substance is ingested in food or air, of causing serious cell damage.

Beta radiation refers either to an electron or to its antiparticle, a positron, emitted from an unstable atom. The emission of an electron entails the formation of an antineutrino, which shares the energy of the nuclear reaction with the electron. For this reason, the energy of the beta particles emitted by a radionuclide changes from 0, when all the energy is collected by the antineutrino, to a maximum energy, when all the energy is collected by the electron. This maximum energy is characteristic of the beta emitter. In the same way, when a positron is emitted, the total energy of the decay is shared with a neutrino. Due to their smaller mass, beta particles have greater penetrating power than alpha particles.

Gamma radiation consists of electromagnetic radiation, which is characteristic of each unstable nucleus. Due to its radiation behaviour gamma radiation has greater penetrating power than alpha and beta particles.

Finally, neutron radiation consists of a free neutron that is usually emitted as a result of spontaneous or induced nuclear fission. Neutron radiation has a high penetrating power due to its null net charge.

The magnitude to measure radioactivity is activity, which is the number of nuclei that decay per unit time. It is measured in Becquerel (Bq) in the international system of units (SI), which is equivalent to disintegrations per second (s^{-1}). The activity of a radioactive source depends on the number of nuclei of the source and a constant λ which is characteristic of the radionuclide following the next equation.

$$A(t) = \lambda \cdot N(t) \quad (2.1)$$

where

A(t) is the activity at time t in Becquerel;

λ is the decay constant second^{-1}; and

N(t) is the number of nuclei in the radioactive source at time t.

Decay constant λ is characteristic of the radionuclide studied and refers to the probability that this radionuclide will decay in a fixed time. This is related to the half-live, which is the time required to reduce the number of the nucleus of a radioactive source to half of its initial value, in accord with Equation 2.2.

$$T_{1/2} = \frac{ln(2)}{\lambda} \quad (2.2)$$

where

$T_{1/2}$ is half-live measured in second; and

λ is the decay constant in second^{-1}.

Since activity depends on the number of nuclides and decay in time, the activity of a radioactive source decreases with time. Radioactive decay is defined by Equation 2.3.

$$A(t) = A_0 \cdot e^{-\lambda t} \quad (2.3)$$

where

A(t) is the activity at time t in Becquerel;

A_0 is the activity at time 0 in Becquerel;

λ is the decay constant in second^{-1}; and

t is the elapsed time in second.

Nevertheless, some radioisotopes do not decay directly to a stable state but undergo a series of decays until a stable isotope is reached. These sequences of disintegrations are

called radioactive chains. Different situations may be reached between two or more radionuclides, depending on the ratio of their decay constant. Consider a parent radionuclide A that decays to a daughter radionuclide B, which in turn decays to a stable nuclide C:

$$A \overset{\lambda_A}{\rightarrow} B \overset{\lambda_B}{\rightarrow} C_{(stable)}$$

Secular equilibrium may occur in a decay chain only when the λ of the daughter (Radionuclide B) is much higher than that of the parent (Radionuclide A). In this situation, the decay rate of A, and hence the production rate of B, is approximately constant because the half-life of A is very long compared with the timescales considered. The number of radionuclides of B grows until the activity of B reaches the activity of A. In a situation of secular equilibrium, the activity of the daughter reaches more than 99 % of the activity of the parent after seven half-lives of the daughter.

When the half-life of the daughter is not negligible compared to the parent's half-life, transient equilibrium may occur. In this situation, the daughter's activity increases and eventually reaches a maximum value that can exceed the parents' activity. Transient equilibrium occurs after approximately four half-lives of the daughter.

In the aforementioned cases of secular and transient equilibrium, the parent radionuclide A is longer-lived than its daughter. In other cases, when $\lambda_A > \lambda_B$, a situation of no equilibrium is achieved. In these cases, the parent decays to a negligible activity, leaving only the daughter radionuclide, which decays with its own half-life.

Furthermore, longer and more complex decay chains may be observed. Some radionuclides disintegrate into more than one daughter following the next decay scheme.

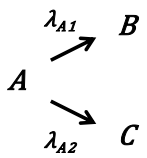

For example, ^{212}Bi in the natural chain of ^{232}Th (please see Figure 1), decay by alpha emission to ^{208}Tl and by beta emission to ^{212}Po. The half-life of the parent nuclide in a branching decay is a function of two decay processes and can be written as,

$$T_{1/2} = \frac{ln(2)}{\lambda_{A1} + \lambda_{A2}} \quad (2.4)$$

where λ_{A1} and λ_{A2} are the decay constants of two independent decay processes.

2.1.1. Effects of ionizing radiation

Despite the different nature of ionizing radiation, all of these types of radioactivity interact with matter in similar ways, and when they reach the electrons of other atoms or other molecules, all of them can produce excitation or ionization. For this reason, radioactivity is also known as ionizing radiation. When this interaction occurs in molecules that are parts of cells of organisms, physico-chemical changes that affect functionality may occur. If these changes occur in macromolecules such as enzymes or proteins, the macromolecules sometimes return to their natural state. Other times, however, the changes are permanent. Besides, the interaction of radioactivity with the water of the cellular cytoplasm can give rise to the formation of free radicals that can recombine or react with other molecules to generate toxic substances such as peroxides for cells.

Risk associated with radioactivity exposure is evaluated by means of equivalent dose, which is measured in Sieverts (Sv), which are equivalent to joules per kilogram. An equivalent dose is the weighted sum of the equivalent dose of all organs and issues. This equivalent dose for each tissue is its absorbed dose weighted by the type and energy of the absorbed radiation. Absorbed dose is the energy deposited per unit of mass. It is measured in Grays (Gy), which are equivalent to joules per kilogram.

The effects of ionizing radiation on human health may be distinguished into deterministic and stochastic effects. Deterministic effects are caused by high dose rate, which irreversibly damages many cells and cause the loss of the functionality of the affected tissues. Many deterministic effects occur shortly after radiation exposure, frequently within a few days or months, so that a link between exposure and health effect is evident. These effects are observed in every individual who receives the same high dose.

In contrast to deterministic effects, the occurrence of a stochastic health effect depends on the modification of a cell that changes its original characteristics without preventing its proliferation, which may induce cancer and genetic disease. These effects are caused by a low dose rate and are inherently random. Not every individual in a community exposed to the same low dose rate suffers health effects after exposure (UNSCEAR, 2012).

2.2. Radioactivity in the environment

Even the effects of ionizing radiation may be disturbing. Humans have been exposed to an environment with a notable presence of natural radioactivity and hence have the ability to withstand a certain dose level. Natural sources are the most relevant in human exposure. However, several economic activities increase the exposure of the population to natural radionuclides, and others produce artificial radionuclides. This section describes the various origins of radioactivity.

2.2.1. Natural radiation

There are several kind of natural radioactivity: cosmic radiation, cosmogenic radionuclides and primordial radionuclides.

Cosmic radiation is high-energy radiation that is generated mainly by solar eruptions and by supernovas or other phenomena outside the solar system. It is composed by high-energy protons, neutrons and alpha particles that produce nuclear reactions with molecules in the high atmosphere. As a result of these interactions, cosmogenic radionuclides are produced. The important isotopes produced by cosmic rays are ^{3}H, ^{7}Be, ^{14}C, ^{22}Na, ^{32}P, ^{33}P and ^{33}S. These isotopes are produced by spallation reactions with atmospheric nitrogen, oxygen and argon, and by high-energy cosmic rays, mostly of protons and neutrons (Warner & Harrison, 1993).

Primordial radionuclides are radioactive nuclides that have been present on the Earth since its formation. Some of these radionuclides give rise to natural radioactive chains, thereby producing more than 20 different radionuclides, most of which are alpha emitters. Just three of these chains are observed in nature. They are commonly called the thorium series, the radium or uranium series, and the actinium series. The mass number of each isotope in these chains can be represented as $A = 4n$, $A = 4n + 2$, and $A = 4n + 3$, respectively. The chain corresponding to mass $A = 4n + 1$ is mainly decayed, such that only the last two of the isotopes involved (^{209}Bi and ^{205}Tl) are found naturally.

Figure 1 and Figure 2 show the radionuclides involved in the thorium series and the uranium series, respectively, together with their decay modes and half-lives. In both figures, the radionuclides included in the Directive 51/2013/EURATOM are highlighted in purple. The data used to create these figures was obtained from the *Laboratorie National Henri Becquerel*.

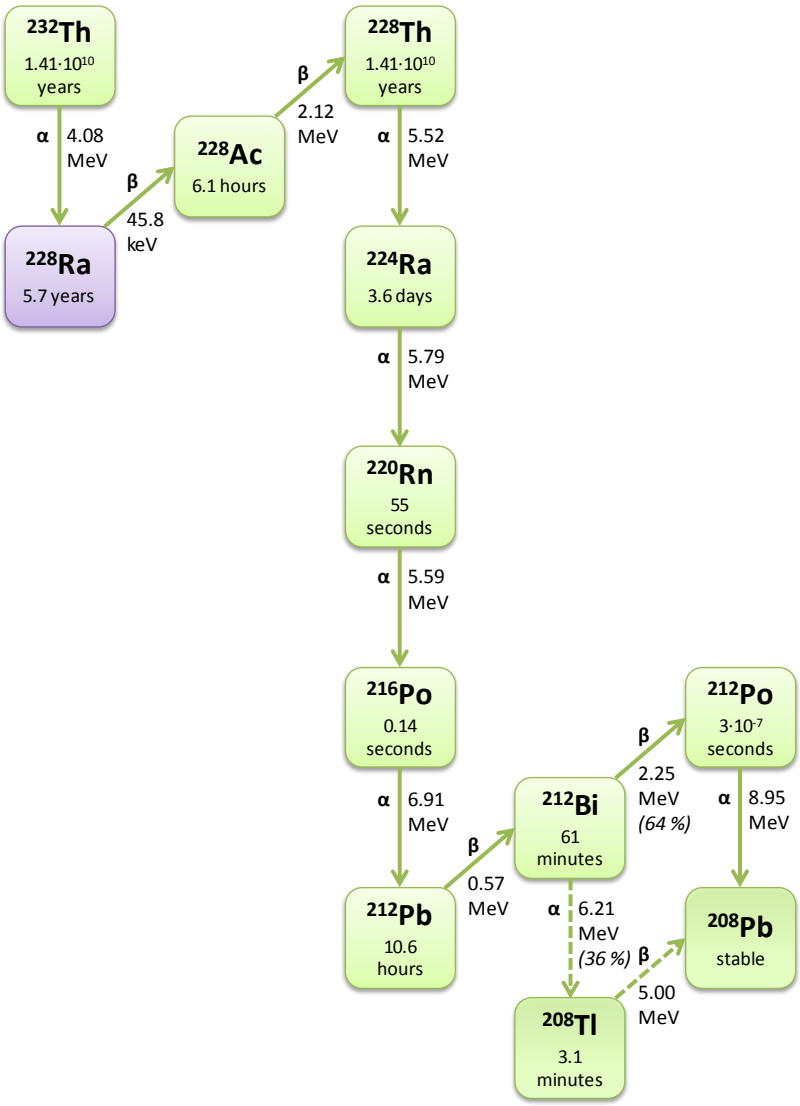

Figure 1. Radionuclides involved in the ^{232}Th natural series with their decay modes, decay energies and half-lives.

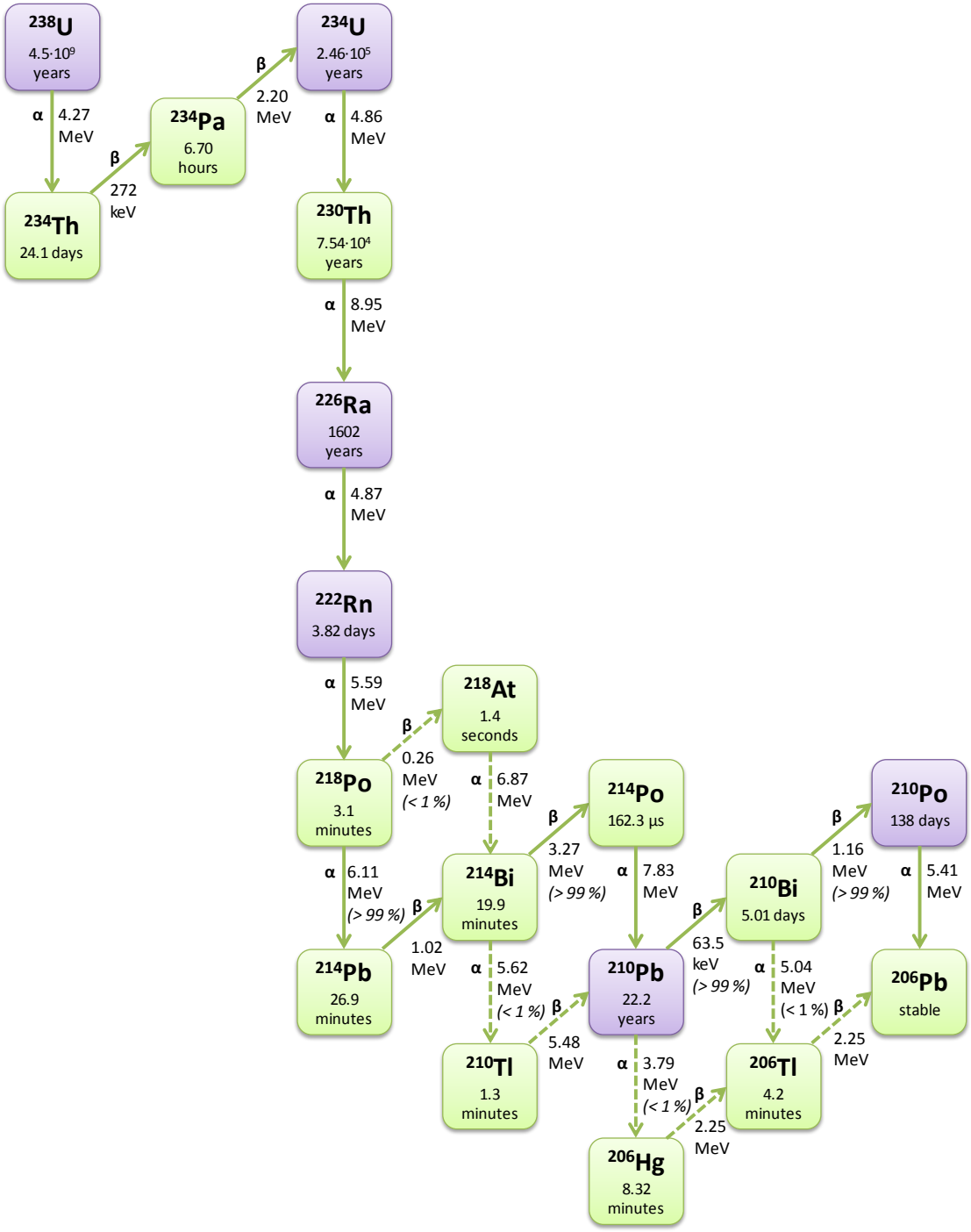

Figure 2. Radionuclides involved in the ^{238}U natural series with their decay modes, decay energies and half-lives.

The various radionuclides of a radioactive chain are not homogenously distributed because they exhibit different chemical behaviours and remain in the environment for a long time. For example, in the uranium series, it is usual to find a disequilibrium between ^{238}U and ^{234}U due to the fact that ^{234}Th is between them in the radioactive chain. The

disequilibrium is observed because uranium is more mobile than thorium in natural systems—particularly in oxidizing environments—due to its high solubility in +6 oxidation state forms. Thorium forms insoluble hydroxides under the same conditions, regardless of redox conditions (Deschamps et al., 2004).

Radon (^{222}Rn), daughter of ^{226}Ra, is a characteristic radionuclide that takes part in the uranium series. Radon is a radioactive noble gas; hence, it can diffuse though soil to the air, where it can be incorporated by inhalation. Furthermore, radon has a high solubility in water, which is why it should be controlled in water sources. Thoron (^{220}Rn), from the thorium series, exhibits the same behaviour but a shorter half live, which makes its radiological impact weaker in most scenarios.

Other primordial radionuclides do occur in radioactive chains, such as ^{113}Cd, ^{123}Te and ^{87}Rb. The most important is ^{40}K, which has a natural isotopic abundance of 0.012 %.

It is important to point out that the distribution of natural radionuclides in Earth's crust may be changed by some industrial activities that use a large amount of materials that contain natural radionuclides called naturally occurring radioactive materials (NORM). Several processes may increase the concentration of natural radionuclides in by-products or residues, and these by-products and residues can increase public exposure if they are not treated properly. Some of the practices involved in NORM are uranium mining and processing, metal mining, coal mining, the use of coal in thermal power plants, practices associated with the phosphogypsum industry, oil and gas extraction including fracking, practices associated with the titanium-oxides industry, and the production of building materials.

2.2.2. Artificial radiation

Artificial radionuclides are generated by human intervention by means of nuclear reactions. In some occasions, these artificial radionuclides are the target of human intervention. For example, artificial radionuclides are produced in particle accelerators, mainly for medical purposes (both diagnosis and treatment).

In other cases, artificial radioactivity is produced as a by-product of another process. This is the case with nuclear power plants (NPP's), in which the objective is the production of electrical energy by means of a sustained and controlled fission reaction. A huge amount of radioactive fission and activation products are produced during fission reactions. Though most of these radionuclides remain in the nuclear reactor and are removed in the

dismantling process with the spent nuclear fuel, some may be released outside the NPP in controlled venting.

For this reason, the NPP has a protocol for surveillance to ensure that no releases have a significant impact on human health or the environment.

In Spain, the Nuclear Safety Council (CSN, its acronym in Spanish) establishes the requirements for environmental radiological monitoring programs, which must be carried out by the NPP owners in the environment surrounding of the installation (Royal Decree 783/2001). The CSN verifies compliance with these requirements by evaluating the programs and their results, conducting periodic inspections and establishing independent control programs.

CSN requires that holders of NPP's and nuclear fuel-cycle facilities develop environmental radiological surveillance programs (PVRA, the acronym in Spanish for these programs) in their surroundings during the phases of the facility's life. The PVRA starts several years before the beginning of the operation of the facilities to determine the radiological conditions of the environment before any discharge of radioactive effluents and to determine their radiological impact.

This surveillance program is based not only on gamma measurements but also on the collection and analysis of samples in the area of influence of the facilities. The samples considered in the program for operative nuclear facilities are the following: drinking water, rain water, superficial and underground water, air, soil, sediment, bio-indicative organisms, milk, agricultural crops, meat, eggs, fish, seafood and honey. To maintain adequate confidence in the results obtained in PVRA, CSN requires the application of quality-assurance systems to environmental radiological monitoring. In addition, 5-15 % of the samples should analysed by two different laboratories, and agreement of the results should be checked.

In addition to CSN—the monitoring program of the holders of the NPP—is an independent environmental radiological-surveillance program (PVRAIN, its acronym in Spanish). Its sampling points, type of samples and analyses performed coincide with those of the PVRA, representing approximately 5 % of the samples of PVRA.

On 11 March of 2011, the Fukushima-Daiichi NPP suffered major damage from equipment failure after an earthquake of magnitude 9.0 and subsequent tsunami. It was the largest civilian nuclear accident since the Chernobyl accident of 1986. It has been estimated that 100 to 500 PBq of ^{131}I and 6 to 20 PBq of ^{137}Cs were released into the environment. The published estimates of the corresponding releases to the atmosphere estimated for the

Chernobyl accident are about 10 % and 20 %, respectively. Much of the released material was dispersed over the Pacific Ocean, but, due to meteorological conditions, a fraction was dispersed over eastern mainland Japan, and radioactive material was deposited on the ground by means of dry deposition and wet deposition with rain and snow (UNSCEAR, 2016).

Apart from the civil uses of nuclear energy, there are also military uses, which also increase the exposure of the population. Since the first nuclear test at the Trinity site, several counties have tested their nuclear weapons atmospherically or in underground explosions. Nuclear explosions in the atmosphere occurred from 1945 to 1980, and radionuclides released by these tests have gradually been deposited on the Earth's crust as fallout. The radionuclides generated in nuclear explosions are similar to those obtained in a nuclear reactor: i.e., mainly ^{14}C, ^{90}Sr, ^{95}Zr, ^{134}Cs and ^{137}Cs.

2.3. Radiation protection: directives and legislation

The dispersion of the radionuclides in the environment is such that different concentrations of radionuclides can be observed in all environmental compartments. The radionuclides present in the atmosphere as gas, aerosol or suspended matter, are dispersed by atmospheric processes and eventually are deposited in the Earth's crust in either soil or water masses. By means of physico-chemical processes, there are also interchanges between the radionuclides of soil and water. Furthermore, interactions with biota have the consequence that radionuclides may be incorporated into animal or plants tissues.

Exposure of humans to radioactivity may occur by way of internal or external irradiation.

External irradiation is produced when the radioactive source is outside the human body. Its main contributors are cosmic radiation and gamma rays from natural or artificial radionuclides. On the other hand, internal irradiation is produced when the radioactive source is incorporated within the organism, commonly by ingestion or inhalation. Since in internal irradiation the radionuclides are near to the organism's tissues, alpha and beta emitters (with low penetrating power) are in this case the main contributors to the internal dose because of their high linear energy transfer (LET). Furthermore, some alpha or beta emitters—such as ^{226}Ra, ^{228}Ra, ^{90}Sr or ^{210}Po—may be incorporated into human tissues, which increases the residence time in the body and thereby increases the effects of radiation.

Several national and international organizations work to control and regulate the ionizing radiation exposure of the human population.

The United Nations Scientific Committee on the Effects of Atomic Radiation (UNSCEAR) was set up by a resolution of the United Nations (UN) General Assembly in 1955. Its mandate in the United Nations system is to assess and report levels and effects of exposure to ionizing radiation. The original committee was composed of senior scientists from 15 designated UN Member States, but several additional countries have been included in this committee over time. Spain was invited in 2011 together with six other UN Member States, thus increasing the membership to 27 States.

UNSCEAR reports are the basis for evaluating radiation risk and for establishing protective measurements for governments and organizations throughout the world.

Table 1. Annual average dose for the worldwide population in mSv from different radioactivity sources (UNSCEAR, 2008).

Source	***Annual average dose (worldwide)***	***Range***	***Comments***
Natural source exposure			
Inhalation (radon gas)	1.26	0.2-10	Much higher in some locations
External terrestrial	0.48	0.3-1	Higher in some locations
Ingestion	0.29	0.2-1	
Cosmic radiation	0.39	0.3-1	Increases with altitude
Total natural	2.4	1-13	Sizeable groups of population receive 10-20 mSv y^{-1}
Artificial source exposure			
Medical diagnosis (excluding therapy)	0.6	From 0 to several tens	Highly dependent on the country
Atmospheric nuclear test	0.005		Higher around test sites
Occupational exposure	0.005	0-20	
Chernobyl accident	0.002		The average in the norther hemisphere has decreased from a maximum of 0.04 mSv un 1986
Nuclear industry	0.0002		
Total artificial	0.6	From 0 to several tens	Individual doses depend primarily on medical treatment, occupational exposure and proximity to test or accident sites.

In 2008, UNCEAR published a report on the sources and effects of ionizing radiation that illustrates the different sources of human exposure. Table 1 includes the main contributors to human exposure, the averages annual dose and the range of exposure for the worldwide population.

As can be seen, the most important contributor to the human dose is natural radiation, which is, on average, 2.4 mSv y^{-1}. Artificial sources contribute 0.6 mSv y^{-1}, on average. This fact is significant, because most of the dose received by the population is due to natural radioactivity if there is no source of contamination.

Directive 2013/51/EURATOM

In October of 2013, the Council of the European Union published Directive 2013/51/EURATOM which specifies requirements for the protection of the health of the general public with regard to radioactive substances in water intended for human consumption (EURATOM, 2013). This directive lays down parametric values, frequencies and performance characteristics of methods for monitoring radioactive substances and substitutes the Directive 98/83/CE of the Council.

The parameters regulated by this directive are ^{3}H and ^{222}Rn activity, concentration and indicative dose. The parametric values established for ^{3}H and ^{222}Rn activity concentration are 100 Bq L^{-1} in both cases. In the case of ID, the parameter value is 0.1 mSv y^{-1}.

If the tritium concentration exceeds its parametric value, an analysis is required for the presence of other artificial radionuclides. As radon activity concentration is highly dependent on the geochemical characteristics of the soil, member states may adjust the parametric value in their national legislations in the range between 100-1000 Bq L^{-1}. However, remedial action is deemed to be justified without further consideration on grounds of radiological protection when radon activity concentrations exceed 1000 Bq L^{-1}.

The *indicative dose* (*ID*) is the committed effective dose for one year of ingestion resulting from all the radionuclides whose presence has been detected in a supply of water intended for human consumption, of natural and artificial origin, but excluding ^{3}H, ^{40}K, ^{222}Rn and short-lived radon decay products considering an annual intake of 730 L for adults. To monitor ID, two screening strategies are proposed in the directive. The first involves screening for individual radionuclides. If one of the activity concentrations exceeds 20 % of the corresponding derived value, an analysis of additional radionuclides is required. The second strategy proposed is based on the measurement of gross alpha and gross beta

activities. For this purpose, the threshold values of 0.1 Bq L^{-1} and 1.0 Bq L^{-1} for gross alpha and gross beta activities are recommended.

If the gross alpha activity and gross beta activity are less than 0.1 Bq L^{-1} and 1.0 Bq L^{-1}, respectively, the member state may assume that the ID is less than the parametric value of 0.1 mSv y^{-1} and radiological investigation is not needed. Otherwise, analysis for specific radionuclides is required.

The directive allows member states to set alternative screening levels for gross alpha activity and gross beta activity if they can demonstrate that the alternative levels are in compliance with an ID of 0.1 mSv.

The ID is to be calculated from measured radionuclides and dose coefficients following Directive 96/29/EURATOM (EURATOM, 1996) for an intake of 730 L per year for an adult. However, when Equation 2.5 is satisfied, member states may assume that the ID is less than the parametric value of 0.1 mSv y^{-1}:

$$\sum_{i=1}^{n} \frac{C_i(obs)}{C_i(der)} \leq 1 \quad (2.5)$$

where

n is the number of detected radionuclides;

$C_i(obs)$ is the observed concentration of radionuclide i; and

$C_i(der)$ is the derived concentration of radionuclide i.

Table 2 list the most common natural and artificial nuclides. These are included in Annex III of Directive 2013/51/EURATOM together with its derived concentration and the required minimum detectable activity MDA for analysis.

Table 2. Derived concentration and required MDA of the methods for the radionuclides included in Directive 2013/51/EURATOM.

Origin	Nuclide	Derived concentration	Required MDA
Natural	^{238}U	3.0 Bq L^{-1}	0.02 Bq L^{-1}
	^{234}U	2.8 Bq L^{-1}	0.02 Bq L^{-1}
	^{226}Ra	0.5 Bq L^{-1}	0.04 Bq L^{-1}
	^{228}Ra	0.2 Bq L^{-1}	0.02 Bq L^{-1}
	^{210}Pb	0.2 Bq L^{-1}	0.02 Bq L^{-1}
	^{210}Po	0.1 Bq L^{-1}	0.01 Bq L^{-1}
Artificial	^{14}C	240 Bq L^{-1}	20 Bq L^{-1}
	^{90}Sr	4.9 Bq L^{-1}	0.4 Bq L^{-1}
	$^{239+240}Pu$	0.6 Bq L^{-1}	0.04 Bq L^{-1}
	^{241}Am	0.7 Bq L^{-1}	0.06 Bq L^{-1}
	^{60}Co	40 Bq L^{-1}	0.5 Bq L^{-1}
	^{134}Cs	7.2 Bq L^{-1}	0.5 Bq L^{-1}
	^{137}Cs	11 Bq L^{-1}	0.5 Bq L^{-1}
	^{131}I	6.2 Bq L^{-1}	0.5 Bq L^{-1}

Furthermore, the directive also list the limits of detection required for analytical methods as 10 Bq L^{-1} for ^{3}H and ^{222}Rn, 0.04 Bq L^{-1} for gross alpha and 0.4 Bq L^{-1} for gross beta.

Royal Decree 314/16

The European Directive 2013/51/EURATOM has recently been transposed to Spanish law by means of the Royal Decree 314/16, which amends the following: Royal Decree 140/2003, laying down sanitary criteria for the quality of water for human consumption, Royal Decree 1798/2010, which regulates the exploitation and commercialization of natural mineral waters and spring bottled waters for human consumption, and Royal Decree 1799/2010, regulating the process of elaboration and commercialization of prepared bottled waters for human consumption. All of these decrees are based on the previous Directive 98/83/CE.

The difference in the parametric values between the directive and the Royal Decree is just in the specified ^{222}Rn activity concentration, which is 500 Bq L^{-1} in the Royal Decree. However, when the ^{222}Rn activity concentration range is between 100 and 500 Bq L^{-1},

actions must be taken to optimize the population protection, without compromising water supply.

2.4. Liquid scintillation spectrometry

Liquid scintillation spectrometry (LSS) was one of the first techniques used for the detection of ionizing radiation. This technique is based on the detection of the pulses of light that are emitted by some substances when ionizing radiations pass through them (L'Annunziata and Kessler, 2012).

Liquid scintillation spectrometry involves mixing the radioactive sample with a scintillation cocktail that is able to accept the energy of nuclear decays. As a result, activated solvent molecules are formed that transfer their energy to organic scintillator. The organic scintillators, or fluor, are organic molecules that can easily accept the energy from the activated solvent to promote into an exited state. These molecules then return to the fundamental state by means of a florescence mechanism, emitting the energy as a flash of light. These light pulses or scintillations are detected by photomultiplier tubes (PMT) and classified in a multichannel (MCA) according to their intensity (number of photons). The intensity of the light pulses is related to the energy of the nuclear decay and the number of pulses with the number of disintegrations produced in the sample. In this way, a spectrum of the sample is obtained that relates the number of disintegrations (counts) as a function of the energy of the disintegration (cannels). A scheme of this process is shown in Figure 3.

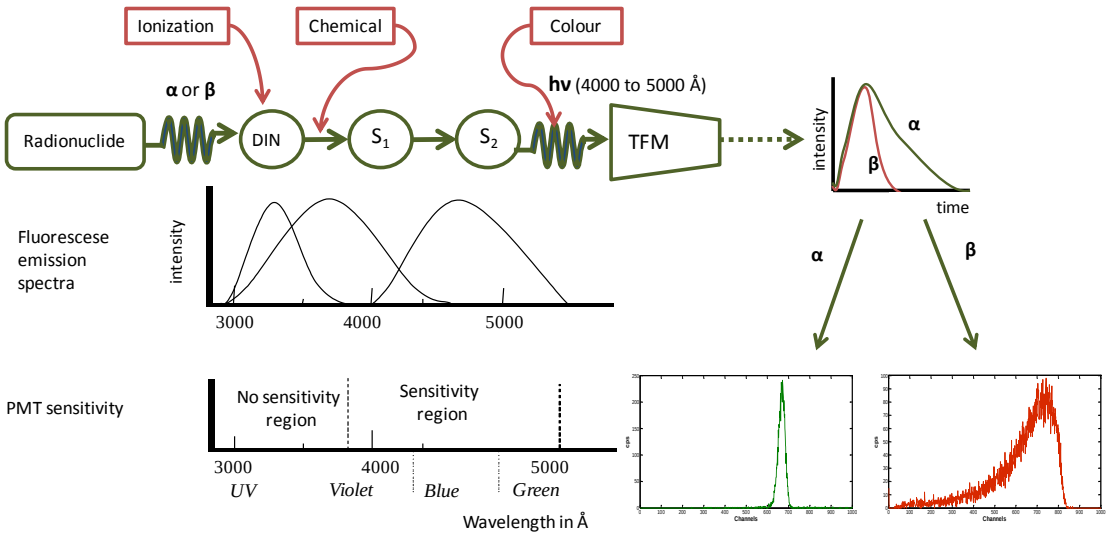

Figure 3. Scheme of scintillation process, highlighting quenching processes, modulation of the emitted energy in order to adequate it to PMT sensitivity and alpha beta separation.

An essential aspect of LSS is the scintillation cocktail. Cocktails are based on a solvent—usually diisopropyl naphthalene (DIN)—that absorbs the energy emitted by the radionuclides contained in the sample. There are other substances in the cocktail—commonly called solutes—that modulate the energy of the activated solvent molecules to adequate the final emitted light pulse to the PMT sensibility region, usually 2,5-diphenyloxazole (PPO) and 1,4-bis(5-phenyloxazol-2-yl) benzene (POPOP).

The selection of these solutes may confer special proprieties on the cocktail such as improvement of alpha/beta separation. Finally, the cocktails used for the determination of aqueous samples need an emulsifier to facilitate the compatibility between organic and aqueous phases.

2.4.1. Quenching

Various phenomena known collectively as quenching hinder energy transference between the particle emitted and the photons detected by the PMT. The quenching phenomena that most affect liquid scintillation measurement are ionization, chemical and colour quenching.

Ionization quenching is related to the density of excited solvent molecules. When the concentration of these molecules is high, the probability of interaction between them is increased. As a result of this interaction, one of the molecules loses the excitation energy while the other becomes overexcited and has a high probability to become ionized. The result is that the initial excitation energy of both molecules is lost, which entails a loss in counting efficiency.

Chemical quenching is the most common mechanism. It is caused by the presence of chemical substances in the sample, including its solvent. These substances obstruct energy transference between the radioactive emission and the fluor and, hence, reduce the efficiency of photon emission. Colour quenching is caused by the presence of coloured substances in the sample that absorb the photons emitted by the fluorine before they can be detected by the PMT. In general, both quenching mechanisms reduce the number of photons detected by the PMT and consequently the apparent energy of the emission (the spectrum shifts to lower energies). Furthermore, this phenomena can also reduce the count rate of the samples and hence the counting efficiency. In addition, previous studies (Pates et al., 1994; Pujol and Sánchez-Cabeza, 1997; Salonen, 2006; Stojkovic, I. et al., 2015) have shown that quenching also affects the degree of α/β misclassification which is a consequence of different manners of its influence on early and delayed components of the light pulse.

For these reasons, LSS efficiency is commonly determined using a quenching curve that describes, for a specific radionuclide, the relation between an instrumental parameter of quenching and the counting efficiency. Quenching curves are prepared by measuring a set of liquid scintillation standard sources with different amounts of quenching agent, either chemical or coloured (Cassette, 2016).

2.4.2. Alpha/beta separation

The differences in scintillation processes produced by alpha and beta particles have been studied since the early use of the LSS technique. These differences are the basis of alpha/beta separation in LSS. Section 2.1 highlights the differences regarding weight, LET and penetrating power of alpha and beta particles. Alpha emitters emit in the range of 2 to 8 MeV, while the common beta emitters do not overtake 3 MeV. However, the LS spectra of alpha emitters with energies around 5 MeV overlap with the spectra of beta emitters with a maximum energy below 2 MeV. For example, Figure 4 shows a spectrum of ^{241}Am pure alpha emitter with an energy of 5.64 MeV and a spectrum of ^{40}K pure beta emitter with a maximum energy of 1.31 MeV.

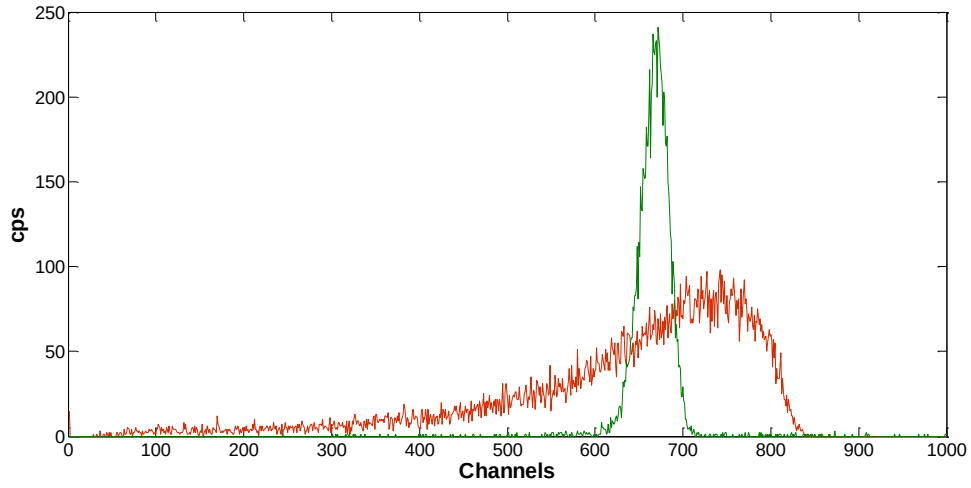

Figure 4. Spectra of a pure alpha emitter in green (^{241}Am) and a pure beta emitter in red (^{40}K) in which can be see their overlapping.

This occurs because alpha particles are more affected by ionization quenching than beta particles. Since alpha particles cause high ionization and have a low penetrating power, the local concentration of ionized molecules of solvent is higher for an alpha than for a beta event; hence, scintillation processes for alpha particles lose efficiency. As a consequence, alpha particles generate around 1 photon per keV while beta particles generate 10 photons per keV (L'Annunziata and Kessler, 2012).

However there are other differences between scintillations produced by alpha and beta particles.

Organic scintillators exhibit both prompt and delayed fluorescence processes. Due to excitation and de-excitation mechanisms, the delayed component in fluorescence is higher for particles of high specific energy loss, such as alpha particles and heavy charged particles. This difference may be determined for each pulse, which makes it possible to classify scintillations as alpha or beta.

2.5. Wallac QUANTULUS 1220 spectrometer

The Wallac Quantulus 1220 (manufactured in Finland, Turku) was used for the measurements done for this thesis. It is a liquid scintillation spectrometer specially designed for the ultra-low level measurement of alpha and beta emitters. The spectrometer has three trays of 20 positions, each with a total capacity of 60 vials of 20 mL each.

The spectrometer is controlled by a personal computer by means of the software *WinQ*. It makes it possible to define protocols respecting the number and position of samples, the configuration of the photomultipliers, the number of repetitions and cycles, and the counting time.

The detection system is basically formed by two front-faced photomultipliers that are arranged on each side of the sample. The signals produced for the disintegration in the sample are detected in coincidence for both photomultipliers. The signals produced for thermal noise in a photomultiplier are not counted in coincidence and hence are rejected.

2.5.1. Background reduction

To achieve a low enough limit of detection, it is necessary to reduce the signal to background ratio or, more specifically, the error of the background determination. For this reason, the background must be minimized, and the instrument must to be stable during the long counting times needed for low-level samples. To accomplish this objective, Quantulus 1220 has two different types of shielding; passive or physical shielding, and active or electronic shielding.

The aim of passive shielding is to prevent environmental radiation from reaching the detection system. This shielding is formed by three layers of different materials. The external layer is an asymmetric block of 630 kg of old lead, the objective of which is to attenuate the cosmic radiation. The asymmetric shape of the shield provides a layer of 20 cm of lead above the detection chamber (the direction with more intense cosmic radiation),

and between 7 and 11 cm in the other directions (where the earth attenuates cosmic radiation). Quantulus 1220 also includes a second layer of cadmium, which absorbs low-energy and thermal neutrons very efficiently. This layer also absorbs X-rays produced in the lead by fluorescence reactions. Finally, a third layer of copper (the wall of the container of the liquid scintillator guard) absorbs the X-rays fluorescence produced in the cadmium formed for the cosmic radiation or lead X-ray.

Fast cosmic particles may cause Cherenkov radiation in the glass of the photomultipliers used for the measurement of the sample, which may increase the background in the counter. To avoid this, Quantulus 1220 includes active shielding. The active shielding is based on the asymmetric liquid scintillation guard formed by a cylinder that contains a mineral-oil scintillator. Two photomultipliers are used to detect scintillation produced in the guard by gamma rays and cosmic radiation. When a signal is detected in coincidence in both guard photomultipliers and sample photomultipliers, the count is registered in another MCA and rejected in the sample counting.

2.5.2. Quenching measurement

As Section 2.4.1 explains, quenching may entail several drawbacks on LSS quantification, including decrease of efficiency, shifting of the spectra and increase of α/β misclassification. To control or even correct these effects, it is necessary to know the quenching level of each measured sample. The quenching index in Quantulus 1220 is SQP[E] (external standard quench parameter). It based on the shifting of the spectra of Compton electrons produced by a gamma source of ^{152}Eu. SQP[E] is defined as 99.5 % of the endpoint channel of this external source. In this way, the lower the SQP[E] is the higher the quenching is in the sample.

2.5.3. Alpha/beta separation

As Section 2.4.2 explains, the scintillations produced by an alpha particle are longer than those produced by a beta particle. Quantulus 1220 uses a pulse-shape analyser (PSA) to separate alpha and beta pulses. PSA is based on the ratio of areas of scintillation pulse after 50 ns and the total area. Before the measurement, the operator sets a PSA value. Pulses with a value lower than the PSA are classified as beta pulses, while those with higher values are classified as alpha pulses.

To obtain an appropriate α/β separation, the PSA value has to be optimized. This optimization used to be conducted by a misclassification study, which looks to minimize the total interference (alpha interference plus beta interference). Alpha interference (τ_α) is

defined as the percentage of counts classified as beta when a pure alpha emitter is counted. In the same way, beta interference (τ_β) is the percentage of count classified as alpha when a pure beta emitter is counted. Both are expressed as shown the following formulas:

$$\tau_\alpha = \frac{cpm_{\alpha\to\beta}}{cpm_{\alpha\to\alpha} + cpm_{\alpha\to\beta}} \quad (2.10) \qquad \tau_\beta = \frac{cpm_{\beta\to\alpha}}{cpm_{\beta\to\alpha} + cpm_{\beta\to\beta}} \quad (2.11)$$

where,

cpm $\alpha \to \beta$ is the counts per minute produced by a pure alpha emitter which are counted in β-MCA;

cpm $\alpha \to \alpha$ is the counts per minute produced by a pure alpha emitter which are counted in α-MCA;

cpm $\beta \to \beta$ is the counts per minute produced by a pure beta emitter which are counted in β-MCA; and

cpm $\beta \to \alpha$ is the counts per minute produced by a pure beta emitter which are counted in α-MCA.

2.6. Computational separation in LSS

As the above section explains, liquid scintillation spectrometry is a meaningful technique that is used for the determination of alpha and beta emitters. However, the poor resolution of this technique hinders the simultaneous determination of different alpha or beta emitters from the same spectrum because their spectra overlap. For alpha emitters, this overlap may be reduced by using photon-electron rejecting alpha-liquid scintillation PERALS® (McDowell and McDowell, 1989). In this method, the alpha emitters from an aqueous sample are extracted with a non-quenched organic solvent and mixed with an organic, highly efficient scintillator. The scintillator spectrometer for PERALS measurement must have an efficient reflector to transmit the maximum amount of produced light to the photomultiplier tube (PMT) and a diffuser reflector to ensure a homogeneous transmission of the light regardless of where on the sample it was produced.

Overlap is unavoidable in the case of beta emitters on account of their continuous spectra. However, several authors have achieved the quantification of several isotopes through the same LSC spectrum. The next sections describe classical and advanced methods for the simultaneous determination of two or more radionuclides from the same LS spectrum.

2.6.1. Classical methods

Exclusion method

The first approach is based on the definition of two counting zones (windows) for the determination of two isotopes: ^{3}H and ^{14}C (Okita et al., 1957). The high-energy window is assumed to contain just counts of the high-energy isotope. However, the low-energy window contains counts of both the low and the high-energy isotopes. The counts of the high-energy window are used to quantify the high-energy isotope; then these counts are used to subtract the contribution of the high-energy isotope in the low-energy window (Okita et al., 1957). To determine the efficiency of both radionuclides in each counting window, it is necessary to perform quenching curves. This method is no longer used because newer and more efficient methods are available for the same purpose.

Inclusion method

The exclusion method was improved by considering two windows with contributions of both isotopes (the inclusion method). The efficiency of each radionuclide in each counting window is determined by considering respective quenching curves. The activity for each radionuclide is obtained by solving a two-equation system in which the total count of each window is equal to the contribution of each radionuclide in this window:

$$CPM_A = A_L * Eff_{LA} + A_H * Eff_{HA} \quad (2.6)$$

$$CPM_B = A_L * Eff_{LB} + A_H * Eff_{HB} \quad (2.7)$$

where

CPM_A	is the total counts of A window (low-energy);
CPM_B	is the total counts of B window (high-energy);
A_L and A_H	is the activities of low- and high energy radionuclide, respectively;
Eff_{LA} and Eff_{LB}	is the efficiency of the low-energy radionuclide in the window A and B, respectively; and
Eff_{HA} and Eff_{HB}	is the efficiency of the high energy radionuclide in the window A and B, respectively.

Nowadays, the inclusion method is used for the determination of several pairs of isotopes, such as ^{55}Fe and ^{59}Fe (Viteri and Kohaut, 1997), ^{3}H and ^{14}C (Shaffer and Langer, 2007) or ^{32}P and ^{33}P (Nakanishi et al., 2009).

Inclusion method with daughters ingrown

In some cases—commonly after a sample treatment that entails a radiochemical separation—there is a fast ingrown of decay products in the sample, and hence in the counting vial. These decay products may interfere with the measurement of the target radionuclide. In the inclusion method, the dependence between the activity of the decay product and the elapsed time between the radiochemical separation and the measurement is used to quantify two or three radionuclides from two counting windows. This method is commonly used for the simultaneous determination of ^{89}Sr and ^{90}Sr (with the ingrown of ^{90}Y) in several kinds of matrix such as water or milk (Kim et al., 2009).

Full Spectrum

Another method used to determine the composition of binary samples is based on the SIS (Spectral Index of the Sample). The SIS is the centre of mass of the spectra and it is specific for a radionuclide in a constant level of quenching. In a binary sample the SIS is a linear combination of the SIS of pure radionuclide standards. Taking this fact into account, the composition of a binary sample can be determined For example, this method was used to determine ^{35}S and ^{32}P (Noor et al., 1995), and ^{3}H and ^{14}C (Noor et al., 1996).

Three over two fitting and digital overlay technique

A further evolution was based on the definition of three windows to determine two isotopes (three over two fitting and digital overlay technique, TOT-DOT). This is an intermediate step between classical methods (inclusion method) and advanced methods (most probable value method). In general, by this technique, several isotopes can be determined by using a number of windows greater than the number of radionuclides. The digital overlay technique also permits quench correction. This technique is described in the patent (Rundtand Kouru, 1992). Although it allows the quantification of radionuclide mixtures, it is typically used to correct quenching effects in single isotopic samples (Kim et al., 2006; Hueber-Becker et al., 2007).

2.6.2. Advanced methods

Most-probable-value method

In this method different counting regions are defined (it is possible to reach a number of regions equal to the number of channels of the MCA). The counts of each window are equal to the sum of the contributions of each radionuclide in that window. In this case, unlike TOD-DOT, an error equation is defined that expresses the difference between the sum of the

individual contributions of each radionuclide and the value measured for each window. The minimum of this function provides the most probable value of the activities for each radionuclide. This method has been used for the determination of up to six radionuclides (Takuie et al., 1991) and to discriminate beta emitters with very similar maximal energies such as ^{14}C (156 keV) and ^{35}S (167keV) (Natake et al., 1996).

Deconvolution of the spectra

Advances in computation have also facilitated the development of new techniques. Some authors have quantified several isotopes by using the same spectra by deconvolution techniques. Software was developed and applied to deconvolute complex spectra from pure spectra standards by taking into account the quenching of the sample and by allowing for the determination of up to six isotopes (Kashirin et al., 2000; Malinovsky et al., 2002) Pure spectra standards were used to resolve ^{85}Sr, ^{90}Sr and ^{90}Y in complex mixtures by fitting (Altzitzoglou, 2008). Other approaches are based on fitting the spectrum of the sample to a linear combination of tailed Gaussian functions (Nebelung and Baraniak, 2007; Nebelung et al., 2009) or to a Fourier series (Remetti and Sessa, 2011; Remetti and Franci, 2012).

Multivariate calibration

Another approach to fulfil the aim of quantify several isotopes from the same scintillation a spectrum is based on multivariate calibration methods. The use of partial least squared (PLS) to avoid interference phenomena and to quantify individual isotopes in composite spectra has been studied for solid (Roig et al., 1999) and plastic scintillation (Bagán et al., 2011). For LSC, a model based on multi-way PLS with energy channels as the primary variable and cocktail sample ratio as the secondary variable has been developed to determine the $^{235}U/^{238}U$ isotope ratio (Mahani et al. 2012).

Improvements have also been made to the data pre-process, such as to the selection of channels to construct the PLS model selected by means of an artificial neural network using a genetic algorithm (Mahani et al., 2007).

This method, which is the used to process LS spectra along this thesis, is explained in the next section.

2.7. Chemometrics and PLS

Our aim is to predict the activity of several alpha and beta emitters in sample spectra by using a calibration set of spectra obtained from samples with a known activity for the radionuclides of interest. To accomplish this aim, the calibration set must be ordered as an

X-Block—an *m* x *n* matrix that contains *n* predictors (or channels) for *m* observations (or standard spectra)—and a Y-Block, which is an *m* x *k* matrix that contains *k* dependant variables (or activity concentration of the different radionuclides of interest) for these *m* observations.

Because LS spectra are used, and because they have a large number of predictors (channels) that are collinear, ordinary multiple regression is not an appropriate regression method. Several approaches have been developed to deal with this problem. One approach is to remove some predictors by using backward elimination, step-wise methods when no statistically significant loss of fit is observed. Another two approaches used to reduce predictors and to solve the problem of co-linearity are principal-components regression (PCR) and partial least-squares regression (PLS). Both are based on constructing new variables that contain most of the information on the spectral data in a smaller number of variables and on fitting a regression equation that uses these new variables. PCR consists of performing a PCA of the X-Block and using the principal components (PC)—which are linear combinations of the predictors and orthogonal between them—as regressors on the Y-Block. The orthogonality of PC solves the multi-collinearity problem. However, the problem of choosing an optimum set of predictors remains, because PCs explain X-Block but are not necessarily relevant in Y-Block prediction (Abdi, 2003).

By contrast, PLS regression searches for a set of components called latent vectors (LV) that perform a simultaneous decomposition of the X-Block and Y-Block with the restriction that these components explain the covariance between *X* and *Y* as much as possible. Because both the *X* and *Y* data are projected to new spaces, PLS methods are known as bilinear factor models. When the LV are obtained, a regression step is performed in which the decomposition of the X-Block is used to predict the Y-Block.

X-Block is decomposed into vectors T and PT, while Y-block is decomposed into U and QT. Equations 2.8 and 2.9 illustrate the decomposition of both matrices in PLS regression. The relationship between the X-Block and the Y-Block is stored in a weight matrix, W:

$$X = TP^T + \mathrm{E} \quad (2.8)$$

$$Y = UQ^T + \mathrm{F} \quad (2.9)$$

where

T and U	are respectively projections of x-score (LV) and Y-score;
P and Q	are respectively orthogonal loading matrixes; and
E and F	are matrixes with the error terms assumed to be independent and with a random normal distribution.

Decompositions of X-Block and Y-Block are performed in a manner that maximizes the covariance between *T* and *U*. Figure 5 depicts a scheme of the construction of a PLS model.

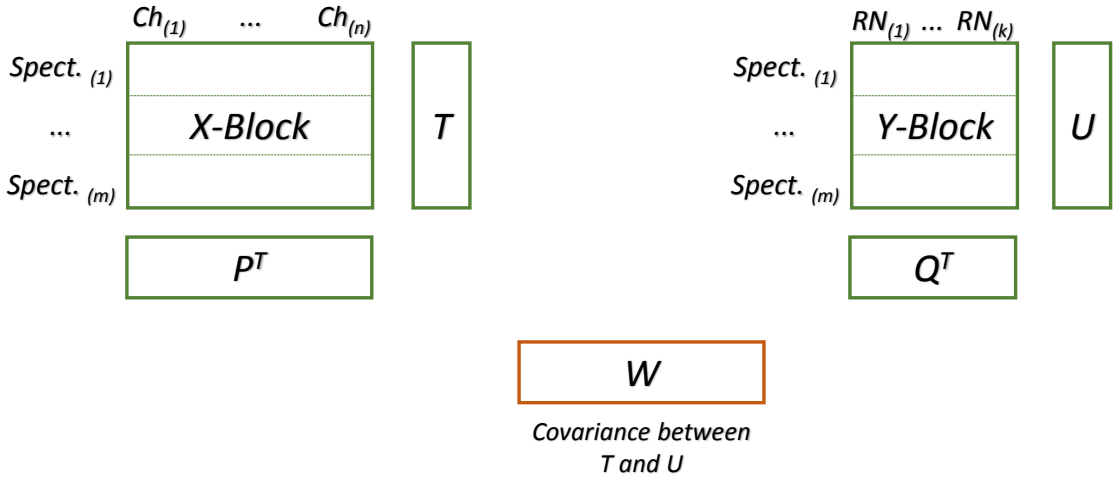

Figure 5. Scheme of PLS model construction from X-Block and Y-Block.

After model construction, the model can be used to predict dependant variables (activity concentration) by means of predictors (LS spectra) by using the vector of weight obtained in the calibration process.

Partial least-square regression (PLS) is a statistical method that reduces the predictors to a smaller set of uncorrelated components and performs least-squares regression on these components, instead of on the original data. PLS regression is especially useful when predictors are highly collinear or when there are more predictors than observations.

A common application of PLS is to model the relationship between spectral measurements near infrared, infrared or ultraviolet, which include many variables that are often correlated with each other, and chemical composition or other physico-chemical properties (Weakley et al., 2016; Muresan et al., 2016; Bourdon et al., 2014). In PLS regression, the emphasis is on developing predictive models that can subsequently be used to predict many variables from the spectral measurements.

In this thesis is studied the feasibility of using PLS to model the relationship between LS spectra and the specific activity concentration of alpha and beta emitters in the sample for different methodologies.

3. OBJECTIVES

The main objective of this thesis is to develop and apply a strategy for the rapid and simultaneous determination of alpha and beta emitters in water samples that focuses on the natural and artificial radionuclides included in the European Directive 2013/51/EURATOM.

This overall aim is divided into specific objectives which are detailed below:

- Development and validation of rapid methodologies not only for the determination of the total content of alpha and beta emitters but also of specific radionuclides mainly based on LSS (liquid scintillation spectrometry) measurements.
- Feasibility study and implementation of chemometric tools for the deconvolution and quantification of specific alpha and beta emitters from LS spectra obtained from rapid methodologies.
- Definition of a strategy for sequentially determining specific alpha and beta emitters and application of the proposed strategy to environmental water sources that may be used as drinking water and to surveillance around nuclear power plants (NPPs).

<u>Development and validation of rapid methodologies</u>

The analytical methodologies studied are the determination of gross alpha and gross beta by concentration method and measurement by liquid scintillation spectrometry ($LSS_{conc.}$); direct measurement of gross alpha and beta by liquid scintillation spectrometry ($LSS_{dir.}$), which is a modification of the first method without the concentration step to measure ^{14}C and ^{3}H; and finally, determination of ^{226}Ra, ^{228}Ra and ^{210}Pb by extraction with a 3M Radium RAD disk and subsequent measurement by LSS. Furthermore, a gamma spectrometry measurement is included in the quantification strategy as a screening method.

Determination of ^{222}Rn, also provided in the European directive, is not considered in this thesis for two reasons. On one hand, several rapid methods exist for ^{222}Rn determination. On the other hand, the potential interference of ^{222}Rn in the determination of other radionuclides can be easily removed from water samples by heating and stirring because it is a gas.

Feasibility study of chemometrics for LS spectra deconvolution

To test the feasibility of PLS models to predict the activity of the aforementioned radionuclides, a database of spectra from $LSS_{conc.}$, $LSS_{dir.}$ and RAD disk methodologies was constructed. It considers different radionuclides, activity levels and quenching levels. Several treatments were tested to improve prediction capabilities.

Definition of a strategy for sequential determination of alpha and beta emitters

The proposed strategy is based on a set of analytical methodologies that provide different information about the sample. The information is combined to quantify several alpha and beta emitters. This strategy has been applied to different kinds of real scenarios, such as determination of tritium in natural water samples, determination of natural radionuclides in environmental water, and determination of natural samples spiked with artificial radionuclides that simulate accidental contamination.

4. VALIDATION OF GROSS ALPHA AND GROSS BETA DETERMINATION

As mentioned in Section 2.3, the Directive 51/2013/EURATOM considers screening parameters like gross alpha and gross beta activities that are useful to evaluate whether the indicative dose is lower than 0.1 mSv y^{-1}. For this reason, and because it is possible to extract more information from the obtained spectra afterwards, we considered the simultaneous determination of gross alpha and gross beta activities by means of LSS. This chapter presents scientific papers regarding the validation of the methodology for gross alpha and gross beta determination by LSS in water samples.

Simultaneous determination of gross alpha, gross beta and ^{226}Ra in natural water by liquid scintillation counting. J. Fons, D. Zapata-García, J. Tent, M. Llauradó. ***Journal of Environmental Radioactivity*** **125 (2013). pp. 56-60.**

This paper considers the simultaneous determination of gross alpha, gross beta and ^{226}Ra activity. A simple and fast method was developed that involves evaporation of the sample to remove ^{222}Rn and its decay products and to improve the detection limits. Furthermore, a mathematical model based on the secular equilibrium conditions between ^{226}Ra and its short-lived decay products is proposed. This model allows for determinations of ^{226}Ra by means of two measurements of gross alpha activity within the first six days after sample preparation. The proposed method was used to determine gross alpha and gross beta and ^{226}Ra for several natural water samples used for human consumption.

A Comparative experimental study of gross alpha methods in natural waters. Montaña, M.; Fons, J.; Corbacho, J.A.; Camacho, A.; Zapata-García, D.; Guillén, J.; Serrano, I.; Tent, J.; Baeza, A.; Llauradó, M.; Vallés, I. ***Journal of Environmental Radioactivity*** **118 (2013). pp. 1-8.**

This article compares the aforementioned method with other two traditional methods for the determination of gross alpha activity: evaporation and co-precipitation methods.

For the evaporation method, the sample is evaporated to dryness and measured by proportional counting or solid scintillations with ZnS. For the co-precipitation method, the radionuclides of the sample are precipitated by the addition of $BaSO_4$ and Fe^{3+} in basic media, and the precipitate is filtered and measured by proportional counting. Precision and accuracy for the three methods was evaluated by using spiked laboratory samples and natural waters that may be used for human consumption.

4.1. Simultaneous determination of gross alpha, gross beta and ^{226}Ra in natural water by liquid scintillation counting

Simultaneous determination of gross alpha, gross beta and ^{226}Ra in natural water by liquid scintillation counting

J. Fons[a *], D. Zapata-García[b], J. Tent[a], M. Llauradó[a]

[a] Laboratory of Environmental Radiology, Analytical Chemistry Department, Universitat de Barcelona, Martí i Franquès 1-11, 3[a] Planta, Catalunya, Barcelona 08028, Spain

[b] Ionizing Radiation Division, Physikalisch-Technische Bundesanstalt, Bundesanstalt, Germany

*corresponding author: jordi.fons@ub.edu

Abstract

The determination of gross alpha, gross beta and ^{226}Ra activity in natural waters is useful in a wide range of environmental studies. Furthermore, gross alpha and gross beta parameters are included in international legislation on the quality of drinking water [Council Directive 98/83/EC]. In this work, a low background liquid scintillation counter (Wallac, Quantulus 1220) was used to simultaneously determine gross alpha, gross beta and ^{226}Ra activity in natural water samples. Sample preparation involved evaporation to remove ^{222}Rn and its short-lived decay daughters. The evaporation process concentrated the sample ten-fold. Afterwards, a sample aliquot of 8 mL was mixed with 12 mL of Ultima Gold AB scintillation cocktail in low-diffusion vials. In this study, a theoretical mathematical model based on secular equilibrium conditions between ^{226}Ra and its short-lived decay daughters is presented. The proposed model makes it possible to determine ^{226}Ra activity from two measurements. These measurements also allow determining gross alpha and gross beta simultaneously. To validate the proposed model, spiked samples with different activity levels for each parameter were analysed. Additionally, to evaluate the model's applicability in natural water, eight natural water samples from different parts of Spain were analysed. The eight natural water samples were also characterised by alpha spectrometry for the naturally occurring isotopes of uranium (^{234}U, ^{235}U and ^{238}U), radium (^{224}Ra and ^{226}Ra), ^{210}Po and ^{232}Th. The results for gross alpha and ^{226}Ra activity were compared with alpha spectrometry characterization, and an acceptable concordance was obtained.

Keywords: Activity growth model, Radioactivity, Environmental samples, Liquid scintillation

Introduction

To determine ^{226}Ra activity concentration is an important task due its high radio-toxicity as review Guogang and Jing (2012). Gross alpha, gross beta and ^{226}Ra activity can be used to establish the TID (Total Indicative Dose). There are various methods of measuring ^{226}Ra, including γ-spectrometry (Kahn et al., 1990; Cazala et al., 2003; Dulaiova and Burnett, 2004), a-spectrometry (Purkl and Eisenhauer 2003; Bojanowski et al., 2005), radon emanometric methods (Lucas et al., 1990; Maharana et al., 2010) and liquid scintillation techniques with radiochemical separation (Salonen, 1993; Repine and Benedik, 2002) or without separation (Salonen, 2006). When liquid scintillation spectrometry without radiochemical separation is applied, the point is to eliminate radon and its short-lived daughters of the sample and to evaluate the increase of the alpha activity between the sample treatment and 21 days after this treatment. The variation was attributed to the increase of ^{222}Rn and its short-lived daughters into the sample vial. This method was tested by several authors and useful results were obtained (Sanchez-Cabeza and Pujol, 1998; Fernandes et al., 2011). However to measure after 21 days of the sample treatment is an important drawback for this method. In this work a mathematical model was developed in order to determinate ^{226}Ra activity measuring the first time just after sample treatment and the second one before 21 days after that treatment. The advantages of this mathematical model application are, on one hand joint the determination of gross alpha, gross beta and ^{226}Ra in one technique and on the other hand avoid radiochemical separation which entails a reduction in sample manipulation and in the reactive consumption.

Methods and materials

Detector

A low background liquid scintillation counter (1220 QUANTULUS, Wallac (Turku, Finland)) was used. The Pulse Shape Analyser (PSA) of the 1220 QUANTULUS discriminates between alpha and beta pulses and separates the pulses into different multi-channels.

The optimal PSA value for the alpha/beta discrimination was established by a misclassification study using ^{236}U and ^{40}K as standards. Please see the report CSN (2011). This detector also has a quench control parameter. The Spectral Quench Parameter of the External Standard (SQP[E]) is the lowest channel below which 99.75% of the counts generated when the sample is irradiated with a ^{152}Eu source, included in the counter, are registered. The SQP[E] was evaluated in all samples. In this study, we used constant quench conditions.

This detector is under the quality control (internal and external) of the Laboratory of Environmental Radiology. (ISO/IEC 17025, ENAC accreditation n° 520/LE1117).

Reagents

High capacity and specially designed for the alpha beta discrimination cocktail Ultima Gold AB (Perkin Elmer, Turku, Finland) was used throughout the work. The radioactive solutions were prepared by weight from the following radioactive standards: ^{230}Th 40.83 ± 0.16 Bq g^{-1} standard supplied by NIST National Institute of Standards and Technology (Gaithersburg, Maryland); ^{226}Ra 176.0 ± 2.4 Bq g^{-1} standard supplied by CIEMAT Centro de Investigaciones Energéticas Medioambientales y Tecnológicas (Madrid, Spain); ^{210}Pb 35,500 ± 700 Bq g^{-1} standard supplied by DAMRI Département des applications et de la métrologie des rayonnements ionitzants France; ^{nat}U 957.2 ± 19.1 Bq g^{-1} standard and ^{236}U 761.1 ± 15.7 Bq g^{-1} standard both supplied by Eckert and Ziegler (Valencia, California). The ^{40}K solutions were prepared from dry KCl salt supplied by Merck (Berlin, Germany). The activity was calculated by applying the natural abundance of ^{40}K.

Material

Twenty-millilitre polyethylene liquid scintillation vials were supplied by Perkin Elmer.

General purpose materials in the laboratory were used.

Analytical procedure

A 100 mL aliquot of a water sample was evaporated to dryness. When the precipitate obtained was cooled to room temperature, it was dissolved in 10 mL of deionised water acidified by HCl to pH = 1.5 as describe Zapata-García et al. (2009).

It was necessary to stir the solution for 5 min to ensure that all the precipitated material was dissolved. With this treatment, ^{222}Rn is completely eliminated from the sample. The elimination of their short-lived daughters occurs by means of radioactive decay.

Fig. 1 show the activity evolution in a ^{226}Ra sample with their decay daughters when ^{222}Rn is removed. To perform this simulation we have used the Laplace transform solution of the equations of radioactive decay. About 3 h and a half are required for a quantitative removal of the short-lived daughters (Catchen, 1984).

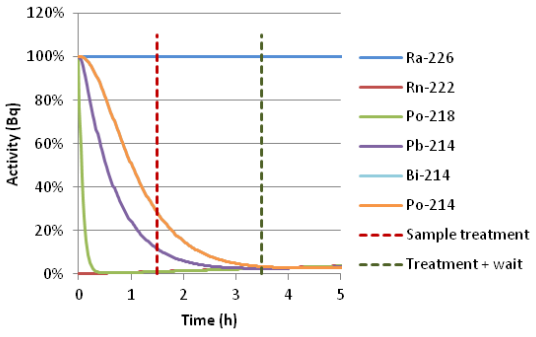

Fig. 1. Activity evolution for ^{226}Ra and its short-lived daughters when ^{222}Rn was completely removed.

An 8 mL aliquot of the evaporated samplewas mixed with 12 mL of the scintillator cocktail in a low diffusion scintillator vial. Under these conditions, the sample remained homogenous andwas stable for several months. The vial was counted in a liquid scintillation counter that was able to discriminate between alpha and beta pulses. It is recommended that the vial should remain in the counter for 2 h before counting to avoid photoluminescence phenomena. The 2 h time period is also necessary to allow the decay of the short-lived daughters of ^{222}Rn. To find the appropriate calibration standard, many alpha emitters (^{230}Th, ^{236}U and ^{241}Am) and beta emitters (^{40}K, ^{137}Cs, ^{90}Sr/Y) were used to conduct a misclassification study (Zapata-García et al., 2012). Both ^{236}U and ^{40}K were selected as calibration standards because they are the emitters with the worst misclassification. Please see the report CSN (2011) for more details.

Samples

Synthetic samples

A synthetic water sample containing 95 mg L^{-1} Ca^{2+}, 51 mg L^{-1} Mg^{2+}, 38 mg L^{-1} Na^{+}, 2 mg L^{-1} K^{+}, 227 mg L^{-1} SO_4^{2-}, 149 mg L^{-1} Cl^{-} and 138 mg L^{-1} HCO_3- was prepared. It was acidified by HNO3 to pH = 1. Several aliquots of this synthetic water sample were spiked with natural isotopes. The composition of these solutions is shown in Table 1.

Natural samples

Eight natural water samples from different parts of Spain were analysed. As shown in Table 2, the selected water samples have different radioactivity contents and a wide range of dry residue. A

100 L volume of water was taken at each sampling point. The water samples were acidified with HNO_3 (1.25 mL L^{-1}) for preservation.

Calibration

Alpha/beta discrimination

The Pulse Shape Analyser is used to discriminate between alpha and beta pulses. With the aim of establishing the optimal PSA value, the misclassification phenomenon was studied using ^{236}U and ^{40}K as standards.

Table 1
^{nat}U, ^{226}Ra, ^{210}Po and gross alpha for the spiked samples.

Code	*U-nat (Bq kg^{-1})*	*Ra-226 (Bq kg^{-1})*	*Po-210 (Bq kg^{-1})*	*Gross alpha (Bq kg^{-1})*
URa 100:0	0.201 ± 0.004	-	-	0.201 ± 0.004
URa 75:25	0.169 ± 0.003	0.108 ± 0.002	0.076 ± 0.002	0.353 ± 0.006
URa 50:50	0.118 ± 0.002	0.128 ± 0.002	0.090 ± 0.002	0.336 ± 0.005
URa 25:75	0.072 ± 0.002	0.181 ± 0.003	0.127 ± 0.002	0.380 ± 0.006
URa 0:100	-	0.208 ± 0.002	0.146 ± 0.002	0.354 ± 0.004
URa	0.214 ± 0.004	0.198 ± 0.003	0.138 ± 0.006	0.550 ± 0.008
URaPo	0.196 ± 0.004	0.202 ± 0.003	0.418 ± 0.010	0.816 ± 0.015

Table 2
Chemical and radiochemical characteristics of the natural water samples.

CODE	*Characteristics*
SUBT-A	Dry residue: 1 g L^{-1}. Activity $^{226}Ra \sim 0.40$ Bq L^{-1}, $^{234+238}U \sim 1.0$ Bq L^{-1}, $^{210}Po \sim 0.02$ Bq L^{-1}
POT-A	Dry residue: 5 g L^{-1}. Activity $^{226}Ra \sim 0.60$ Bq L^{-1}, $^{234+238}U \sim 1.0$ Bq L^{-1}, $^{210}Po \sim 0.06$ Bq L^{-1}
SUP-A	Dry residue: 1.5 g L^{-1}. Activity $^{234+238}U \sim 0.10$ Bq L^{-1}
POT-B	Dry residue: 0.4 g L^{-1}. Activity $^{226}Ra \sim 0.002$ Bq L^{-1}
POT-C	Dry residue: 0.9 g L^{-1}. Activity $^{234+238}U \sim 0.08$ Bq L-1, $^{226}Ra \sim 0.002$ Bq L^{-1}
POT-D	Dry residue: 4.7 g L^{-1}. Activity $^{226}Ra \sim 1.0$ Bq L^{-1}, $^{228}Ra \sim 0.03$ Bq L^{-1}, $^{234+238}U \sim 1.0$ Bq L^{-1}
SUP-B	Dry residue: 0.6 g L^{-1}. Activity $^{226}Ra \sim 0.01$ Bq L^{-1}, $^{234+238}U \sim 0.06$ Bq L^{-1}
SUBT-B	Dry residue: 0.9 g L^{-1}. Activity $^{226}Ra \sim 0.10$ Bq L^{-1}, $^{234+238}U \sim 1.0$ Bq L^{-1}

In this study one vial for each one of the standards was prepared and measured at different PSA values. The optimal PSA is found as the value in which the total misclassification, alpha plus beta, is lower.

Fig. 2 shows the graphical representation of this misclassification study. We can see that the optimal PSA value is around 100. In this PSA value the misclassification is lower than 10% for both alpha and beta emitters.

Results and discussion

Mathematical model

The aim of this study was to establish a mathematical function that describes the alpha evolution in a closed system with ^{226}Ra and without ^{222}Rn and its short-lived daughters.

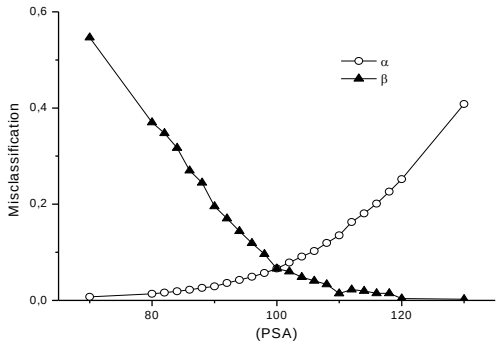

Fig. 2. Alpha and beta misclassification versus PSA value.

A simple case is considered in which the parent nuclide A decays to a daughter nuclide B, which in turn decays to a stable nuclide C. In such decay chains, the number of atoms of B as a function of time is described by Equation (1):

$$N_B(t) = \frac{\lambda_A}{\lambda_B - \lambda_A} N_A^0 \left(e^{-\lambda_A t} - e^{-\lambda_B t}\right) + N_B^0 e^{-\lambda_B t} \quad (1)$$

where

$N_B(t)$ is the number of atoms of B at time (t); λ_A and λ_B are the decay constants of A and B, respectively; N^0_A and N^0_B are the numbers of atoms of A and B, respectively, at time zero and t is the elapsed time.

Secular equilibrium conditions and an absence of B atoms at time zero are considered in Equation (2):

$$A_B(t) = A_A^0 * \left(1 - e^{-\lambda_B t}\right) \quad (2)$$

where

$A_B(t)$ is the activity of B at time (t) in Bq; λ_B is the decay constant of B in s^{-1}; A^0_A is the activity of A at time zero in Bq and t is the elapsed time in s.

In Equation (2), a null B activity at time zero is shown. At later time points, the B

activity is equal to the A activity when secular equilibrium is reached (Annunziata, 1998). A priori, this equation cannot describe our problem because ^{226}Ra is a parent radionuclide with a numerous daughters. However, it is possible to apply the philosophy of Equation (2) because ^{222}Rn, the first of the daughter of ^{226}Ra, has the longest half-life within the decay series and all the other short-lived daughters remain in secular equilibrium with ^{222}Rn while it is still being generated. ^{226}Ra has three alpha emitter short-lived daughters: ^{222}Rn, ^{218}Po and ^{214}Po. Considering the secular equilibrium between ^{222}Rn and all the short-lived daughters, the alpha activity in a closed system with only ^{226}Ra at time zero is described by Equation (3):

$$Act_{\alpha}{}^{226}Ra(t) = 3Act(^{226}Ra)^{0} * \left(1 - e^{-\lambda_{Rn}t}\right) + Act(^{226}Ra)^{0} \quad (3)$$

where

Act^{226}Ra(t) is the alpha activity in a closed system (which only contains ^{226}Ra at time zero) elapsed at t time in Bq; Act(^{226}Ra)^{0} is the ^{226}Ra activity at time zero in Bq and λ_{Rn} is the ^{222}Rn decay constant in s^{-1}.

Considering that our closed system may contain nuclides other than ^{226}Ra and considering that their activities do not decay significantly in the considered time, the alpha activity in the system is described by Equation (4):

$$Act_{\alpha}(t) = A * \left(1 - e^{-b*t}\right) + C \quad (4)$$

where

Act (t) is the alpha activity in the closed system elapsed at t time in Bq; A is a parameter corresponding to the maximum increase in the alpha activity and is equal to 3*Act(^{226}Ra)^{0} in Bq; b is the ^{222}Rn decay constant in s^{-1} and C is the parameter corresponding to the gross alpha at time zero in Bq.

It should be noted that the current model (Equation (4)) is indicative of the real alpha activity in closed systems where only short-lived daughters of ^{226}Ra are generated.

Table 3
Fitted model parameters and bias in the gross alpha and ^{226}Ra activities for samples with similar gross alpha activities and increasing ^{226}Ra activities.

Samples	*Fitted parameters*			*Bias*	
	A (Bq kg^{-1})	*b (h^{-1})*	*C Gross alpha at t_0 (Bq kg^{-1})*	*Gross alpha*	*^{226}Ra activity*
URa 0:100	0.578 ± 0.051	0.006 ± 0.002	0.382 ± 0.022	7.9 %	7.4 %
URa 25:75	0.556 ± 0.026	0.006 ± 0.001	0.350 ± 0.060	-7.9 %	2.4 %
URa 50:50	0.434 ± 0.006	0.006 ± 0.003	0.226 ± 0.018	-32.7 %	16.7 %
URa 75:25	0.220 ± 0.029	0.006 ± 0.003	0.235 ± 0.033	-33.4 %	-32.1 %
URa 100:0	0.000	-	0.193 ± 0.024	-4.0 %	-

Table 4
Fitted model parameters and bias in the gross alpha and ^{226}Ra activities for samples with similar ^{226}Ra activities and increasing gross alpha activities.

Samples	*Fitted parameters*			*Bias*	
	A (*Bq kg^{-1}*)	*b* (*h^{-1}*)	*C* *Gross alpha at t_0 (Bq kg^{-1})*	*Gross alpha*	*^{226}Ra activity*
Ra 0:100	0.578 ± 0.051	0.006 ± 0.002	0.382 ± 0.022	7.9 %	-7.4 %
URa	0.628 ± 0.057	0.007 ± 0.001	0.512 ± 0.041	-7.5 %	5.7 %
URaPo	0.632 ± 0.049	0.005 ± 0.002	0.717 ± 0.024	-12.1 %	4.3 %

Model's verification using synthetic samples

To validate the proposed theoretical model, several synthetic samples (shown in Table 1) were analysed. Each sample was measured at several time points (2, 24, 72, 144, 240, 504 and 720 h) after the sample treatment.

^{226}Ra proportion effect

To evaluate the ^{226}Ra proportion effect in the evolution profiles, synthetic samples with similar gross alpha values, but increasing ^{226}Ra contributions, were prepared. Fig. 3 shows the mean and standard deviation of replicate measurements of alpha activity evolution over time. Error bars represent the standard deviation of each replicate. The modelled activity evolution for each sample is also shown (solid line). As shown in Fig. 3, the alpha activity of the URa 100:0 sample with no ^{226}Ra content remains constant. Furthermore, the alpha activity of all the samples containing ^{226}Ra increases over time. Fig. 3 also demonstrates that the experimental data match the proposed model. The fitted model parameters are shown in Table 3. This table also shows the bias between the calculated and spiked gross alpha and ^{226}Ra activities. (Table 4).

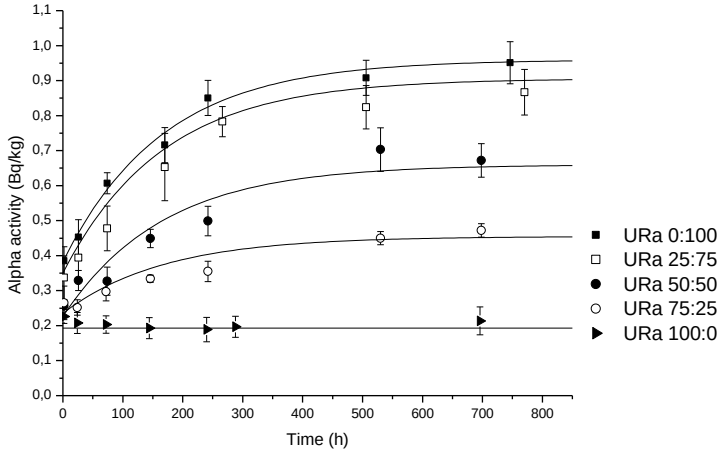

Fig. 3. Evolution of the alpha activity over time for samples with similar gross alpha values and increasing ^{226}Ra activity. The solid lines represent the model evolution.

Gross alpha effect

To evaluate the gross alpha effect in the evolution profiles, synthetic samples with similar 226Ra activities (approximately 0.200 Bq L^{-1}) but increasing gross alpha activities (adding ^{nat}U or ^{nat}U and ^{210}Po) were prepared. Fig. 4 shows the mean and standard deviation of replicate measurements of alpha activity evolution over time.

Error bars represent the standard deviation of each replicate. The modeled activity evolution for each sample is also shown (solid line). As demonstrated in Fig. 4, the three samples with the same ^{226}Ra activity have profiles that remain equidistant. The only difference between the profiles is the addition of a constant component. Fig. 3 also shows that the experimental data match the proposed model.

The fitted model parameters are shown in Table 3. This table also presents the bias between the calculated and spiked gross alpha and ^{226}Ra activities.

Model's application to natural samples

The proposed model, Equation (4), permits the calculation of gross alpha activity at time zero and the ^{226}Ra activity. For this purpose, two gross alpha determinations at two different times are required. To test the proposed model in natural samples, several analyses were performed. Two measurements of gross alpha at two different times were made for each of the eight natural samples. The first measurement was performed two hours after sample treatment. The second measurement was conducted six days after the sample treatment.

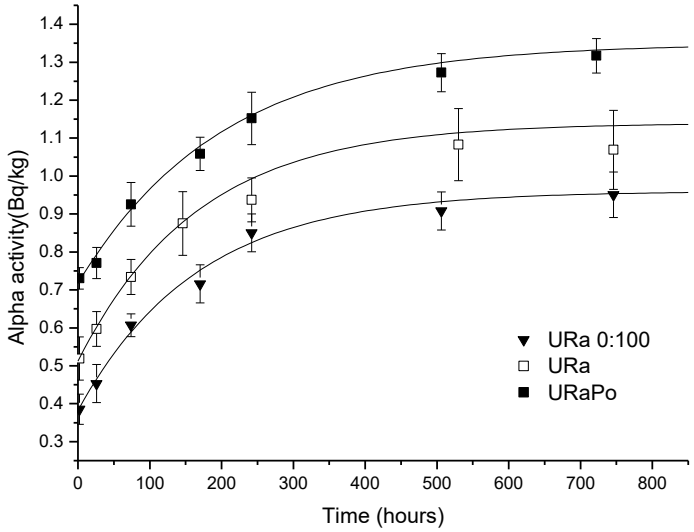

Fig. 4. Evolution of the alpha activity over time for samples with similar 226Ra activities and increasing gross alpha activities. The solid lines represent the model evolution.

Table 5
Alpha activities, fitted model parameter, reference values and bias calculation for gross alpha and ^{226}Ra activity for each natural sample.

	Measure		*Fitted parameters*			*Reference values*[c]		*Bias*	
Sample	*Activity 1*[a]	*Activity 2*[b]	*A*	*C (Actα)*	*Act ^{226}Ra*	*Act α*	*Act ^{226}Ra*	*Act α*	*Act ^{226}Ra*
	(Bq kg^{-1})	*(Bq kg^{-1})*	*(Bq kg^{-1})*	*(Bq kg^{-1})*	*(Bq kg^{-1})*	*(Bq kg^{-1})*	*(Bq kg^{-1})*	*%*	*%*
SUBT-A	1.974 ± 0.176	2.703 ± 0.155	1.129 ± 0.313	1.957 ± 0.640	0.376 ± 0.104	2.170 ± 0.206	0.467 ± 0.114	-9.8 %	-19.5 %
SUBT-B	6.283 ± 0.152	6.507 ± 0.164	0.347 ± 0.303	6.278 ± 0.624	0.116 ± 0.101	6.225 ± 0.583	0.134 ± 0.018	0.9 %	-13.4 %
POT-A	1.315 ± 0.078	2.330 ± 0.088	1.572 ± 0.162	1.292 ± 0.453	0.524 ± 0.054	1.385 ± 0.175	0.552 ± 0.064	-6.7 %	-5.1 %
POT-D	0.315 ± 0.010	0.697 ± 0.037	0593 ± 0.056	0.306 ± 0.241	0.198 ± 0.019	0.280 ± 0.038	0.214 ± 0.033	9.3 %	-7.7 %
POT-B	< 0.025	< 0.025	-	-	-	0.038 ± 0.013	0.002 ± 0.001	-	-
POT-C	0.031 ± 0.017	0.047 ± 0.013	0.025 ± 0.028	0.031 ± 0.192	0.008 ± 0.009	0.060 ± 0.015	0.004 ± 0.001	-48.7 %	100.0 %
SUP-A	0.182 ± 0.010	0.173 ± 0.034	-0.014 ± 0.052	0.182 ± 0.055	-0.005 ± 0.017	0.186 ± 0.029	0.005 ± 0.003	-2.1 %	-209.5 %
SUP-B	0.098 ± 0.023	0.105 ± 0.028	0.011 ± 0.050	0.098 ± 0.081	0.004 ± 0.017	0.099 ± 0.024	0.004± 0.001	-1.1 %	-7.0 %

[a] Activity 1: Alpha activity measured 2 h after sample treatment.
[b] Activity 2: Alpha activity measured 144 h after sample treatment.
[c] Reference values: Actα sum of current alpha emitters determined by alpha spectrometry. Act ^{226}Ra determined by alpha spectrometry.

During the six-day measurement period, the increase of alpha activity was significant, which permitted the estimation of ^{226}Ra activity. Equations (5) and (6) show the values of the model parameters A (maximum growth) and C (gross alpha at time zero):

$$A = \frac{Act_2 - Act_1}{e^{-bt_1} - e^{-bt_2}} \quad (5)$$

$$C = \frac{Act_2(1 - e^{-bt_1}) - Act_1(1 - e^{-bt_2})}{e^{-bt_2} - e^{-bt_1}} \quad (6)$$

Table 5 contains both activities measured at two hours and six days after the sample treatment, the fitted model parameters and the bias in the gross alpha and ^{226}Ra determination. Table 5 also contains the reference values used to calculate bias. The reference value for ^{226}Ra is the mean of three replicates, as evaluated by alpha spectrometry after a radiochemical separation. For gross alpha, the reference value is the sum of the isotopes found in natural water: ^{234,235,238}U, ^{226,228}Ra, ^{210}Po and ^{232}Th. For ^{226}Ra determination, samples containing on the order of 10^{-1} Bq kg^{-1} ^{226}Ra have a bias less than 20%. However, when the sample contains on the order of 10^{-3} Bq kg^{-1} of ^{226}Ra, the bias obtained is unacceptable. The results obtained from applying the model to gross alpha determination generally have a bias below10%, which is as low as the bias obtained from single determination. However, a large bias was obtained for the POT-C sample. A very low alpha activity (near the Minimum Detectable Activity) is the cause of this unacceptable bias.

Conclusions

The proposed model makes it possible to quantify ^{226}Ra activity in a closed system using two measurements of alpha activity. To make this measurement possible, it is necessary for all the ^{226}Ra short-lived daughters to be removed during the treatment of the sample. The model permits the second measurement to be conducted within the first 21 days after sample treatment instead of waiting until secular equilibrium is reached. A liquid scintillation vial containing the cocktail and the treated sample approximates the described closed system. The proposed model can be applied for two gross alpha measurements to estimate ^{226}Ra activity. Biases lower than 20% were obtained for samples with ^{226}Ra activities on the order of 10^{-1} Bq kg^{-1}.

Acknowledgements

This study was supported by the Catalan government (AGAUR 2009SGR1188), the Spanish government (CYCIT contract CTM2011- 27211) and by the Spanish Nuclear Safety Council (projects “Study

of existing problems in the gross alpha determination in drinking water. Proposal of procedures" and "Rapid methods for the simultaneous determination of alpha and beta emitters by liquid scintillation spectrometry in water").

References

Annunziata, M.F., 1998. Nuclear radiation. Its interaction with matter and radioisotope decay. In: "Handbook of Radioactivity Analysis" (Chapter 1e5). Academic Press, San Diego, California, pp. 53-67.

Bojanowski, R., Radecki, Z., Burns, K., 2005. Determination of radium and uranium isotopes in natural waters by sorption on hydrous manganese dioxide followed by alpha-spectrometry. Journal of Radioanalytical and Nuclear Chemistry 264 (2), 437-443.

Catchen, J.G., 1984. Application of the equation of radioactive growth and decay to geochronological models and explicit solution of the equations by Laplace transform. Isotope Geosciences 1984 (2), 181-185.

Cazala, C., Reyss, J.L., Decossas, J.L., Royer, A., 2003. Improvement in the determination of 238U, 228,234Th, 226,228Ra, 210Pb, and 7Be by g spectrometry on evaporated fresh water samples. Environmental Science and Technology 37 (21), 4990-4993.

Council Directive 98/83/EC of 3 November 1998 on the Quality of Water Intended for Human Consumption.

Dulaiova, H., Burnett, W.C., 2004. An efficient method for g-spectrometric determination of radium-226, 228 via manganese fibers. Limnology and Oceanography. Methods 2, 256-261.

Fernandes, P., Sousa, O., Juliao, Q.C., Dantas, M., 2011. Development and validation of a technique for the determination of 226Ra and 228Ra by liquid scintillation in liquid samples. Radiation Protection Dosimetry 144, 335-338.

Guogang, J., Jing, J., 2012. Determination of radium isotopes in environmental samples by gamma spectrometry, liquid scintillation counting and alpha spectrometry: a review of analytical methodology. Journal of Environmental Radioactivity 106, 98-119.

Kahn, B., Rosson, R., Cantrell, J., 1990. Analysis of 228Ra and 226Ra in public water supply by a g-ray spectrometry. Health Physics 59, 125-131.

Lucas, H.F., Markun, F., Boulenger, R., 1990. Methods for measuring radium isotopes: emanometry. In: The Environmental Behaviour of Radium (Chapter 3-2). Technical Reports Series No. 310, vol. 1. International Atomic Energy Agency, Vienna, pp. 149-172.

Maharana, M., Eappen, K.P., Sengupta, D.J., 2010. Radon emanometric technique for 226Ra estimation. Journal of Radioanalytical and Nuclear Chemistry 285, 469-474.

Purkl, S., Eisenhauer, A., 2003. A rapid method for a-spectrometric analysis of radium isotopes in natural waters using ion-selective membrane technology. Applied Radiation and Isotopes 59 (4), 245-254. Repine, U.,

Benedik, L., 2002. Development of a method for the determination of 226Ra by liquid scintillation counting. Journal of Radioanalytical and Nuclear Chemistry 254, 181-185.

Salonen, L., 2006. Alpha/Beta liquid scintillation spectrometry in surveying Finnish groundwater samples. Radiochemistry 48, 606-612.

Salonen, L., 1993. A rapid method for monitoring of uranium and radium in drinking water. Science of the Total Environment 130/131, 23-35.

Sanchez-Cabeza, J.A., Pujol, L., 1998. Simultaneous determination of radium and uranium activities in natural water samples using liquid scintillation counting. Analyst 123, 399-403.

Zapata-García, D., Llauradó, M., Rauret, G., 2009. Establishment of a method for the rapid measurement of gross alpha and gross beta activities in sea water. Applied Radiation and Isotopes 67, 978-981.

Zapata-García, D., Llauradó, M., Rauret, G., 2012. The implications of the particle energy an acidic media on gross alpha and gross beta determination using liquid scintillation. Applied Radiation and Isotopes 70, 705-711.

4.2. A comparative experimental study of gross alpha methods in natural waters

A comparative experimental study of gross alpha methods in natural waters

M. Montaña[a *], J. Fons[b], J.A. Corbacho[c], A. Camacho[a], D. Zapata-García[b], J. Guillén[c], I. Serrano[a], J. Tent[b], A. Baeza[c], M. Llauradó[b], I. Vallés[a]

[a] Institut de Tècniques Energètiques, Universitat Politècnica de Catalunya, Barcelona, Spain

[b] Laboratori de Radiologia Ambiental, Universitat de Barcelona, Spain

[c] Laboratorio de Radiactividad Ambiental, Universidad de Extremadura, Spain

*corresponding author: montse.montana@ubc.edu

Abstract

The aim of the present work was to compare the results obtained with gross alpha methods such as evaporation, co-precipitation and total evaporation by liquid scintillation counting and to check whether these results are representative of the real total alpha activity concentration on the sample. The study was carried out on eight natural waters with very different radioactive characteristics. For all the samples uranium (^{238}U, ^{235}U, and ^{234}U), radium (^{226}Ra and ^{224}Ra), ^{210}Po, and ^{232}Th isotopes were also assayed by using radiochemical separation and alpha spectrometry in order to determine the sum of the activities of these alpha emitters.

Precision (expressed as relative standard deviation) was below 28% for evaporation and below 18% for co-precipitation. In the case of total by liquid scintillation counting it was below 10% for samples with Total Alpha activity above 0.1 Bq/L (this value is about three times the MDA). Furthermore, for most of the studied waters, the Total Alpha activity and the gross alpha activity determined by the three methods were comparable. The obtained bias by the evaporation, co-precipitation, and total evaporation by liquid scintillation counting methods was lower than 40%, 25% and 20%, respectively.

The ANOVA test was applied to find out if there was significant variability among the methods. For the samples with the most common radiochemical characteristics there were no significant differences among the three studied methods. However differences were detected for samples with a high saline content or with a very low activity level.

Keywords: Gross alpha activity, Evaporation and co-precipitation methods, Total evaporation and measurement by liquid scintillation counting

Introduction

Due to the importance of water to human life, its quality must be strictly controlled. For this reason standard methods are used to evaluate drinking water for human consumption in order to guarantee that they have a low level of radioactivity.

The radioactivity in drinking water may be either man made, resulting from waste discharges and atomic bomb fallout, or produced naturally, from the dissolution of gases and rock minerals. The most common radioactivity is naturally produced and includes isotopes of uranium and thorium and their daughter products: ^{226}Ra, ^{228}Ra, ^{222}Rn, ^{210}Pb and ^{210}Po (UNSCEAR, 2000).

According to the World Health Organization (WHO) guidelines (2011), the Total Dose Indicative (TDI) parameter must be measured in drinking water to ensure that it is safe for consumption. The WHO (2011) and the European Directive 98/83/EC (EC, 1998) fixed parameter values for TDI (0.1 mSv/year). It is specified that TDI excludes tritium, ^{40}K, radon and radon decay products. A more practical approach is to use a screening procedure, where the total radioactivity present in the form of alpha and beta radiation is first determined (gross alpha/beta activity determination) since this is one of the simplest radioanalytical procedures (Jobbágy et al., 2010), without regard to the identity of specific radionuclides.

In Spain, the health criteria governing water quality for human consumption were published in 2003 in decree no. 140/2003. This decree established the highest permissible values for gross alpha (0.1 Bq/L), gross beta excluding ^{40}K contribution (1 Bq/L) and tritium activity (100 Bq/L) (RD, 140/2003). Below these screening levels, drinking water is acceptable for human consumption, and no further action is required.

In general, gross alpha is more of a concern than gross beta for natural radioactivity in waters, when considering health effects from natural radioactivity (Semkow and Parekh, 2001).

Different methods are used to measure gross alpha activity. Two of them are based on evaporation (EPA, 1980) or coprecipitation (EPA, 1984) of the sample, using either a gas flow proportional on total evaporation of the sample and measurement by liquid scintillation counting (total evaporation/LSC) (ASTM,1996), is being increasingly used.

Gross alpha activity is intended to approximate the Total Alpha activity concentration (TAAC) of the sample. However, this parameter is subject to several factors (e.g., alpha particle energies, calibration standard used and time elapsed from sample preparation to measurement) that can cause a high degree of

variability (Ardnt, 2010), basically because a mixed radionuclide composition has to be simultaneously measured (Jobbágy et al., 2010).

The elapsed time is an important influential factor. Two different times must be considered: the time between sample collection and preparation, and the time between sample preparation and analysis. When a sample contains ^{226}Ra, the contribution of ^{226}Ra progeny to the gross alpha activity increases with the time between preparation and analysis. For example, Oural et al. (1988) found that the gross alpha activity of replicate samples could vary by two orders of magnitude when analysed by different laboratories. This was attributed to ^{222}Rn progeny. For samples containing ^{224}Ra, Parsa (1998) found a large variation in the gross alpha activity with time when the period between sample collection and analysis ranged from days to weeks. In addition, Parsa et al. (2000) found that the gross alpha activity of some replicate water samples analysed within 48 h of collection could vary by over one order of magnitude and showed the variation to be due to ^{224}Ra, ^{212}Pb, and/or ^{214}Pb/^{214}Bi.

Taking into account the methods previously mentioned, the elapsed time between sample preparation and analysis may vary between 3 h and three days after sample preparation. For example, gross alpha by the evaporation method (EPA, 1980) stipulates that once the sample is prepared it should be stored for at least three days prior to measuring its gross alpha activity. On the other hand, the co-precipitation method (EPA, 1984) stipulates that once the sample is prepared it should be measured 3 h after preparation. However, in a previous study (CSN, 2011) carried out by our research group, at least a two days delay was suggested because during the sample preparation, and just after filtration step, ^{222}Rn from the air is trapped in the precipitate and produces the alpha emitters ^{218}Po and ^{214}Po increasing and varying the alpha contribution in the blank and the sample during 48 h after preparation, more specifically in low-background laboratories and when samples have low alpha activities. In the case of the total evaporation/ LSC method, measurement was done after 2 h of vial preparation in order to prevent photoluminescence phenomena (L'Annunziata, 1998), which interferes with the measurement. In routine laboratory work, perhaps it is not possible to ensure that measurement is done 2 h after completing the preparation. This is not a cause of problems in the total evaporation/LSC, as a spectral output is obtained and it is possible to detect the ^{226}Ra contribution in these spectra because the signal appears due to the presence of ^{214}Po (CSN, 2011). In this case, fresh sample prepara-

tion and measurement 2 h later is required. If there is no ^{226}Ra in the sample, quantification may be carried out with a delay longer than 2 h.

For the reasons mentioned above, it was of interest to study the gross alpha activity obtained by different methods placing utmost importance on the elapsed time between sample preparation and measurement with the intention to establish a maximum of this elapsed time in order to get comparable results. Therefore, the aim of the present work was to compare the results obtained with gross alpha evaporation, co-precipitation and total evaporation/LSC methods, and to check whether these results are representative of the sum of the activities of the alpha emitters present in the samples. The study was carried out on eight natural water samples of very different radioactive characteristics. For all the samples, uranium (^{238}U, ^{235}U, and ^{234}U), radium (^{226}Ra and ^{224}Ra), ^{210}Po, and ^{232}Th isotopes were also assayed using radiochemical separation and alpha spectrometry in order to determine the sum of activities of these alpha emitters. Then, a temporal evolution in gross alpha activity for the eight natural waters was studied to evaluate the influence of elapsed time between sample preparation and measurement taking into account the different time established in all three methods. Precision and accuracy (expressed by the bias) were calculated for these methods and differences among them were also statistically studied using ANOVA and "t" tests in order to consider whether there was significant variability among the three methods.

Materials and methods

Three accredited laboratories (ISO/IEC 17025) took part in the study. A specific method for gross alpha determination was assayed by each laboratory and radiochemical procedures for specific alpha emitters were applied by the three laboratories. All three test procedures were validated using a synthetic water matrix spiked with different radionuclides and gross alpha activity values were calculated with different alpha emitting radionuclide standard counting efficiencies to see which standard was the best for gross alpha activity determinations (CSN, 2011).

Sample collection

A total of eight natural waters from different parts of Spain (Fig. 1), with differing radioactive levels, and with a wide range of dissolved solids, were analysed.

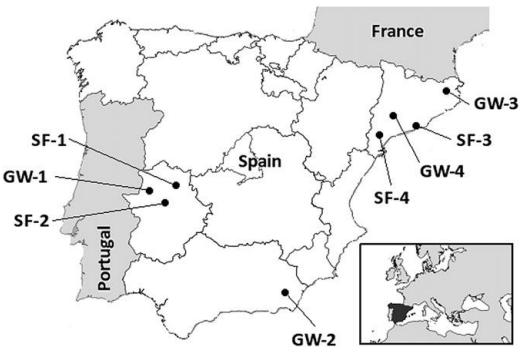

Fig. 1. Sampling sites in Spain.

Table 1
Summary of the types, dry residue, conductivity, original pH, sulphate amount and reservoir geology of waters studied.

Sample Code	*Type of water*	*Residue (g/L)*	*Conductivity (mS/cm)*	*Original pH*	*Sulphate (mg/L)*	*Reservoir geology*
GW-1	Groundwater	1	1.225	7.2	79	Granitic
GW-2	Groundwater	0.5	0.700	7.0	51	Gypsum-bearing
GW-3	Groundwater	4.7	1.295	7.1	32	Basaltic
GW-4	Groundwater	2.1	2.145	7.1	458	Old lignite mines
SF-1	Surface	1.5	1.318	7.8	116	Detrital
SF-2	Surface	0.4	0.214	7.7	22	Detrital
SF-3	Surface	0.9	1.896	7.7	73	Detrital
SF-4	Surface	0.7	0.415	7.8	113	Calcareous

Table 1 lists the type of water, residue, conductivity, original pH, sulfates and the reservoir geology of the waters studied. A volume of 100 L of water was taken at each sampling point. To preserve the water samples, they were acidified with HNO3 (1.25 mL/L). The origins of four samples were surface waters (SF), while the other samples were groundwater (GW). All the samples were treated water except GW-4 which was raw water.

Gross alpha activity methods

Evaporation method

The procedure used (CSN, 2011) allows the simultaneously determination of the gross alpha and beta activity. This procedure is similar to the standard method (UNE 73311-4:2002) widely used in Spain for determining the gross beta activity in non-saline water that is basically the same as the EPA 900.0 method (EPA, 1980) with a few modifications to improve the distribution of salt residues on the stainless steel planchets and to reduce the variability associated with the preparation of mass efficiency curves. The basis of this method is firstly a mild reducing evaporation of a given volume of water sample. Subsequently, when the volume has been reduced to about 5-8 mL, the sample is transferred to a stainless steel planchet of 4.7 cm diameter and oven-dried at 105 °C. The optimal mass density of the residue for determining the gross alpha activity is 5 mg/cm^2. To improve the uniformity of evaporated water residues, the polished bottoms of the planchets were roughened using a 37% HCl treatment. Both the steel planchet and the deposit are weighed and stored in a desiccator. Finally, the sample is measured in a gas flow proportional counter (Berthold LB770). Measurements were performed after two days but within a maximum of five days to minimise ingrowth of ^{224}Ra and to prevent a significant increase in alpha counting due to ^{226}Ra progeny). For the con-

struction of a mass efficiency curve, a solution spiked with ^{230}Th was prepared.

The range of the surface density that we covered in the mass efficiency was within 1.5 and 10 mg/cm^2.

Co-precipitation method

This sample preparation technique incorporates both an EPA approved methodology (EPA, 1984) and the method proposed by Suarez Navarro et al. (2002) for gross alpha determination, together with a few improvements in order to provide details that are relevant for achieving good reproducibility (CSN, 2011).

A 500 mL water sample, usually preserved with HNO_3, was neutralized with 6N NH_4OH. 20 mL of 2N H_2SO_4 and a magnetic stir bar were then added to each sample. The sample was stirred and heated to boiling for 5 min to purge radon and CO_2. The sample was then cooled to 50 °C and 1 mL of Ba^{2+} carrier was added to the sample while it was stirred. The barium-radium sulphate precipitate formed was stirred for 30 min at 50 °C in order to obtain optimum precipitate formation (Suarez Navarro et al., 2002). To coprecipitate the actinides, 1 mL of Fe^{3+} carrier was added to the solution and 6N NH_4OH was added in drops until the precipitate was produced.

Bromocresol purple indicator was used to control the pH of the precipitation (about 7 ± 0.5). It was continuously stirred without heating for 30 min. Finally, the combined precipitates were cooled to room temperature, filtered and collected onto a pre-weighed 0.45 mm pore size filter of cellulose nitrate using a vacuum filtration system. At this point, it is important to consider that a good filtration takes at least about 10 min to ensure that the precipitate is collected perfectly by removing the maximum amount of water and to avoid losing precipitate. Afterwards, the filter with the precipitate was placed on a stainless steel planchet, secured with a retaining ring and dried in the heater at 105 °C for 1 h. Finally, the planchet was then cooled to room temperature inside a desiccator for 15 min, weighed and then counted in a ZnS(Ag) scintillation detector, using a thin plastic screen of ZnS(Ag) placed on the planchet, or directly in a gas flow proportional counter (Berthold LB770). It is recommended that alpha counting should be delayed two days (CSN, 2011). Using a ^{230}Th standard, the alpha detection efficiencies were determined and an appropriate masse efficiency curve was derived for this standard as an alpha-calibration source (Montaña et al., 2012).

Total evaporation/LSC method

A 100-mL aliquot of a water sample was evaporated to dryness. When the precipitate obtained was cooled to room temperature, it was then dissolved in 10 mL

of deionized water acidified by HCl to pH = 1.5. Some samples with a high salt content needed more acidic solution to be completely dissolved. The solution was then stirred for 5 min in order to ensure that the entire residue was dissolved. With this treatment ^{222}Rn and all its short-lived decay daughters were eliminated in the sample. An 8-mL aliquot of the evaporated sample was mixed with 12 mL of the scintillation cocktail Ultima Gold AB (Perkin Elmer Life Science, Boston, MA, USA) in a low diffusion scintillator vial. Under these conditions the sample remained homogenous and chemically stable for some months. The vial was counted in a liquid scintillation counter which could discriminate between alpha and beta pulses (Wallac 1220 Quantulus, Perkin Elmer Life Science, Boston, MA, USA). It is recommended that the vial should remain within the counter for 2 h before the start of counting in order to prevent photoluminescence phenomena (L'Annunziata, 1998). Furthermore, this time is necessary for the short-lived ^{222}Rn daughters to decay. To find the appropriate calibration standard, many alpha emitters such as (^{230}Th, ^{236}U, ^{241}Am) and some beta emitters (^{40}K, ^{137}Cs, ^{90}Sr/Y) were used to carry out a misclassification study (Zapata-García et al., 2012). The Pulse Shape Analyzer (PSA) level was optimized using ^{236}U and ^{40}K calibration standards as they showed the best performance in the misclassification study and an optimized value of 100 was obtained. The alpha window was set from channel 500 to 800; the beta window from 250 to 1024. See CSN (2011) for more details.

Radiochemical procedures for specific alpha emitter determinations

Below there is a description of the different procedures applied by the laboratories.

Uranium and thorium

Procedure 1. To determine the uranium and thorium content in the water samples, ^{232}U/^{228}Th in secular equilibrium or ^{229}Th were added as tracers. The uranium and thorium content was then co-precipitated with $Fe(OH)_3$. The precipitate was dissolved and separated in a Dowex resin AG1X8. The uranium and thorium were retained in the column and subsequently eluted. A detailed description of the experimental procedure has been reported in Vallés (1994). Finally, the alpha sources were prepared by co-precipitation with NdF_3 (Sill, 1987) or were electrodeposited onto stainless steel planchets (Hallstadius, 1984).

Procedure 2. ^{232}U/^{228}Th in secular equilibrium was added initially for recovery control of the process. The separation scheme consisted of the evaporation of samples to dryness and further dissolution in 5 mL of 3M HNO_3-0.5M $Al(NO_3)_3$.

Sample solutions were then transferred to the UTEVA column and eluted (Horwitz et al., 1992). Eluted solutions were evaporated to dryness for coprecipitation of the radionuclides as fluorides. Co-precipitation of Th was done in the presence of Nd and nitric media (Horwitz et al., 1993), while U was co-precipitated in the presence of Ce and hydrochloric media (Horwitz et al., 1992).

Radium

Procedure 1. The radium content in the water was absorbed in MnO_2 precipitate. ^{133}Ba was added as a tracer. The precipitate was then dissolved in 5M HNO_3, and the uranium and thorium present in the samples was extracted with TBP (tributyl phosphate). Finally, the radium was co-precipitated as $Ba(Ra)SO_4$ (Baeza et al., 1998). Recovery was determined by γ-spectrometry of ^{133}Ba and ^{226}Ra by alpha spectrometry.

Procedure 2. Radium isotopes (^{226}Ra and ^{224}Ra) were determined by co-precipitation from a 1-L sample with barium and lead carriers adding 9M H_2SO_4. The solution was then purified by barium sulphate precipitation at pH 5-5.3 in the presence of EDTA.

A detailed description of the procedure has been reported in Vallés (1994). Both ^{226}Ra and ^{224}Ra activities were measured using a ZnS(Ag) scintillation counter by measuring the planchets at two and twenty-one days after radium separation.

Polonium

2.3.3.1. Procedure 1. In the determination of ^{210}Po content, ^{208}Po was used as a tracer. The polonium content was co-precipitated with $Fe(OH)_3$. The precipitate was then dissolved in 8M HCl and diluted to 1.5M HCl. The polonium was deposited onto silver planchets and measured by alpha spectrometry (Bolívar et al., 2002).

Procedure 2. ^{210}Po was determined by spontaneous deposition onto a silver planchet. ^{209}Po was used as a tracer. The water sample was previously concentrated by evaporation at 90 °C to a volume of 25 mL. The solution was transferred to a 40 mL Teflon cell, and 5 mL of 20% hydrochloride hydroxylamine, 2 mL of 25% sodium citrate and 1 mL of Bi^{+3} carrier were added and stirred.

Finally, the polonium was deposited for 3 h at a temperature of 90-95 °C, with agitation of the solution (Vallés, 1994).

Alpha spectrometry

Uranium isotope activities (^{234}U, ^{235}U and ^{238}U), ^{232}Th, ^{210}Po and ^{226}Ra (procedure 1) were determined by alpha spectrometry using PIPS detectors with a 450 mm2 active area (Canberra). The detectors were energy-calibrated using a NIST traceable mixed standard alpha source containing ^{239}Pu, ^{241}Am and ^{244}Cm. The energy slope of the spectrum was about 1.5 keV per channel, and the region of

observation selected was from 4 to 8 MeV. The counting efficiency of the detectors was between 18 and 30%. The activity concentration was calculated using Genie 2000 software. The samples were generally measured about 5 mm from the detectors and during 250,000 s in order to achieve adequate minimum detectable activities (MDA) of 0.1 mBq/L (U), 0.1 mBq/L (Th), 0.4 mBq/L (Po), 0.9 mBq/L (Ra). 2.4. Temporal evolution of gross alpha activity The temporal evolution in gross alpha activity for the 8 natural waters was studied to evaluate the influence of elapsed time from sample preparation to measurement in the gross alpha results. Different measurements, between 0 and 30 days, were performed for each method studied.

ANOVA and "t" tests

A One-factor ANOVA test was applied to determine if there were significant differences in the results provided by the three methods. The variance of each method was compared to the global variance for the seven natural waters which had gross alpha activities higher than the MDA. The study was carried out considering three replicates of the analysis for each method and a confidence level of 95%.

A t-test was applied comparing the results of each of the studied methods with the TAAC in order to find the cause of differences found with the ANOVA test. This test was done for three replicated (evaporation and total evaporation/LSC) and four replicated (coprecipitation) samples.

Results and discussion

Activity concentration of alpha emitting radionuclides

The results of the activity concentration of specific alpha emitters in the waters are given in Table 2. TAAC was calculated by summing the quantified specific alpha emitter activity. If the activity was lower than the minimum detectable activity, this value was not used to calculate TAAC. Activities were expressed in mBq/L because of the very low values for some radionuclides.

According to the results presented in Table 2, groundwater showed higher TAAC than surface waters. In fact, all the studied groundwater presented gross alpha activities above the screening level of 100 mBq/L, while only one of the four studied surface waters exceeded this value. The activity concentration (mBq/L) of ^{234}U, ^{235}U and ^{238}U in the natural waters varied from 18 to 2900, from <1 to 90 and from 8 to 3000, respectively.

Table 2
^{238}U, ^{235}U, ^{234}U, ^{232}Th, ^{226}Ra, ^{224}Ra, ^{210}Po activity concentrations (mBq/L) in the 8 natural waters.

Alpha activity concentration (mBq/L)								
Code	*^{238}U[a]*	*^{235}U[a]*	*^{234}U[a]*	*^{232}Th[a]*	*^{226}Ra[a]*	*^{224}Ra[a]*	*^{210}Po[a]*	*Total alpha activity concentration (Σ isotopes)[b]*
GW-1	240 ± 20	10 ± 3	1330 ± 90	<5	470 ± 60	80 ± 20	36 ± 4	2200 ± 200
GW-2	370 ± 20	13 ± 6	390 ± 60	<8	550 ± 40	40 ± 10	28 ± 3	1400 ± 200
GW-3	8 ± 4	<1	18 ± 5	<9	210 ± 20	27 ± 6	0.6 ± 0.4	260 ± 40
GW-4	3000 ± 200	90 ± 20	2900 ± 200	<10	130 ± 10	17 ± 4	110 ± 10	6200 ± 600
SF-1	70 ± 10	<2	90 ± 10	9 ± 5	5 ± 1	<2	<0.3	170 ± 30
SF-2	11 ± 5	<3	21 ± 6	8 ± 5	2.3 ± 0.4	<1	1 ± 0.3	40 ± 10
SF-3	20 ± 5	<2	34 ± 6	<5	4.0 ± 0.8	<2	0.8 ± 0.4	60 ± 15
SF-4	34 ± 8	<2	48 ± 9	<5	2.6 ± 0.7	<2	1.2 ± 0.5	90 ± 20

[a] The overall uncertainty (coverage factor k = 2) was given as the average uncertainty of individual results, corresponding to three replicates by the three laboratories for each sample. This arose mainly from counting uncertainty.

[b] Uncertainty of Alpha Total activity was given as the combined uncertainty of the average uncertainty of each isotope, with a coverage factor k =2, corresponding to a level of confidence of 95%.

The high activity concentration of uranium observed in the GW-4 sample was due to the rock present in the reservoir which was mainly lignite containing elevated levels of uranium. The arithmetical mean of the ^{234}U/^{238}U activity ratio for all samples resulted in 2.0 ± 1.5 (relative standard deviation, RSD = 73%) thus confirming a different disequilibrium in the samples studied. The fact that ^{226}Ra concentration in groundwater was higher than in surface water was also observed. The minimum ^{226}Ra activity concentration was 2.3 mBq/L (SF-2) and the maximum value was 550 mBq/L (GW-2). Significant activity concentration of ^{224}Ra was also measured in the four selected groundwater samples. ^{210}Po activity concentration was determined for most of the samples, but its contribution to Alpha Total was below 2.5%. The minimum activity concentration of ^{210}Po was 0.6 mBq/L and the maximum activity concentration was 110 mBq/L (GW-4). Contribution of ^{232}Th was insignificant due to its low solubility in water and it was not detected in most of the studied waters. Uranium and radium isotopes are the main contributors to the TAAC in these samples and produced more than 90% of the activity. Uranium isotopes (^{238}U+^{234}U) were usually present to a higher percentage (more than 70%) compared with ^{226}Ra (usually less than 20%). The exceptions were GW-2 and GW-3 with 40% and 80% of ^{226}Ra, respectively. 3.2. Temporal evolution of gross alpha activity By way of example,

Fig. 2 shows the gross alpha activities measured repeatedly for up to one month for water sample GW-3 (80% ^{226}Ra) using evaporation, co-precipitation and total evaporation/ LSC methods. Some results for the different preparation techniques at different times are missing from the graph since no measurement was performed at those times. In Fig. 2, as might be expected for samples with ^{226}Ra, it is clear that gross alpha activity varies with time and therefore can be overestimated depending on the method chosen and the time elapsed.

Evaporation showed the highest gross alpha activities in the temporal study, for example 800 mBq/L, while co-precipitation reached 660 mBq/L and total evaporation/LSC reached 540 mBq/L after 21 days of elapsed time.

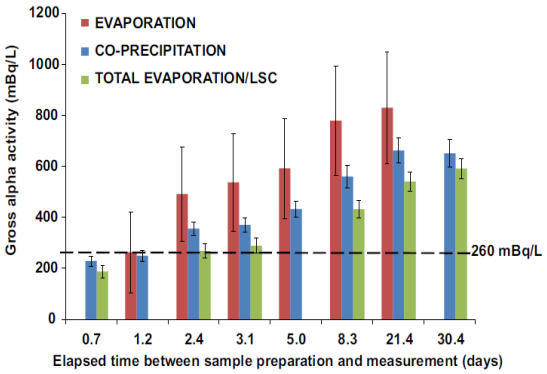

Fig. 2. Temporal evolution of gross alpha activity in the GW-3 sample by evaporation, co-precipitation and total evaporation/LSC methods. The dashed line is the TAAC in the sample. The error bars represent the overall uncertainty (coverage factor k = 2).

The ratio calculated by dividing the measured gross alpha activity and the Alpha Total activity ranged from 1.0 to 3.2 for evaporation, from 0.9 to 2.6 for co-precipitation and from 0.7 to 2.1 for total evaporation/LSC (elapsed time between 1 and 21 days). According to these results, evaporation overestimated gross alpha activity, more than did co-precipitation or total evaporation/LSC, in waters with ^{226}Ra as the main contributor (80%) to Alpha Total. It should be noted that evaporation also shows greater variability in the results. The recommendation to measure samples prepared by the evaporation and co-precipitation methods after two days of their preparation does not provide satisfactory results for sample GW-3. But it is important to consider three points. First; using ^{230}Th as a calibration standard for samples with significant amounts of ^{226}Ra will tend to overestimate gross alpha activity because ^{226}Ra and its daughters emit higher energy alpha particles than does ^{230}Th. On the other hand, samples containing ^{226}Ra can be measured immediately after preparation, but this recommendation carries some drawbacks under routine laboratory work. Finally, in a previous investigation (CSN, 2011) it was observed that natural waters in Spain with non-negligible ^{226}Ra content are unusual. Therefore, the initial recommendations are suitable for most natural waters in Spain.

Table 3 shows some statistical parameters (arithmetic mean, relative standard deviation, minimum and maximum values and the number of data) for gross alpha activity using the evaporation, co-precipitation and total evaporation/LSC methods in the temporal evolution study (0-30 days) in the eight selected waters. Uncertainty corresponds to average uncertainty for individual measurements which mainly arises from counting statistics, and RSD gives information about temporal variation in the measured activity. Both parameters are compared and if no differences between them are found, no gross alpha activity variations occur over time. However, this time should be considered as an important factor that needs to be defined. High uncertainties are associated with low activities (SF-2 or SF-3) with values near the MDA. The evaporation method shows a higher uncertainty than the co-precipitation and total evaporation/ LSC methods. On the other hand, RSDs for radioactivity in groundwaters from the three methods were usually higher than the mean uncertainty.

Table 3
Average of gross alpha activity (mBq/L) obtained at different elapsed times and statistical parameters for the three methods.

Sample code	Statistical parameters	Evaporation	Co-precipitation	Total evaporation/LSC
GW-1	Mean (uncertainty[a])	2006 (± 10%)	2451 (± 8%)	2300 (± 4%)
	Range (min-max)	(1432 - 2842)	(1935 - 3259)	(1800 - 2900)
	RSD (data)	20% (37)	16% (55)	36% (9)
GW-2	Mean (uncertainty[a])	918 (± 10%)	2144 (± 5%)	1700 (± 5%)
	Range (min-max)	(643 - 1161)	(1249 - 2805)	(1200 - 2400)
	RSD (data)	14%(45)	21% (78)	47% (9)
GW-3	Mean (uncertainty[a])	665 (± 29%)	550 (± 8%)	427 (± 8)
	Range (min-max)	(247 - 1929)	(229 - 1070)	(194 - 678)
	RSD (data)	42% (42)	35% (62)	34% (12)
GW-4	Mean (uncertainty[a])	3836 (± 8%)	5374 (± 8%)	6400 (± 5%)
	Range (min-max)	(3111 - 4457)	(4562 - 6113)	(6100 - 6700)
	RSD (data)	8% (29)	7% (56)	19% (6)
SF-1	Mean (uncertainty[a])	106 (± 10%)	151 (± 9%)	178 (± 16%)
	Range (min-max)	(63 - 140)	(126 - 175)	(123 - 223)
	RSD (data)	22% (17)	8% (55)	3% (6)
SF-2	Mean (uncertainty[a])	12 (± 60%)	7 (± 28%)	<MDA
	Range (min-max)	(<1 - 48)	(3 - 18)	-
	RSD (data)	112% (26)	58% (52)	-
SF-3	Mean (uncertainty[a])	33(± 132%)	51 (± 12%)	40 (± 50%)
	Range (min-max)	(<3 - 81)	(44 - 79)	(0 - 70)
	RSD (data)	56% (29)	17% (49)	2% (6)
SF-4	Mean (uncertainty[a])	59 (± 64%)	87 (± 10%)	100 (± 20%)
	Range (min-max)	(26 - 87)	(49 - 113)	(70 - 130)
	RSD (data)	32% (29)	22% (69)	2% (6)

The number of data used in calculation is indicated in brackets.
[a] All data average uncertainty k = 2.

Table 4
Gross alpha activity obtained for each method in mBq/L. The mean value obtained among the three methods is also presented.

Code	*Evaporation*			*Co-precipitation*			*Total evaporation/LSC*			*Average activity among methods*		
	Act.	*Unc.[a]*	*RSD(%)*	*Act.*	*Unc.[a]*	*RSD(%)*	*Act.*	*Unc.[a]*	*RSD(%)*	*Act*	*Unc.[b]*	*RSD(%)*
GW-1	1860	460	17(3)	2235	193	8(4)	1970	70	9(3)	2020	190	9
GW-2	1120	280	28(3)	1604	134	9(4)	1320	60	6(3)	1350	243	18
GW-3	380	200	20(3)	321	30	11(4)	210	30	9(3)	310	90	29
GW-4	3780	920	8(3)	5591	295	15(4)	6830	250	2(3)	5170	1278	25
SF-1	150	70	17(3)	144	13	9(4)	180	30	5(3)	160	20	13
SF-2	<MDA			<MDA								
SF-3	60	40	5(3)	52	7	18(4)	30	20	55(3)	50	16	33
SF-4	60	40	16(3)	76	9	25(4)	100	20	26(3)	80	18	23

The number of data used in each calculation is indicated in brackets.
[a] Uncertainty is given as average uncertainty, corresponding to three replicates for each sample which arises mainly from counting uncertainty
[b] Uncertainty is given as a standard deviation, corresponding to the three methods.

One characteristic of studied groundwater is the presence of significant ^{226}Ra activities. Ingrowth of ^{226}Ra daughters means that elapsed time has an influence on count rate and ideally would require measurements to be carried out as soon as possible. However, one must decide on a compromise between the theoretically ideal time and each laboratory's work routine. Consequently, to limit the variability associated with the elapsed time after source preparation, an optimal range for measurement delay should be established. It is recommended that the elapsed time for the evaporation and co-precipitation methods be after 2 days and before a maximum of 5 days. The differences between the values for the same sample obtained at two and five days (Fig. 2) were calculated and found to be 21% for both methods. This value is less than the threshold reference value of 50% for gross alpha derived from the IAEA-CU-2010-03 world-wide open proficiency test on the determination of natural radionuclides in water and ^{226}Ra in soil (IAEA, 2010). Additionally, if there is a non-negligible presence of ^{226}Ra in samples with activities around 0.1 Bq/L, not enough time has passed for its descendants to significantly increase the gross alpha count rate in that maximum elapsed time proposed. By contrast, for the total evaporation/LSC method, recommending a maximum is not necessary since a spectral output with the ^{214}Po signal can be used to assess the ^{226}Ra contribution. A large variation in gross alpha activity (RSD) was also observed for sample SF-2 which had detectable activity at or slightly above the MDA.

Gross alpha activity (two days or 2 h values after preparation): comparative study among methods

Table 4 shows the data for the eight waters studied and presents a comparison among gross alpha activities measured by the three methods. Additionally, the average activity among the three meth-

ods is given. As the optimal elapsed time between sample preparation and measurement is different for each method, the gross alpha activity after two days of measurement for evaporation and co-precipitation and after 2 h for total evaporation/LSC are presented in order to compare results among these methods. RSD between methods was less than 30% with the exception of sample SF-3, whose gross alpha activity is near the minimum detectable activity for the total evaporation/LSC method. In order to test if this deviation entails a no significant variation, an ANOVA test was applied.

ANOVA results

In order to test statistically whether there was significant variability among the three methods, an ANOVA test was applied to the results from the eight natural water samples. SF-2 was excluded because its activity was below the MDA for all three methods. This test was applied to the data obtained at the optimal elapsed time for each method (two days for evaporation and co-precipitation and 2 h for total evaporation/LSC). The conclusions derived from this test involve only the methods when the measure is performed at this optimal elapsed time. The ANOVA results are presented in Table 5.

For five of the seven water samples tested there were no significant differences among the three studied methods. There were significant differences among methods for samples SF-3 and GW-4. In order to find the cause of these differences a t-test was applied comparing the results of each of the studied methods with the TAAC. This test was done for three replicated (evaporation and total evaporation/LSC) and four replicated (co-precipitation) samples.

Table 6 showed the t-test results. In general, for all water samples, the results obtained for the studied method (evaporation, co-precipitation or total evaporation/LSC) were not significantly different for alpha spectrometry determination. This finding is concordant with the ANOVA test results.

Table 5
ANOVA test results for comparison of gross alpha activity determination methods in natural water samples.

Sample code	*Fcal*	*F'*	*Differences between methods*	*Degrees of freedom*
SF-1	2.95	4.75	No diff.	9
SF-2	-	-	-	-
SF-3	4.85	4.75	Sig. diff.	9
SF-4	4.55	5.41	No diff.	8
GW-1	1.60	4.75	No diff.	9
GW-2	4.10	4.75	No diff.	9
GW-3	5.78	6.59	No diff.	7
GW-4	17.38	4.75	Sig. diff.	9

Fcal: Calculated value from the F distribution.
F': 0.05 critical value from the F distribution (evaporation and concentration 3 degrees of freedom, co-precipitation 4 degrees of freedom.

Table 6
T test between each sample for each method and the alpha spectrometry results.

Sample code	*Evaporation*			*Co-precipitation*			*Total evaporation/LSC*		
	t_{cal}	t'	*Equal to α spect.*	t_{cal}	t'	*Equal to α spect.*	t_{cal}	t'	*Equal to α spect.*
GW-1	1.407	3.182	Equal	0.508	4.715	Equal	1.133	3.182	Equal
GW-2	1.267	3.182	Equal	1.525	4.527	Equal	0.606	3.182	Equal
GW-3	2.102	3.182	Equal	1.368	4.551	Equal	1.778	3.182	Equal
GW-4	6.457	3.182	Sig. diff.	1.034	4.337	Equal	0.167	3.182	Equal
SF-1	1.615	3.182	Equal	2.357	4.724	Equal	0.223	3.182	Equal
SF-2	-	-		-	-		-	-	
SF-3	0.226	3.182	Equal	0.734	4.603	Equal	1.954	3.182	Equal
SF-4	2.468	3.182	Equal	1.659	4.773	Equal	0.044	3.182	Equal

tcal: Calculated value from the t distribution
t': 0.05 critical value from the t distribution (evaporation and concentration 3 degrees of freedom ,co-precipitation 4 degrees of freedom.

However, there were differences between the evaporation method and the alpha spectrometry determination for sample GW-4.This allows us to attribute to the evaporation method the significant differences detected between the three methods using the ANOVA test. The inability of the evaporation method to determine gross alpha activity in sample GW-4 was due to the high residue of the sample. A high saline content in the sample is a drawback for the evaporation method as it implies a high mass residue which increases autoabsorption. Moreover, the high sulphate content in sample GW-4 (unusual in natural waters in Spain) generated residues with an autoabsorption greater than that obtained with the nitrates matrix used in the calibration. This fact involves an underestimation of the gross alpha content. However, for sample SF-3 there were differences between methods but there were no differences between each method and the TAAC. This apparent contradiction could be justified on the basis of the MDA of the methods, since the evaporation/LSC method has a MDA one order of magnitude higher than the other two methods, and similar to the level of activity of sample SF-3. This means that the differences between methods were detected by the ANOVA test but in the comparison of each method with the TAAC, the high dispersion in the total evaporation/LSC method provides the non-significant result.

Precision and accuracy

A comparison of the gross alpha activity results, excluding SF-2, for each method and the TAAC was also reported as a bias (Fig. 3). Bias was calculated by the following equation:

$$Bias\ (\%) = \frac{Gross\ alpha - TAAC}{TAAC} \cdot 100$$

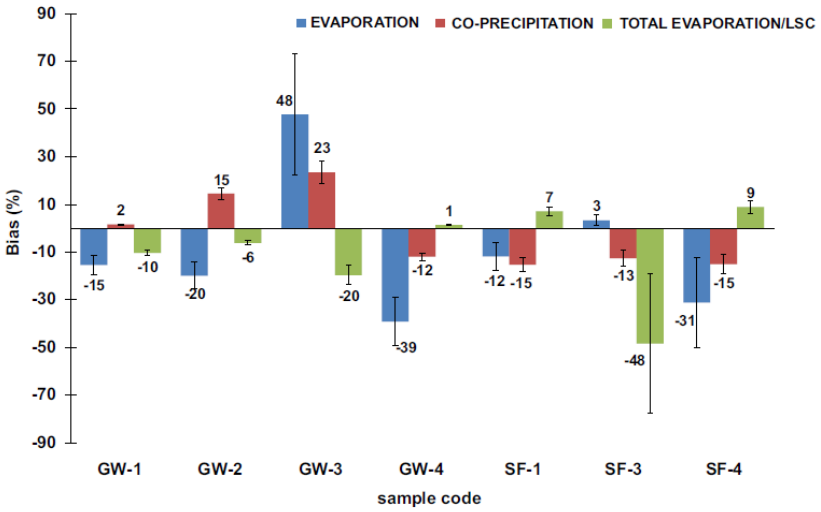

Fig. 3. Bias (%) obtained by the three methods (evaporation, co-precipitation and total evaporation/LSC) and the TAAC for the natural water samples studied. The error bars represent the overall uncertainty (coverage factor k = 2).

Total evaporation/LSC has usually the lowest bias (generally <10%) with the exception of GW-3 and SF-3. SF-3 presented gross alpha activity close to the MDA of this method. On the other hand, significant biases (positive) in the evaporation and co-precipitation methods were shown for sample GW-3 due to the significant contribution of ^{226}Ra, 80% of the TAAC. Results obtained for the other samples presented an acceptable bias (less than -20%) for the three methods. When the bias is greater than 20% it is due to low activity levels, as in samples SF-1, SF-3 and SF-4. Gross alpha activity determined by the evaporation method is often underestimated as a negative bias was obtained for most of the samples. Gross alpha activity determined by the co-precipitation method has a bias below 25% for all the samples irrespectively of the activity. Gross alpha activity determined by the total evaporation/LSC method and the TAAC were comparable when the samples contained significant activity.

Conclusions

Uranium and radium isotopes are the main contributors to TAAC in eight natural surface water and groundwater samples from different regions of Spain, each with different radioactive characteristics. Groundwater shows higher gross alpha activities than does surface waters. The comparison of results for gross alpha activity obtained by the three methods (evaporation, co-precipitation and total evaporation/LSC) show an acceptable deviation (RSD less than 30%). For practical uses, especially because radiological laboratories sometimes process a large number of samples in a small window of time, gross alpha measurements should

be carried out after two days and preferably before five days after sample preparation for the evaporation and co-precipitation methods in order to obtain results which are not largely overestimated, especially in waters in which the main contributor is ^{226}Ra. ANOVA tests were used to identify differences among evaporation, co-precipitation and total evaporation/LSC methods. For the samples with the most common radiochemical characteristics there were no significant differences among the three studied methods. However differences were detected for samples with a high saline content or with a very low activity level. Precision (as RSD) was below 28% for evaporation and below 18% for co-precipitation, while in the case of total evaporation/LSC it was below 10% for samples with TAAC above 0.1 Bq/L. The biases obtained by the evaporation, co-precipitation, and total evaporation/LSC methods were lower than 40%, 25% and 20%, respectively.

Acknowledgements

The present work was made possible by finance from the Spanish "Consejo de Seguridad Nuclear" under the project "Estudio de la problemática existente en la determinación del índice de actividad alfa total en aguas potables. Propuesta de procedimientos".

References

Ardnt, M.F., 2010. Evaluation of Gross Alpha and Uranium Measurements for MCL Compliance. Water Research Foundation. ASTM, American Society for Testing and Materials, 1996. Standard Test Methods for Alpha Particle Radioactivity of Water. Method: D1. 943-996.

Baeza, A., del Río, L.M., Jiménez, A., 1998. Procedure for simultaneous determination of ^{223,224,226,228}Ra by Alpha and Gamma Spectrometry. Radiochimica Acta 83, 53-60.

Bolívar, J.P., García-Tenorio, R., Mas, J.L., Vaca, F., 2002. Radioactive impact in sediments from an estuarine system affected by industrial wastes releases. Environ. Int. 27 (8), 639-645.

CSN (Consejo de Seguridad Nuclear), 2011. Es Acuerdo específico de colaboración entre el consejo de seguridad nuclear y la universidad de Extremadura para el estudio de la problemática existente en la determinación del índice de actividad alfa total en aguas potables. Propuesta de procedimientos. 10 Noviembre de 2011. Internal report (in Spanish).

EC, December 1998. Council directive 98/83/EC of 3 November 1998 on the quality of water intended for human consumption. Off. J. Eur. Communities. L 330/32.

EPA (Environmental Protection Agency) 600/4-80-032, 1980. Prescribed Procedures for Measurement of Radioactivity in Drinking Water. In: Gross Alpha and Gross Beta Radioactivity in Drinking Water, Method 900.0. Environmental Protection Agency.

EPA (Environmental Protection Agency) 520/5-84-006, 1984. Radiochemical determination of gross alpha activity in drinkingwater by co-precipitation, method 00- 02. In: Radiochemistry Procedures Manual, Eastern Environmental, Radiation Facility. Environmental Protection Agency. Modified in August 1987.

Hallstadius, L., 1984. A method for the electrodeposition of actinides. Nucl. Instruments Methods Nucl. Res. 223, 266e267.

Horwitz, E.P., Chiarizia, R., Dietz, M.L., Diamond, H., 1992. Separation and preconcentration of uranium from acidic media by extraction chromatography. Analytica Chim. Acta 266, 25e37.

Horwitz, E.P., Chiarizia, R., Dietz, M.L., Diamond, H., 1993. Separation and preconcentration of actinides from acidic media by extraction chromatography. Analytica Chim. Acta 281, 361e372.

IAEA-CU-2010-03, 2010.World-wide Open Proficiency Test on the Determination of Natural Radionuclides in Water and Ra-226 in Soil. http://nucleus.iaea.org/rpst/.

ISO/IEC 17025, 2005. General Requirements for the Competence of Testing and Calibration Laboratories.

Jobbágy, V., Wätjen, U., Mere_sova, J., 2010. Current status of gross alpha/beta activity analysis in water samples: a short overview of methods. J. Radioanalytical Nucl. Chem. 286, 393-399.

L'Annunziata, M., 1998. Handbook of Radioactivity Analysis. Academic Press, San Diego.

Montaña, M., Camacho, A., Serrano, I., Vallés, I., 2012. Experimental analysis of the mass efficiency curve for gross alpha activity and morphological study of the residue obtained by the

co-precipitation method. Appl. Radiat. Isot. 70, 1541-1548.

Oural, C.R., Upchurch, S.B., Brooker, H.R., 1988. Radon progeny as sources of gross-alpha radioactivity anomalies in ground water. Health Phys. 55 (6), 889-894.

Parsa, B., 1998. Contribution of short-lived radionuclides to alpha-particle radioactivity in drinking water and their impact on the safe drinking water act regulations. Radioact. Radiochem. 9, 41e50.

Parsa, B., Nemeth,W.K., Obed, R.N., 2000. The role of radon progenies in influencing gross alpha-particle determination in drinking water. Radioact. Radiochem. 11, 11-22.

RD (Real Decreto) 140/2003, esde 7 de febrero, por el que se establece los criterios sanitarios de la calidad del agua de consumo humano, Boletin Oficial del Estado (Official Bulletin of Government) 21 de Febrero del 2003, 7228.

Sill, C.W., 1987. Precipitation of actinides as fluorides or hydroxides for highresolution alpha spectrometry. Nucl. Chem. Waste Manage. 7 (3e4), 201e215.

Suarez Navarro, J.A., Pujol, Ll., de Pablo, M.A., 2002. Rapid determination of gross alpha-activity in sea water by co-precipitation. J. Radioanalytical Nucl. Chem. 253 (1), 47-52.

Semkow, T.M., Parekh, P.P., 2001. Principles of gross alpha and beta radioactivity detection in water. Health Phys. 81, 567-574.

(Spanish standard) UNE 73311-4:2002, 2002. Determination of the Total Beta Activity Index in Water by Means of a Proportional Meter.

UNSCEAR, United nations Scientific Committee on Effects of Atomic Radiation (UNSCEAR), 2000. Sources and Effects of Ionizing Radiation. United Nations, New York.

Vallés, I. 1994. Development of the Analytical Procedures to Measure the radioactivity in waters and its application to drinking water. Doctoral thesis. Barcelona, Spain: University of Barcelona., pp. 52-84 (in Spanish).

World Health Organization, 2011. Chapter 9: radiological aspects. In: Guidelines for Drinking-water Quality, fourth ed.. Geneva, isbn, 978-92-154815-1.

Zapata-García, D., Llauradó, M., Rauret, G., 2012. The implications of particle energy and acidic media on gross alpha and gross beta determination using liquid scintillation. Appl. Radiat. Isotope. 70, 705-711.

4.3. Discussion

Give the results obtained in the two scientific papers of this chapter, it must be emphasized that the development and validation of an analytical procedure for simultaneous determination of gross alpha and gross beta activity has been described. Furthermore, an estimation of ^{226}Ra activity is also made by means of a second measurement of the sample considering the increase of alpha activity due to the ingrowth of ^{222}Rn and its short-lived daughters. This methodology has been validated and compared with other classical techniques for the determination of gross alpha activity—such as evaporation and co-precipitation methods with subsequent measurement by solid scintillation with ZnS or proportional counter.

The developed procedure involves evaporating an aliquot of 100 mL of the sample to dryness. When the precipitate obtained is cooled at room temperature, it is dissolved in 10 mL of deionised water acidified by HCl to pH 1.5. An aliquot of 8 mL of the concentrated sample is then mixed with 12 mL of the scintillation cocktail (Ultima Gold AB) in low-diffusion polyethylene vials. After 2 hours of waiting for photoluminescence decay, the sample is measured in a Wallac QUANTULUS 1220 for 400 minutes by using the alpha beta counting mode. The instrumental parameter PSA (pulse shape analyser) used to separate the alpha and beta events is optimized by means of interference studies by using ^{236}U as a pure alpha emitter and ^{40}K as a pure beta emitter.

We have also developed a mathematical model to estimate the activity of ^{226}Ra from a second measurement of the counting vial within the 21 first days after sample treatment. This model also makes it possible to determine gross alpha activity without the contribution of ^{222}Rn and their short-lived decay products, as is indicated by the directive. The premises for the correct application of this model are as follows:

- All ^{222}Rn must been removed from the sample during treatment. Two hours must be allowed for the decay of alpha emitters and short-life daughters (^{218}Po, ^{214}Pb and ^{214}Po).
- The counting vial should be sealed in other to avoid ^{222}Rn release.
- The procedure can only be used to estimate ^{226}Ra samples that do not contain other radionuclides that may modify the alpha activity in the counting vial, like ^{228}Ra.

The increase of alpha activity over time after sample treatment was evaluated by using samples spiked with different contributions of gross alpha activity and with different proportions of ^{226}Ra activity concentration. Figure 6 shows the evolution of alpha activity over time for different spiked samples. Each experimental measurement is shown and the

error bars represent the counting uncertainty. The lines represent the proposed model for each spiked sample. Figure 6a shows the evolution of samples with a constant ^{226}Ra activity concentration and increasing gross alpha activity. Figure 6b shows that the samples contain a similar gross alpha activity and increasing ^{226}Ra activity concentration. The experimental data match the proposed model.

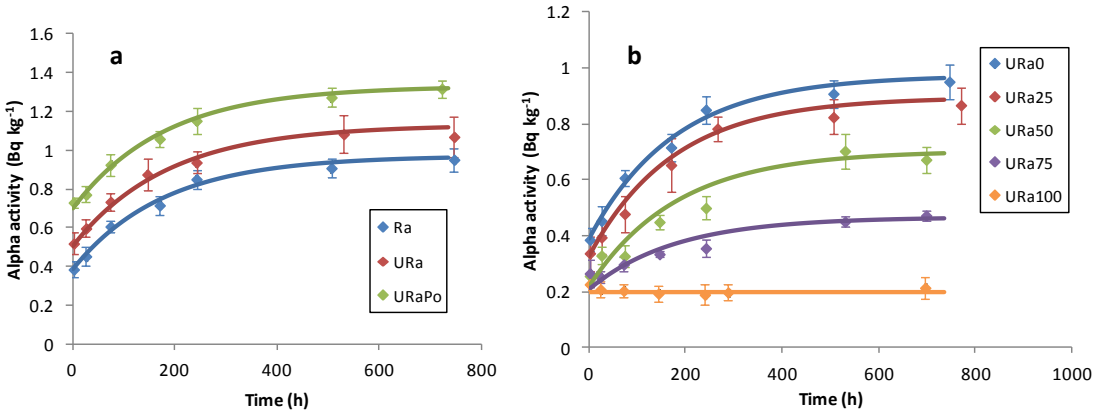

Figure 6. Evolution of alpha activity in samples with the same activity of ^{226}Ra and increasing gross alpha activities (a) and with similar gross alpha activities and an increasing activity concentration of ^{226}Ra.

The analytical procedure and mathematical model has been validated by using spiked samples with different proportions of gross alpha activity and ^{226}Ra. The detection limits were established as 0.025 Bq kg^{-1} and 0.095 Bq kg^{-1} for gross alpha and gross beta respectively.

Then, natural water samples were analysed by applying the proposed method, and the results were compared by selective procedures with alpha spectrometry measurements. Generally, the results obtained for gross alpha determination have a bias below 10 %. However one sample with an activity close the detection limit shows a higher bias.

Regarding ^{226}Ra, it was observed that samples with activity concentrations around 0.1 Bq kg^{-1} are determined with bias lower than 20 %, while the bias is unacceptable in samples that contain on the order of 10^{-3} Bq kg^{-1}.

This procedure has been compared with the procedure of evaporation and proportional counter measurement and the procedure of co-precipitation and solid scintillation measurement.

The procedure of evaporation and proportional counter measurement is based on the concentration of the sample to dryness on a stainless steel planchet. Due to the relatively

low power of penetration of alpha particles compared with beta particles, the amount of precipitate on the planchet should be lower (on the order of 5 mg cm^{-2}, while when gross beta is measured it can be 25 mg cm^{-2}), to reduce the self-absorption (USEPA, 1980; Llauradó et al., 2004; Llauradó et al., 2005).

In the co-precipitation procedure, barium and iron carriers are added to the sample and are subsequently precipitated as $BaSO_4$ and $Fe(OH)_3$ by adding basic media. Radium isotopes co-precipitate with $BaSO_4$, while other elements like actinides or polonium are absorbed into $Fe(OH)_3$. The precipitate is then filtered, dried and after that measured by solid scintillation with ZnS (Montaña et al., 2012).

A comparative study of the three methods was carried out based on the analysis of spiked samples with different alpha emitters and with natural samples characterized with total content of alpha emitters by alpha spectrometry.

The content of alpha emitters in natural samples was characterized by using radiochemical separations to determine specific radionuclides. The alpha emitters determined in the natural waters are: ^{238}U, ^{235}U, ^{234}U, ^{232}Th, ^{226}Ra, ^{224}Ra and ^{210}Po. From this small set of samples, it can be seen that more than 90 % of gross alpha activity is produced by the contribution of uranium and radium isotopes. Furthermore, uranium isotope contribution is the most important in 70 % of the cases while radium is most important in less than 20 %. This observation has been confirmed in larger datasets (Corbacho et al., 2016).

A t-test was used to determine whether there are significant differences between each method and the summation of activity concentration of all the specific alpha emitters for each sample. The result shows that just for one sample (GW-4) with a high salt content, the procedure of evaporation and measurement by proportional counter shows significant differences. This can be easily explained due to the high saline content, which is a drawback for the evaporation method as it implies a high mass residue which increases auto-absorption. Moreover, the high sulphate content on sample GW-4 has the consequence that the residue obtained causes a higher auto-absorption than the nitrate matrix used in the calibration, which entails an underestimation of gross alpha activity.

An ANOVA test for each sample was applied to determine whether there are significant differences among the studied methods. In general, no differences were observed except for sample GW-4 and SF-3. Regarding GW-4, the observed difference is caused by the autoabsorption issue of the evaporation method.

Regarding sample SF-3, an apparent contradiction is observed, because the result obtained for each method is not significantly different from the summation of alpha emitters. But the results differ among them. This can be explained on basis of the MDA of the methods, since a concentration method with LSS measurement has an MDA that is one order of magnitude higher than evaporation and co-precipitation methods and that is close to the activity of SF-3. For this reason, even the results obtained by the three methods have significant differences. The high variability of the LSS method for a sample close the MDA means that no differences can be observed between this value and the summation of alpha emitters.

5. VALIDATION OF RADIUM ISOTOPES DETERMINATION BY MEANS OF RADIUM RAD DISK

After the development and validation of simultaneous determination of gross alpha and gross beta activities, specific methodologies have to been developed in order to deal with radionuclides which progeny ingrown in short time after sample treatment. This chapter presents a methodology that entails a rapid radiochemical separation for the determination of ^{226}Ra, ^{228}Ra and ^{210}Pb using Radium RAD disk and direct LSS measurement.

On the direct measurement of ^{226}Ra and ^{228}Ra using 3M Empore™ RAD disk by liquid scintillation spectrometry. J. Fons-Castells, M. Vasile, H. Loots, M. Bruggeman, M. Llauradó, F. Verrezen. *Journal of Radioanalytical and Nuclear Chemistry* 309 (2016). pp. 1123-1131.

Methodologies that use RAD disk for radium isotopes determination are based on a selective extraction of Ra and a subsequent elution in order to measure by classical methods (emanation techniques for ^{226}Ra and gamma spectrometry via ^{228}Ac for ^{228}Ra) or by LSS. However, the solution for the elution of radium from the RAD disk is not always compatible with LSS cocktails. For this reason, and in order to simplify and streamline the method, a direct measurement of the RAD disk into counting vial has been evaluated. This paper is a feasibility study of the determination of ^{226}Ra and ^{228}Ra. It describes direct measurement of *3M Empore™* radium RAD disk.

Simultaneous determination of ^{226}Ra, ^{228}Ra and ^{210}Pb in drinking water using 3M Empore™ RAD disk by LSC-PLS. J. Fons-Castells, J. Oliva, J. Tent-Petrus, M. Llauradó. *Applied Radiation and Isotopes* 124 (2017). pp. 83-89.

Once the direct measurement of radium RAD disk was evaluated as a viable methodology for ^{226}Ra and ^{228}Ra determination, the problem of interference between ^{228}Ra and ^{210}Pb had to be solved. Both are low energy beta emitters with similar maximal energies (45.8 keV for ^{228}Ra and 63.5 keV for ^{210}Pb), which, due to the quenching caused by the RAD disk in the vial, cannot be decomboluted. This paper presents a procedure in which elution of ^{210}Pb from the RAD disk and PLS model are combined to simultaneously determine ^{226}Ra, ^{228}Ra and ^{210}Pb. Furthermore, the quantification of the spectra by means of multilinear calibration using PLS model was also used to improve the determination of ^{210}Pb.

5.1. On the direct measurement of ^{226}Ra and ^{228}Ra using 3M EMPORE™ RAD disk by liquid scintillation spectrometry

On the direct measurement of ^{226}Ra and ^{228}Ra using 3M Empore™ RAD disk by Liquid Scintillation Spectrometry

Fons-Castells J.[1*], Vasile M.[2], Loots H.[2], Bruggeman M.[2], Llauradó M.[1], Verrezen F.[2]

[1] Analytical Chemistry Department, University of Barcelona, Diagonal 647, 08028 Barcelona, Spain

[2] Belgian Nuclear Research Center SCK·CEN, Boeretang 200, B-2400 Mol, Belgium

*corresponding author: jordi.fons@ub.edu

Abstract

A study on the use of 3M Empore™ Radium RAD disk for the rapid and direct determination of ^{226}Ra and ^{228}Ra concentration in drinking water samples by means of liquid scintillation spectrometry is described. Three cocktails and several treatments were tested in order to improve the knowledge on the energy transfer between the alpha or beta – particle emissions of the isotopes fixed in the RAD disk and the cocktail. The sources of variability of this method were compared with the elution method, in which radium is stripped from de RAD disk and measured by liquid scintillation spectrometry using a Quantulus 1220™.

Keywords: RAD Disk, Solid Phase Extraction, ^{226}Ra, ^{228}Ra, ^{210}Pb, Rapid methods

Introduction

Determination of ^{226}Ra and ^{228}Ra is important from the point of view of environmental protection and radiation protection. Determination of radium isotopes is considered in a huge range of environmental studies related to NORM and TE-NORM (Technologically-Enhanced, Naturally-Occurring Radioactive Materials).

Since radium is a bone-seeking element, and ^{226}Ra and ^{228}Ra have high radiotoxicity, these nuclides are considered potential contributors to the human Indicative Dose (ID). As it can be found in UNSCEAR 2000 [1], drinking water is one of the major sources in human intake of radium. For this reason ^{226}Ra and ^{228}Ra are also included in the new European directive for drinking water [2] for which derived levels have been specified.

Solid Phase Extraction (SPE) is a widely used alternative to $BaSO_4$ co-precipitation methods [3,4] to pre-concentrate radium from aqueous solutions. SPE techniques commonly use chromatographic resins [5] or ionic exchange columns [6,7] in order to separate and concentrate radium. After that, radium isotopes can be measured by liquid scintillation spectrometry [6], alpha spectrometry [7,8] or gamma spectrometry [9]. However these methods are often time-consuming and may involve the use of large amounts of reagents. In the late '90s the RAD disk has been introduced as a very practical SPE method for the concentration of radium [10,11]. Radium RAD disks are available from vendors like 3M Empore™.

The radium RAD disks used in this study are circular 47 mm diameter filters composed by crown ether covalently bound to an inert substrate which selectively extracts Ra^{2+} from acid solutions [12]. These filters are used to extract and concentrate radium from aqueous samples. Detailed studies on the interfering elements in the extraction process were performed and reported by Scapitta and Miller in 1996 [10]. After filtration of the sample through the RAD disk, several procedures may be applied for the subsequent radioactivity determination of ^{226}Ra and ^{228}Ra. For ^{228}Ra it is recommended by the supplier [13] to store the filter for 14 to 28 days to allow for the decay of ^{224}Ra and its decay products that interfere the measurement. This time is enough to achieve the ingrowth of ^{228}Ac, and to subsequently elute ^{228}Ac to be counted by LSC or by a proportional counter. ^{226}Ra may be determined via ^{222}Rn by an emanation technique by elution with ethylene diamino tetraacetic acid (EDTA) and transferring in a radon bubbler [11]. However, methods that use radium RAD disk described in the literature commonly

involve the elution of radium with EDTA [14-18] or diammonium hydrogen citrate (DHC) [11,19] or both [20,21] and a subsequent measurement by LSC.

Scapitta and Miller [10] suggested the possibility of performing a direct measurement of the Radium RAD disk by liquid scintillation spectrometry transferring the filter directly inside a counting vial, adding scintillation cocktail and measuring it as such. This method is faster and reduces the use of reagents but may entail several problems that are not yet systematically reported. Seely and Osterheim in 1998 used a similar approach for strontium by direct measurement of the Strontium RAD disks by liquid scintillation spectrometry [22].

In this paper, different factors that hinder the direct measurement of the radium RAD disk by liquid scintillation spectrometry were studied with the aim to understand them and, if possible, to eliminate or minimise their effect. Additionally, some observations associated with the elution of radium isotopes from RAD disk with basic EDTA and the subsequent measurement by LSC are reported.

Experimental

Apparatus

All the measurement results that are reported here were performed with an ultra-low level liquid scintillation spectrometer Wallac Quantulus™ 1220 in alpha-beta separation mode and low coincidence bias. The counting time was 60 minutes for each sample and 1 minute for the SQP[E] (Spectral Quench Parameter of the External standard) determination. The target isotopes were, ^{226}Ra (alpha emitter with the energies 4.78 MeV (93.8 %) and 4.60 MeV (6.2 %)), ^{228}Ra (weak beta emitter E_{max} = 39.0 keV (60%) and 14.5 keV (40 %)) and ^{210}Pb (weak beta emitter E_{max} = 16.5 keV (80 %) and 63.0 keV (20 %))[23].

Reagents and Materials

The samples were prepared using reverse osmosis water and diluted standard solutions; such as a ^{226}Ra certified standard solution (containing ^{210}Pb) and a ^{228}Ra solution both supplied by National Institute of Standards and Technology (NIST) and a ^{210}Pb solution supplied by National Physical Laboratory (NPL). For the pulse shape analysis (PSA) optimization, diluted standards of ^{14}C supplied by CERCA-LEA and ^{241}Am by the National Physical Laboratory (NPL) were used.

Four different liquid scintillation cocktails, OptiPhase Hisafe™ III, Optiphase SuperMix™, Ultima Gold™ AB and Insta-Gel Plus supplied by Perkin Elmer, were tested for use with the RAD disk.

3M Empore™ Radium RAD disks were used for the extraction of radium and lead.

20 mL PE vials supplied by Perkin Elmer were used in this study.

For the filtration of the water samples, a 3M Empore™ filtration system was coupled to a N 840 FT.18 LABOPORT® vacuum pump.

All reagents used were of analytical grade.

Optimization of the Pulse Shape Analysis (PSA) level

The PSA was optimized for three cocktails (Hisafe™ III, Ultima Gold™ AB and Insta-Gel Plus) using ^{241}Am as pure alpha emitter and ^{14}C as pure beta emitter. The PSA was not optimized for Optiphase Super-Mix™ because this cocktail was just used in elution method to check phase stability.

The vials for the optimization were prepared by adding a conditioned RAD disk obtained after filtration of 20 mL of 2 M HNO_3. Then, a known amount of the standard (^{241}Am or ^{14}C) was added together with 20 mL of the cocktail into the vial. These vials were counted for 10 minutes using different values of the PSA level in order to obtain a misclassification curve [24]. The optimal PSA was obtained as the value with the minimum total interference. For Hisafe™ III, a second method for the optimization of the PSA level was also tested by using a sample containing 1 Bq of ^{226}Ra standard solution which was filtered through a previously conditioned RAD disk and transferred in a polyethylene LS vial with 20 mL of cocktail [25]. These results were compared with the standard PSA determination method. In order to avoid a misinterpretation in the alpha/beta separation caused by the ingrowth of the short lived decay products of ^{226}Ra, the vial was stored 28 day to allow secular equilibrium to be reached prior to the PSA tests. Then, the vial was counted at several PSA levels for 60 minutes.

All the results and conclusions are dealt with in following paragraphs.

Determination of ^{226}Ra and ^{228}Ra by direct measuring of the RAD disk

Preliminary tests showed that measurements of ^{226}Ra by direct counting of the RAD disk by LSC are subject to several sources of bias. The measurements performed right after the sample preparation show crosstalk from alpha particles in the beta window. Additionally, the spectra clearly shift to high energies (mainly in the alpha window) with time.

In order to optimize the measurement conditions and to investigate the source of the problems mentioned above several experimental parameters were investigated.

At first, a poor energy transfer between the ionizing particle emitted from the radionuclide fixed in the RAD disk and the cocktail were believed to be responsible for the observations made. In order to check this hypothesis, several tests were performed as described below.

For all the tests, the sample was prepared as follows: the RAD disk was conditioned with 20 mL of 2 M HNO_3, then the 250 mL sample spiked with known amount of ^{228}Ra (3 Bq) or ^{226}Ra (1 Bq) acidified to pH < 2 with concentrated HNO_3 was filtered through the RAD disk. In all cases the flow rate was lower than 50 mL min^{-1}.

The first test consisted of studying the impregnation of the RAD disk with different types of cocktail. After the sample preparation, as described above, each filter was transferred into a LSC vial, where 20 mL of scintillation cocktail was added. Respectively, Hisafe™ III (S_1 – S_3), Ultima Gold™ AB (S_4) or Insta-Gel Plus (S_5) were used (see Table 1), followed by 1 hour of cooling down in darkness to avoid photoluminescence phenomena. Then each sample was measured for 60 minutes.

In the second test we applied different treatments believing to have an impact on the way the disk is impregnated by the cocktail: mixing for 30 minutes in an ultrasonic bath (S_6), or for 10 minutes in a vortex agitator (S_7), drying of the RAD disk on a watch glass for 1 hour on a hot plate (S_8) after filtration of the sample (see Table 1).

Another treatment which was tested was to impregnate the RAD disk with the cocktail by suction, using the same filtration system as is used to filter the sample. 10 mL of Hisafe™ III were sucked through the RAD disk and the eluted fraction was collected in a separate LS vial prepared also for counting after addition of another 10 mL of fresh cocktail.

The RAD disk impregnated with cocktail in this way was then transferred into another LSC vial and 20 mL of Hisafe™ III were added (S_9) (see Table 1).

Table 1
Radionuclides considered, treatment after filtration and impregnation methods and cocktails used for each sample.

Test code	*Radionuclide(s)*	*Treatment after filtration*	*Cocktail*
S_1	$^{226}Ra/^{210}Pb$	Direct	Hisafe™ III
S_2	^{228}Ra	Direct	Hisafe™ III
S_3	^{210}Pb	Direct	Hisafe™ III
S_4	$^{226}Ra/^{210}Pb$	Direct	Ultima Gold™ AB
S_5	$^{226}Ra/^{210}Pb$	Direct	Insta-Gel Plus
S_6	$^{226}Ra/^{210}Pb$	Ultrasonic	Hisafe™ III
S_7	$^{226}Ra/^{210}Pb$	Vortex	Hisafe™ III
S_8	$^{226}Ra/^{210}Pb$	Dry	Hisafe™ III
S_9	$^{226}Ra/^{210}Pb$	Cocktail suction	Hisafe™ III
S_{10}	$^{226}Ra/^{210}Pb$	Direct creased	Hisafe™ III
S_{11}	$^{226}Ra/^{210}Pb$	Direct folded	Hisafe™ III

An overview of different types of cocktails and different treatments applied is presented in Table 1.

In all these tests, the RAD disk was positioned inside the LS vial along its walls (see Fig. 1).

Since the counting geometry of the LS vial with the RAD disk inside is not necessary symmetric with respect to the position of the photomultipliers tubes (PMT) of the LSC, the position of the LS vial in the counter has to be considered. In order to evaluate the influence of the vial position on the counting rate or on the shape of the spectra, sample S_1 was measured at several orientations (0°, 45°, 90°, 135° and 180°) after 28 days, when ^{226}Ra reached the secular equilibrium with its daughter products.

Two other ways of inserting the disk in the vial were considered: one by folding the disk in a specific way and another by creasing the disk. Fig.1 shows a schematic representation of the folding and different orientations of the vial with respect to the PMT.

Elution of radium and lead from the RAD disk

In the methods that entail elution of the radium isotopes from the RAD disk after the filtration, the EDTA is the most commonly extractant used [14-18]. We also tested this method. Samples were prepared in the same way as for the direct measurement, but radium was eluted from the disk using 20 mL of a 0.25 M basic EDTA solution.

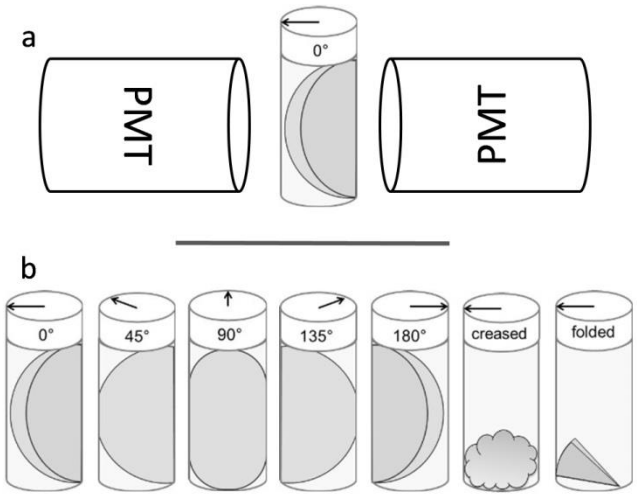

Fig. 1. Schematic representation of the folding of the filter in the vials in the counter (a) and different orientations and geometries of the RAD disk inside the LS vials (b) with respect to the PMT.

An elution curve for ^{226}Ra and ^{210}Pb was obtained by collecting the eluted fraction every 2 mL. Furthermore, several tests were performed in order to check the amount of EDTA solution accepted by the cocktails (we tested four different cocktails); no radioactive tracers were added in these tests.

Results and discussion

Optimization of the Pulse Shape Analysis (PSA) level

The results of the alpha and beta calibration with ^{241}Am and ^{14}C for Insta-Gel Plus show, at the optimal PSA level set at 40, an interference around 20 %, which is too high to achieve valid results in samples that may contain both alpha and beta emitters. For Optiphase Hisafe™ III and Ultima Gold™ AB the misclassification was much lower (less than 1 %) at the optimum PSA level set at 90 for Hisafe™ III and 70 for Ultima Gold™ AB using the missclasification method.

For Optiphase Hisafe™ III we also performed the alpha and beta calibration by means of Feng's method [24] in the absence of pure alpha or beta emitter, but just by using a ^{226}Ra source. This method assumes that around the optimum PSA level there is an inflection in the misclassified counts. The data near the inflection point can be fitted to a cubic polynomial function ($y=ax^3+bx^2+cx+d$) and the optimum PSA level is obtained by investigating where the second derivative of the fitted function ($y''=3ax+b$) is equal to 0. The optimal PSA is equal to $-b/3a$.

In Fig. 2 the counting rate in the alpha window relative to the total count rate is plotted against the PSA level. The mathematical fitting of the curve by a cubic polynomial is also shown.

With this method, the optimum PSA level obtained is 75, which is fifteen units below the value obtained in the misclassification study with ^{241}Am and ^{14}C. The main advantage of this alternative method is to perform the calibration with the same radionuclides that are measured in the samples. However, in our case, this is not completely possible since the calibration standard was measured at secular equilibrium between ^{226}Ra and its short-lived decay products, while the actual samples are measured as soon as possible. This fact can be the cause of the difference in the PSA level obtained by classical method and the one obtained by Feng's method. For this reason, the classical method was considered more appropriate and hence, for the measurements of our samples we decided to use Hisafe™ III as cocktail with a PSA level set at 90.

Determination of ^{226}Ra and ^{228}Ra by direct counting of the RAD disk

As shown by the preliminary studies, the measurements of ^{226}Ra with the wet RAD disk inserted into a vial and then adding the cocktail (Hisafe™ III), show several sources of measurement bias. The measurements performed just after the sample treatment have crosstalk from alpha particles in the beta window.

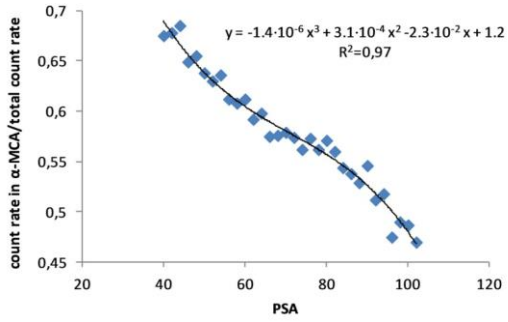

Fig. 2. Ratio between count rate in the alpha multichannel and total count rate *versus* PSA value and fitting with a cubic polynomial

This misclassification decreases during the first 5 hours after the preparation of the vial and stabilizes for times exceeding 5 hours. Fig. 3 shows the evolution of the spectra as a function of the delay between sample preparation and counting, for sample S_1, the delay is 1 hour (a) and 5 hours (b). Fig. 3 clearly shows that counts move from the beta window to the alpha window as a function of time. After 5 hours delay between the preparation and the counting) the spectra still show further evolution mainly in the alpha window where it is observed that the spectrum shifts to higher energies. This effect can be seen in Figure 4 where spectra of sample S_1 without considering alpha-beta separation are shown respectively 1, 3 and 5

hours after vial preparation. A similar counting vial was prepared using a sample spiked at 1 Bq/sample with ^{228}Ra (S_2) and the same effects were observed for the alpha counts of ^{224}Ra. However, for sample S_3 which just contains ^{210}Pb, these phenomena are not observed. In Figure 5 the evolution of spectral parameters during the first 20 hours after the preparation of a sample S_1 is shown. The misclassification, defined as the ratio between beta and alpha counts, and the spectral shifting defined as the shift in channels measured at the channel with the maximum counts, are presented. The figure equally shows the mean value (continuous line) and 2σ standard deviation (dashed lines) for the misclassification and shifting parameters once they are stable. As can be seen, misclassification evolves during the first 5 hours after sample preparation while the shifting evolves during the first 8 hours after sample preparation.

An experimental parameter that combines radium recovery and counting efficiency was determined after 8 hours of the LS vial preparation when misclassification and shifting are stable. Values of (100 ± 2) % for ^{226}Ra and (48 ± 2) % for ^{228}Ra were obtained. With these results we can conclude that the chemical yield for radium is 100 %.

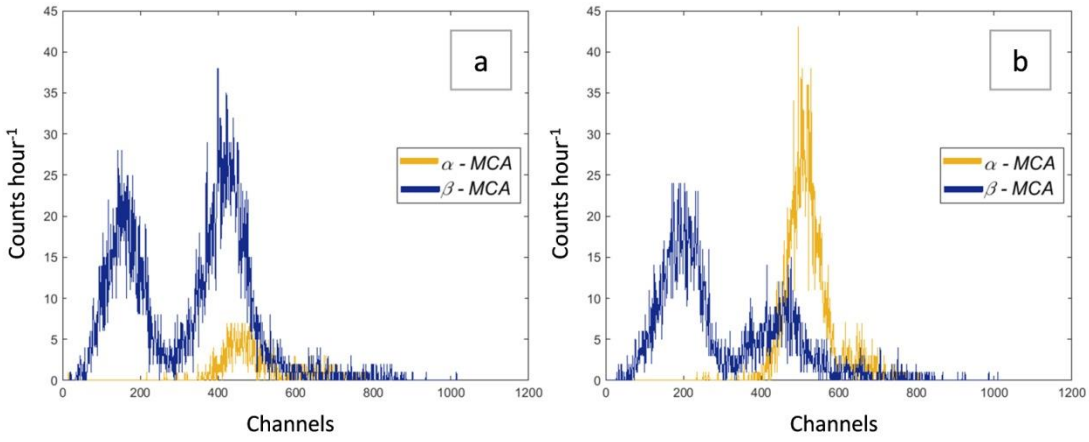

Fig. 3. Spectra of sample S_1, with alpha beta separation 1 hour after vial preparation (a) and 5 hours after vial preparation (b).

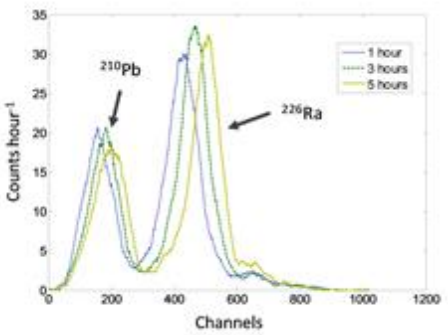

Fig. 4. Spectra of S_1 after 1 hour (doted in blue), 3 hours (dashed in green) and 5 hours (yellow) of delay between sample preparation and LSC. No alpha beta separation is applied. Spectra were smoothed using Savitzky-Golay filter to better illustrate the shifting.

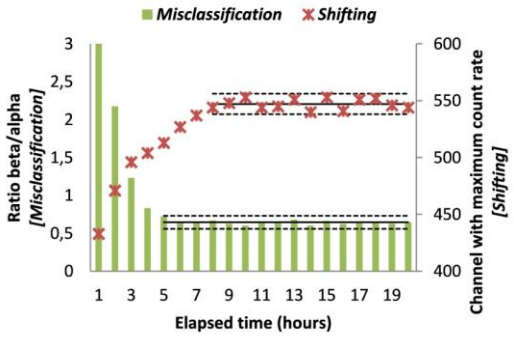

Fig. 5. Evolution of the misclassification (as ratio of the beta/alpha counts) and shifting (as channel with maximum number of counts) for the sample S_1.

The efficiency is 100 % for the alpha emission of ^{226}Ra and 48 % for ^{228}Ra, a low beta emitter. However lead is also retained in the radium RAD disks and may interfere in ^{228}Ra measurements due to the overlapping between both LS spectra [10-11,14-16]. These results are consistent with the literature, were 100 % of radium and lead retention is reported. Regarding the efficiency, Wallner et. al. report values of 100 % for ^{226}Ra and 57 % for ^{228}Ra [18].

However, these results were obtained eluting radium from the RAD disk and measuring the solution. In our case, ^{226}Ra and ^{228}Ra are directly measured from the RAD disk and hence the efficiency for ^{228}Ra, low energy beta emitter, decreases.

It is known from literature that quenching may affect the alpha beta separation [26, 27] and that it also affects the shape of the spectrum. However, the quenching, read from the SQP[E], remained constant during the measurements, at a value of about 765, and only in the first measurement is was slightly lower (775). It has to be pointed out that an increase of SQP[E] entails a decrease of the quenching. Although SQP[E] remained constant, we assumed that the variations observed during the first hours after sample preparation are caused by changes in the energy transfer between the ionizing particle emitted from the radionuclide fixed in the RAD disk and the cocktail. The SQP[E] parameter may not describe this loss of energy before the excitation of the cocktail since the quenching parameter is obtained from the spectra of Compton electrons produced in the vial by an external source. To explain the observations discussed, two possible causes

were considered. One possible cause is explained by considering that radionuclides fixed in the RAD disk slowly migrate into the cocktail during the first hours after sample preparation. The other possible cause, assuming that nuclides do not migrate, is attributed to a slow impregnation of the disk by the cocktail. When the filter is not yet fully impregnated some radiation may lose energy before it can interact with the cocktail. When the filter is fully impregnated, the emitted particles transfer their energy in a unique way to the cocktail. In order to prove that one of these explanations was true, the RAD disk from the sample S_2 was removed from the vial (after 21 h, once the spectrum is stable) and was transferred to a new vial containing fresh cocktail. Next, the new vial (containing the RAD disk) and the initial vial with the cocktail that has been in contact with the RAD disk for 21 hours where counted again.

Fig. 6 shows the spectra that were obtained from both samples. It can be seen that only ^{220}Rn and some beta decay products leached out in the cocktail, while the radium isotopes (^{224}Ra and ^{228}Ra) clearly remain fixed in the RAD disk.

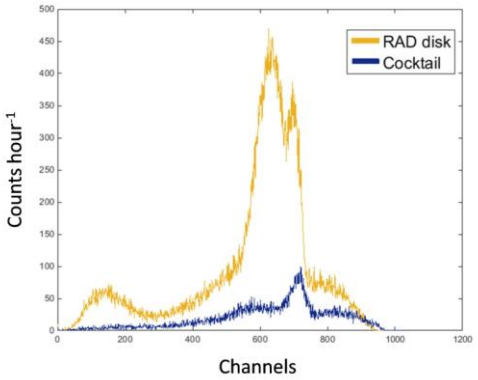

Fig. 6. Spectrum of the cocktail of S_2 when the RAD disk is removed after 21 h (blue), and spectrum of the RAD disk of sample S_2 with fresh cocktail (yellow).

Since radium does not migrate from the disk to the cocktail, we assume that the evolution of the grade of impregnation of the RAD disk by the cocktail evolves for several hours once the RAD disk is inserted in the vial, causing the misclassification and shifting of the spectra. For this reason, different cocktails and procedures that affect the impregnation of the RAD disk were tested. Direct measurement of a RAD disk containing a mixture of ^{226}Ra and ^{210}Pb was also performed using both, Ultima Gold™ AB (S_4) and Insta-Gel Plus (S_5) as cocktail. For Ultima Gold™ AB misclassifications were observed until 5 hours after sample preparation, and shifting until 8 hours after sample preparation as was observed for Optiphase Hisafe™ III. These results were consistent because both cocktails are based on di-isopropylnaphthalene (DIN). However, for Insta-Gel Plus

(1,2,4-Trimethylbenzene based cocktail) the misclassification does not change in time although it is high (~20 %). Also the spectral shifting is observed only for the first three hours after sample preparation. Insta-Gel Plus clearly impregnates the RAD disk faster, but the high misclassification does not allow an accurate determination of ^{226}Ra due to the high contribution of the cross talk.

The different treatments applied to improve the impregnation speed of the RAD disk by the cocktail (S_6, S_7 and S_8) show similar results as for the sample S_1. The envisaged methods (ultrasonic and drying) did not appreciable shorten the time of impregnation. The time needed for the stabilization of misclassification was decreased from 5 to 4 hours and from 7 to 8 hours for shifting of the spectra.

Still another attempt was tried to speed up the impregnation of the RAD disk with cocktail. This was done by suction of the cocktail (S_9) through the filter after filtration of the sample. This method showed that no misclassification or shifting occurred after the first hour after the sample preparation. The alpha beta separation was correct, and the channel with the maximum counts did not change (and stayed at 550 ± 5 channels). Furthermore, when the cocktail is sucked through the RAD disk after filtration of the sample, part of ^{210}Pb that may interfere in ^{228}Ra determination is also removed. Fig. 7 shows the spectra of the RAD disk impregnated through suction of the cocktail (S_9) (a) and the eluted cocktail collected during the impregnation by suction of the RAD disk (b). It was observed that 50 % of ^{210}Pb was stripped from the RAD disk with Hisafe™ III while ^{226}Ra remains on the RAD disk (less than 1 % is eluted in the cocktail fraction).

The measurements of the sample S_1 show that the orientation of the LS vial in the counter with respect to the PMT has no influence on the counting efficiency or on the shape of the spectra when the RAD disk is inserted along the vials wall. The measurements for the creased and folded filter show loss of efficiency, misclassification problems and shifting of the spectra to lower energies.

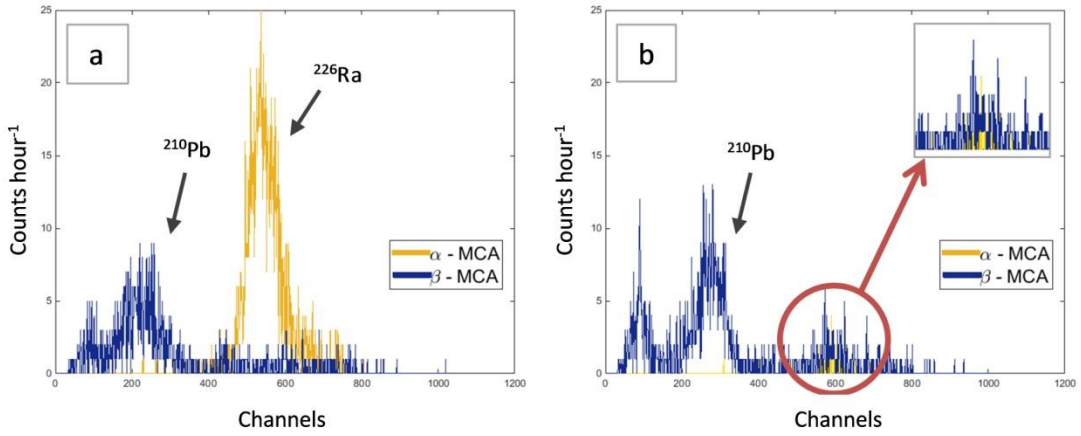

Fig. 7. Alpha and beta spectra for a RAD disk with forced impregnation with cocktail (a) and the cocktail fraction used to impregnate it (b) samples S_9.

For example, for the folded RAD disk (S_{11}) only 40 % of efficiency for ^{226}Ra is achieved 8 hours after sample treatment.As a summary of the test performed, it is possible to determine ^{226}Ra and ^{228}Ra by direct measurement of RAD disks under some considerations. One liter of sample acidified to pH < 2 with HNO_3 is filtered through a RAD disk. To achieve the maximum efficiency and no problems of misclassification or shifting of the spectra, the RAD disk has to be inserted along the vials wall and a good impregnation of the RAD disk has to be achieved by means of waiting 8 hours or sucking the cocktail through the RAD disk. Direct measuring of ^{228}Ra will overestimate the real value when the sample contains ^{210}Pb due to its chemical and spectral interference.

Elution of radium and lead from the RAD disk

The elution curves for ^{226}Ra and ^{210}Pb are shown in the Fig. 8 and are consistent with the literature. Möbius et al. reported that lead (^{210}Pb) is more concentrated than radium in the first 5 mL of basic EDTA fraction [20].

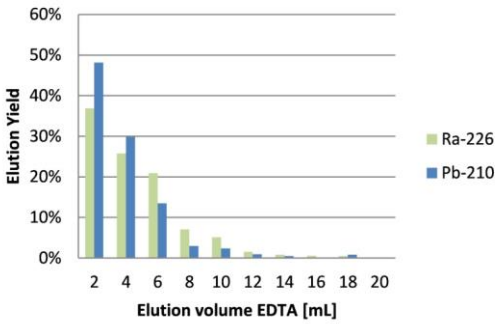

Fig. 8 Elution curves for ^{226}Ra and ^{210}Pb from radium RAD disk by EDTA.

Table 2
EDTA/cocktail ratio, cocktail used and appearance after 2 hours cooling down at 14 °C for test of sample acceptance.

CODE	*EDTA/cocktail ratio*	*Cocktail*	*Observations*
E_1	2/18	Ultima Gold™ AB	Milky aspect
E_2	10/10	Ultima Gold™ AB	Milky aspect and phase separation
E_3	2/18	Insta-Gel Plus	Milky aspect
E_4	10/10	Insta-Gel Plus	Milky aspect
E_5	2/18	SuperMix™	Clear
E_6	10/10	SuperMix™	Milky aspect
E_7	2/18	Hisafe™ III	Clear
E_8	5/15	Hisafe™ III	Phase separation
E_9	5/10[(1)]	Hisafe™ III	Phase separation
E_{10}	5/10[(2)]	Hisafe™ III	EDTA crystallization
E_{11}	10/18[(3)]	Hisafe™ III	Milky aspect

[(1)] 5 mL of 0.25 M EDTA + 5 mL of Reverse Osmosis water + 10 mL of cocktail
[(2)] 5 mL of 0.25 M EDTA + 5 mL 0.25 M HNO_3 + 10 mL of cocktail
[(3)] 10 mL of 0.25 M EDTA evaporated to 2 mL + 18 mL of cocktail

There is a need to elute radium and lead from the RAD disk with at least 10 mL of 0.25 M basic EDTA in order to achieve a yield of more than 95 %.

The remaining 5 % is eluted with another 10 mL of EDTA. Less than 0.5 % of the activity remains in the RAD disk after stripping with 20 mL of basic EDTA. Taking into account the volume of EDTA needed to strip 95 % of radium and lead, we tested the acceptance of the EDTA eluted by different cocktails. The ratio EDTA to cocktail, the type of the cocktail used and the observations of these tests are presented in Table 2.

The samples were prepared and cooled down for 2 hours at 14 °C. As is shown in Table 2, samples with a ratio 2/18 for SuperMix™ (E_5) and Hisafe™ III (E_7) have a homogeneous and clear aspect and are perfectly suitable for liquid scintillation measurement. Samples E_2, E_8, E_9 and E_{10} are not stable and present phase separation and hence are not suitable for liquid scintillation measurement. The dilution (E_9) or neutralization (E_{10}) of EDTA does not increase the sample acceptance in the cocktail. The other samples show a milky aspect that, even when homogeneous, indicates that the mixtures are close to immiscible point. If these mixtures are measured by liquid scintillation counting, a check after measurement has to be done in order to ensure than no phase separation has occurred during the counting. Milky homogeneous samples were obtained for E_6 and E_{11}.

Conclusions

Determination of ^{226}Ra and ^{228}Ra may be performed by means of the direct measurement of the Radium RAD disk by liquid scintillation counting under some considerations. To ensure a good alpha and beta separation and good stability of the spectra after the sample preparation, it is necessary to wait at least 8 hours between sample preparation and counting. The RAD disk has to be inserted unfolded with the disk along the wall of the vial in order to achieve the maximum counting efficiency. ^{228}Ra is overestimated in samples containing ^{210}Pb due to interference.

The waiting time between sample preparation and measurement can be reduced if the RAD disk is impregnated by the forced flow of the cocktail. One valid procedure to achieve this is to suck the cocktail through the RAD disk using a vacuum system. When this impregnation procedure is applied, the waiting time needed is just to avoid photoluminescence. Moreover the impregnation by suction of the cocktail also removes up to 50 % of ^{210}Pb from the RAD disk and therefore, reduces its interference.

For the elution of radium from the RAD disk, at least 10 mL of 0.25 M basic EDTA solution are needed to achieve a 95 % recovery for lead and radium. The selection of a cocktail compatible with the EDTA solution is critical. In case of working with milky solutions, the sample needs to be controlled before and after the counting.

Acknowledgements

J. Fons-Castells wishes to acknowledge the Spanish Nuclear Safety Council for the project “Rapid methods for the simultaneous determination of alpha and beta emitters by LSC in water” and the Spanish ministry of economy and competitively for the PhD grant FPI BES 2012-052590.

References

1. United Nations (2000) Annex B: Exposures from natural radiation sources In: UNSCEAR 2000 report Vol. I Sources and effects of ionizing radiation
2. Council Directive 2013/51/Euratom of 22 October 2013 laying down requirements for the protection of the health of the general public with regard to radioactive substances in water intended for human consumption. Official journal of the European Union. L296: 12-21
3. Chalupnik S, Lebecka J, Mielnikov A, Michalk B (1996) Determining radium in water: comparison of methods. LSC 1994, Advances in Liquid Scintillation Spectrometry. 103-109
4. Rusconi R, Azzellino A, Bellinzona S, Forte M, Gallini R, Sgorbati G (2004) Assessment of drinking water radioactivity content by liquid scintillation counting: set up of high sensitivity and emergency procedures. Anal. Bioanal. Chem. 379:247-253
5. Brunett WC, Cable PH, Moser R (1995) Determination of Radium-228 in natural waters using extraction chromatographic resins. Radioactiv Radiochem. 6:36-43
6. Nour S, El-Sharkawy A, Brunett WC, Horwitz EP (2004) Radium-228 determination of natural waters via concentration on manganese dioxide and separation using Diphonix ion exchange resin. Appl. Radiat. Isot. 61:1173-1178
7. Jia G, Torri G, Innocenzi P, ocone R, Di Lullo A (2005) Determination of radium isotopes in mineral and environmental water by alpha-spectrometry. J Radioanal Nucl Chem. 267:505-514
8. Alvarado JS, Orlandini KA, Erickson MD (1995) Rapid determination of radium isotopes by alpha spectrometry. J Radioanal Nucl Chem. 194:163-172
9. Inoue M, Komura K (2007) Preliminary application of low-background gamma-spectrometry to volcanic ground water: low-levels of ^{7}Be, ^{22}Na, ^{137}Cs

and radium isotopes as new geochemical tracers in a ground water flow system. J Radioanal Nucl Chem. 273:177-181
10. Scapitta SC, Miller PW (1996) Evaluation of 3M Empore™ Rad disks for radium determination in water. 42nd Annual Conf. on Bioassay, Analytical and Environmental Radioactivity, San Francisco
11. Ďureková A (1997) Contribution to the simultaneous determination of ^{228}Ra and ^{226}Ra by using 3M's Empore™ radium Rad disks. J Radioanal Nucl Chem. 223:225-228
12. Jia G, Jia J (2012) Determination of radium isotopes in environmental samples by gamma spectrometry, liquid scintillation and alpha spectrometry: a review of analytical methodology. J Environ Radioactiv. 106:98-119
13. 3M (2009) Test Method RA-195: Rapid determination of radium-228 in water by elution of ingrown actinium-228 from Empore™ Radium RAD disks. USA 1/09
14. Schönhofer F, Wallner G (2001) Very rapid determination of ^{226}Ra, ^{228}Ra and ^{210}Pb by selective adsorption and liquid scintillation counting. Radioactiv Radiochem. 37:355-372
15. Wallner G (2002) Determination of ^{228}Ra, ^{226}Ra and ^{210}Pb in drinking water using liquid scintillation counting. LSC 2001, Advances in Liquid Scintillation Spectrometry. 269-274
16. Wallner G, Steininger G (2006) Radium isotopes and ^{222}Rn in Austrian drinking waters. J Radioanal Nucl Chem. 274:511-516
17. Schönhofer F, Maringer FJ (2006) The EU drinking water directive, the Austrian standard, and an ultra low-level liquid scintillation spectrometry approach for assuring compliance. LSC 2005, Advances in Liquid Scintillation Spectrometry. 1-11
18. Wallner G, Wagner R, Katzlberger C (2008) Natural radionuclides in Austrian mineral water and their sequential measurements by fast methods. J Environ Radioactiv. 99:1090-1094
19. Ďureková A, Ďurec F, Autxová L, Adámek P (1999) Determination of 226Ra and 228Ra in mineral and drinking waters using 3M's Empore™ radium Rad disks. Czech J Phys. 49:119-125
20. Möbius S, Kamolchote K, Rakotoarisoa T (2002) Extractive methods for fast radium analysis. LSC 2001, Advances in Liquid Scintillation Spectrometry. 283-292
21. Möbius S, Rakotoarisoa T, Lauria DC, Zafimanjato L (2006) Fast survey for key nuclides and group parameters in drinking water. LSC 2005, Advances in Liquid Scintillation Spectrometry. 149-156
22. Seely DC, Osterheim JA (1998) Determination of radium isotopes in environmental samples by gamma spectrometry, liquid scintillation and alpha spectrometry: a review of analytical methodology. J Radioanal Nucl Chem. 236:175-180
23. Dulieu, C. et. al. (2010) Table of radionuclides. Volume 5. Bureau International des Poids et Mesures. Sèvres, France.
24. L'Annunziata M F, Kessler M J (2012) In: L'Annunziata M F (ed) Handbook of Radioactivity Analysis, 3rd edn. Academic Press, San Diego
25. Feng X, He Q, Wang J, Chen J (2014) A method for optimum PSA setting in the absence of pure α or β emitter and its application in the determination of ^{237}Np/^{233}Pa. Appl Radiat Isotopes. 93:114-119
26. Sanchez-Cabeza JA, Pujol L (1998) Simultaneous determination of radium and uranium activities in natural waters samples using liquid scintillation counting. Analyst 122:383-385
27. Feng X, He Q, Wang J, Chen J (2013) Simultaneous determination of ^{152}Eu and ^{241}Am in liquid solution by liquid scintillation counting. J Radioanal Nucl Chem. 295:1495-1503

5.2. Simultaneous determination of ^{226}Ra, ^{228}Ra and ^{210}Pb in drinking water using 3M Empore™ RAD disk by LSC-PLS

Simultaneous determination of ^{226}Ra, ^{228}Ra and ^{210}Pb in drinking water using 3M Empore™ RAD disk by LSC-PLS

Jordi Fons-Castells*, Javier Oliva, Joana Tent-Petrus, Montserrat Llauradó

Department of Chemical Engineering and Analytical Chemistry, University of Barcelona, Martí i Franquès 1-11, 08028 Barcelona, Spain.

*corresponding author: jordi.fons@ub.edu

Abstract

A procedure for the rapid and simultaneous determination of ^{226}Ra, ^{228}Ra and ^{210}Pb in drinking water by means of extraction with a 3M Empore™ Radium RAD disk and liquid scintillation spectrometry is described. The selective elution of ^{210}Pb from the RAD disk and a multivariate calibration using partial least squares regression (PLS) are tested as methods to avoid overlap in the spectra between ^{228}Ra and ^{210}Pb. The validated procedure was tested with mixtures of radionuclides and interlaboratory materials; finally, it was applied to natural waters.

Keywords: ^{226}Ra, ^{228}Ra, ^{210}Pb, RAD disk, Multivariate Calibration

Introduction

^{226}Ra, ^{228}Ra and ^{210}Pb are radionuclides included in the European Directive for drinking water (Council Directive 2013/51/Euratom) due to their radiotoxicity and because they are common radionuclides in natural waters. Recently, in Spain, the new Royal Decree 314/2016 included ^{226}Ra, ^{228}Ra and ^{210}Pb as target radionuclides that have to be analysed in drinking water. For this reason, rapid methods for evaluating these radionuclides are required.

Several methods for performing ^{210}Pb determination based on radiochemical separation are described in the literature as well as for ^{226}Ra and ^{228}Ra.

Regarding ^{210}Pb, the common methods of separation are performed using sulfate co-precipitation method (Wallner, 2002) or extraction chromatography using Sr-Spec resin (Vajda et al., 1997; Vrecek et al., 2004).

Regarding radium isotopes, Ba(Ra)SO_4 and or Pb(Ra)SO_4 coprecipitation and cation-exchange resin absorption are the most commonly used techniques to preconcentrate radium isotopes (Guogang & Jing, 2012).

Another procedure based on the absorption of radium isotopes on MnO_2-coated disk is described in the literature (Eikenberg et al., 2001). In this procedure, a rapid determination of ^{226}Ra and ^{224}Ra (alpha emitters) is achieved with low-level alpha spectrometry. However, the determination of ^{228}Ra is performed via ^{228}Th after a standing time of approximately six months.

In the late 1990s, the Radium RAD disk was introduced as a rapid SPE (solid phase extraction) method for concentrating radium (Scapitta & Miller, 1996). Radium RAD disks are circular 47-mm diameter inert supports with a covalently bonded crown ether that selectively retains radium isotopes (Durekova, 1997). It is important to note that although the RAD disk is a practical separation method for radium, these filters also retain lead isotopes and this may be an important drawback (Scapitta & Miller, 1996; Ďureková, 1997; Ďureková et ál., 1999; Möbius, 2006; Schönhofer & Maringer, 2006; Wallner et al., 2008).

There are different procedures to evaluate radium using the RAD disk. In brief, they can be sorted into two classes. In the first one, radium is eluted from the RAD disk, which is usually achieved with a solution of basic EDTA (ethylenediaminetetraacetic acid) (Möbius, 2006; Schönhofer & Maringer, 2006; Wallner et al., 2008). When these methods are used, 100 % of radium is eluted, but all the retained lead is also eluted. If this solution is measured by LSC with alpha beta separation, ^{226}Ra can be determined, but

^{210}Pb interferes with ^{228}Ra (a low beta emitter) (Möbius, 2006; Schönhofer & Maringer, 2006; Wallner et al., 2008).

A method to avoid this interference between ^{210}Pb and ^{228}Ra is based on the previous elimination of interferents like ^{210}Pb or ^{90}Sr from the RAD disk. In the experiments done by Ďureková et ál., DHC (Diammonium hydrogen citrate) is used for both to elute interferents and after that to elute radium isotopes as well. In a first step lead and strontium were removed from the RAD disk with 20 mL of DHC $6{\cdot}10^{-4}$ mol L^{-1}, after wait the ingrown of ^{228}Ac (48 hours) it was eluted from the RAD disk with 20 mL of DHC $3{\cdot}10^{-4}$ mol L^{-1} and measured in a proportional counter to determine ^{228}Ra. Finally radium isotopes were removed from the RAD disk with 40 mL of DHC 0.2 mol L^{-1} adjusted to pH 7.8 and ^{226}Ra is counted by conventional radon emanation technique (Ďureková, 1997; Ďureková et al., 1999). This method solves the problem of interference between ^{228}Ra and ^{210}Pb but requires of time consuming classical techniques.

Following similar strategy, a new method has been recently developed for the determination of ^{210}Pb and ^{226}Ra/^{228}Ra (Eikenberg et. al. 2014). This is based on the extraction of lead from the RAD disk with 5 mL of DHC 0.2 mol L^{-1} and followed by the extraction of radium isotopes with 6 mL of 0.25 mol L^{-1} basic EDTA. On this work, triple-to-double coincidence ratio TDRC was used for efficiency tracing.

The second approach for evaluating radium and lead include direct measurements from the RAD disk as Scapitta & Miller suggest in 1996 for strontium RAD disk. Recently, some authors measured radium isotopes using this approach but overlapping ^{228}Ra and ^{210}Pb spectra are also a problem (Vasile et al., 2016; Fons-Castells et al., 2016). In these cases, the authors do not determine ^{210}Pb and notice that in presence of ^{210}Pb, ^{228}Ra may be overestimated.

Several methods for LSC spectra deconvolution that can solve the problem of overlapping have been described in the literature. In the last years, PLS (Partial Least Squares) has been described as a practical tool for quantifying mixtures of alpha and beta emitters from LSC spectra (Mahani et al., 2012; Fons-Castells et al., 2017).

PLS is based on a reduction of variables by the use of a new coordinate system performed from new axes called latent variables (LVs), which are linear combinations of the original variables (in our case, the count in each channel of the LSC spectra). These LVs are chosen to explain the maximum correlation between the original variables and activity of each isotope. In a first step, a PLS model was

created using a set of spectra for single or multiple isotope samples and the certified activity of these samples. Afterwards, the PLS model can be used to determine the activity of a sample with its LSC spectrum.

In this paper two strategies to eliminate the interference between ^{228}Ra and ^{210}Pb are studied to propose a procedure for simultaneously determining ^{226}Ra, ^{228}Ra and ^{210}Pb; selective extraction of lead isotopes with DHC from the RAD disk and PLS quantification. Both strategies were validated with prepared mixtures and a quality control material. Then, the method was applied for evaluating the ^{226}Ra, ^{228}Ra and ^{210}Pb in water samples collected from five different sources, which may be used for human consumption.

Experimental

Apparatus

Retention test analyses were measured with a BEGe 3830 CANBERRA high resolution gamma spectrometer. In the retention test, the target radionuclides were ^{228}Ac 911.21 keV, [26.60 %] measured to follow the retention of ^{228}Ra when the secular equilibrium is reached 3 days after the sample treatment and ^{210}Pb 46.5 keV, [4 %]. The counting time was sufficient to achieve a proper measure statistics.

A Wallac QUANTULUS 1220 low level liquid scintillation spectrometer was used for quantification of massic activities of ^{226}Ra, ^{228}Ra and ^{210}Pb. The counting time was 100 min for each sample and 1 min for the spectral quench parameter of the external standard (SQP[E]). The target radionuclides were ^{226}Ra (alpha emitter with the energies 4.78 MeV [93.8 %] and 4.60 MeV [6.2 %]), ^{228}Ra (weak beta emitter E_{max} = 39.0 keV [60%] and 14.5 keV [40 %]) and ^{210}Pb (weak beta emitter E_{max} = 16.5 keV [80 %] and 63.0 keV [20 %]) (Wallner, 2002).

Reagents

Nitric acid (69 %) was used to acidify water samples to pH 2. DHC (Diammonium hydrogen citrate) was used as extracting solution to elute ^{210}Pb from the RAD disk. All reagents were of analytical grade. ^{226}Ra and ^{228}Ra were certified standard solutions from Eckert and Ziegler and ^{210}Pb certified standard solution from DAMRI, all of which had 3 % uncertainty with a coverage factor k=2. The scintillation cocktail used in this study was Optiphase Hisafe III.

Preliminary studies

To evaluate the influence of the sample volume in the retention of radium and lead isotopes in radium RAD disk, some preliminary tests were performed. Two volumes were tested, 1 L and 5 L. Two tests for both volumes were performed from spiking with 3 Bq of ^{228}Ra or ^{210}Pb, respectively. For each test two RAD disk were used, the first one was used to filter each sample. Then, the filtered water for each experiment was filtered again through the second RAD disk. Both RAD disks were measured by gamma spectrometry to determine the retained ^{228}Ra and ^{210}Pb.

Elution

According to the literature, basic EDTA solution is commonly used to elute radium and lead isotopes from the RAD Disk (Möbius, 2006; Schönhofer & Maringer, 2006; Wallner et al., 2008). However, the amount of EDTA needed to achieve a recovery near 100 % is not accepted by commonly used cocktails (Fons-Castells et al., 2016); hence, the volume of sample added to the counting vial has to be reduced. To avoid the hindrance that increases the detection limits, the proposed procedure radium isotopes were directly measured on the RAD Disk.

As mentioned previously, one of the key issues for evaluating the ^{228}Ra using the RAD disk is the interference of ^{210}Pb due to its overlapping spectra. To minimize this interference, DHC was used to elute lead isotopes.

RAD disk retention

Several DHC concentrations and pH values for the extraction solution were tested to optimize the extraction ^{210}Pb from the RAD disk. The pH values were selected considering the constant of complex formation of DHC with Ra and Pb. In Table 1, the compositions of the tested solutions were described.

Table 1
DHC concentration and pH of the tested extraction solutions.

Code	*Concentration DHC (mol L^{-1})*	*pH*
E_1	0.05	6.50
E_2	0.05	8.50
E_3	0.05	5.75
E_4	0.01	6.50

Elution tests were performed using different solutions to remove lead from the RAD disk. One-liter sample was spiked with 1 Bq L^{-1} of ^{210}Pb and 1 Bq L^{-1} of ^{226}Ra. A total of 20 mL of each solution described in Table 1 was used to elute lead from the RAD disk. 10 fractions, 2 mL each, were collected. After the elution fraction was collected, the RAD disks were transferred in a LS vial, 20 mL of scintillation cocktail had been added and measured by LSC. To avoid shifting of the spectrum or misclassification problems, the RAD disk was counted 8 hours after it was placed into a counting vial. This procedure ensured good impregnation with

the cocktail (Fons-Castells et al., 2016). The counting time was 100 min.

Optimization of the Pulse Shape Analyser (PSA)

The optimization of the alpha beta discriminator parameter, PSA, was performed with an interference study using ^{236}U as an alpha emitter and ^{40}K as a beta emitter. The optimal PSA value was established as 100.

Interferents evaluation

^{226}Ra decay products

To avoid misclassification issues caused by the incomplete impregnation of the RAD disk by the cocktail, the waiting time was at least eight hours. Consequently, several short lived decay products of ^{226}Ra may have grown into the counting vial. For this reason, ^{226}Ra activity is corrected by taking into account the time that elapsed between the sample preparation and measurement. Furthermore, the ^{226}Ra standard contains 14 % ^{210}Pb because the standard was not recently separated. For this reason, in all samples, the presence of ^{210}Pb in the ^{226}Ra standard was considered.

^{228}Ra decay products

^{224}Ra, as ^{228}Ra, occurs in the decay chain of ^{232}Th. ^{224}Ra, as a radium isotope, is retained in RAD disks and could interfere with the determination of ^{226}Ra because it is an alpha emitter. However, the ^{224}Ra alpha emission (5.78 MeV) is more energetic than the emission of ^{226}Ra (4.87 MeV) and does not overlap (Cook & Kleinschmidt, 2011).

^{90}Sr

Strontium, as radium, is an alkaline earth metal; hence, their chemical proprieties are similar. For this reason, ^{90}Sr is an interferent that has to be considered when radiochemical separation is required for radium isotope determination. Furthermore, some authors evaluated an important retention of ^{89}Sr in radium RAD disks (Scapitta & Miller, 1996).

To evaluate the interference of ^{90}Sr in the determination of ^{226}Ra, ^{228}Ra and ^{210}Pb in the developed method, a retention test was performed. Following the optimized procedure, although ^{90}Sr is retained, more than 97 % is eluted with DHC solution. For this reason, ^{90}Sr does not significantly interfere with determination of ^{226}Ra and ^{228}Ra. However, the presence of ^{90}Sr in a sample may cause overestimation of ^{210}Pb.

Counting efficiency

The counting efficiency has to be determined for each radionuclide of interest in both the RAD disk and solutions used to elute ^{210}Pb. The efficiency in the RAD disk for each radionuclide was evaluated at two massic activity concentration levels

(1.0 and 0.1 Bq kg^{-1}) in triplicate. This efficiency was determined by filtering known levels of standards, ^{226}Ra, ^{228}Ra or ^{210}Pb, and considering the results obtained on RAD disk retention study of each element. The spectra obtained from the standards used to evaluate the efficiency were also used as calibration standards for the PLS models.

The counting efficiency of ^{210}Pb in DHC was determined by spiking with a known amount of ^{210}Pb standard, which was previously purified by eliminating ^{210}Bi and ^{210}Po with Sr-Specific resin, a DHC solution and mixing it with the scintillation cocktail Optiphase Hisafe III.

As is mentioned above, the quenching was controlled by means of SQP[E] parameter in both, RAD disk and eluted fraction. The quenching level of spiked samples, intercomparison material and natural samples measured was comparable and evaluated around the 830 ± 10 for RAD disk and 810 ± 10 for DHC fraction. For the application of this method to different kind of samples (e.g. marine water or waste water) the role of quenching on the counting efficiency has to be considered.

Analytical procedure

The results obtained in the preliminary tests allow the optimization of the procedure for ^{226}Ra, ^{228}Ra and ^{210}Pb determination. In this section, the optimized procedure and samples analysed by means of it are described.

Prepared mixtures

Several mixtures of radionuclides were prepared in the laboratory by adding a known amount of radioactive standard to test the veracity of the procedure. In Table 2, the massic activity of the three radionuclides in each mixture is presented. In order to remove ^{224}Ra from the ^{228}Ra standard two sequential separations were performed. Triskem U/TEVA™ resin was used to retain the ^{228}Th contained in ^{228}Ra standard. After 21 days of the separation the activity of ^{224}Ra decays until 3 % of the initial activity. At this point a second separation of ^{228}Th was performed to ensure than the standard of ^{228}Ra contains less than 1.5 % of ^{224}Ra during the course of the experiments. High resolution γ-spectrometry was used to confirm the activity of ^{228}Ra via ^{228}Ac and the decay of non supported ^{224}Ra.

Table 2
Massic activity added and its uncertainty with a coverage factor k=2 for ^{226}Ra, ^{228}Ra and ^{210}Pb in laboratory prepared mixtures.

CODE	^{226}Ra Bq kg^{-1}	^{228}Ra Bq kg^{-1}	^{210}Pb Bq kg^{-1}
M_1	1.00 ± 0.05	-	0.96 ± 0.10
M_2	1.00 ± 0.05	-	0.19 ± 0.02
M_3	0.10 ± 0.01	-	0.89 ± 0.09
M_4	0.11 ± 0.01	-	0.09 ± 0.01
M_5	1.01 ± 0.05	0.12 ± 0.01	0.10 ± 0.01
M_6	0.10 ± 0.01	1.09 ± 0.06	0.02 ± 0.01
M_7	0.10 ± 0.01	0.11 ± 0.01	0.02 ± 0.01
M_8	-	1.14 ± 0.06	0.08 ± 0.01
M_9	-	0.13 ± 0.01	0.09 ± 0.01
M_{10}	0.10 ± 0.01	0.13 ± 0.01	0.09 ± 0.01
M_{11}	1.02 ± 0.05	0.12 ± 0.01	0.19 ± 0.02

Quality control

The method was validated for determining ^{226}Ra with a quality control material IAEA-TEL-2014-03 sample 03 that contains 24.5 ± 0.2 Bq kg^{-1} of $^{90}Sr/^{90}Y$, 26.3 ± 0.2 Bq kg^{-1} of ^{134}Cs, 19.6 ± 0.1 Bq kg^{-1} of ^{137}Cs, 17.9 ± 0.1 Bq kg^{-1} of ^{226}Ra, 5.48 ± 0.04 Bq kg^{-1} of ^{nat}U and 20.0 ± 0.1 Bq kg^{-1} of ^{241}Am.

Natural samples

After the validation, five natural samples from different places in Spain and different radiochemical proprieties were analysed according to the developed procedure. In Table 3, the type of water, dry residue, conductivity, pH and geological reservoir type for each sample are presented.

Optimized Procedure

For all the samples, prepared mixtures, quality control material and natural samples, the following procedure was applied. A radium RAD disk was mounted in a vacuum filtration tramp and it was connected to a vacuum pump. Twenty millilitres of 2 mol L^{-1} HNO_3 were filtered through the RAD disk to condition it. Then, 5 L of sample that was acidified to pH < 2 with HNO_3 was filtered through the RAD disk, and the funnel was cleaned with 20 mL of 2 mol L^{-1} HNO_3. Afterwards, 7 mL of DHC 0.05 mol L^{-1} at pH 5.75 were used to elute ^{210}Pb from the RAD disk, and they were collected in a polyethylene (PE) vial. An aliquot of 5 mL of this solution was mixed with 15 mL of Optifase Hisafe III. This vial was measured in a Wallac QUANTULUS for 100 min after waiting 2 hours to avoid photoluminescence phenomena. The RAD disk was transferred into another PE vial to which 20 mL of Hisafe III were added. This vial was measured for 100 min after waiting 8 hours to ensure correct impregnation of the RAD disk with the cocktail, which prevents a bad alpha beta classification and shifting of the spectra during the measurement (Fons-Castells et al., 2016).

Table 3
Chemical and geological characteristics of natural waters.

CODE	Type of water	Residue (g L^{-1})	Conductivity (mS cm^{-1})	pH	Reservoir geology
S_1	Groundwater	1.0	1.22	7.2	Granitic
S_2	Drinking water	0.5	0.70	7.0	Gypsum-bearing rocks
S_3	Drinking water	4.7	1.96	7.1	Basaltic
S_4	Groundwater	2.1	2.15	7.1	Old lignite mines
S_5	Surface	1.5	1.32	7.8	Detrital

Optimized Procedure

For all the samples, prepared mixtures, quality control material and natural samples, the following procedure was applied. A radium RAD disk was mounted in a vacuum filtration tramp and it was connected to a vacuum pump. Twenty millilitres of 2 mol L^{-1} HNO_3 were filtered through the RAD disk to condition it. Then, 5 L of sample that was acidified to pH < 2 with HNO_3 was filtered through the RAD disk, and the funnel was cleaned with 20 mL of 2 mol L^{-1} HNO_3. Afterwards, 7 mL of DHC 0.05 mol L^{-1} at pH 5.75 were used to elute ^{210}Pb from the RAD disk, and they were collected in a polyethylene (PE) vial. An aliquot of 5 mL of this solution was mixed with 15 mL of Optifase Hisafe III. This vial was measured in a Wallac QUANTULUS for 100 min after waiting 2 hours to avoid photoluminescence phenomena. The RAD disk was transferred into another PE vial to which 20 mL of Hisafe III were added. This vial was measured for 100 min after waiting 8 hours to ensure correct impregnation of the RAD disk with the cocktail, which prevents a bad alpha beta classification and shifting of the spectra during the measurement (Fons-Castells et al., 2016).

Data treatment

Two different data treatment were taken in consideration for the quantification of ^{226}Ra, ^{228}Ra and ^{210}Pb. In the first one, the activity of each radionuclide is determined by integration of the counts detected in each counting window. The counting windows defined were for RAD disk measurement, from channel 530 to 950 of the α-MCA for ^{226}Ra and from 20 to 300 of the β-MCA for ^{228}Ra. For the measurement of DHC eluted fraction, the chánnels from 60 to 460 of the β-MCA were integrated for determine the activity of ^{210}Pb. The uncertainty and the detection limits were calculated for this method following ISO 11929:2010 considering uncertainty on the sample preparation and elution yields and counting uncertainty.

To ensure a better separation between ^{228}Ra and ^{210}Pb a second data treatment based on a PLS model which was handled using MATLAB 2009b (MathWorks, Inc. Natic, MA, USA) and SMPLS algorithm with a Statistics Toolbox (Eigenvector Research) was tested.

A PLS model correlates an X-Block, which contains the predictors (spectra), with a Y-Block, which contains variables (activity of the radionuclides of interest). First, the model is created with the data from the calibration standards. Afterwards, the model can be used for determination of the massic activity of the radionuclides of interest using the spectra of each sample as predictors.

Three different PLS models were constructed to determine the ^{226}Ra, ^{228}Ra and ^{210}Pb. Each model was constructed using a specific region of all spectra obtained in the measurements of calibration standards.

The model for determining ^{226}Ra was constructed using channels 530 to 950 from the alpha region of the measurement of the RAD disk, while the model for the determination of ^{228}Ra using the channels from 20 to 300 of the beta region of the RAD disk measurement. In the case of the model for determining the ^{210}Pb, it was constructed using channels from 60 to 460 for the beta spectra of the DHC solution measurement.

The Y-Block's for all models were the activities of ^{226}Ra, ^{228}Ra and ^{210}Pb added to each calibration standard. The procedure for constructing PLS models for determining several alpha and beta emitters is fully described in (Fons-Castells et al., 2017).

The uncertainty of the predicted activities was estimated using simple Faber 96 method (Faber et al., 1996; Zhang & Garcia-Munoz, 2009).

To estimate the limit of detection for each model, a set of blanks (samples that do not contain the radionuclide of interest but that may contain other interfering radionuclides) were analysed according to the developed procedure. In other words, the set used to estimate the MDA of the method for ^{226}Ra contain mixtures spiked with ^{228}Ra and ^{210}Pb, but none were spiked with ^{226}Ra. The limit of detection for each radionuclide was evaluated as the arithmetic mean plus three times the standard deviation of each set (Fons-Castells et al., 2017).

In Fig. 1, the spectra of a mixture of ^{226}Ra, ^{228}Ra and ^{210}Pb for RAD disk and eluted fraction are represented together with the counting windows used for its determination for both treatments, window quantification and PLS model.

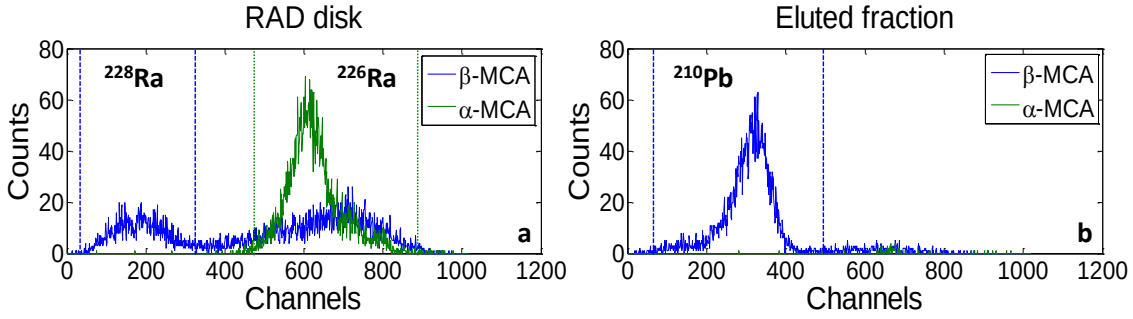

Fig. 1. Spectra of the RAD disk after the elution (a) and the eluted fraction of ^{210}Pb (b) for a spiked sample with ^{226}Ra, ^{228}Ra and ^{210}Pb together with the counting windows used for its determination.

Results and discussion

Preliminary studies

RAD disk retention

The retention of radium in one litre samples by the RAD disk was 97.5 ± 2.9 %. The retention of lead by the RAD disk was 88.4 ± 2.4 %. No significant differences in the retention between 1 L and 5 L samples were observed.

Elution

In Fig. 2, the accumulated extraction levels of ^{226}Ra and ^{210}Pb in function of the volume of the extracting solution are represented for each solution.

For E_2 and E_4 tests, the eluted radium was low with 20 mL of extracting solution, 1 % and 2 %, respectively.

However, the total eluted lead was clearly below 100 %. In the case of E_2, the maximum extraction was achieved at 8 mL of extracting solution and is evaluated as approximately 70 %. For test E_4, the lead extraction is constantly increasing, but the accumulated extraction obtained at 20 mL is approximately 90 %. In test E_1, the maximum extraction of ^{210}Pb was achieved with 10 mL of extracting solution and was evaluated as 85 %. With 10 mL of this solution, 1 % of ^{226}Ra was extracted from the RAD disk. Finally, for test E_3 99.2 % of lead and 1.4 % of radium were eluted with 7 mL of extracting solution. Considering these results, 7 mL of DCH 0.05 mol L^{-1} at pH 5.75 was selected as the extracting solution to elute ^{210}Pb from the RAD disk.

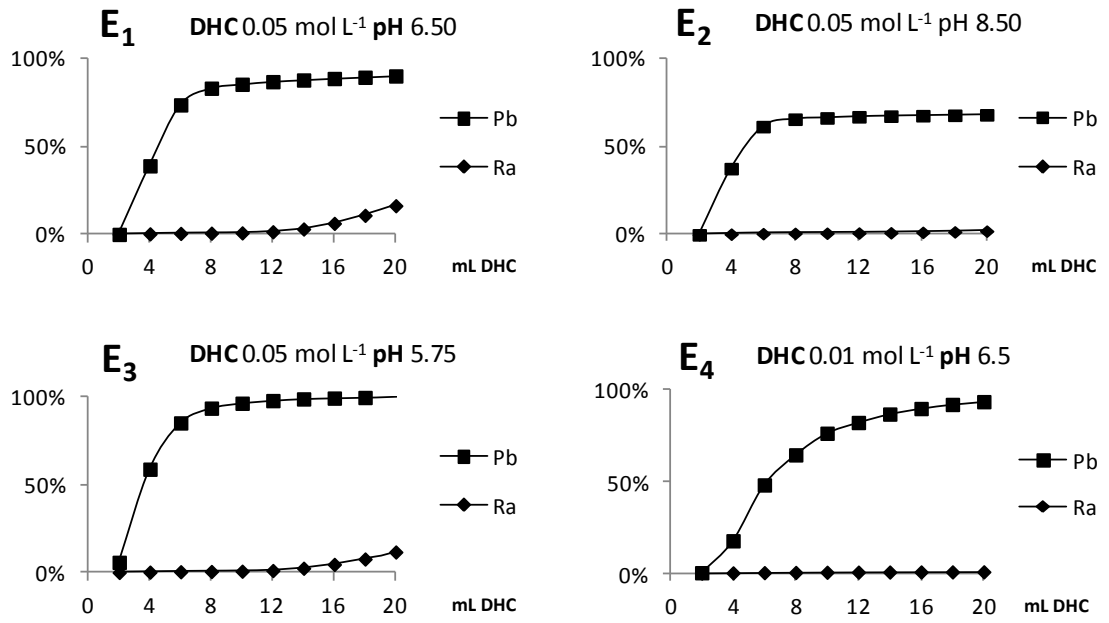

Fig. 2. Percentage of radium and lead eluted at increasing volumes of extracting solutions, E_1, E_2, E_3 and E_4.

Table 4
Quality parameters for ^{226}Ra, ^{228}Ra and ^{210}Pb.

	^{226}Ra	^{228}Ra	^{210}Pb
Initial retention (%)	97.5 ± 2.9	97.5 ± 2.9	88.4 ± 2.4
Eluted with DHC (%)	1.4 ± 0.7	1.4 ± 0.7	99.2 ± 1.0
Global retention (%)	96.1 ± 2.9	96.1 ± 2.9	-
Global elution (%)	-	-	87.7 ± 2.8
Counting efficiency (%)	98.7 ± 3.7	35.6 ± 2.1	92.6 ± 3.7

Counting efficiency

Table 4 summarizes the results obtained for retention, elution and efficiency for ^{226}Ra, ^{228}Ra and ^{210}Pb. Global retention refers to the radium retained on the RAD disk after the elution step, while global elution refers to the percentage of lead eluted regarding the initial amount.

Data treatment

The criterion used in this work for optimizing the number of latent variables (LVs) in PLS models was based on the minimization of the root mean square error of the cross validation (RMSECV). The PLS models for determining ^{226}Ra and ^{228}Ra were constructed with 3 LVs, while the one for ^{210}Pb was constructed with 1 LV. This is because ^{226}Ra and ^{228}Ra are determined using the spectra of the RAD disk where some decay produces ingrowth. These results make it more difficult to explain the spectra of the RAD disk; hence, more LVs are needed to achieve sufficient correlation between the initial variables (channels of the spectra) and activity of each isotope.

In Table 5, the coefficient of determination for the calibration (R^2) and root mean square error of the calibration for each model are shown. The coefficient of determination of the linear regression between the added activity and that determined by the model were for radium isotopes higher than 0.99 and for ^{210}Pb approximately 0.97.

Table 5
R^2 of the calibration and root mean square error of cross validation (RMSECV) for each radionuclide.

	R^2	*RMSECV*
^{226}Ra	0.997	0.128
^{228}Ra	0.997	0.076
^{210}Pb	0.973	0.102

The detection limits obtained were 0.02 Bq kg^{-1} for ^{226}Ra, 0.03 Bq kg^{-1} for ^{228}Ra and 0.02 Bq kg^{-1} for ^{210}Pb with 5 L for the sample volume and 100 min for the counting time. The detection limits obtained are sufficiently low to fulfil the request of the European Directive.

Prepared mixtures

Table 6 shows the massic activity spiked in the prepared mixtures described in Table 2, and the activity determined using both methods, window quantification

and PLS model for ^{226}Ra, ^{228}Ra and ^{210}Pb. The reported uncertainty is reported with a coverage factor k=2 and the bias between the determined activity and the added is showed in brackets.

As seen in Table 6, for both radium isotopes, the maximum bias obtained is observed in the samples with low massic activity (0.1 Bq kg^{-1}) and is evaluated as approximately 10 % for both methods. Furthermore, no effects of interference between radionuclides were observed because the bias observed in these mixtures is comparable to that obtained with pure standards.

On contrary, for ^{210}Pb determination a slightly higher bias is observed. For windows quantification, the bias registered goes up to 30 % for samples with ^{228}Ra and a low activity of ^{210}Pb (M_8) which is in part explained with 1.4 % of ^{228}Ra eluted in lead fraction. This high bias is partially solved using PLS quantification which removes ^{228}Ra contribution from ^{210}Pb fraction.

However, the bias obtained for ^{210}Pb determined by PLS model is higher than the obtained for radium isotopes. This fact is consistent with the results of R^2 for ^{210}Pb shown in Table 5, which is lower than that obtained for radium isotopes. The highest bias observed is approximately 20 % for one sample with low massic activity (0.2 Bq kg^{-1}). For the other of the samples, the bias was below 10 %.

The results confirm an improvement in the crosstalk between ^{228}Ra and ^{210}Pb that was achieved using two different separation strategies; the specific elution of ^{210}Pb with DHC and the use of a multivariate calibration (PLS) for quantifying both, eluted and retained fraction. For the quantification of radium isotopes, the bias is below than 10 % considering both methods while for ^{210}Pb the use of PLS models is need to reduce the bias below 20 %.

Quality control

The procedure was then validated for to determine the ^{226}Ra with the quality control provided from IAEA. The massic activity determined with the procedure was 18.6 ± 0.6 Bq kg^{-1} instead of the 17.9 ± 0.1 Bq kg^{-1} that was provided for the organizer.

Natural samples

The validated procedure was applied to determine the massic activity of ^{226}Ra, ^{228}Ra and ^{210}Pb in five natural samples, which may be used for human consumption. Table 7 shows the results obtained for these samples with their uncertainty. When the determined massic activity is below the limit of detection, it is shown as < MDA.

Table 6

Added massic activity of the prepared mixtures and massic activity determined with PLS method and window method with the relative bias between them in brackets for each mixture and radionuclide.

CODE	^{226}Ra			^{228}Ra			^{210}Pb		
	Added	*Det. Wind (Bias)*	*Det. PLS (Bias)*	*Added*	*Det. Wind (Bias)*	*Det. PLS (Bias)*	*Added*	*Det. Wind (Bias)*	*Det. PLS (Bias)*
	Bq kg^{-1}	*Bq kg^{-1} (%)*	*Bq kg^{-1} (%)*	*Bq kg^{-1}*	*Bq kg^{-1} (%)*	*Bq kg^{-1} (%)*	*Bq kg^{-1}*	*Bq kg^{-1} (%)*	*Bq kg^{-1} (%)*
M_1	1.00 ± 0.05	1.02 ± 0.15 (1 %)	0.96 ± 0.09 (-4 %)	-	< 0.06	< 0.03	0.96 ± 0.10	1.02 ± 0.15 (6 %)	0.98 ± 0.09 (3 %)
M_2	1.00 ± 0.05	0.95 ± 0.14 (-5 %)	0.97 ± 0.09 (-3 %)	-	< 0.06	< 0.03	0.19 ± 0.02	0.21 ± 0.03 (9 %)	0.20 ± 0.02 (6 %)
M_3	0.10 ± 0.01	0.11 ± 0.02 (10 %)	0.11 ± 0.02 (11 %)	-	< 0.06	< 0.03	0.99 ± 0.09	1.07 ± 0.16 (8 %)	0.95 ± 0.09 (-4 %)
M_4	0.11 ± 0.01	0.10 ± 0.02 (-5 %)	0.10 ± 0.01 (-2 %)	-	< 0.06	< 0.03	0.09 ± 0.01	0.10 ± 0.02 (12 %)	0.10 ± 0.01 (5 %)
M_5	1.01 ± 0.05	1.00 ± 0.15 (-1 %)	1.03 ± 0.09 (2 %)	0.12 ± 0.01	0.13 ± 0.02 (10 %)	0.12 ± 0.02 (1 %)	0.10 ± 0.01	0.12 ± 0.02 (15 %)	0.09 ± 0.01 (-6 %)
M_6	0.10 ± 0.01	0.09 ± 0.01 (-10 %)	0.10 ± 0.01 (0 %)	1.09 ± 0.06	1.13 ± 0.17 (4 %)	1.18 ± 0.10 (9 %)	0.02 ± 0.01	< 0.06	< 0.02
M_7	0.10 ± 0.01	0.09 ± 0.01 (-7 %)	0.10 ± 0.01 (-4 %)	0.11 ± 0.01	0.11 ± 0.02 (0 %)	0.12 ± 0.02 (9 %)	0.02 ± 0.01	< 0.06	< 0.02
M_8	-	< 0.04	< 0.02	1.14 ± 0.06	1.16 ± 0.17 (3 %)	1.23 ± 0.11 (8 %)	0.08 ± 0.01	0.12 ± 0.02 (33 %)	0.10 ± 0.01 (14 %)
M_9	-	<0.04	< 0.02	0.13 ± 0.01	0.13 ± 0.02 (5 %)	0.12 ± 0.02 (-4 %)	0.09 ± 0.01	0.10 ± 0.02 (17 %)	0.10 ± 0.01 (15 %)
M_{10}	0.10 ± 0.01	0.11 ± 0.02 (8 %)	0.10 ± 0.01 (-5 %)	0.13 ± 0.01	0.12 ± 0.02 (-5 %)	0.12 ± 0.02 (-5 %)	0.09 ± 0.01	0.11 ± 0.02 (21 %)	0.10 ± 0.01 (9 %)
M_{11}	1.02 ± 0.05	1.03 ± 0.15 (0 %)	1.03 ± 0.09 (1 %)	0.12 ± 0.01	0.14 ± 0.02 (13 %)	0.13 ± 0.02 (10 %)	0.15 ± 0.02	0.12 ± 0.02 (-20 %)	0.16 ± 0.02 (10 %)

Table 7
Massic activity of ^{226}Ra, ^{228}Ra and ^{210}Pb determined with the PLS method for the five natural samples described in Table 3.

CODE	**^{226}Ra** *Bq kg^{-1}*	**^{228}Ra** *Bq kg^{-1}*	**^{210}Pb** *Bq kg^{-1}*
S_1	< 0,02	< 0,03	< 0,02
S_2	< 0,02	< 0,03	< 0,02
S_3	0,51 ± 0.05	< 0,03	< 0,02
S_4	0,08 ± 0.01	< 0,03	< 0,02
S_5	0,19 ± 0.02	< 0,03	0,13 ± 0.02

As seen in Table 7, for all samples, the ^{228}Ra massic activity is below the detection limit. For ^{210}Pb, just S_5, has an activity that is higher than the detection limit, but it is below the derived level established by the European Directive. In the case of ^{226}Ra, S_3, S_4 and S_5 has higher activity than the detection limit, but S_3 has an activity that is greater than that established in the directive. With these results, all samples may be used for human consumption, except for S_3, due to the high ^{226}Ra level.

Conclusions

A procedure for rapidly and simultaneously evaluating ^{226}Ra, ^{228}Ra and ^{210}Pb based on separation using a radium RAD disk and LSC-PLS measurement has been described. This procedure combines the strength of the selective extraction of ^{210}Pb using DHC 0.05 mol L^{-1} at pH 5.75 from a RAD disk and multivariate calibration to avoid interference between ^{228}Ra and ^{210}Pb. Radium isotopes can be determined directly from the counting of the RAD disk and ^{210}Pb from the eluted fraction without PLS model obtaining similar biases. The procedure was validated and applied to determine three natural radionuclides in five water sources in Spain that have potential use as drinking water. Four of these sources were evaluated as suitable for human consumption, while the other one was close to the limit of the European Directive for ^{226}Ra.

Acknowledgements

The authors wish to acknowledge the Spanish Nuclear Safety Council for the project “Rápid methods for the simultáneous determination of alpha and beta emitters by LSC in wáter” the Spánish science and innovation ministry [grant number CTM2014-55191] and the Catalan government [grant number AGAUR 2014SGR1277]. Jordi Fons Castells also wishes to acknowledge the Spanish ministry of economy and competitively for the PhD grant FPI BES 2012-052590.

References

Cook M, Kleinschmidt R (2011) Simultaneous determination of ^{226}Ra and ^{228}Ra in water by liquid scintillation spectrometry. Aust J Chem 64:880-884

Council Directive 2013/51/Euratom of 22th October 2013 laying down requirements for the protection of the health of the general public with regard to radioactive substances in water intended for human consumption. Off J Eur Union L296:12-21

Ďureková A (1997) Contribution to the simultáneous determination of ^{228}Ra and ^{226}Ra by using 3M's EMPORE™ Radium Rad disks. J Radioanal Nucl Chem 223:225-228

Ďureková A, Ďurec F, Autxová L, Adámek P (1999) Determination of ^{226}Ra and ^{228}Ra in mineral and drinking waters using 3M's Empore™ radium Rad disks. Czech J Phys. 49:119-125

Eikenberg J, Tricca A, Vezzu G, Bajo S, Ruethi M, Surbeck H (2001) Determination of ^{228}Ra, ^{226}Ra and ^{224}Ra in natural water via absorption on MnO_2-coated discs. J Env Radioactiv 54:109-131

Eikenberg J, Beer H, Jäggi M (2014) Determination of ^{210}Pb and ^{226}Ra/^{228}Ra in continental water using HIDEX 300SL LS-spectrometer with TDCR efficiency trácing ánd optimized α/β-discrimination. App Radiat Isot. 93:64-69

Faber K, Kowalsku BR (1996) Prediction error in least square regression: Further critique in the deviation used in The Unscrambler. Chemom Intell Lab Syst. 34:283-292

Fons-Castells J, Tent-Petrus J, Llauradó M. (2017). Simultaneous determination of specific alpha and beta emitters by LSC-PLS in water samples. J Env Radioactiv 166:195-201

Fons-Castells J, Vasile M, Loots H, Bruggeman M, Llauradó M, Verrezen F. (2016). On the direct measurement of ^{226}Ra and ^{228}Ra using 3M Empore™ RAD disk by liquid scintillation spectrometry. J Radioanal Nucl Chem 309:1123–1131

Guogang J, Jing J, (2012). Determination of radium isotopes in environmental samples by gamma spectrometry, liquid sicintillation counting and alpha spectrometry: a review of analytical methodology. J Env Radioactiv 106:98-119

ISO 11929:2010 Determination of the characteristic limits (decision threshold, detection limit and limits of the confidence interval) for measurements of ionizing radiation Fundamentals and application

Mahani M, Ghomi SH, Mazloomifer A, Salimi B (2012) Application of multi-way partial least squares calibration for simultaneous determination of radioisotopes by liquid scintillation technique. Nucl Technol Radiar Prot 27(2) 125-130

Möbius S, Rakotoarisoa T, Lauria DC, Zafimanjato L (2006) Fast survey for key nuclides and group parameters in drinking water. LSC 2005, Advances in Liquid Scintillation Spectrometry. 149-156

Scapitta SC, Miller PW (1996) Evaluation of 3M EmporeTM RAD disk for radium determination in water. In: 42nd annual conference on bioassay, analytical and environmental radioactivity, San Francisco.

Schönhofer F, Maringer FJ (2006) The EU drinking water directive, the Austrian standard, and an ultra low-level liquid scintillation spectrometry approach for assuring compliance. LSC 2005, Advances in Liquid Scintillation Spectrometry. 1-11

Shabana EI, Qutub MMT, Kinsara AA (2015) Sensitivity and Precision of Determination of ^{210}Pb in Groundwater. Int J Water and Wastewater Treatment

Vajda N, LaRosa J, Zeisler R, Danesi P, Kis-Benedek, Gy (1997) A novel technique for the simultaneous determination of ^{210}Pb and ^{210}Po using crown ether. J Environ Radioactiv. 37:355-372

Vasile M, Loots H, Jacobs K, Verheyen L, Sneyers L, Verrezen F, Bruggeman M (2016) Determination of ^{210}Pb, ^{210}Po, ^{226}Ra, ^{228}Ra and uranium isotopes in drinking water in order to comply with the requirement of the EU 'Drinking Wáter Directive'. App Rádiát Isot 109:465-469

Vrecek P, Benedik L, Pihlar B (2004) Determination of ^{210}Pb and ^{210}Po in sediment and soil leachates and in biological materials using a Sr-resin column and evaluation of column reuse. App Radiat Isot 60:717-723

Wallner G (2002) Determination of ^{228}Ra, ^{226}Ra and ^{210}Pb in drinking water using liquid scintillation counting. LSC 2001, Advances in Liquid Scintillation Spectrometry. 269-274

Wallner G, Wagner R, Katzlberger C (2008) Natural radionuclides in Austrian mineral water and their sequential measurements by fast methods. J Environ Radioactiv. 99:1090-1094

Zhang L, Garcia-Munoz S (2009) A comparison of different methods to estimate prediction uncertainty using Partial Least Squares (PLS): A practitioner's perspective. Chemom Intell Lab Syst. 97:152-158

5.3. Discussion

From the results obtained in the two scientific papers from this chapter, it has to be mentioned that a procedure has been validated for the simultaneous determination of ^{226}Ra, ^{228}Ra and ^{210}Pb by means of solid phase extraction using a radium RAD disk and subsequent measurement by liquid scintillation spectrometry.

The first paper considers the feasibility of the direct measurement of radium isotopes from the RAD disk into the counting vial. The problems that entail the direct measurement are, on the one hand, that a shifting to channels of high energy of the spectra of ^{226}Ra is observed when the RAD disk is sequentially measured over time. On the other hand, the counts of ^{226}Ra (an alpha emitter) are misclassified in the beta multichannel until eight hours after the sample preparation.

SQP[E] was monitored during the first 20 hours after sample treatment, but no significant differences were detected.

We considered several hypotheses to explain the shifting of the spectrum and the misclassification issues.

On the one hand, we considered that radionuclides retained in the RAD disk may slowly migrate to the cocktail during the first hours of sample preparation. This may explain the better detection after eight hours without α/β misclassification and with no shifting of the spectrum. However, this hypothesis was rejected after separately measuring the cocktail from a sample prepared 20 hours before after removing the RAD disk. The RAD disk was also measured with a fresh cocktail. The results show that radium isotopes and decay products remain in the RAD disk while ^{222}Rn migrates to the cocktail.

On the other hand, assuming that the radionuclides of interest do not migrate to the cocktail, the aforementioned issues may be attributed to a slow impregnation of the RAD disk by the cocktail. In this way, while the RAD disk is impregnated, the transference of energy from the radionuclide is retained in the filter and the cocktail improves, which explain the differences in both spectra position and α/β classification changes. This hypothesis was proved by impregnating the RAD disk just after sample filtration by sucking the cocktail trough the filter. The results obtained with this experiment just after sample preparation are equivalent to those obtained by the usual procedure after eight hours. Furthermore, part of the ^{210}Pb retained on the RAD disk was eluted with the cocktail used to impregnate the RAD disk.

For the aforementioned reasons, the shifting and misclassification problems observed in the first hours after sample preparation may be explained by considering that the RAD disk needs a certain amount of time to become properly impregnated with cocktail. Hence, the evolution of the grade of RAD disk impregnation with cocktail interferes in the determination of radium.

Figure 7 depicts the evolution of the shifting of the ^{226}Ra spectra and its misclassification. The shifting is represented as the channel with the maximum number of counts, which increased during the first eight hours after the sample preparation. After that, the maximum in ^{226}Ra spectrum remains constant. The misclassification is represented as the ratio between beta and alpha counts. This decreases within the first five hours after sample preparation and remains constant after that.

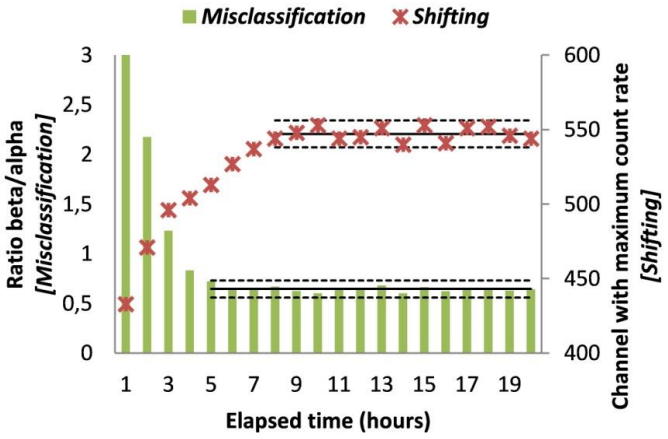

Figure 7. Evolution of misclassification and shifting of the spectra for a sample that contains ^{226}Ra.

Furthermore, the folding and the position of the RAD disk into the counting vial has been evaluated and, regarding the folding of the RAD disk, it has to be positioned along the LS vial walls to achieve maximum efficiency. No effect of the vials position inside the scintillation spectrometer was observed.

It was found that the complete elution of radium isotopes from the RAD disk can be performed by using basic ethylenediamine tetraacetic acid (EDTA) solutions. Though three different scintillation cocktails were tested, the volume required to achieve complete elution and concentration and media of EDTA required for this elution is not compatible with any cocktail. For this reason, to obtain a stable counting solution without phase separation, just an aliquot of the total volume used for the elution can be added into the counting vial to decrease the detection limit.

In addition, as lead isotopes are also retained in the RAD disk, the determination of ^{228}Ra is affected by the presence of ^{210}Pb, since both are beta emitters with close energies.

For this reason, several elution solutions at different dihydrogen ammonium citrate (DHC) concentrations and pH values were tested to determine the selective extract lead isotopes from the RAD disk. The optimal elution conditions were established as 0.05 mol L^{-1} of DHC at pH 5.75. In this way, radium isotopes, mainly ^{226}Ra and ^{228}Ra, were determined directly from the measurement of the RAD disk, while ^{210}Pb is determined from the fraction eluted with DHC. The results obtained in spiked mixtures containing ^{226}Ra, ^{228}Ra and ^{210}Pb for radium isotopes exhibit a bias of 10 % for both. However, for ^{210}Pb, some samples have a bias higher than 30 %. Even the contribution of ^{210}Bi—which increases in the eluted fraction from ^{210}Pb after the extraction is subtracted—may provide an explanation for the high bias observed.

For this reason, multivariate calibration by means of PLS models were applied for the determination of ^{226}Ra, ^{228}Ra in the RAD disk and ^{210}Pb in the eluted fraction. To achieve this quantification, a calibration set with spectra of single radionuclides at different levels of activity concentration was used. The results obtained show that the bias for radium isotopes does not significantly change and remain around 10 %. However, the bias observed in mixtures of radionuclides for ^{210}Pb decreases with this quantification method to 10 %.

From all this investigation, the prospered procedure was based on selective extraction of radium and lead isotopes by means of a 3M Empore™ Radium RAD disk. These 47 mm diameter filters are composed of crown ether covalently bounded to an inert substrate. In the optimized procedure, RAD disk are preconditioned by filtering 20 mL of 2 mol L^{-1} HNO_3. Afterwards, an aliquot from 1 to 5 L of sample acidified to pH lower than 2 with HNO_3 are filtered thought the RAD disk by using a vacuum filtering system. Lead isotopes are then eluted from the RAD disk. 7 mL of DHC 0.05 mol L^{-1} at pH 5.75 were collected in a polyethylene vial. This solution was mixed with 15 mL of Optifase Hisafe™ III and measured in a Wallac QUANTULUS for 100 min after waiting two hours to avoid photoluminescence phenomena. Besides this, the RAD disk was transferred into another PE vial to which 20 mL of Hisafe III was added. This vial was measured for 100 min after waiting eight hours to ensure correct impregnation of the RAD disk with the cocktail, which prevents a bad alpha/beta classification and shifting of the spectra during the measurement.

The detection limits of the procedure that uses 1 L of sample are 0.04 Bq kg^{-1}, 0.06 Bq kg^{-1} and 0.06 Bq kg^{-1} for ^{226}Ra, ^{228}R and ^{210}Pb, respectively.

This procedure has been validated with reference materials and has been used for quantification of drinking-water samples.

6. PARTIAL LEAST SQUARES REGRESSION APPLIED TO LIQUID SCINTILLATION SPECTROMETRY DECOMBOLUTION

Finally, the last step for the simultaneous determination of several isotopes from one single LS spectrum concerns the feasibility of PLS models to conduct this deconvolution. PLS models will be constructed by using LS spectra obtained by means of several procedures, such as those used to determine gross alpha and gross beta activities (described in the papers of Chapter 4) or those used to determine ^{226}Ra, ^{228}Ra and ^{210}Pb using RAD disk (described in the papers of Chapter 5). A database of spectra of the radionuclides listed in the Directive 2013/51/EURATOM at three levels of activity concentration and at different quenching levels was created to construct PLS models.

Simultaneous determination of specific alpha and beta emitters by LSC-PLS in water samples. J. Fons-Castells, J. Tent-Petrus, M. Llauradó. *Journal of Environmental Radioactivity* 166 (2017) pp. 195-201.

This paper studies the feasibility of PLS regression based on LS spectra with alpha/beta separation. A set of calibration spectra that include three replicates at three different activity concentrations for seven radionuclides was used to quantify prepared mixtures of these radionuclides and inter-comparison materials. Furthermore, we tested quantification using a PLS model in the presence of a radionuclide that was not include in the calibration model.

Effect of quenching on efficiency, spectra shape and alpha-beta discrimination in liquid scintillation spectrometry. J. Fons-Castells, V. Díaz, A. Badía, J. Tent-Petrus, M. Llauradó. Send for publication at *Applied Radiation and Isotopes.*

Since PLS models are based on the shape of spectra, and because these are highly affected by quenching, an exhaustive study was performed on the effects of colour and chemical quenching on efficiency, spectrum shape and alpha/beta separation using different alpha and beta emitters. The main objectives of this study were, on one hand, to evaluate the changes in alpha and beta spectra and to thereby determine which families of radionuclides present the same behaviour. On the other hand, a database of spectra of the studied radionuclides at different quenching levels was created to construct PLS models by using quenched standards to quantify quenched samples.

6.1. Simultaneous determination of specific alpha and beta emitters by LSC-PLS in water samples

Simultaneous determination of specific alpha and beta emitters by LSC-PLS in water samples

J. Fons-Castells *, J. Tent-Petrus, M. Llauradó

Chemical Engineering and Analytical Chemistry Department, University of Barcelona, Diagonal 647, 08028 Barcelona, Spain

*corresponding author: jordi.fons@ub.edu

Abstract

Liquid scintillation counting (LSC) is a commonly used technique for the determination of alpha and beta emitters. However, LSC has poor resolution and the continuous spectra for beta emitters hinder the simultaneous determination of several alpha and beta emitters from the same spectrum. In this paper, the feasibility of multivariate calibration by partial least squares (PLS) models for the determination of several alpha (^{nat}U, ^{241}Am and ^{226}Ra) and beta emitters (^{40}K, ^{60}Co, ^{90}Sr/^{90}Y, ^{134}Cs and ^{137}Cs) in water samples is reported. A set of alpha and beta spectra from radionuclide calibration standards were used to construct three PLS models.

Experimentally mixed radionuclides and intercomparision materials were used to validate the models. The results had a maximum relative bias of 25% when all the radionuclides in the sample were included in the calibration set; otherwise the relative bias was over 100% for some radionuclides.

The results obtained show that LSC-PLS is a useful approach for the simultaneous determination of alpha and beta emitters in multi-radionuclide samples. However, to obtain useful results, it is important to include all the radionuclides expected in the studied scenario in the calibration set.

Keywords: Alpha emitters, Beta emitters, Simultaneous quantification, Multivariant calibration, Partial least squares

Introduction

Liquid scintillation counting (LSC) is a meaningful technique for the determination of alpha and beta emitters. It has appropriate detection efficiency but poor resolution. This poor resolution hinders the simultaneous determination of different emitters in the same spectrum because of their spectra overlap. In the case of beta emitters this overlapping is unavoidable on account of their continuous spectra. However, several authors have achieved quantification of different isotopes through the same LSC spectrum. The first approach purposed was based on the definition of two counting zones (windows) for the determination of two isotopes ^{3}H and ^{14}C (Okita et al., 1957). The high energy window was assumed to contain just counts of the high energy isotope. However, the low energy window contains counts of both the low and the high energy isotopes. The counts of the high energy window are used to quantify the high energy isotope and then these counts are used to subtract the contribution of the high energy isotope in the low energy window (Okita et al., 1957).

This technique was improved by considering two windows with contributions of both isotopes (the inclusion method). Nowadays, the inclusion method is used for the determination of several pairs of isotopes such as ^{55}Fe and ^{59}Fe (Viteri and Kohaut, 1997), ^{3}H and ^{14}C (Shaffer and Langer, 2007) or ^{32}P and ^{33}P (Nakanishi et al., 2009).

Another method used to determine the composition of binary samples is based on the SIS (spectral index of the sample). The SIS is the center of mass of the spectra and it is specific for a radionuclide in a constant level of quenching. In a binary sample the SIS is a linear combination of the SIS of pure radionuclide standards. This method was used to determine ^{35}S and ^{32}P (Noor et al., 1995), and ^{3}H and ^{14}C (Noor et al., 1996).

A further evolution was based on the definition of three windows to determine two isotopes (three over two fitting and digital overlay technique). In general, by this technique several isotopes could be determined by using a number of windows greater than the number of isotopes. The digital overlay technique also permits quench correction. This technique was described in patents (Rundt and Kouru, 1989, 1992). Although it allows the quantification of radionuclide mixtures, it is typically used to correct quenching effects in single isotopic samples (Kim et al., 2006; Hueber-Becker et al., 2007).

The advances in computation also permitted the development of new techniques. Some authors quantified several isotopes using the same spectra by deconvolution techniques. Software was

developed and applied to deconvolute complex spectra from pure spectra standards taking into account the quenching of the sample and allowing determination of up to six isotopes (Kashirin et al., 2000; Malinovsky et al., 2002). Pure spectra standards were used to resolve ^{85}Sr, ^{90}Sr and ^{90}Y in complex mixtures by fitting (Altzitzoglou, 2008). Other approaches are based on fit the spectrum of the sample to a linear combination of tailed Gaussian functions (Nebelung and Baraniak, 2007; Nebelung et al., 2009) or to a Fourier series (Remetti and Sessa, 2011; Remetti and Franci, 2012).

Another approach to fulfill the aim of quantify several isotopes by the same scintillation spectra is based on multivariate calibration methods. The use of partial least squared (PLS) to avoid interference phenomena and quantify individual isotopes in composite spectra has been studied for solid scintillation (Roig et al., 1999) and for plastic scintillation (Bagan et al., 2011). For LSC, a model based on multi-way PLS with energy channels as the primary variable and cocktail sample ratio as the secondary variable was developed to determine the ^{235}U/^{238}U isotope ratio (Mahani et al., 2012).

There were also improvements in the data preprocess, such as the selection of channels to construct the PLS model selected by means of an artificial neural network using a genetic algorithm (Mahani et al., 2007).

In this work the feasibility of multivariate calibration by partial least squares (PLS) models based on LSC spectra with alpha beta discrimination is studied in order to determine simultaneously different alpha (^{nat}U, ^{241}Am and ^{226}Ra) and beta emitters (^{40}K, ^{60}Co, ^{90}Sr/^{90}Y, ^{134}Cs and ^{137}Cs) in water samples without radiochemical separation. The isotopes were selected to cover a wide energy range of both alpha emissions (from 4.20 MeV of ^{238}U to 5.49 MeV of ^{241}Am) and beta emissions (from 0.31 MeV of ^{60}Co to 2.28 MeV of ^{90}Y). The PLS was based on a reduction of the variables by the use of new coordinate system performed from new axes called latent variables (LV), which are linear combinations of the original variables.In this study the original variables were counts in each channel of the multichannel analyzer (MCA). These LVs are chosen as the ones to explain the maximum correlation between original variables and the activity of each isotope. The weights for each variable to each LV are called loadings and the weights for each LV to each sample are called scores.

Material and methods

Detector

An ultra-low level LSC spectrometer (1220 QUANTULUS, Wallac (Turku, Finland)) with alpha-beta pulse shape ana-

lyzer (PSA) and logarithmic amplification was used. The quenching control of the samples was performed by means of the Spectral Quench Parameter of the External Standard (SQP[E]) with a source of ^{152}Eu.

Reagents

High capacity scintillation cocktail Ultima Gold AB supplied by Perkin Elmer was used throughout the work. Radioactive solutions were prepared diluting a weighed amount of the following radioactive liquid standards: ^{60}Co 73.9 ± 1.1 kBq g^{-1}, ^{134}Cs 37.0 ± 0.6 kBq g^{-1}, ^{nat}U 0.96 ± 0.03 kBq g^{-1}, ^{226}Ra 0.89 ± 0.03 kBq g^{-1} and ^{236}U 0.76 ± 0.02 kBq g^{-1} supplied by Eckert & Ziegler (Valencia, USA); ^{90}Sr 4.07 ± 0.03 kBq g^{-1} standard in secular equilibrium with ^{90}Y supplied by Amersham International (Braunschweig, Germany); and ^{137}Cs 849 ± 6 kBq g^{-1} and ^{241}Am 43.9 ± 0.7 Bq g^{-1} standard supplied by CERCA LEA (Paris, France). ^{40}K solutions were prepared from dry salt supplied by Merck (Berlin, Germany). Its activity was calculated by applying the natural abundance of ^{40}K and its semidisintegration period. All these solutions are traceable to NIST.

Samples

Radionuclide calibration standards

For each radionuclide, three aliquots of 500 mL were labeled at different activity levels by dilution of the standard with HNO3 1%. Table 1 shows the spiked activity and its uncertainty with a coverage factor k = 2 for each sample. The spectra obtained from the analysis of these radionuclide calibration standards were treated and used to construct the models.

Linear combination of radionuclide calibration standards spectra

By means of linear combinations among radionuclide calibration standards spectra, 57 simulated composite spectra were calculated. All the possible combinations of isotopes, from binary samples to a six isotope mixture were calculated.

Table 1
Massic activity of the 24 radionuclide calibration standards and their uncertainty.

Radionuclide	*High activity (Bq kg^{-1})*	*Intermediate activity (Bq kg^{-1})*	*Low activity (Bq kg^{-1})*
^{40}K	10.84 ± 0.54	8.49 ± 0.42	1.88 ± 0.09
^{60}Co	53.10 ± 1.59	26.83 ± 0.81	10.14 ± 0.30
^{90}Sr/^{90}Y*	42.83 ± 0.64	21.43 ± 0.32	8.18 ± 0.12
^{137}Cs	41.99± 0.63	21.04 ± 0.32	6.62 ± 0.10
^{nat}U**	10.40 ± 0.62	5.19 ± 0.31	2.24 ± 0.13
^{241}Am	12.74 ± 0.38	6.23 ± 0.19	1.25 ± 0.04
^{134}Cs***	61.23 ± 1.84	30.32 ± 0.90	12.18 ± 0.36
^{226}Ra***	10.00 ± 0.50	5.20 ± 0.26	0.90 ± 0.04

** Activity of ^{90}Sr (the samples also contains ^{90}Y in secular equilibrium).*
*** Activity of ^{234}U + ^{238}U (the sample also contains ^{234}Th and ^{234m}Pa in secular equilibrium).*
**** These standards were used to calibrate the models for the determination of quality control samples*

Table 2
Massic activity added for each radionuclide in mixtures of radionuclides, along with their uncertainty.

Code	*^{40}K (Bq kg^{-1})*	*^{60}Co (Bq kg^{-1})*	*$^{90}Sr/^{90}Y$ (Bq kg^{-1})*	*^{137}Cs (Bq kg^{-1})*	*^{nat}U (Bq kg^{-1})*	*^{241}Am (Bq kg^{-1})*	*^{134}Cs (Bq kg^{-1})*
BETA	14.59±0.73	30.55±0.92	23.18±0.35	16.43±0.25	-	-	-
MIX	-	-	23.85±0.36	16.38±0.25	6.12±0.37	5.42±0.16	-
INTERF	13.57±0.68	29.99±0.90	23.06±0.35	16.34±0.25	6.32±0.38	5.22±0.16	20.46±0.61

Each linear combination was performed by addition, using a random replicate of the intermediate activity solution for n isotope and subtracting n-1 blank spectra. The actual activity for each isotope in each spectrum was obtained also by addition.

These simulated spectra were used to make a preliminary test of the model and to estimate the minimum detectable activity (MDA) for each isotope.

Experimentally mixed radionuclides

Three mixtures of radionuclides of 500 mL were prepared with a massic activity near to the intermediate activity of the radionuclide calibration standards (Table 1). The BETA mixture contained four beta emitters that covered a wide range of beta emissions (from 0.31 MeV of ^{60}Co to 2.28 MeV of ^{90}Y). The MIX mixture contained both alpha and beta emitters. The INTERF mixture contained the six radionuclides studied (^{40}K, ^{60}Co, ^{90}Sr/^{90}Y, ^{137}Cs, ^{nat}U and ^{241}Am) and ^{134}Cs (0.66 MeV maximal energy), an intermediate energy beta emitter not included in the calibration set and used here as an interferent. Table 2 shows the spiked massic activities and uncertainties with a coverage factor k = 2 for each composite.

The spectra obtained from the analysis of these mixtures of radionuclides were used to evaluate the bias of the PLS model.

Quality control and intercomparison materials

In order to verify the procedure to construct the PSL models, an intercomparison exercise was done and a quality control material was analyzed. However, these materials contained other radionuclides than the used for model calibration, and hence, two new models had to be created.

Table 3
Massic activity of IAEA-TEL-2014-03 sample 03.

	IAEA-TEL-2014-03 sample 03	
	Activity (Bq kg^{-1})	*Uncertainty (Bq kg^{-1})*
^{90}Sr/^{90}Y	24.5	0.2
^{134}Cs	26.3	0.2
^{137}Cs	19.6	0.1
^{226}Ra	17.9	0.1
^{nat}U*	5.48	0.04
^{241}Am	20.0	0.1

The materials used were IAEA-TEL-2014-03 sample 03, a spiked water quality control material with a known massic activity (see Table 3), and IAEA-TEL-2015-03 sample 01, spiked water with an unknown activity of anthropogenic gamma emitters and ^{90}Sr.

Analytical procedure

The analytical procedure used was based on evaporating to dryness a 100 mL aliquot of the sample. The precipitated obtained is dissolved in 10 mL of deionised water acidified by HCl to pH = 1.5. Afterwards 8 mL aliquot of this dissolution is mixed with 12 mL of Ultima Gold AB in PE vials. The vial is counted with the ultra-low level liquid scintillation spectrometer QUANTULUS 1220, after 2 h remaining in darkness to avoid photoluminescence phenomena. The vial was counted using α/β discrimination counting mode after 2 h remaining in darkness to avoid photoluminescence phenomena.

The calibration of PSA (Pulse Shape Analyzer) used in the alpha/beta discrimination was performed by means of a misclassification study with ^{236}U as pure alpha emitter and ^{40}K as pure beta emitter (Fons et al., 2013). The optimal discrimination was obtained at PSA value of 100. In these conditions the interference was below 6% for both alpha and beta emitters. For all the samples analyzed the quenching remained constant and SQP[E] values were between 790 and 800. This minimum variation did not affect the spectral response. However, for natural water samples, the presence of some metallic ions (Ni^{2+}, Fe^{3+}) or organic matter may cause quenching effects. In that case, the PLS model would have to be constructed with single radionuclide calibration standards at different levels of quenching.

Data treatment

The data treatment and PLS model were handled in MATLAB2009b version (MathWorks, Inc., Natick, MA, USA) using SIMPLS algorithm by means of Statistics Toolbox (Eigenvector Research). The aim of the PLS was to correlate a matrix of predictors (XBlock) with a matrix of measured activities of each radionuclide (YBlock) for the different samples. In order to achieve the best correlation and improve the prediction power of the model, several pretreatments had to be done. Radionuclide calibration standard spectra, for ^{40}K, ^{60}Co, $^{90}Sr/^{90}Y$, ^{137}Cs, ^{nat}U and ^{241}Am, were stored by rows in a matrix (XBlock). Each row contained 2040 variables, 1020 concerning the counts of the channels in beta spectrum and 1020 concerning the counts of the channels in alpha spectrum. It should to be noted that in both alpha and beta spectrum the corresponding blank was subtracted. In order to minimize the computation time and to reduce the complexity of the model, the region of interest (ROI) for alpha

(454-915) and beta (75-895) spectra were selected. This procedure entails a reduction from 2040 to 1196 variables. Afterwards, each spectrum in the matrix was smoothed using a Savitzky-Golayfilter with polynomial order 1 and a window width of 31. Before the PLS model construction this matrix was mean centered. At the end of this treatment, XBlock was a matrix of 54 rows, one for each radionuclide calibration standard spectra (6 radionuclides per 3 levels of activity per 3 replicates), and 1196 columns (containing the counts of alpha and beta ROI). For each radionuclide calibration standard, the activities in the counting vial of each radionuclide were stored by columns in another matrix (YBlock). Each row contained the activity of each radionuclide (^{40}K, ^{60}Co, ^{90}Sr/^{90}Y, ^{137}Cs, ^{nat}U and ^{241}Am) for each spectrum.

Since the analytical procedure entails a sample concentration, the activity in the vial was calculated from the values of massic activity concentration (Table 1) by means of Equation (1). YBlock was a matrix of 54 rows (one for each spectra) and 6 columns (containing the activity for each radionuclide).

$$A^i_{vial} = \frac{A^i_{sample} * m_{sample} * m_{add}}{m_{dis}} \quad (1)$$

where;

A^i_{vial} is the activity of the radionuclide i introduced into the counting vial in Bq.

$A^i_{standard}$ is the added activity of the radionuclide i in the radionuclide calibration standards corrected at measure date in Bq kg^{-1}.

$m_{standard}$ is the mass of radionuclide calibration standard evaporated in kg.

m_{dis} is the mass of solution after the precipitate dissolution in kg.

m_{add} is the mass of the aliquot added in the vial in kg.

The added activity for each linear combination is also a linear combination of the activities of the radionuclide calibration standards used to generate the spectrum. The same data treatment used for reference radionuclide spectra was applied for the linear combinations of reference radionuclide standards and the experimentally mixed radionuclides.

Optimization of the number of latent variables

One of the critical points in a PLS model construction is the determination of the optimal number of latent variables (LVs) used to construct it. In this work, the criterion to select the number of LV was based on the root mean square error of cross validation (RMSECV). The number of LV was sequentially increased until the last addition did not improve the RMSECV. The cross validation was performed by means of the 'venetian blinds' algorithm with seven data splits (Rubingh et al., 2006).

Fig. 1 shows the RMSECV for each radionuclide against the number of LV. As can be seen this error decreased in few LV for some radionuclides but 6 LV were needed to reduce the RMSECV for all radionuclides below an acceptable threshold (0.1%).

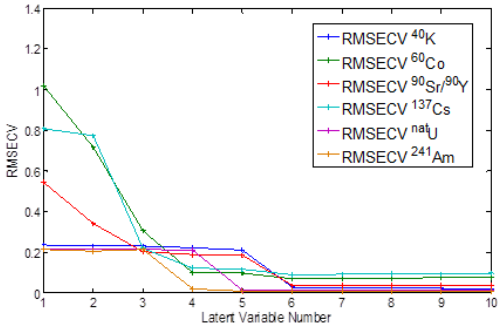

Fig. 1. Root mean square error of cross validation vs. latent variable number for each radionuclide.

Selectivity ratio

Selectivity ratio was calculated as the ratio between explained and residual variance of the spectral variables and proves useful to identify which variables are the most important in the discrimination of groups of samples (Rajalahti et al., 2009). For this reason, selectivity ratios spectra for ^{90}Sr/^{90}Y, ^{nat}U and ^{241}Am are plotted in Fig. 2. As can be seen the most important predictors for this radionuclides did not overlap, and have high maximum values (over 200). For the alpha emitters, the most important variables for the discrimination exactly correspond to the shape of their spectra. For ^{90}Sr/^{90}Y the selectivity ratio spectrum matches with the channels of higher energy in beta spectrum and in the higher energy of alpha spectrum corresponding to the misclassified counts of ^{90}Y.

However, for the other beta emitters (^{40}K, ^{60}Co and ^{137}Cs) the higher selectivity ratio was in all cases below 1, and they overlapped. For this reason a higher interference for these beta emitters is expected than for ^{90}Sr/^{90}Y and the alpha emitters. In Fig. 3 shows the spectrum of selectivity ratio for ^{40}K, ^{60}Co and ^{137}Cs.

In summary, ^{40}K, ^{60}Co and ^{137}Cs may be more affected by interference than ^{90}Sr/^{90}Y, ^{nat}U and ^{241}Am.

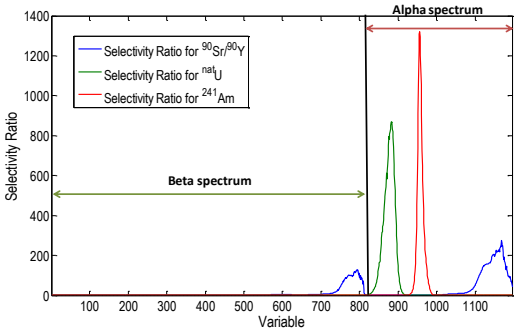

Fig. 2. Spectrum of selectivity ratio for ^{90}Sr/^{90}Y, ^{nat}U and ^{241}Am.

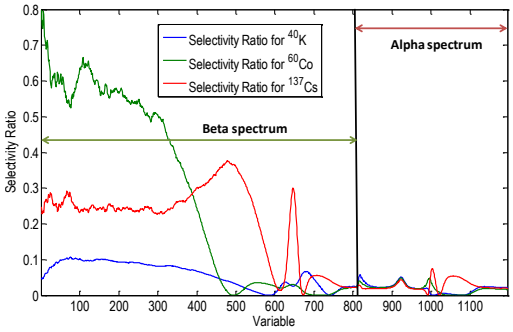

Fig. 3. Spectrum of selectivity ratio for ^{40}K, ^{60}Co and ^{137}Cs.

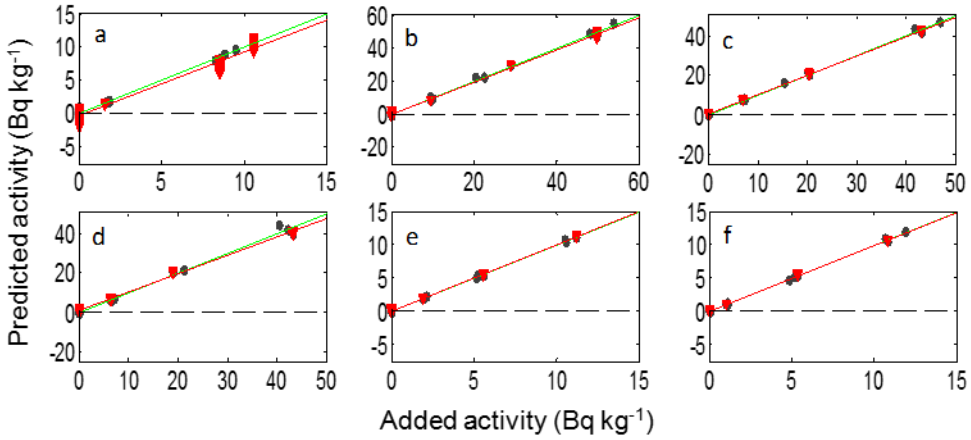

Fig. 4. Determined activity vs added activity for radionuclide calibration standards spectra (in black) and its linear combination (in red) for ^{40}K (a), ^{60}Co (b), ^{90}Sr/^{90}Y (c), ^{137}Cs (d), natU (e), and ^{241}Am (f).

Results and discussion

Validation with simulated spectra

Before testing the PLS model with experimentally mixed radionuclides, the model was tested with simulated composite spectra in order to evaluate the prediction error and the minimum detectable activity (MDA).

The activity of the six radionuclides studied was determined by the PLS model for each of the 54 simulated composite spectra. Linear regressions represented on Fig. 4 show the relation between the added activity and the determined using the model for the six radionuclides studied. The black dots represent cross validation of the radionuclide calibration standards, and the red dots are from the linear combination of standards spectra.

In Table 4 coefficient of determination of the calibration (R^2), root mean square error of cross validation (RMSECV) and root mean square error of prediction of linear combination standards spectra (RMSEP) are shown. Coefficient of determination of the linear regressions between determined and added activities were 0.99 or greater for all the radionuclides, so the model can determinate the activity of the radionuclide calibration standards used to create them. Furthermore, focusing the attention on RMSECV and RMSEP, we can see that clearly ^{nat}U and ^{241}Am are the radionuclides that were better explained by the model. Both have RMSECV around 0.1 and RMSEP below 0.2.

For ^{90}Sr/^{90}Y, the other radionuclide pair that had a high and non overlapped selectivity ratio values, and for ^{40}K, the error for cross validation and for prediction was higher than that obtained for the alpha emitters.

Table 4
R^2 of the calibration, RMSECV and RMSEP for each radionuclide.

Radionuclide	*R^2*	*RMSECV*	*RMSEP*
^{40}K	0.990	0.336	0.882
^{60}Co	0.997	0.865	1.328
^{90}Sr/^{90}Y	0.999	0.457	0.633
^{137}Cs	0.993	1.092	1.574
^{nat}U	0.999	0.119	0.175
^{241}Am	0.999	0.086	0.160

For ^{60}Co and ^{137}Cs, the errors for cross validation (around 1) and prediction of linear combination of standard spectra (around 1.5) were the highest. For this reason, it was expected that there would be more interference in the quantification of mixtures of radionuclides for ^{60}Co and ^{137}Cs.

Minimum detectable activity

In order to estimate the minimum detectable activity (MDA) for each radionuclide, the 57 linear combination of standard spectra were quantified by the model. The MDA for each radionuclide was established as the arithmetical mean plus two times the standard deviation of the determined activity for the radionuclide considered in the linear combination of standard spectra which was not actually present. To illustrate this, in Fig. 5, a wide view of Fig. 4c is plotted. The variability on activity determined of ^{60}Co in linear combinations that did not contain such radionuclide (e.g. linear combination of radionuclide calibration standard spectra of ^{40}K + ^{137}Cs + ^{241}Am), was used to estimate the MDA.

Table 5 shows the MDA estimated following the aforementioned criteria in the vial and in the sample, taking into account the concentration pretreatment of the samples.

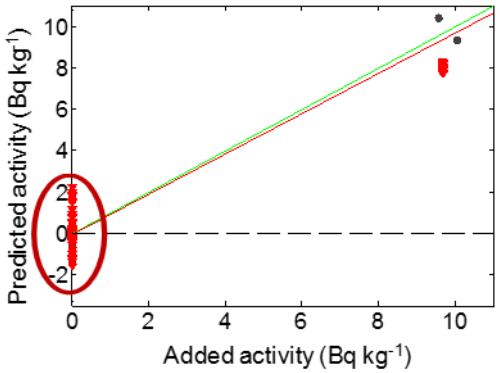

Fig. 5. Wide view of Fig. 4c: the determined activity vs added activity for reference radionuclide calibration standards (black) and its linear combination (red) for ^{60}Co.

Validation with experimentally mixed radionuclides

After estimation of the MDA, the three mixtures of radionuclides (BETA, MIX and INTERF) were analyzed in triplicate, following the same procedure as for the reference standards. The spectra obtained from this analysis were pretreated in the same way as the reference radionuclide calibration standards, and the activities of the mixtures were determined using the PLS model described above.

Table 5
MDA in the vial and in the sample for each radionuclide for model A.

	MDA (Bq/vial)	*MDA (Bq/kg)*
^{40}K	0.074	0.92
^{60}Co	0.123	1.54
^{90}Sr/^{90}Y	0.034	0.42
^{134}Cs	-	-
^{137}Cs	0.095	1.19
^{nat}U	0.023	0.28
^{241}Am	0.013	0.15

Table 6
Activity added in the vial, activity determined with model based on measurement of the mixture and relative bias for each mixture and radionuclide.

	BETA			*MIX*			*INTERF*		
	Added (Bq kg^{-1})	*Predicted (Bq kg^{-1})*	*Rel. Bias*	*Added (Bq kg^{-1})*	*Predicted (Bq kg^{-1})*	*Rel. Bias*	*Added (Bq kg^{-1})*	*Predicted (Bq kg^{-1})*	*Rel. Bias*
^{40}K	14.6 ± 0.7	16.2 ± 0.7	11.0%	-	< 0.9	-	13.6 ± 0.7	12.3 ± 0.4	-9.1%
^{60}Co	30.6 ± 0.9	34.2 ± 0.7	12.0%	-	< 1.5	-	30.0 ± 0.9	30.4 ± 0.9	1.7%
^{90}Sr/^{90}Y	23.2 ± 0.4	22.1 ± 0.6	-4.6%	23.9 ± 0.4	23.8 ± 0.3	0.4%	23.1 ± 0.4	23.8 ± 1.2	3.7%
^{134}Cs	-	-	-	-	-	-	20.5 ± 0.6	-	-
^{137}Cs	16.4 ± 0.3	20.4 ± 1.0	24.4%	16.4 ± 0.3	20.1 ± 0.8	23.5%	16.3 ± 0.3	35.2 ± 1.0	115.8%
^{nat}U	-	< 0.3	-	6.1 ± 0.4	6.0 ± 0.2	-0.7%	6.3 ± 0.4	5.9 ± 0.1	-6.4%
^{241}Am	-	< 0.2	-	5.4 ± 0.2	5.3 ± 0.1	-1.3%	5.2 ± 0.2	5.1 ± 0.2	-2.3%

In Table 6 the activity added into the vial, the activity determined from the measured spectra by means of PLS model and the relative bias for each mixture and each radionuclide is shown. For the activity added, the uncertainty with a coverage factor k = 2 is given. For the determined activity the uncertainty corresponds to standard deviation between the three replicates analyzed.

As can be seen in Table 6, the maximum relative bias for ^{40}K and ^{60}Co was around 10% in all the mixtures. For ^{137}Cs the relative bias was around 25% for BETA and MIX mixtures. For the mixture INTERF, which contains 20 Bq kg^{-1} of ^{134}Cs, the relative bias of ^{137}Cs was higher than 100%. Paying attention to the determined activity of ^{137}Cs in the INTERF mixture (35.2 ± 1.0 Bq kg^{-1}), we can see that there is no significant difference between it and the sum of ^{134}Cs and ^{137}Cs (36.7 ± 1.3 Bq kg^{-1}). Hence, it can be deduced that all the contribution of ^{134}Cs is miss-classified as ^{137}Cs, and it does not affect the quantification of the other radionuclides in the mixture.

In the case of ^{90}Sr/^{90}Y the relative bias was below 5% in the three mixtures. It should be noted that this better quantification for ^{90}Sr/^{90}Y compared to ^{40}K and ^{60}Co is caused by the high energy ^{90}Y that is counted in a region without interferents. For this reason, even in a mixture with an interferent not include in the calibration set, the error in the quantification of ^{90}Sr/^{90}Y remains below 5%.

For alpha emitters ^{nat}U and ^{241}Am, the relative bias was around 5%. Weak interference between alpha and beta emitters is reported due to the optimization of the PSA and because of the interference of ^{90}Y in alpha spectrum does not overlap with alpha peaks. The interference between both emitters is also weak for two reasons. The first one is the significant difference in the energy emission, close to 1 MeV, greater than the resolution at full width at half maximum of Quantulus 1220 (about 300 keV at best) for alpha

peaks (Quantulus 1220 Instrument Manual, 2002). The other reason is the improvement of the quantification by means of multivariate calibration instead of the classical window counting. Regarding MDA, the activity determined for the radionuclides that are not actually present in a mixture (^{nat}U and ^{241}Am in BETA mixture and ^{40}K and ^{60}Co for MIX mixture) were in all cases below the MDA and are reported in Table 6 as <MDA. This confirms that the method used to estimate the limit of detection is useful for our purpose.

Validation with quality control samples

Another two models were constructed following the procedure described above in order to be tested with natural samples. The first one includes ^{134}Cs in order to solve the problem of misclassification between ^{134}Cs and ^{137}Cs, observed in experimentally mixed radionuclides. The new model was constructed with 7 LV and the detection limits were slightly higher. This model was tested in an intercomparison (IAEA-TEL-2015-03 sample 01). The activities for each radionuclide reported by the organizer, determined using the PLS model and the performance statistics of the intercomparison are shown in Table 7. For the other radionuclides the activities determined were in all the cases below the detection limit. The relative bias between the activity determined using the PLS model and the value reported by the organizer was below 15% for ^{90}Sr/^{90}Y, ^{134}Cs and ^{137}Cs. To determine the activity in the quality control material IAEATEL- 2014-03 sample 03, a third model was constructed using the reference radionuclide calibration standards of ^{90}Sr/^{90}Y, ^{134}Cs, ^{137}Cs, ^{nat}U and ^{241}Am. Furthermore, spectra of ^{226}Ra were included in the model calibration. It has to be pointed out that samples have to be strictly measured just after 2 h of sample treatment. Otherwise, the ingrowth of the progeny of ^{226}Ra may interfere with the measurement.

Although, it is important delay the measurement 2 h after sample treatment to avoid photoluminescence phenomena.

Table 7
Activity determined and reported by the organizer and performance statistics for IAEA-TEL-2015-03 sample 01.

	Organizer		***Predicted***		***Perfomance statistics***		
	Activity (Bq kg^{-1})	*Uncertainty (Bq kg^{-1})*	*Activity (Bq kg^{-1})*	*Uncertainty (Bq kg^{-1})*	*Rel. Bias*	*Robust SD*	*z-score*
^{90}Sr/^{90}Y	29.6	0.8	34.1	3.4	15 %	3.0	1.5
^{134}Cs	30.0	0.9	31.9	3.2	6 %	1.8	1.1
^{137}Cs	30.1	0.9	32.9	3.3	10 %	1.0	2.8

Table 8
Activity determined and certified by the organizer and relative bias for the quality control material IAEA-TEL-2014-03 sample 03.

	IAEA-TEL-2014-03 sample03		
	Certified (Bq kg^{-1})	*Predict (Bq kg^{-1})*	*Rel. Bias*
^{90}Sr/^{90}Y	24.5 ± 0.2	22.60 ± 2.3	-8 %
^{134}Cs	26.3 ± 0.2	31.6 ± 3.2	20 %
^{137}Cs	19.6 ± 0.1	15.2 ± 1.5	-22 %
^{226}Ra	17.9 ± 0.1	15.2 ± 1.5	-15 %
^{nat}U*	5.48 ± 0.04	6.3 ± 0.6	14 %
^{241}Am	20.0 ± 0.1	17.0 ± 1.7	-15 %

**sum of ^{234}U and ^{238}U*

In this case, the model was constructed with 6 LV and the detection limits obtained were comparable with the obtained for the other models.

The activities determined with the PLS model, the values certified by the organizer and the relative bias are shown in Table 8.

For this sample, the precision of the models calculated as relative bias for all the radionuclides is around 20%.

Conclusions

A PSL model for LSC spectrawas proposed for the determination of ^{40}K, ^{60}Co, ^{90}Sr/^{90}Y, ^{137}Cs, ^{nat}U and ^{241}Am. The 6 LV model was validated with simulated composite spectra and good correlations between the added activity and activity determines using the PLS model was obtained (correlation coefficient above 0.99). By evaluating the variability on the activity determined for a radionuclide in linear combinations that do not contain this radionuclide, the MDAs were estimated. This estimation proved useful for our purpose since prediction of radionuclides not included on a mixture was always below the MDA. The influence of interferents was also tested by measuring a sample with all the radionuclides included in the model and ^{134}Cs. In this case the prediction relative bias for all the radionuclides excluding ^{137}Cs was not change. For ^{137}Cs the relative bias goes over 100% because all the ^{134}Cs was misclassified as ^{137}Cs. For this reason, it is important include all the expected radionuclides for the studies scenario in the calibration set.

With the same procedure two other models were constructed and validated with an intercomparision exercise and a quality control material. As is expected, the increased number of radionuclides in the sample decreased the precision of the method. However, the bias obtained for these reference materials was for all the radionuclides below 25%. For the tested cases, the PLS model allowed relative bias for ^{nat}U, ^{241}Am, ^{226}Ra and ^{90}Sr/^{90}Y was below 15%, around 10% for ^{40}K and ^{60}Co and near to 25% for ^{137}Cs. However, these results may be affected by the number of alpha or beta emitters and their proportions in the sample.

Acknowledgements

The authors would like to thank the financial support of the Catalan Government (AGAUR2014SGR1277), the Spanish Government (CYCIT contract

CTM2011-27211) and the Spanish Nuclear Safety Council (project "Rapid methods for the simultaneous determination of alpha and beta emitters by liquid scintillation spectrometry in water"). J. Fons also thanks the Spanish Ministry of Economy and Competitiveness for the PhD grant FPI BES-2012-052590.

References

Altzitzoglou, T., 2008. Radioactivity determination of individual radionuclides in a mixture by liquid scintillation spectra deconvolution. Appl. Radiat. Isot. 66 (6e7), 1055-1061.

Bagán, H., et al., 2011. Mixture quantification using PLS in plastic scintillation measurements. Appl. Radiat. Isot. 69 (6), 898-903.

Fons, J., et al., 2013. Simultaneous determination of gross alpha, gross beta and 226Ra in natural water by liquid scintillation counting. J. Environ. Radioact. 125, 56-60.

Hueber-Becker, F., et al., 2007. Occupational exposure of hairdressers to [14C]-paraphenylenediamine-containing oxidative hair dyes: a mass balance study. Food Chem. Toxicol. Int. J. Publ. Br. Ind. Biol. Res. Assoc. 45 (1), 160-169.

Kashirin, I., et al., 2000. Liquid scintillation determination of low level components in complex mixtures of radionuclides. Appl. Radiat. Isot. Incl. Data Instrum. Methods Use Agric. Ind. Med. 53 (1-2), 303-308.

Kim, Y.J., et al., 2006. Determination of 129I using liquid scintillation counting. In:

Chalupnik, S., Sch€onhofer, F., Koakes, J. (Eds.), LSC 2005. "Advances in Liquid Scintillation Spectrometry." Radiocarbon, University of Arizona, Tucson, pp. 273-276.

Mahani, M., et al., 2012. Application of multi-way partial least squares calibration for simultaneous determination of radioisotopes by liquid scintillation technique. Nucl. Technol. Radiat. Prot. 27 (2), 125-130.

Mahani, M.K., et al., 2007. A new method for simultaneous determination of 226Ra and uranium in aqueous samples by liquid scintillation using chemometrics. J. Radioanal. Nucl. Chem. 275 (2), 427-432.

Malinovsky, S.V., et al., 2002. Mathematical aspects of decoding complex spectra applied to liquid scintillation counting. In: M€obius, S., Noakes, J.E., Sch€onhofer, F. (Eds.), LSC 2001. "Advances in Liquid Scintillation Spectrometry." Radiocarbon, University of Arizona, Tucson, pp. 127-135.

Nakanishi, T., et al., 2009. Simultaneous measurements of cosmogenic radionuclides 32P, 33P and 7Be in dissolved and particulate forms in the upper ocean. J. Radioanal. Nucl. Chem. 279 (3), 769-776.

Nebelung, C., Baraniak, L., 2007. Simultaneous determination of 226Ra, 233U and 237Np by liquid scintillation spectrometry. Appl. Radiat. Isot. 65 (2), 209-217.

Nebelung, C., J€ahnigen, P., Bernhard, G., 2009. Simultaneous determination of beta nuclides by liquid scintillation spectrometry. In: Eikenberg, J., et al. (Eds.), LSC 2008. "Advances in Liquid Scintillation Spectrometry." Radiocarbon, University of Arizona, Tucson, pp. 193-201.

Noor, A., et al., 1996. Pulse height spectral analysis of 3H : 14C ratios. Appl. Radiat. Isot. 47 (8), 767e775.

Noor, A., Kasim, N., L'Annunziata, M.F., 1995. Application of pulse height spectral analysis to double-label counting of 35S-32P. Appl. Radiat. Isot. 44 (8), 791-797.

Okita, G.T., et al., 1957. Assaying compounds containing tritium and carbon-14. Nucleonics 15 (6), 111-114.

Rajalahti, T., et al., 2009. Discriminating variable test and selectivity ratio plot: quantitative tools for interpretation and variable (biomarker) selection in complex spectral or chromatographic profiles. Anal. Chem. 81 (7), 2581-2590.

Remetti, R., Franci, D., 2012. ABCD-Tool, a software suite for the analysis of a/b spectra from liquid scintillation counting. J. Radioanal. Nucl. Chem. 292 (3), 1115-1122.

Remetti, R., Sessa, A., 2011. Beta spectra deconvolution for liquid scintillation counting. J. Radioanal. Nucl. Chem. 287 (1), 107-111.

Roig, M., et al., 1999. Determination of a mixture of gamma-emitting radionuclides using solid scintillation detectors and multivariate calibration. Anal. Chim. Acta 379.

Rubingh, C.M., et al., 2006. Assessing the performance of statistical validation tools for megavariate metabolomics data. Metabolomics 2 (2), 53-61.

Rundt, K., Kouru, H., 1992. Apparatus and a Method for Measuring the Activity of Radioactive Samples Containing a Multiple of Radioactive Isotopes.

Rundt, K., Kouru, H., 1989. Liquid Scintillator Counter for Measuring the Activity of Radioactive Samples Containing a Multiple of Radioactive Isotopes.

Science, P.E.L., 2002. Instrument Manual 1220 Quantulus.

Shaffer, C.L., Langer, C.S., 2007. Metabolism of a 14C/3H-labeled GABAA receptor partial agonist in rat, dog and human liver microsomes: evaluation of a dualradiolabel strategy. J. Pharm. Biomed. Anal. 43 (4), 1195-1205.

Viteri, F.E., Kohaut, B.A., 1997. Improvement of the Eakins and Brown method for measuring 59Fe and 55Fe in blood and other iron-containing materials by liquid scintillation counting and sample preparation using microwave digestion and ion-exchange column purification of iron. Anal. Biochem. 244 (1), 116-123.

6.2. Effect of quenching on efficiency, spectra shape and alpha-beta discrimination in liquid scintillation spectrometry

Implications of quenching in efficiency, spectrum shape and alpha/beta separation

Jordi Fons-Castells*, Vladimir Díaz, Andrea Badia, Joana Tent-Petrus, Montserrat Llauradó

Department of Chemical Engineering and Analytical Chemistry, University of Barcelona, Martí i Franquès 1-11, 08028 Barcelona, Spain.

*corresponding author: jordi.fons@ub.edu

Abstract

Liquid scintillation spectrometry (LSS) is a meaningful technique for the determination of alpha and beta emitters. However, this technique is highly affected by quenching phenomena, which reduce the counting efficiency, shift the spectra to low energies and may cause misclassification problems. In this paper, a selection of chemical and colour quench agents was evaluated to study the influence of alpha and beta energy and quenching effect on the detection efficiency, the shape of the spectra and the α/β misclassification.

Keywords: Chemical quenching, Colour quenching, Liquid scintillation spectrometry, Alpha-beta separation.

Introduction

Liquid scintillation spectrometry (LSS) is one of the most commonly used techniques for the determination of alpha and beta emitters due to its high efficiency. LSS involves mixing the radioactive sample with a scintillation cocktail, which is able to convert the nuclear decay energy into light pulses which are detected by photomultiplier tubes (PMT). Modern scintillation cocktails are based on a safe solvent, usually diisopropyl naphthalene (DIN), which absorb the energy emitted by the radionuclides contained in the sample. In the cocktail there are other substances, commonly called solutes or fluor, which modulate the energy of the activated solvent molecules to adequate the final emitted light pulse to the PMT sensibility region, usually 2,5-diphenyloxazole (PPO) and 1,4-bis-2-(5-phenyloxazolyl)benzene (POPOP). Moreover, some cocktails contain solutes that strengthen the differences between the light pulse of alpha and beta events, in order to facilitate the α/β separation. Pulse-shape discrimination (PSD) is the common method used for the counters for α/β separation and is commonly based on the relation between early and delayed component of the light pulse or in the length of the pulse.

There are different phenomena that hinder the energy transference between the particle emitted and the photons detected by the PMT, known as quench. The quenching phenomena which highly affect in liquid scintillation measurement are chemical and colour quenching. Chemical quenching is the most common mechanism and is caused by the presence of chemical substances in the sample, including its solvent. These substances obstruct the energy transference between the radioactive emission and the fluor and hence, reduce the efficiency of photon emission. Colour quenching is caused by the presence of coloured substances in the sample which may absorb the photons emitted by the fluorine before they can be detected by the PMT. In general, both quenching mechanism, reduce the number of photons detected by the PMT and consequently the apparent energy of the emission (the spectrum shifts to lower energies). Furthermore, this phenomena can also reduce the count rate of the samples and hence the counting efficiency. In addition, previous studies (Pates, J.M., et al., 1994; Pujol, Ll. & Sánchez-Cabeza, J.A., 1997; Salonen, L., 2006; Stojkovic, I., 2015) have shown that quenching also affects the degree of α/β misclassification which is a consequence of different manners of its influence on early and delayed components of the light pulse.

For these reasons, in LSS efficiency is commonly determined using a quenching curve which describes, for a specific radionuclide, the relation between an in-

strumental parameter of quenching and the counting efficiency. Quenching curves are prepared measuring a set of liquid scintillation standard sources with different amounts of quenching agent either chemical or coloured (Cassette, P., 2016).

In the latest years, methods for the simultaneous determination of several alpha and beta emitters by deconvoluting liquid scintillation spectrum have been developed. One of the methods used for deconvolution is fitting the spectrum of the sample to a linear combination of experimental standard spectra (Altzitzoglou, T., 2008), to a tailed Gaussian functions (Nebelung, C., et al., 2009) or to a Fourier series (Remetti, R. & Franci, D., 2012). Furthermore, other authors use methods based on multilinear calibration as PLS model construction (Mahani, M., et al., 2008; Fons-Castells, J., et al., 2017). These methods work on quenching controlled conditions, but the presence of a quenching source in the sample jeopardizes the veracity of the results. For all these reasons, understand and model the influence of quenching on efficiency, spectrum shape and α/β misclassification is a key point in simultaneous determination of alpha and beta emitters by LSS in changing quenching conditions.

To fulfil this aim, the influence of chemical and colour quenching on the efficiency, the spectrum shape and the α/β misclassification has been studied for different radionuclides.

In this paper different chemical and colour quenching agents were tested to identify different behaviours and select an agent of each type to perform the quenching curves. Then, the selected agents were used to perform chemical and colour quenching curves for seven radionuclides. A wide energy range of beta emitters were covered with ^{3}H (18.6 keV [100 %]), ^{60}Co (317.3 keV [99.9 %]), ^{137}Cs (514.0 keV [94.4 %]), ^{40}K (1131.1 keV [89.3 %]) and $^{90}Sr/^{90}Y$ (545.9 keV [100 %] / 2278.7 keV [99.98 %]). ^{241}Am (5.49 MeV) was selected as alpha emitter and ^{nat}U as a mixture of alpha and beta emitters. The influence on the efficiency, the spectrum shape and the α/β misclassification has been studied for all the radionuclides for chemical and colour quenching. Furthermore, the influence of quenching on the optimal PSD was evaluated using ^{241}Am and $^{90}Sr/^{90}Y$ as calibration standards.

Materials and methods

The quenching agents studied were: coloured solutions from inorganic salts ($CuSO_4 \cdot 5H_2O$, $NiNO_3 \cdot 6H_2O$ and $FeCl_3$), organic inks (bromocresol green and methyl red) and uncoloured organic substances (nitromethane, dimetil keton, nitric acid).

The samples were measured with Ultima Gold AB (Perkin Elmer) as liquid scintil-

lation cocktail in 20 mL polyethylene vials (Perkin Elmer) in a Wallac Quantulus™ 1220 counter with α-β separation mode for 100 minutes. The Pulse Shape Analyser (PSA) was set as 100, which is the optimal PSA established in the laboratory for the simultaneous determination of gross alpha and gross beta using ^{236}U and ^{40}K as standards (Fons, J., et al., 2013). The quenching index in Quantulus™ 1220 is SQP[E] (External Standard Quench Parameter) and is based on the shifting of the spectra of Compton electrons produced by a gamma source of ^{152}Eu. SQP[E] is defined as the 99.5 % of the endpoint of this external source.

Selection of a quenching agent for chemical and colour quenching

Five concentrations for each quenching agent (5 coloured and 3 uncoloured) were assayed by duplicate. The quenching standards were prepared mixing different volumes of each quenching agent with water acidified with HCl at pH 1.5 until 8 mL and spiking with 30 Bq of ^{3}H. The amount of quenching agent added were: for the coloured solutions of inorganic salts from 1 to 7 ml of 0.1 mol L^{-1} solution, for organic inks from 1 to 7 mL of 0.01 mol L^{-1} solution, from 25 µL to 200 µL of nitromethane, from 1 to 7 mL of dimethyl ketone and from 0.5 to 2 mL of nitric acid (50 %). Counting vials are then completed with 12 mL of Ultima Gold AB as scintillation cocktail. From these experiments the differences between chemical quenching agents and colour quenching agents were evaluated.

Evaluation of efficiency, spectrum shape and α/β misclassification

The selected quenching agents were nitromethane and $FeCl_3$ for chemical and colour quenching respectively because are the ones which cover a wider range of SQP[E]. For each one of the studied radionuclides (^{3}H, ^{40}K, ^{60}Co, $^{90}Sr/^{90}Y$, ^{137}Cs, ^{nat}U and ^{241}Am), chemical and colour quenching curves were prepared following the procedure explained above, using the selected quenching agents. For all the samples analyzed efficiency, spectrum shape and α/β classification were studied.

PSA optimization in changing quenching conditions

$^{90}Sr/^{90}Y$ and ^{241}Am samples used to perform quenching curves, were also measured at different PSA values to achieve misclassification curves at different quenching levels for both, colour and chemical quench.

Data treatment

All the spectra obtained were treated in MATLAB2009b version (MathWorks, Inc., Natick, MA, USA). From each one was calculated the count rate in alpha multichannel analyser (α-MCA) and in β-MCA, and also the global count rate to evaluate the role of quenching on the

efficiency. The ratio between beta counts and alpha counts was also calculated as a parameter to control the α/β classification.

To analyze the shifting of the spectra, the mass centre of spectrum (MCS) was calculated for all spectra. It was calculated as the weighted mean of the channels of the spectrum with their count rate as weights.

$$MCS = \frac{\sum_i^{1024} i * cpm_i}{\sum_i^{1024} cpm_i} (1)$$

where i are the channels of the MCA and cpm_i are the count rate for each channel.

The charts in which efficiency, shifting of spectra and α/β separation is represented in function of SQP[E] for all the radionuclides studied are provided in supplementary material (SM) from Fig. 1S to Fig. 21S. The spectra of ^{40}K, ^{60}Co, ^{90}Sr/^{90}Y ^{137}Cs, ^{nat}U and ^{241}Am for different concentrations of $FeCl_3$ and nitromethane are also provided in supplementary material from Fig. 22S to Fig. 32S.

The calculation of quenching curves was performed using QUENCH software, which is specifically designed for the determination of quenching curves with uncertainties (Cassette, P., 2016). This software fits logarithmic or polynomial functions to experimental data with uncertainties in both quenching and efficiency. Since the program allows to calculate quenching and efficiency with uncertainties by interpolating, we use it to plot the quenching curves with its uncertainty.

Results and discussion

Selection of a quenching agent for chemical and colour quenching

Influence of quenching on efficiency and spectrum shape of ^{3}H were evaluated for different colour agents. In Fig. 1, efficiency (a) and mass centre of spectrum (b) of ^{3}H in front of SQP[E] are represented for all colour quenching agents.

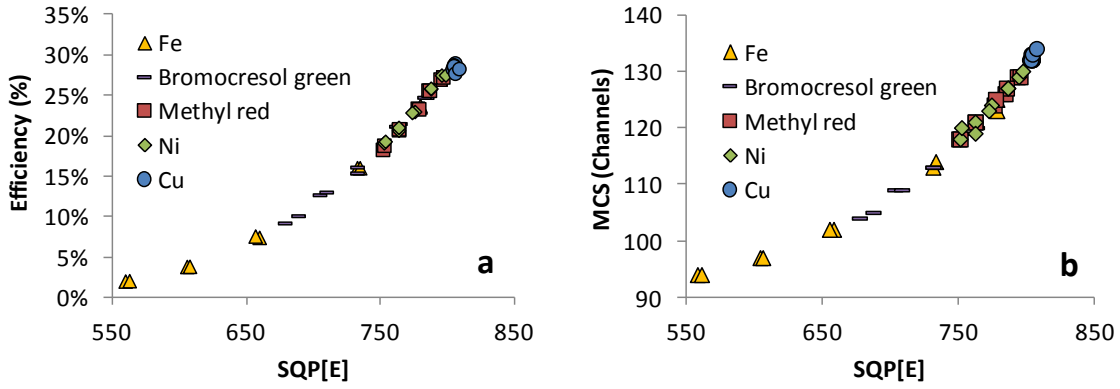

Fig. 1. Efficiency (a) and mass centre of spectrum (b) of ^{3}H in front quenching (SQP[E]) for five colour quenching agents studied.

Cu^{2+} solution (blue) does not undergone quenching due to it does not absorb light in the wavelength emitted by the scintillator. The SQP[E] for all the standards solution was 805 ± 2 while its efficiency 28.5 ± 0.4 %, regardless of the Cu^{2+}concentration. Ni^{2+} (green) and methyl red (red) solutions cause an intermediate grade of quenching. In both cases SQP[E] is in the range between 800 and 750, and the efficiency between 30 and 20 %. When the concentration of quenching agent increases, both SQP[E] and efficiency of ^{3}H decrease. Bromocresol green and Fe^{3+}, both yellow solutions, follow the same pattern than Ni^{2+} and methyl red but its range of SQP[E] is larger from 800 to 680 for bromocresol green and from 800 to 550 for Fe^{3+}. This is because the absorption of yellow solutions is in the wavelength range of emission of the scintillator. Spite of that, as the Fig 1a shows, the tendency of efficiency of ^{3}H in front of SQP[E] is the same for all the colour quenching agents, regardless the covered range of SQP[E].

Similarly, in Fig. 1b it is seen that effect of all the colour quenching agents tested in the mass centre of the spectrum follows the same tendency. When SQP[E] decreases the spectrum of ^{3}H shifts to lower energies and hence MCS decreases.

In the same way, the influence of quenching on efficiency and spectrum shape of ^{3}H were evaluated for different chemical agents. In Fig. 2 efficiency (a) and mass centre of spectrum (b) of ^{3}H in front of SQP[E] are represented for three chemical quenching agents.

The observed range of SQP[E] is between 800 and 730 for dimethyl keton and nitric acid, while it goes from 800 to 580 for nitromethane. Chemical agents addition results with the same tendency for both, efficiency and MCS dependence on SQP(E) as colour quenching agents induce.

Since $FeCl_3$ and CH_3NO_2 are the quenching agents which cover the wide range of SQP[E], they were selected as agents to

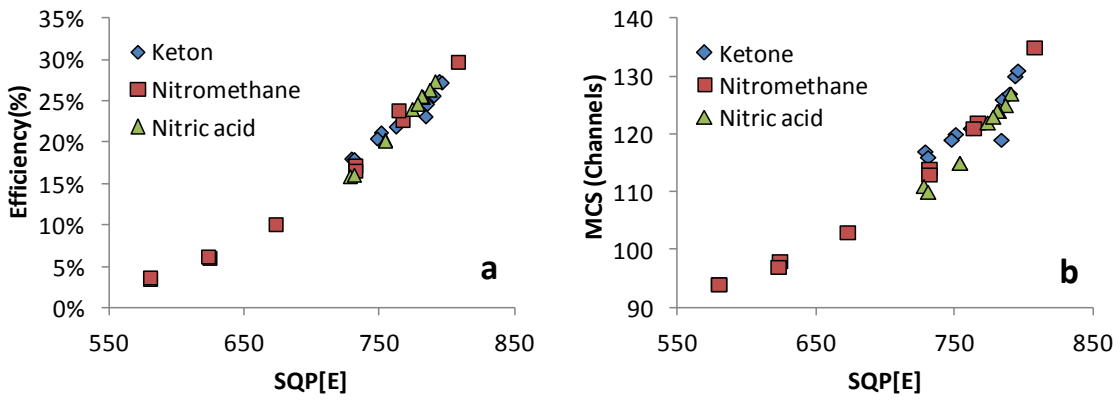

Fig. 2. Efficiency (a) and mass centre of spectrum (b) of ^{3}H in front of quenching (SQP[E]) for three chemical quenching agents studied.

perform colour and chemical quenching curves, respectively.

In Fig. 3, quenching curves of $FeCl_3$ and CH_3NO_2 were plotted to show the different tendencies between colour and chemical agents.

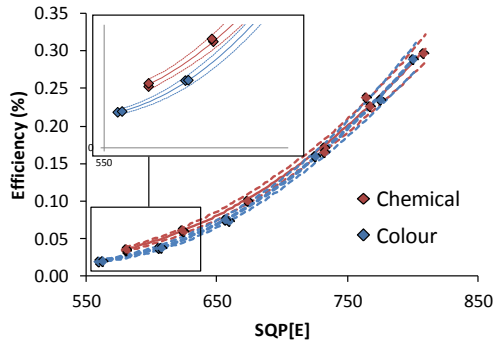

Fig. 3. Efficiency quenching curves for $FeCl_3$ and CH_3NO_2 with an enlargement of low SQP[E] values.

As illustrates Fig. 3, two different tendencies can be observed when colour and chemical quenching are compared. As it can be seen, at high values of SPQ[E] (low quenching effect), colour and chemical quenching cannot be differentiated. However, at low values of SQP[E] (high quenching effect) the coloured substances decrease the counting efficiency more than the non coloured. This reflects that colour and chemical quenching cause different effect on efficiency for low energy beta emitters and may cause different effects on the other parameters studied. Consequently, colour and chemical quenching were studied separately for different radionuclides, using $FeCl_3$ and CH_3NO_2 for colour and chemical quenching respectively.

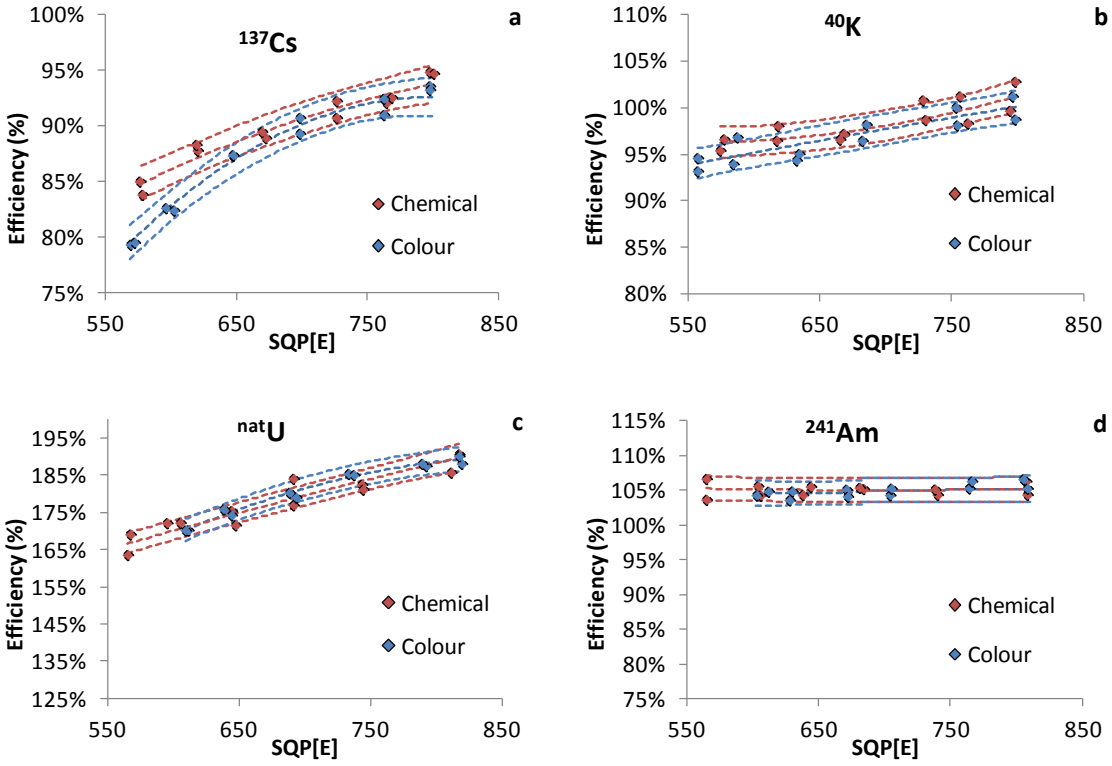

Fig. 4. Efficiency in function of SQP[E] for colour and chemical quenching for ^{137}Cs (a), ^{40}K (b), ^{nat}U and ^{241}Am (d).

Evaluation of efficiency, spectrum shape and α/β misclassification

Efficiency

In Fig. 4, quenching curves (efficiency in function of SQP[E]) for colour and chemical quenching are represented for ^{137}Cs (a), ^{40}K (b), ^{nat}U(c) and ^{241}Am (d). In this case total efficiency (without considering alpha and beta separation) was considered.

As can be seen in Fig. 4a, for ^{137}Cs an intermediate energy beta emitter (514.0 keV [94.4 %]), the efficiency decreases with the increase of quenching for both, chemical and colour quenching, but this effect is more pronounced in lowest SQP[E] values for colour agent, in the same way as the observed for ^{3}H (Fig. 3). On contrary, for high energy beta emitters like ^{40}K (1131.1 keV [89.3 %]) the efficiency just slightly decreases with quenching and no significant differences were observed between chemical and colour quenching. For ^{241}Am (a 5.49 MeV alpha emitter), either chemical or colour quenching do not cause a decrease on the total efficiency. As can be seen in Fig. 4d, constant efficiency in the studied range of SQP[E] is observed for both, colour and chemical quenching. Finally, as Fig. 4c shows, for ^{nat}U, which is a mixture of alpha and beta emitters the pattern observed is close to the observed for high beta emitters. No differences between colour and chemical quenching were observed and both cause a slight decrease of efficiency at low values of SQP[E].

Spectrum shape

In Fig. 5, mass centre of spectrum (MCS) in function of SQP[E] for colour and chemical quenching is represented for ^{3}H, a low beta emitter (a), ^{90}Sr/^{90}Y a mixture of medium an high beta emitters (b) and ^{241}Am an alpha emitter. Fig. 5 d shows MCS for ^{90}Sr/^{90}Y, ^{40}K, ^{137}Cs and ^{60}Co in front of SQP[E] without distinguish between colour and chemical quenching. As it can be seen in Fig. 5a and 5b, for beta emitters there is no significant difference in the shifting of the spectra between colour and chemical quenching. For low energy beta emitters (^{3}H), the MCS decreases with increasing quenching in the same way as efficiency. For intermediate and high energy beta emitters, this decrease follows a linear behaviour between MCS and SQP[E].

In Fig. 5d, a comparison of different medium and high energy beta emitters (^{90}Sr/^{90}Y [545.9 keV/2278.7 keV], ^{40}K [1131.1 keV], ^{137}Cs [514.0 keV] and ^{60}Co [317.3 keV]) shows that in all cases MCS decreases linearly with the decrease of SQP[E] in the studied range.

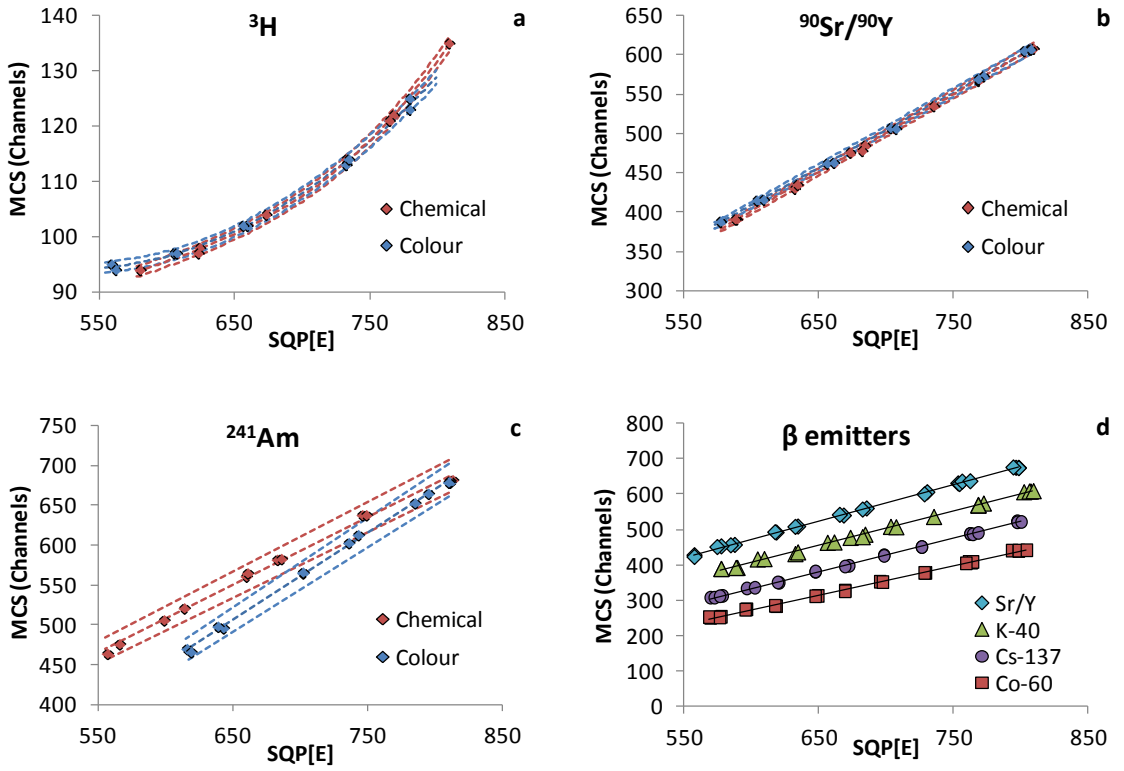

Fig. 5. Mass centre of spectrum shift in channels in front of SQP[E] for colour and chemical quenching for ^{3}H (a), ^{90}Sr/^{90}Y (b), ^{241}Am (c) and comparison of medium and high energy beta emitters (d).

On the contrary, for alpha emitters (^{241}Am), different behaviour for colour and chemical quenching is observed. In both cases, MCS decreases linearly with the decrease of SQP[E] but with different slope for colour and chemical quenching (Fig. 5c). For alpha emitters, the influence of quenching on the shifting of the spectra is higher for colour than for chemical quenching.

The difference observed between alpha and beta emitters regarding the influence of quenching type in the shifting of spectra can be explained considering the way in which SQP[E] is measured.

SQP[E] is defined as the 99.5 % of the endpoint of the Compton spectra of an external gamma source, usually ^{152}Eu or ^{226}Ra. The inelastic scattering of the gamma photons by electrons of the atoms in the counting vial provides a source of electrons with continuous energy in the counting solution, which conform the Compton spectra. In this way, SQP[E] informs about the shifting (99.5 % of the endpoint) of an spectra of intermediate energy electrons, and hence it is expected to correlate linearly with the shifting (MCS) of medium high energy beta emitters, regardless the type of quenching. For alpha emitters the way in which colour or chemical quenching affect the shifting is not the same than the observed for beta emitters or Compton electrons, and for this reason, the behaviour of MCS for colour and chemical

quench is significantly different as shown Fig. 5c.

Furthermore, other changes in the shape of spectrum can occur when quenching is increased. ^{137}Cs is an intermediate energy beta emitter (E_{max} 514 keV) and its identification is further determined by the monoenergetic conversion electron peak of ^{137m}Ba at 625 keV (Kaihola, L., 2006). The influence of quenching on the spectra of this monoenergetic peak is dependant from the type (colour or chemical) of quenching. Fig. 6 shows spectra of ^{137}Cs at different quench levels for colour (a) and chemical (b) quenching.

As illustrates Fig. 6, not only MCS changes between colour and chemical quenching, but also spectrum shape. At high levels of quenching (SQP[E] below 600) the monoenergetic peak disappears when quenching is caused by a coloured agent, but remains visible when it is caused by a chemical agent. This fact occurs because colour quenching aggravates more the resolution than chemical quenching. This may be explained with the fact that chemical quenching induces a loss of energy from the excited solvent in a non-radiative process and hence production of fewer photos per disintegration, which further causes the loss of efficiency in the photons detected by the PMT. This loss of photons emission mainly depends on the concentration of the chemical agent in the counting solution and as it is homogeneous, the loss of efficiency is also constant. On the contrary, in colour quenching, photons emitted by the fluors are absorbed by coloured substances in the sample. The number of photons detected by the PMT depends on the optical path length between the point where the disintegration occurs and the wall of the vial. Since disintegration may occur in the centre or close to the wall of the vial, disintegrations with the same energy may be detected with different energy depending on the place where they occur. For this reason, and due to the random distribution of disintegrations along the counting vial, colour quenching may cause significant loss of resolution (ten Haff, F.E.L., 1972).

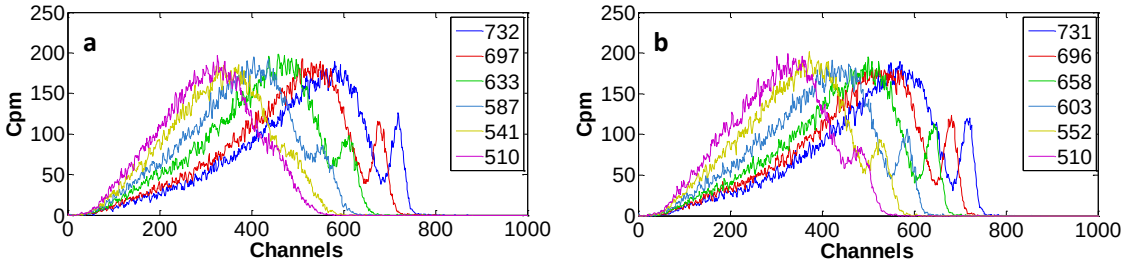

Fig. 6. Spectra of ^{137}Cs at different quench levels for colour (a) and chemical (b) agents. The values of the legend are the SQP[E] level for each spectra.

This loss of resolution can be also observed for the alpha peak of ^{241}Am, please find in supplementary material figures 31S and 32S.

α/β misclassification

For all the radionuclides studied, the ratio between the counts in the β-MCA and the α-MCA was represented as function of SQP[E] and in all the cases the pattern observed was similar. All the samples were measured at PSA value of 100 which was optimized using ^{236}U and ^{40}K as calibration standards. At this PSA level, the misclassification was the minimum achievable, and it was around 5 %.

As an example, in Fig. 7 the ratio between the counts in the β-MCA and the α-MCA measured at PSA 100 is represented as function of SQP[E] for colour and chemical quenched standards of ^{nat}U.

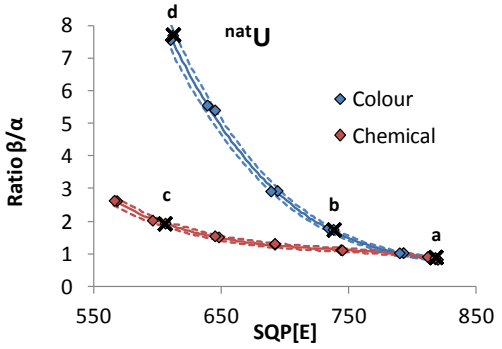

Fig. 7. Ratio between β and α counts as function of SQP[E] for colour and chemical quench in ^{nat}U standards.

Similar effects to the ones illustrated in Fig. 7 were observed for all radionuclides studied, where it can be seen that small changes in SQP[E] do not significantly affect α/β classification. When there are greater changes in SQP[E] two different patterns where observed for colour and chemical quenching respectively. The β/α ratio increases markedly when SQP[E] decreases in colour quenched samples since alpha counts of ^{234}U and ^{238}U are being counted in the β-MCA. On the contrary, for chemical quenching this misclassification occurs at low values of SQP[E] (below 650) and just in a moderate way.

In Fig. 8, spectra of ^{nat}U with different degrees of quenching are shown. Each spectrum corresponds to a characteristic point in Fig. 7 where are highlighted with letters.

It has to be noted that in this context non-quenched refers to samples prepared without any quenching agent apart from the 8 mL of acidified water.

When we compare a non-quenched sample (Fig. 8a) with all the quenched samples (Figures 8b, 8c and 8d), it can be seen that the spectra shifts to lower channels and the counts corresponding to ^{234}U and ^{238}U were classified in β-MCA instead of α-MCA.

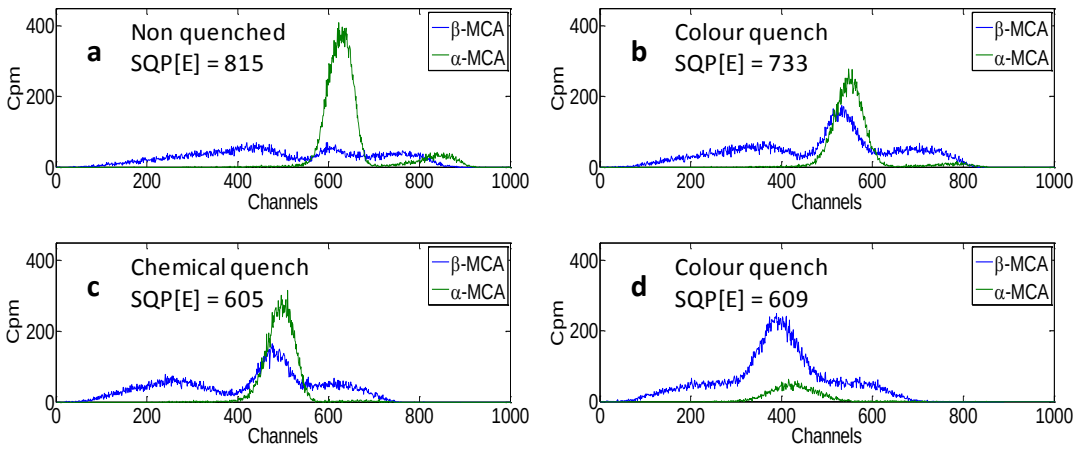

Fig. 8. Spectra in α-MCA and β-MCA of ^{nat}U for non quenched (a), moderately colour quenched (b), highly chemical quenched (c) and highly colour quenched.

At the same value of SQP[E] (~600) (Figures 8b and 8c) colour quenching aggravates more the interference than chemical quenching.

As it was said before, the results showed above were obtained measuring at the same value of PSA. In order to find how the optimal PSA and the minimum interference are affected for changing quenching conditions, misclassification study for $^{90}Sr/^{90}Y$ and ^{241}Am were performed at different PSA values (from 70 to 130) and different quenching conditions (SQP[E] 800 from to 550) for colour and chemical quenching.

The results obtained are shown in Fig. 9 where optimal PSA and total interference are represented in function of SQP[E].

In general, when SQP[E] decreases (quenching increase) the optimal PSA (PSA value with the lower total interference) decreases, and total interference at optimum PSA increases. For chemical quench, at low quenching region (SQP[E] from 700 to 800) the total interference at the optimal PSA remains constant below 10 %. On the contrary, for colour quenching, the total interference at the optimal PSA increase from SQP[E] 800.

When chemical and colour quenching are compared, it can be observed that colour quench modifies in a higher degree optimum PSA and total interference than chemical quenching.

In supplementary material figures S33 and S34, interactive 3 dimensions Matlab™ figures are provided. There, total interference is represented as function of PSA and SQP[E] for colour and chemical quenching.

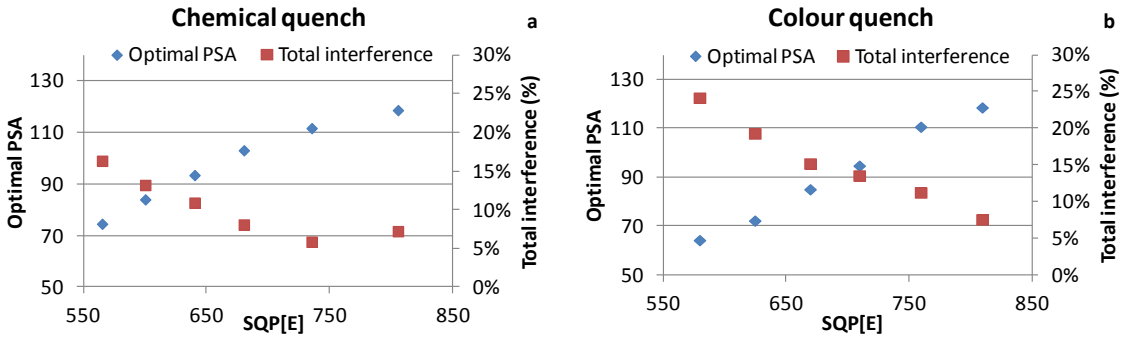

Fig. 9. Optimal PSA and total interference as function of SQP[E] for chemical (a) and colour (b) quenching.

Conclusions

From a set of quenching agents, $FeCl_3$ solutions and nitromethane have been selected to perform colour and chemical quenching curves respectively since they cover a width range of SQP[E].

The efficiency is highly affected by quenching for low energy beta emitters, and just moderately affected for high energy beta emitters. In the case of alpha emitters, quenching does not clearly affect the efficiency. For radionuclides affected, colour quench reduce more the efficiency than chemical quenching at low values of SQP[E].

Regarding the spectrum shape, when quench increases spectrum shifts to lower energies in all the examined cases. For beta emitters the correlations between SQP[E] and MCS are linear and equal for chemical and colour quench. On the contrary, for alpha emitters two different behaviours for chemical quenching and colour quenching were observed. This can be explained because SQP[E] is a quench parameter based on the shifting of the spectrum of Compton electrons generated by the external source, which are more representative of beta emissions than alpha emissions. In general, MCS may be an appropriate parameter to follow the shape of the spectra. However, each radionuclide and each type of quenching (chemical or colour) have to be evaluated because complex phenomena on the shape of spectrum may occur mainly due to the loss of resolution at high quenching levels.

Finally, regarding α/β separation; when quenching of the sample increases, alpha emissions are more susceptible to be classified in the β-MCA. For low energy beta emitters (^{3}H) this cannot be observed since there are no misclassified counts in α-MCA. For high energy beta emitters (^{40}K, ^{60}Co $^{90}Sr/^{90}Y$ and ^{137}Cs) the misclassified counts in α-MCA decrease with the increased quenching. For alpha emitters (^{241}Am) the counts misclassified in the β-MCA increase with the increasing quenching. With increasing quenching level the optimal PSA decreases and the total interference measured at this optimal PSA increases.

In all the studied cases, colour quenching modifies in a higher degree α/β classification than chemical quenching.

In brief, at the same SQP[E] value, at high quenching levels (SQP[E] below of 600), colour quenching has more influence on efficiency reduction, shifting of the spectra and α/β separation than chemical quenching. At low quenching levels (SQP[E] from 700 to 800) colour and chemical quenching have similar effects on the evaluated parameters.

For these reasons, the nature of the quenching in real samples has to be properly studied in order to set up the PSD, select a quenching agent to perform quenching curves and, if necessary, correct the shifting of the spectra.

Acknowledgements

This study was funded by the Spanish Ministry of Economy and Competitiveness (CTM2014-55191), the Catalan government (AGAUR2014SGR1277) and the Spanish CSN with the project "*Metodología rápida para la determinación de emisores alfa y beta en aguas*". J. Fons-Castells also thanks the financial support of the Ministry of Economy and Competitiveness for the PhD grant FPI BES-2012-052590.

References

Altzitzoglou, T., 2008. Radioactivity determination of individual radionuclides in a mixture by liquid scintillation spectra deconvolution. Applied Radiation and Isotopes, 66(6-7), 1055-61.

Cassette, P., 2016 QUENCH: A software package for the determination of quenching curves in liquid scintillation counting. Appl. Radiat. Isot., 109, 301-307.

Fons, J., Zapata-Garcia, D., Tent, J., Llauradó, M., 2013. Simultaneous determination of gross alpha, gross beta and ^{226}Ra in water by liquid scintillation counting. J Enviorn. Radioact. 125, 56-60.

Fons-Castells, J., Tent-Petrus, J., Llauradó, M., 2017. Simultaneous determination of specific alpha and beta emitters by LSC-PLS in water samples. J Enviorn. Radioact. 166, 195-201.

Kaihola L., 2006. Gamma monitoring capabilities of Quantulus. In S. Chalupnik, et al., eds. LSC 2005. "Advances in Liquid Scintillation Spectrometry." Tucson: Radiocarbon, University of Arizona. 435-438.

Mahani, M. K., Chaloosi, M., Khanchi A. R., Maragheh M.G., Salimi, B., Asgharizadeh, F., 2008. A new method for simultaneous determination of ^{226}Ra and uranium in aqueous samples by liquid scintillation using chemometrics. J. Radioanal. Nucl. Chem., 275(2), 427-432.

Nebelung, C., Jähnigen, P., Bernhard, G., 2009. Simultaneous determination of beta nuclides by liquid scintillation spectrometry. In J. Eikenberg et al., (Eds.) LSC 2008. "Advances in Liquid Scintillation Spectrometry." Tucson: Radiocarbon, University of Arizona. 193-201.

Pates, J.M., Cook, G.T., McKenzie, A.B., Passo, C.J., 1994 Quenching and its effect on alpha/beta separation liquid scintillation spectrometry. Radiocarbon 1996 75-85.

Pujol, Ll., Sanchez-Cabeza, J.A., 1997. Role of quenching on alpha/beta separation in liquid scintillation counting for several high capacity cocktails. The Analyst 122, 383-385.

Remetti, R. & Franci, D., 2012. ABCD-Tool, a software suite for the analysis of α/β spectra from liquid scintillation counting. J. Radioanal. Nucl. Chem., 292(3), 1115-1122.

Salonen, L., 2006 Alpha spillover depends on alpha energy: a new finding in alpha/beta liquid scintillation spectrometry. In S. Chalupnik, et al., (Eds.) LSC 2005. "Advances in Liquid Scintillation Spectrometry." Tucson: Radiocarbon, University of Arizona. 135-148.

Stojkovic, I., Tenjovic, B., Nikov, J., Todorovic, N., 2015. Radionuclide, scintillation cocktail, and chemical/color quench influence on discrimination setting in gross alpha/beta measurements by LSC. J Enviorn. Radioact. 144, 41-46.

ten Haff, F.E.L., 1972 Colour quenching in liquid scintillation coincidence counters. In Liquid scintillation counting 1971 Vol. 2. M.A. Crook, P. Johnson, B. Scales (Eds.) London Heyden & Son Ltd, 39-48.

6.3. Discussion

From the results obtained in the two scientific papers in this chapter, it must be noted that the determination of specific radionuclides from spectra obtained by determining gross alpha and gross beta activities using PLS models provides satisfactory results.

However, when attempting to quantify samples that contain a radionuclide that is not included in the calibration set, the results obtained using PLS models may not be correct for all radionuclides. It is therefore necessary, as much as possible, to include in the calibration set all the expected radionuclides in the studied sample.

This fact is illustrated with the results obtained from a spiked sample that was quantified by using two different PLS models: one that contains all the radionuclides present in the sample (A), and another from which one radionuclide is missing (B).

Table 3 shows these results. The activities are presented in Bq kg^{-1}, and the relative bias in %.

Table 3. Added and predicted activity for two models together with its bias.

RN	Added	Predicted model A	Predicted model B	Bias model A	Bias model B
^{40}K	13.6 ± 0.4	13.0 ± 0.4	12.3 ± 0.4	-4.4 %	-9.1 %
^{60}Co	30.0 ± 0.9	30.5 ± 0.9	30.4 ± 0.9	1.7 %	1.7 %
$^{90}Sr/^{90}Y$	23.1 ± 0.4	23.7 ± 1.1	23.8 ± 1.2	2.6 %	3.7 %
^{134}Cs	20.5 ± 0.6	19.9 ± 0.8	-	-2.9 %	-
^{137}Cs	16.3 ± 0.3	15.8 ± 0.7	35.2 ± 1.0	-3.1 %	115.8 %
^{nat}U	6.3 ± 0.4	6.0 ± 0.1	5.9 ± 0.1	-4.8 %	-6.4 %
^{241}Am	5.2 ± 0.2	5.2 ± 0.2	5.1 ± 0.2	-0.7 %	-2.3 %

The studied sample was spiked with different radionuclides. Model A was constructed with all radionuclides, and Model B was constructed with all except ^{134}Cs. As a result, in the prediction of Model B, ^{134}Cs is misclassified as ^{137}Cs; hence, a bias higher than 100 % is obtained.

The model construction was validated with reference materials to obtain satisfactory results.

The limits of detection for each radionuclide in a model was established as the arithmetical mean plus two times the standard deviation of the determined activity for the radionuclide considered in the standards, which did not contain this radionuclide.

In addition, critical issues regarding the determination of specific radionuclides from liquid scintillation spectra using PLS models include efficiency, the shape of the spectrum (characteristic of radionuclide of interest) and the α/β separation.

It is known two clearly different behaviours can be observed in liquid scintillation-quenching agents. The first step in this study was to select one agent to study colour quenching and another to study chemical quenching from a set of quenching agents. $FeCl_3$ and nitromethane were considered for the study of colour and chemical quenching, respectively.

As seen in the study of the quenching effect on efficiency, shape of the spectrum and α/β separation, these effects exhibit different degrees depending on the type of agent: chemical or colour. On the one hand, it has been observed that the efficiency of low-energy beta emitters greatly decreases with quenching, while for high-energy beta emitters this effect is moderate. For alpha emitters there is not observed a clear quenching effect on the efficiency. For beta emitters at the same SQP[E] value, colour quenching reduces the efficiency more than chemical quenching.

Regarding the spectrum shape, both, alpha and beta emitters are affected. The spectrum of alpha and beta emitters shifts to lower energies for both colour and chemical quenching.

Finally, with regard to α/β separation, when quenching increases, the optimal PSA decreases and total interference at that PSA value increases. These effects are more significant for colour quenching than for chemical quenching. Figure 8 shows the variation of interference at several PSA values in a range of quenching levels for colour (a) and chemical quenching (b).

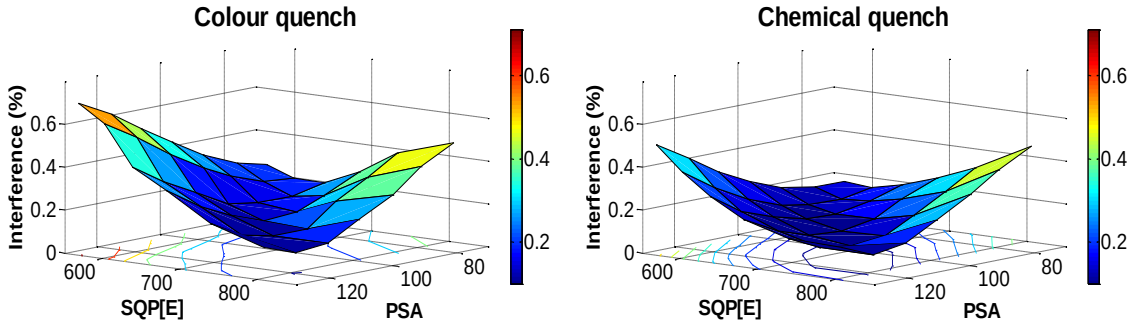

Figure 8. Variation of interference at several PSA values in a range of quenching levels for colour (a) and chemical quenching (b).

For all of these reasons, when an attempt to determine specific radionuclides is made in samples which matrix cause high quenching levels, it is necessary to use libraries that

contain standard spectra of the radionuclides expected in the sample using different levels of colour and chemical quenching.

In this way, calibration sets must be constructed using the spectra of the expected radionuclides at the SQP[E] levels closer to those observed in the sample. It may be interesting also to include SQP[E] spectra in the calibration set that are used for the construction of PLS models.

Finally, the work conducted facilitates the construction of a database of ^{3}H, ^{40}K, ^{60}Co, $^{90}Sr/^{90}Y$, ^{137}Cs, ^{nat}U and ^{241}Am for colour and chemical quenching.

7. VALIDATION OF THE STRATEGY FOR ALPHA AND BETA EMITTERS DETERMINATION. GLOBAL DISCUSSION OF THE RESULTS

This section presents a strategy for the determination of the radionuclides included in Annex III of the Directive 2013/51/EURATOM for protection of the health of the general public with regard to radioactive substances in water intended for human consumption.

The strategy presented includes all of what is explained in previous chapters. Among the methodologies used are the determination of gross alpha and gross beta activities by $LSS_{conc.}$, which is described in Chapter 4, and the determination of ^{226}Ra, ^{228}Ra and ^{210}Pb described in Chapter 5. These spectra are treated by means of the multivariate calibration described in Chapter 6.

It has to be mentioned that the determination of ^{222}Rn is not considered in this strategy for two reasons. On one hand, several rapids methods for ^{222}Rn determination already exist: e.g., direct measurement of the sample by two-phase LSS methods. On the other hand, the potential interference of ^{222}Rn in the determination of other radionuclides can be easily removed from water samples by heating and stirring because it is a gas. Hence, to accomplish the directive, an independent analysis of ^{222}Rn should also be performed.

7.1. Summary of methodologies

The methodologies selected for the strategy of determination of the alpha and beta emitters are the following:

- *High-resolution gamma spectrometry:* Has been used as a screening methodology to control the presence of gamma emitters such as ^{241}Am, ^{134}Cs and ^{137}Cs. The procedure entails a direct measurement of the sample in a 500 mL geometry using both calibrations in energy and in efficiency established in the routine protocols of the laboratory. The measurement was performed in a high-purity germanium detector CANBERRA BEGe 3830. If suspended matter was observed in the sample, a filtration step was performed. As the objective is to obtain rapid methods the counting time was always lower than 24 hours, and usually between one and six hours.

- *Concentration method with LSS measurement ($LSS_{conc.}$):* This procedure was used to determine gross alpha and gross beta activities and screening parameters included in the Directive 2013/51/EURATOM. Furthermore, the alpha and beta spectra obtained were used to determine specific radionuclides by means of PLS

models. In this procedure, 100 mL of the sample were evaporated to dryness. When the precipitate obtained is cooled at room temperature, it was dissolved in 10 mL of deionised water acidified by HCl to pH 1.5. An aliquot of 8 mL of the concentrated sample was mixed with 12 mL of the scintillation cocktail (Ultima Gold AB) in low-diffusion polyethylene vials. After two hours of waiting for photoluminescence extinction, the sample was measured in a Wallac QUANTULUS 1220 for 400 minutes by using the alpha-beta counting mode. The instrumental parameter PSA (pulse shape analyser) used to separate between alpha and beta events was optimized by means of interference studies using ^{236}U as a pure alpha emitter and ^{40}K as a pure beta emitter.

- *Direct method with LSS measurement ($LSS_{dir.}$):* This procedure is based on a direct measurement by LSS of a vial prepared with 8 mL of sample mixed with 12 mL of the scintillation cocktail. The water sample was previously stirred for 2-3 minutes to remove ^{222}Rn. The counting vial is measured for 400 minutes in the same conditions described for $LSS_{conc.}$ method. This method is based on the procedure for the determinations of ^{14}C in water samples ISO 13162. Since the steps of acidification and concentration of the sample were removed, this procedure allows the determination of ^{3}H and ^{14}C by means of a multivariate calibration using PLS models.

- *Selective extraction using radium RAD disk and measurement by LSS:* In this procedure, selective extraction of radium and lead isotopes is performed by means of a 3M Empore™ Radium RAD disk. These 47 mm diameter filters are composed of crown ether that is covalently bound to an inert substrate. In the optimized procedure, RAD disks are preconditioned by filtering 20 mL of 2 mol L^{-1} HNO_3. Afterwards, an aliquot from 1 to 5 L of sample acidified to pH lower than 2 with HNO_3 are filtered through the RAD disk using a vacuum filtering system. Lead isotopes are then eluted from the RAD disk by using 7 mL of dihydrogen ammonium citrate (DHC) 0.05 mol L^{-1} at pH 5.75, which were collected in a polyethylene vial. 5 mL of this solution was mixed with 15 mL of Optifase Hisafe™ III and measured in a Wallac QUANTULUS for 100 min after waiting two hours to avoid photoluminescence phenomena. Besides this, the RAD disk was transferred into another PE vial to which 20 mL of Hisafe III was added. This vial was measured for 100 min after waiting eight hours to ensure correct

impregnation of the RAD disk with the cocktail, which prevents bad alpha-beta classification and shifting of the spectra during the measurement.

The experimental work conducted in the framework of this thesis has been conducted in the laboratory of environmental radioactivity of the University of Barcelona (LRA-UB) accredited by the National Accreditation Body under ISO/IEC 17025 with ENAC accreditation number LE/1117. Gamma spectrometry and simultaneous determination of gross alpha and gross beta emitters by $LSS_{conc.}$ are in the scope of this accreditation, Furthermore, ^{226}Ra, ^{228}Ra and ^{210}Pb determination using RAD disk and LSS measurement is in process of accreditation.

7.2. PLS Model construction

7.2.1. Spectra database

To test the feasibility of PLS models to predict the activity of the studied radionuclides, a database of spectra from $LSS_{conc.}$, $LSS_{dir.}$ and RAD disk methodologies was constructed. Furthermore, γ-spectrometry measurements of the radionuclides with gamma emissions were also conducted.

For $LSS_{conc.}$ models, 33 single radionuclide standard solutions were prepared and analysed by triplicate. The radionuclides used to prepare these standard solutions are ^{40}K, ^{60}Co, $^{90}Sr/^{90}Y$, ^{134}Cs, ^{137}Cs, ^{210}Pb, ^{226}Ra, ^{228}Ra, ^{nat}U, $^{239+240}Pu$ and ^{241}Am at three levels of activity concentration.

For $LSS_{dir.}$ models, 39 single radionuclide standard solutions were prepared and analysed by triplicate. The radionuclides used to prepare these standard solutions are ^{3}H, ^{14}C, ^{40}K, ^{60}Co, $^{90}Sr/^{90}Y$, ^{134}Cs, ^{137}Cs, ^{210}Pb, ^{226}Ra, ^{228}Ra, ^{nat}U, $^{239+240}Pu$ and ^{241}Am at three levels of activity concentration.

For RAD disk models, nine single radionuclide standard solutions were prepared and analysed by triplicate. The radionuclides used to prepare these standard solutions are ^{210}Pb, ^{226}Ra and ^{228}Ra at three levels of activity concentration and per triplicate. It has to be pointed out that, for this method, two different vials were prepared for each sample. One containing the fraction eluted with DHC (lead fraction) and another containing the RAD disk with radium isotopes.

Table 4 shows the three levels of activity concentration analysed for the radionuclides studied. ^{40}K is included in the study because, though it is not included in the directive concerning drinking water, it is a radionuclide that can be found in natural water samples, and its presence may interfere with the quantification of other radionuclides if it is not considered in the calibration set.

Table 4. Activity concentration for the levels studied for each radionuclide. (H) high, (O) intermediate and (L) low activity concentration.

	Activity (Bq kg^{-1})		
Radionuclide	**(H)**	**(O)**	**(L)**
^{3}H	100	50	25
^{14}C	100	50	25
^{40}K	10	5	2
^{60}Co	50	25	10
$^{90}Sr/^{90}Y$	50	25	10
^{134}Cs	50	25	10
^{137}Cs	50	25	10
^{210}Pb	10	5	1
^{226}Ra	10	5	1
^{228}Ra	10	5	1
$^{234+238}U$	10	5	1
$^{239+240}Pu$	10	5	1
^{241}Am	10	5	1

For both LSS methods ($LSS_{conc.}$ and $LSS_{dir.}$) two spectra were obtained for each replicate of the sample (alpha and beta). For the RAD disk method, the spectra used to construct the PLS models are the alpha and beta of the RAD disk fraction and the beta of the fraction eluted with DHC. The SQP[E] spectra for each measurement were used to select the level of quenching of the standards used to construct the PLS model to quantify each sample. Figure 9 shows the scheme of the database of spectra used to construct PLS models for simultaneous determination of several alpha and beta emitters.

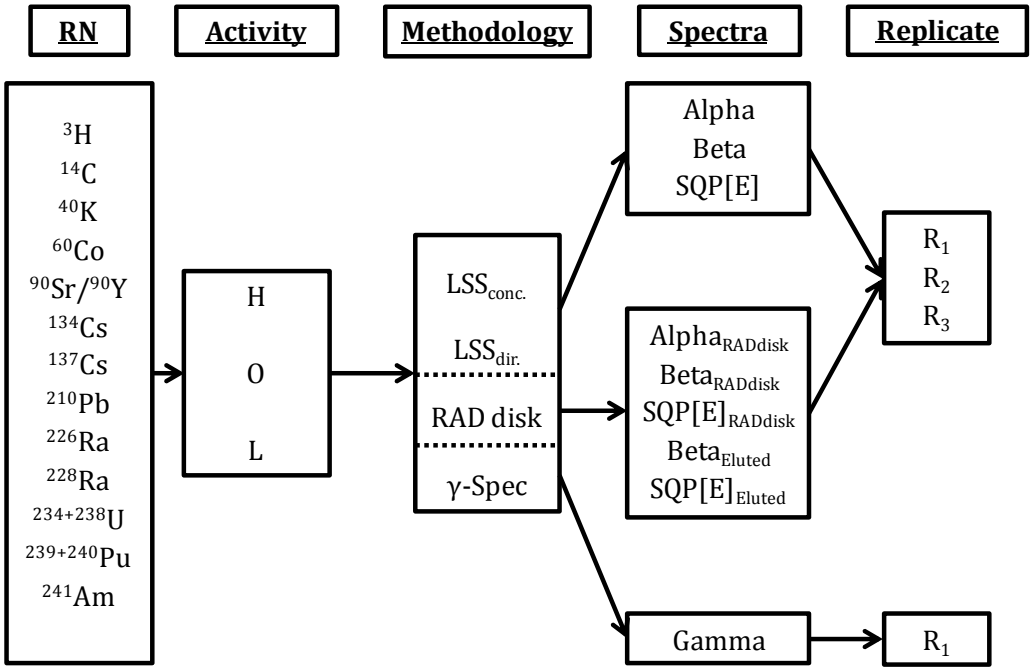

Figure 9. Scheme of the database of spectra used for PLS models construction.

7.2.2. Data pre-treatment

The procedure to construct a PLS model consists of selecting from the database the spectra of the radionuclides of interest (taking into account the results obtained in other methodologies). The SPQ[E] of each measurement is considered to select the database that will be used to quantify each sample. After this, the region of interest (ROI) is selected depending on the methodology and the radionuclides included in the model. The ROI for each standard (alpha and beta for LSS and beta region of eluted fraction for RAD disk method) are joined in the same vector, and then all the standards are stored in a matrix. The matrix obtained was then smoothed using a Savitzky-Golay filter and mean centred. This is the calibration set or X-Block.

As an example, the construction of a PLS model with LSS$_{conc.}$ spectra for ^{40}K, ^{60}Co, ^{90}Sr/^{90}Y, ^{137}Cs, ^{nat}U and ^{241}Am is described.

To include the information of the alpha and beta spectra in the same vector, the channels of each of the spectra containing information have been selected. For this, the ROI is selected as all channels except those that do not contain accounts in 95 % of the spectra. It has been found that the ROI that provide information and with which we work are between channels 545 and 915 for the alpha spectrum and between channels 75 and 895 for the beta spectrum. Figure 10 shows the alpha spectrum (red) and the beta spectrum (blue), both of which correspond to a ^{90}Sr sample in a secular equilibrium with ^{90}Y, where the window is

selected for each spectrum. It should be pointed out that the signal that appears in the α-MCA is due to interference caused by ^{90}Y (high-energy beta emitter 2.28 MeV).

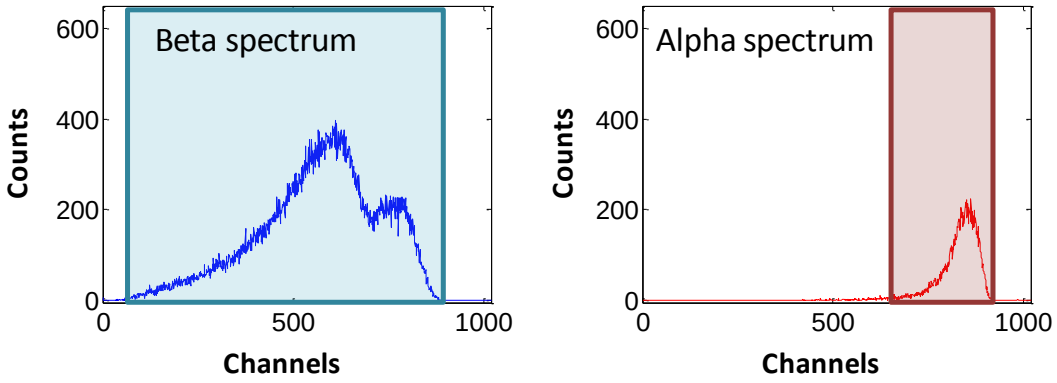

Figure 10. Beta and alpha spectra of $^{90}Sr/^{90}Y$. The shaded region indicates the selected ROI.

When alpha and beta ROI are selected, both are joined in a same vector. For this purpose, the matrix that contains beta ROIs of all the selected standards is enlarged in the direction of the rows, adding as new columns the matrix that contains alpha ROIs. Figure 11 shows a graphic representation of the matrix enlarged in the rows direction for each studied radionuclide.

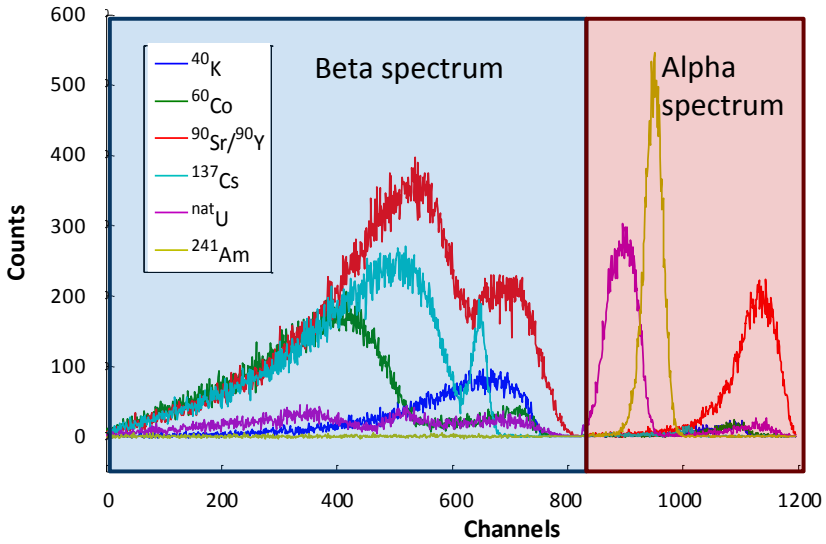

Figure 11. Graphic representation of the matrix enlarged in the rows direction which contains alpha and beta ROI for a replicated of a standard of high activity for the six radionuclides.

The matrix was the smoothed and mean centred. The smoothing was performed by means of Savitzky-Golay filter with polynomial order 1 and a window width of 31 channels.

In other words, groups of 31 points of each spectrum were interpolated into a line, and this interpolation was used to obtain the new, smoothed vector. With this process, small variations in the spectra caused by instrumental noise are neglected in subsequent calculations. The mean centring process consists of subtracting from each spectrum the mean of the entire matrix on the rows direction following the next equations:

$$X_{ik}^{*} = X_{ik} - \overline{X_k} \quad (7.1) \qquad\qquad \overline{X_k} = \frac{\sum_{k=1}^{K} X_{ik}}{K} \quad (7.2)$$

where

X_{ik} and X_{ik}^{*} are the original and the mean-centred vectors of spectra, respectively;

$\overline{X_k}$ is a row vector composed of the mean of each column; and

K is the number of rows of the X-Block.

Although this procedure does not entails a large improvement of the prediction of the model, it is a necessary step before the PLS model construction. Figure 12 is a graphic representation of the X-Block matrix, which contains alpha and beta spectra from 54 standard solutions (three replicates at three activity concentrations for six radionuclides). Figure 12a shows original data while Figure 12b shows the smoothed and mean-centred matrix.

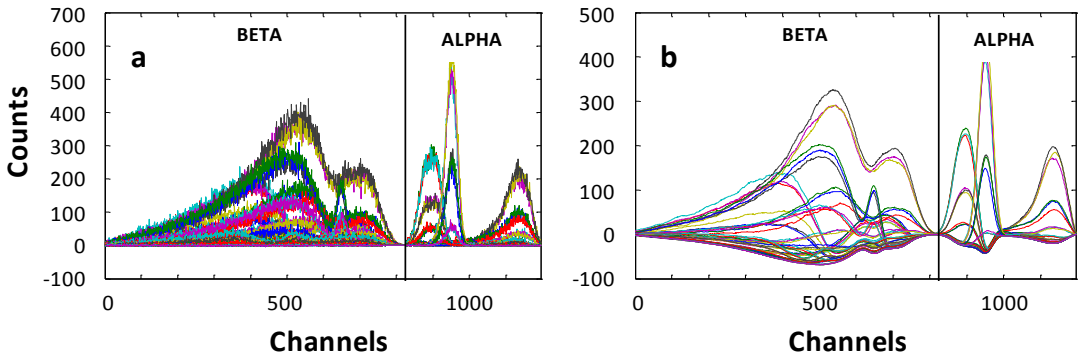

Figure 12. Original matrix which contains 54 standard solution spectrum (a) and smoothed and mean-centered matrix (b).

On the other hand, the activity for each radionuclide in each of the spectra obtained was calculated following Equation (7.3). In this way, a second matrix (Y-Block) with 54 rows (one for each spectrum) and six columns (one for each radionuclide) was obtained:

$$A_v^i = \frac{A_m^i * m_m * m_v}{m_{dis}} \quad (7.3)$$

where

A_v^i is the activity of the radionuclide *i* in the counting vial in Bq;

A_m^i is the activity of the radionuclide *i* in the standard at measurement date in Bq kg^{-1};

m_m is the mass of sample in kg;

$m_{dis}$is the mass after dissolution of the sample evaporated to dryness in kg; and

m_v is the mass of solution added into the counting vial in kg.

In this way the X-Block matrix (which contains the alpha and beta spectrum of the standards of the radionuclides of interest) and the Y-Block matrix (which contains the activity corresponding to the X-Block spectra) were obtained and can be used to construct a PLS model. This PLS model makes it possible to quantify the activity concentration of samples that contain mixtures of ^{40}K, ^{60}Co, ^{90}Sr/^{90}Y, ^{137}Cs, ^{nat}U and/or ^{241}Am.

7.3. Strategy

It was seen that even the determinations of specific alpha and beta emitters by LSS-PLS are accurate when the target radionuclides are included in the PLS model, this is highly affected by interferents not included on it. Furthermore, including radionuclides that are not in the sample in the PLS model makes it unnecessarily more complex. For these reasons, a strategy was defined to screen and select the radionuclides that have to be included in the calibration step for PLS model construction. Figure 13 is a flowchart for the application of the different methodologies studied and the PLS model construction. For each methodology, the volume of sample analysed is shown at the top left, the time of preparation is shown on the lower left side, and the counting time is shown on the lower right side.

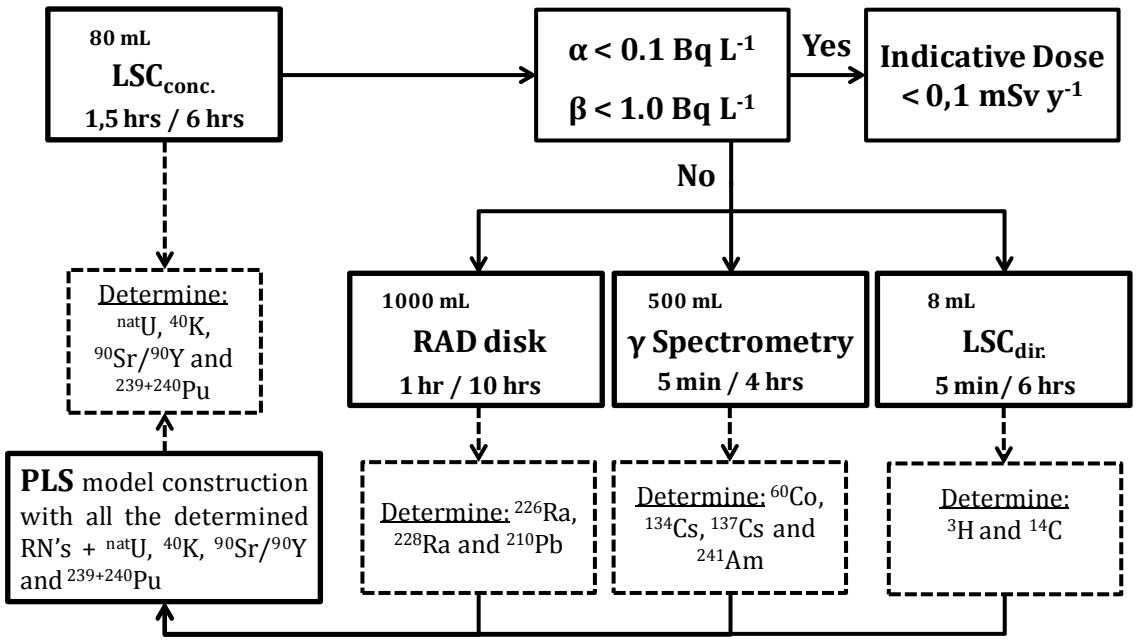

Figure 13. Application flowchart of the different studied methodologies and PLS model construction.

Firstly, gross alpha and beta determination is performed by means of the $LSS_{conc.}$ method. If gross alpha and gross beta activities are below 0.1 Bq L^{-1} and 1.0 Bq L^{-1} respectively, it can be assumed that no further analysis has to be performed because the indicative dose is below 0.1 mSv y^{-1}, as recommend the Directive 2013/51/EURATOM. Otherwise, the sample has to be measured following the other three methodologies: high-resolution gamma spectrometry, selective extraction using radium RAD disk and measurement by LSS, and the direct method with LSS measurement ($LSS_{dir.}$). The presence of ^{60}Co, ^{134}Cs, ^{137}Cs and ^{241}Am in the sample is assessed by high-resolution gamma spectrometry. In the same way, ^{210}Pb, ^{226}Ra and ^{228}Ra are assessed by extraction with the RAD disk and the LSS measurement. From the results obtained, a PLS model is constructed by using the standard spectra of the $LSS_{dir.}$ method. The radionuclides that have to be included in the model are all those detected by the aforementioned methodologies plus ^{3}H, ^{14}C, ^{40}K, $^{90}Sr/^{90}Y$, ^{nat}U and $^{239+240}Pu$. By means of this model, ^{3}H and ^{14}C can be quantified. Furthermore, ^{40}K, $^{90}Sr/^{90}Y$ ^{nat}U and $^{239+240}Pu$ can be detected, but they will be quantified by using the PLS model constructed with $LSS_{con.}$ method spectra, due to its lower detection limits. Table 5 summarizes the data shown in Figure 13, which graphically depicts the methodology by which each radionuclide has been determined.

Table 5. Radionuclides studied together with the methodology used to determine them.

Radionuclides	Methodology
^{60}Co, ^{134}Cs, ^{137}Cs and ^{241}Am	γ Spec.
^{226}Ra, ^{228}Ra and ^{210}Pb	RAD disk
^{3}H and ^{14}C	$LSS_{dir.}$-PLS
^{40}K, ^{90}Sr/^{90}Y, ^{nat}U and $^{239+240}$Pu	$LSS_{conc.}$-PLS

It has to be pointed out that the determination of ^{222}Rn is neglected in the flowchart of the strategy even though it is a parameter that has to be determined to accomplish the directive because it can be independently determined.

7.4. Application to natural samples

7.4.1. $LSS_{dir.}$-PLS: Tritium determination on environmental water samples (PVRA)

Direct measurement by liquid scintillation spectrometry methodology ($LSS_{dir.}$) was used to determine the ^{3}H activity concentration of several water samples in the framework of PVRA around NPP of Vandellós II in the period between 2012 and 2015. Different matrices—such as marine water, superficial water, underground water and drinking water—were analysed by means of both the accredited method used in the laboratory based on a distillation process, and by $LSS_{dir.}$ with PLS quantification. Then the results obtained for both methods were compared.

The accredited method consists of taking an aliquot of 300 mL of water sample, basifying it with 2 g of NaOH and adding 75 mg of $KMnO_4$ for continental water samples and 100 mg for marine water. The sample is then introduced into a distillation system, heated until the boiling point and refluxed for 60 minutes to ensure a homogeneous distribution of hydrogen isotopes. After that, the sample is distilled; the first 30 mL is discarded and then 150 mL is collected. An aliquot of 8.6 mL of the distilled sample is mixed with 11.4 mL of Optiphase Hisafe III scintillation cocktail. The sample is measured for 24 hours by LSS considering a quenching curve.

The PLS model used to quantify the $LSS_{dir.}$ measurements was constructed by using a calibration set and the standards of ^{3}H, ^{14}C and ^{40}K, which are the radionuclides expected in these samples. Table 6 presents the results of ^{3}H obtained by both methods with their uncertainties. No replicate from either method was analysed.

Table 6. ^{3}H activity concentration for ten natural samples measured by distillation and $LSS_{dir.}$-PLS method.

	Distillation method		**$LSS_{dir.}$-PLS method**		
CODE	*Activity* *Bq kg^{-1}*	*Uncert.* *Bq kg^{-1}*	*Activity* *Bq kg^{-1}*	*Uncert.* *Bq kg^{-1}*	*Bias* *%*
Mar. 2012	407.5	27.3	367.3	36.7	-10 %
Mar. 2013	69.1	4.7	66.6	6.7	-4 %
Sup. 2012	3.07	0.62	3.55	0.70	16 %
Sup. 2013	< 1.88	-	< 3.15	-	-
Sup. 2014	10.10	1.01	8.90	0.89	12 %
Sup. 2015	< 1.66	-	< 3.15	-	-
Und. 2012	3.75	0.67	3.25	0.64	-13 %
Und. 2013	2.63	0.60	< 3.15	-	-
Und. 2014	4.91	0.80	3.59	0.72	-27 %
Und. 2015	< 1.65	-	< 3.15	-	-
Dri. 2014	7.85	0.81	7.85	0.79	0 %
Dri. 2015	6.63	1.49	6.02	0.60	-9 %

When the ^{3}H activity concentration determined by both methods are compared, it can be seen that, in general, the bias obtained around 10 %. Just for the water samples near the AMD (Sup. 2012, Und. 2012 and Und. 2014), the bias observed is higher and in some cases near to 30 %. This may be explained by the high variability of the results near the MDA, which could be controlled by measuring replicates. It has to be pointed out that the MDA for the accredited method is lower than the value obtained with the $LSS_{dir.}$-PLS method. For this reason, some samples (just *Und. 2013* on the studied set) may present a ^{3}H activity concentration that is below the MDA for the new proposed method but can be detected by the distillation method. For the $LSS_{dir,}$ method, the activity concentration of ^{40}K is below the AMD (0.35 Bq kg^{-1}) for all the samples except the marine ones. The ^{40}K activity concentration for these samples is 8.6 ± 0.9 Bq kg^{-1} and 7.7 ± 0.8 Bq kg^{-1} for Mar. 2012 and Mar. 2013, respectively. Finally, for the entire set of samples, the activity concentration of ^{14}C was below the detection limit (0.39 Bq kg^{-1}).

7.4.2. Natural radionuclides in environmental water samples

The results of a set of natural drinking water samples analysed using RAD disk methodology (included in the paper, "*Simultaneous determination of ^{226}Ra, ^{228}Ra and ^{210}Pb in*

drinking water using 3M Empore™ RAD disk by LSC-PLS") and $LSC_{conc.}$-PLS (included in the paper *"Simultaneous determination of gross alpha, gross beta and ^{226}Ra in natural water by liquid scintillation counting"*) are discussed in this section. The natural water samples analysed in the context of this thesis contain only natural radionuclides.

The selected samples are a set of five natural water sources that have potential for use as drinking water. Gross alpha and gross beta activities were determined by means of the procedure explained in section 4. The results obtained by the $LSS_{conc.}$ method are listed in Table 7, and gross alpha was compared with a reference value obtained by summing the contribution of ^{234}U, ^{235}U, ^{238}U, ^{224}Ra, ^{226}Ra and ^{210}Po determined by alpha spectrometry.

Table 7. Gross alpha and gross beta activities for the set of five natural samples.

	LSS method (Bq kg^{-1})		**Reference**	**Bias**
Code	*Gross α*	*Gross β*	*Gross α*	*Gross α*
S_1	1.29 ± 0.45	0.78 ± 0.06	1.39 ± 0.18	- 7 %
S_2	6.28 ± 0.62	5.52 ± 0.29	6.2 ± 0.58	1 %
S_3	0.18 ± 0.06	0.33 ± 0.07	0.19 ± 0.03	-2 %
S_4	< 0.03	< 0.10	0.04 ± 0.01	-
S_5	0.10 ± 0.08	0.29 ± 0.07	0.10 ± 0.02	-1 %

Following the criterion of the directive, according to which gross alpha and gross beta activities may be indicative of the ID, it can be seen that S_2 overtakes the derived activity concentration regarding gross beta (1.0 Bq L^{-1}) and that samples S_1, S_2 and S_3 exceeds the limit of gross alpha (0.1 Bq L^{-1}).

Nevertheless, all the samples were analysed using the RAD disk method for the determination of ^{226}Ra, ^{228}Ra and ^{210}Pb, and the spectra obtained from the analysis of gross alpha and gross beta activities were deconvoluted to quantify ^{nat}U and ^{40}K.

Table 8 reports the results obtained applying the strategy and reference values. The reference values for the different natural radionuclides were determined by accredited methods using *α* spectrometry for ^{226}Ra and ^{nat}U, by extraction with specific resin and LSS determination for ^{210}Pb, and by atomic-absorption spectrometry for ^{40}K considering the natural abundance.

For all the samples, the results obtained from applying the proposed strategy are consistent with those obtained via reference procedures. A bias below 15 % was obtained in all the cases.

Table 8. ^{210}Pb, ^{226}Ra and ^{nat}U activity concentration for five natural water samples using the proposed strategy and reference procedures.

	Strategy (Bq kg^{-1})			**Reference (Bq kg^{-1})**			**Bias (%)**		
Code	^{210}Pb	^{226}Ra	^{nat}U	^{210}Pb	^{226}Ra	^{nat}U	^{210}Pb	^{226}Ra	^{nat}U
S_1	<0.02	0.51	0.80	0.028	0.55	0.78	-	-7	3
S_2	0.13	0.19	6.10	0.11	0.16	5.90	13	15	3
S_3	<0.02	<0.02	0.18	<0.0003	0.005	0.16	-	-	13
S_4	<0.02	<0.02	<0.03	0.001	0.002	0.032	-	-	-
S_5	<0.02	0.08	0.09	0.001	0.070	0.082	-	14	4

For ^{210}Pb, S_2 has activity above the detection limit, and the other samples were below 0.02 Bq kg^{-1}. ^{226}Ra was found in a range below the detection limit (0.02 Bq kg^{-1}) to 0.51 Bq kg^{-1}, and ^{nat}U was found below the detection limit (0.03 Bq kg^{-1}) to 6.1 Bq kg^{-1}.

Regarding ^{228}Ra and ^{40}K, the activity concentration in all the samples was below the limits of detection of 0.03 Bq kg^{-1} and 0.9 Bq kg^{-1}, respectively.

From the results obtained by applying Equation 2.5 it can be seen that the ID of S_3, S_4 and S_5, considering a consumption of 730 L per year, is below 0.1 mSv y^{-1}, while S_1 (mainly by ^{226}Ra contribution) and S_2 (mainly for ^{nat}U contribution) exceed this value.

7.4.3. Artificial radionuclides in environmental water samples

Since no artificial radionuclides were observed in the natural water samples analysed, the application of the proposed strategy for their determination was evaluated by means of quality control materials and inter-comparison exercises. This section discusses the results obtained by applying the strategy explained in Section 7.3 for IAEA-TEL-2014-03 Sample 03 and IAEA-TEL-2015-03 Sample 01.

Regarding the inter-comparison of IAEA-TEL-2015-03, Sample 01 is a spiked water sample for which the organizer requests the activity of anthropogenic gamma emitters and ^{90}Sr. First, a high-resolution gamma spectrometry measurement was performed to determine the caesium isotopes activity concentration. ^{134}Cs and ^{137}Cs were determined and no further gamma emitters were detected. After this, a PLS model for $LSS_{conc.}$ method was

constructed by using ^{134}Cs, ^{137}Cs and ^{90}Sr/^{90}Y spectra as standards. The results obtained for γ spectrometry and $LSS_{conc.}$-PLS are shown in Table 9.

Table 9. Activity concentration of the inter-comparison exercise IAEA-TEL-2015 Sample 01 obtained by γ spectrometry and $LSS_{conc.}$-PLS compared with that given by the organizer. The values obtained by following the proposed strategy are highlighted in shading.

RN	**γ-Spec. (Bq kg^{-1})**	**$LSS_{conc.}$-PLS (Bq kg^{-1})**	**Organizer (Bq kg^{-1})**	***Statistics performance***		
				Relative Bias	*Robust SD*	*z-score*
^{90}Sr	-	34.1 ± 3.4	29.6 ± 0.8	7.4 %	3	0.7
^{134}Cs	28.5 ± 2.2	31.9 ± 3.2	30.0 ± 0.9	-5.0 %	1.8	0.8
^{137}Cs	30.2 ± 2.4	32.9 ± 3.3	30.1 ± 0.9	0.3 %	1	0.1

From these results, which are partially shown in the paper "*Simultaneous determination of specific alpha and beta emitters by LSC-PLS in water samples*", from Chapter 5, two conclusions can be derived. On one hand, γ spectrometry makes it possible to determine gamma emitters with low bias, and, furthermore, makes it possible to identify the gamma emitters that must be included in the PLS model to achieve a more realistic scenario. On the other hand, the $LSS_{conc.}$-PLS method, is not only useful for the determination of ^{90}Sr/^{90}Y but also allows for the quantification of ^{134}Cs and ^{137}Cs with a low uncertainty.

Regarding the quality-control material IAEA-TEL-2014-03 Sample 03, the organizer reports the radionuclides present in the sample and its activity concentrations. However, the strategy described in Section 7.3 was applied to this sample, as no information about the sample was given. Gross alpha and gross beta activities were evaluated as 35.5 ± 2.5 Bq kg^{-1} and 81 ± 5 Bq kg^{-1}, respectively. After this, γ spectrometry measurement was performed and ^{134}Cs, ^{137}Cs and ^{241}Am were determined. ^{40}K, ^{60}Co, ^{210}Pb, and ^{228}Ra (via ^{228}Ac) were not detected. ^{226}Ra (via ^{214}Pb) was detected, but since no secular equilibrium was reached when the measurement was performed, ^{226}Ra was underestimated. The RAD disk methodology was applied to determine ^{226}Ra and to evaluate the presence of ^{228}Ra and ^{210}Pb. Values of 18.6 ± 0.6 Bq kg^{-1} and 9.4 ± 0.5 Bq kg^{-1} were determined for ^{226}Ra and ^{210}Pb, respectively, while for ^{228}Ra, the results were below the detection limit. With this information, the PLS model using spectra of $LSS_{dir.}$ was constructed to quantify ^{3}H and ^{14}C. The radionuclides included in the model are all the listed in **Table 4** except for ^{60}Co and ^{228}Ra, which are excluded because they were discarded by other methodologies. ^{3}H and ^{14}C were below the detection limit, as was ^{40}K. Regarding $^{239+240}$Pu, its activity concentration was determined to be above the detection limit. However, the activity concentration of

$^{239+240}$Pu (3.2 ± 0.6 Bq kg^{-1}) and that of ^{241}Am (14.5 ± 1.5 Bq kg^{-1}), determined by LSS$_{dir.}$-PLS method, were around the activity concentration of ^{241}Am determined by γ spectrometry. This fact suggests, as is the case with ^{134}Cs and ^{137}Cs in *"Simultaneous determination of specific alpha and beta emitters by LSC-PLS in water samples"*, there is an interference of ^{241}Am in the determination of $^{239+240}$Pu, both with close energy on its characteristic alpha emission (5.49 MeV and ~ 5.25 MeV, respectively). For this reason, $^{239+240}$Pu was excluded from the PLS model construction. With the new PLS model, the ^{241}Am activity concentration determined by γ spectrometry and that determined by LSS$_{dir.}$-PLS were concordant.

Since ^{40}K may be determined with lower detection limits with LSS$_{conc.}$ method, it was included in the LSS$_{conc.}$-PLS model. Thus, the radionuclides included in LSS$_{conc.}$-PLS model are the following: ^{40}K, ^{90}Sr/^{90}Y, ^{134}Cs, ^{137}Cs, ^{226}Ra, ^{nat}U and ^{241}Am. By means of this model, the spectrum previously used to determine gross alpha and gross beta activities was analysed. Table 10 shows the results obtained by the four studied methodologies. The methodology used to determine each radionuclide is highlighted in shading. Table 10 also includes the relative bias between the shaded value and the value reported by the organizer.

Table 10. Activity concentration of the quality control material IAEA-TEL-2014-03 Sample 03 obtained following the proposed strategy compared with that given by the organizer. The results with which relative bias was calculated are highlighted in shading.

RN	γ-Spec. (Bq kg^{-1})	RAD disk (Bq kg^{-1})	LSS$_{dir.}$-PLS (Bq kg^{-1})	LSS$_{conc.}$-PLS (Bq kg^{-1})	Organizer (Bq kg^{-1})	Relative Bias (%)
^{3}H	-	-	< 5.2	-	-	-
^{14}C	-	-	< 3.8	-	-	-
^{40}K	< 10.7	-	< 3.6	< 0.4	-	-
^{60}Co	< 0.3	-	-	-	-	-
^{90}Sr/^{90}Y	-	-	19.3 ± 2.9	22.6 ± 2.3	24.5 ± 0.2	-8 %
^{134}Cs	23.2 ± 0.4	-	35.2 ± 5.3	31.6 ± 3.2	26.3 ± 0.2	-12 %
^{137}Cs	19.3 ± 0.3	-	12.8 ±1.9	15.2 ± 1.5	19.6 ± 0.1	-2 %
^{210}Pb	12.0 ± 2.7	9.4 ± 0.5	7.6 ± 1.2	9.1 ± 0.9	-	-
^{226}Ra	8.2 ± 0.4[1]	18.6 ± 0.6	15.5 ±2.3	15.2 ± 1.5	17.9 ± 0.1	4 %
^{228}Ra	< 1.6[2]	< 0.03	-	-	-	-
^{nat}U[3]	-	-	7.1 ± 1.1	6.3 ± 0.6	5.48 ± 0.04	14 %
$^{239+240}$Pu	-	-	-	-	-	-
^{241}Am	21.3 ± 0.3	-	21.1 ±3.2	17.0 ± 1.7	20.0 ±0.1	-6 %

[1] Via ^{214}Bi (609.31 keV, not in secular equilibrium)

[2] Via ^{228}Ac (911.21 keV)

[3] Sum of ^{234}U and ^{238}U

These results—partially shown in the paper, "*Simultaneous determination of specific alpha and beta emitters by LSC-PLS in water samples*" ($LSS_{conc.}$-PLS method) and in the paper, "*Simultaneous determination of ^{226}Ra, ^{228}Ra and ^{210}Pb in drinking water using 3M Empore™ RAD disk by LSC-PLS*" (RAD disk method)—illustrate the usefulness of the proposed strategy.

^{3}H and ^{14}C were found below the detection limit by the $LSS_{dir.}$-PLS method.

^{40}K was found below the detection limit for all the methodologies used, but the result reported is that obtained by $LSS_{con.}$-PLS, which provides the lower detection limit.

^{60}Co was below the detection limit for γ spectrometry and hence was not included in the LSS_{dir} and LSS_{conc}. PLS models.

$^{90}Sr/^{90}Y$ and ^{nat}U were detected by both the $LSS_{dir.}$-PLS and $LSS_{conc.}$-PLS. However, since the $LSS_{conc.}$-PLS method has lower detection limits and uncertainty, the results of both radionuclides were given by this method.

^{134}Cs, ^{137}Cs and ^{241}Am were determined by γ spectrometry and were included in PLS models to consider the radionuclides present in the sample.

Finally, ^{210}Pb, ^{226}Ra and ^{228}Ra were determined by means of RAD disk methodology, although they may be also determined by γ spectrometry, $LSS_{dir.}$-PLS or $LSS_{conc.}$-PLS methods. This selection was made because RAD disk is the method with the higher selectivity and the lowest limit of detection. Furthermore, the determination of ^{226}Ra via ^{214}Bi by γ-spectrometry must meet some requirements. On one hand, the sample should not contain unsupported ^{222}Rn, because ^{214}Bi is in equilibrium with ^{222}Rn; hence, ^{226}Ra will be overestimated. On the other hand, the counting geometry must be sealed to avoid ^{222}Rn releases, and one must wait until secular equilibrium between ^{226}Ra and ^{222}Rn has been achieved. This requirement makes ^{226}Ra via ^{214}Bi by γ-spectrometry a slow procedure.

Is has to be noted that the results obtained by the $LSS_{conc.}$ and LSS_{dir} methods for radionuclides such as ^{134}Cs, ^{137}Cs, ^{210}Pb, ^{226}Ra and ^{241}Am are also concordant with that provided by the organizer.

In less than 24 hours,

7.5. Further applications

The proposed strategy makes it possible to determine even 13 radionuclides from a sample of 1.5 L in less than 24 hours. Furthermore, the strategy makes it possible to significantly reduce the reagents used because the methods used entail a minimum

radiochemical separation. For all these reasons, the proposed strategy has been shown to be rapid screening method.

The analytical procedures used, together with PLS models quantification, realize a rapid determination of alpha and beta emitters in waters. For this reason, the quantification of LS spectra by means of PLS in other matrices, such as soil lixiviates or urine samples, should be explored in situations that require rapid screening methods as emergency events.

8. CONCLUSIONS

From the research conducted in the present doctoral thesis, the following conclusions can be inferred:

Regarding the determination of gross alpha and gross beta activities by LSS,

1. A procedure for the rapid determination of gross alpha and gross beta activities by LSS has been optimized and validated for the measurement of water samples.

2. The activity of ^{226}Ra can be simultaneously estimated by means of a second measurement of the counting vial after six days of sample treatment.

3. The validated procedure provides results that are comparable with the classical methods—like evaporation and co-precipitation methods—for gross alpha determination and summation of alpha emitters.

Regarding the determination of ^{226}Ra, ^{228}Ra and ^{210}Pb by RAD disk extraction and LSS measurement,

4. A procedure for rapid determination of ^{226}Ra, ^{228}Ra and ^{210}Pb using Radium RAD disk and LSS was developed and validated.

5. Direct measurement of Radium RAD disk by LSS may be performed under some conditions. The most important of them is to ensure a good impregnation of the filter to avoid α/β separation issues and shifting of the spectra. To achieve this impregnation of the RAD disk, there is need to wait eight hours or to force this impregnation by sucking the scintillation cocktail trough the RAD disk.

6. To achieve an appropriate determination of ^{228}Ra and to avoid interference between ^{210}Pb and ^{228}Ra, DHC can be used to selectively elute ^{210}Pb from the RAD disk in order to separately measure lead and radium isotopes.

Regarding the PLS models for LS spectra deconvolution,

7. The studies conducted to test the feasibility of PLS models for LS spectra deconvolution have proven that this is a valid procedure for the determination of several radionuclides from LS spectra. However, it must be noted that, to obtain reliable results, it is critical to include in the calibration set all the radionuclides expected in the studied scenario.

8. PLS models have been proved valid for the quantification of specific radionuclides from LS spectra not only for procedures that determine global

alpha and beta activities but also for procedures that entail a radiochemical separation, such as RAD disk extraction.

9. The quantification of LSS by means of PLS in other matrices should be explored for situations that require rapid methods such as accidental events.

Regarding quenching effects in efficiency, spectrum shape and α/β separation,

10. The efficiency is highly affected for low-energy beta emitters and just moderately for high-energy beta emitters, while alpha emitters are not clearly affected.

11. Colour quenching modifies α/β classification in to a higher degree than chemical quenching.

12. The nature of quenching in real samples must be properly studied to select the best quenching agent to perform the quenching curves and hence to set up the PSD, correct the efficiency, and, if necessary, correct the shifting of the spectra.

Regarding the strategy for applying the developed methodology,

13. A strategy has been proposed to sequentially determine the radionuclides included in the Annex III of the Directive 2013/51/EURATOM, which combines the procedures developed in this thesis and other classical measurements like γ spectrometry.

14. This strategy, either entire or partially, satisfactorily determined the activity of specific radionuclides in water samples of PVRA, sources with potential use as drinking water, and spiked quality-control materials.

15. The proposed strategy makes it possible to determine even 13 radionuclides in a rapid way (less than 24 hours) with a minimum radiochemical separation which entails a significant reduction of the used reagents.

REFERENCES

Abdi, H. (2003) Partial Least Sqares (PLS) Regression. In Lewis-Beck, M., Briman, A., Futing T. (eds.) *Encyclopedia of Social Sciences Research Methods*. Thousand Oaks (CA): Sage.

Altzitzoglou, T. (2008) Radioactivity determination of individual radionuclides in a mixture by liquid scintillation spectra deconvolution, *Applied Radiation and Isotopes, 66*(6-7), pp. 1055–1061. doi: 10.1016/j.apradiso.2008.02.052.

Bagán, H., Tarancón, A., Rauret, G. and García, J.F. (2011) Mixture quantification using PLS in plastic scintillation measurements. *Applied radiation and isotopes, 69*(6), pp. 898–903. doi: 10.1016/j.apradiso.2011.02.039.

Bourdon, F., Lecoeur, M., Odou, P., Vaccher, C. and Foulon, C. (2014) Complementarity of UV-PLS and HPLC for the simultaneous evaluation of antiemetic drugs. *Talanta, 120*, pp. 274–282. doi: 10.1016/j.talanta.2013.12.015.

Cassette, P. (2016) QUENCH: A software package for the determination of quenching curves in liquid scintillation counting. *Applied Radiation and Isotopes, 109*, pp. 301-307.

Corbacho, J.A., Zapata-García, D., Montaña, M., Fons, J., Camacho, A., Guillén, J., Serrano, I., Baeza, A., Llauradó, M. and Vallés, I. (2016) Selection of the appropriate radionuclide source for the efficiency calibration in methods of determining gross alpha activity in water. *Journal of Environmental Radioactivity, 151*, pp. 22–27 doi: 10.1016/j.jenvrad.2015.07.029.

Deschamps, P., Hillaire-Marcel, C., Michelot, J.L., Doucelance, R., Ghaleb, B. and Buschaert, S. (2004) $^{234}U/^{238}U$ Disequilibrium along stylolitic discontinuities in deep Mesozoic limestone formations of the Eastern Paris basin: evidence for discrete uranium mobility over the last 1-2 million years. *Hydrology and Earth System Sciences Discussions, European Geosciences Union, 8* (1), pp. 35-46. doi: 10.5194/hess-8-35-2004.

EURATOM 1996, Council Directive 96/29/EURATOM of 13 May 1996 laying down basic safety standards for the protection of the health of workers and the general public against the dangers arising from ionizing radiation. L 159/1.

EURATOM 2013, Directive 2013/51/EURATOM of 22 October 2013, laying down requirements for the protection of the health of the general public with regard to radioactive substances in water intended for human consumption. L 296/12.

Hueber-Becker, F., Nohynek, G.J., Dufour, E.K., Meuking, W.J., de Nie, A.T., Toutain, H. and Bolt, H.M. (2007) Occupational exposure of hairdressers to [^{14}C]-para-phenylenediamine-containing oxidative hair dyes: a mass balance study. *Food and chemical toxicology : an international journal published for the British Industrial Biological Research Association, 45*(1), pp. 160–169. doi: 10.1016/j.fct.2006.08.002.

ISO, International Organization for Standardization. ISO 13162:2011 Water quality — Determination of carbon 14 activity — Liquid scintillation counting method. Switzerland.

ISO, International Organization for Standardization. ISO/IEC 17025:2005 General requirements for the competence of testing and calibration laboratories. Switzerland.

Kashirin, I., Ermakov, A.I., Malinovsky, S.V., Belanov, S.V., Sapozhnikov, A., Efimov. K.M., Tikhomirov, V.A. and Sobolev, A.I. (2000) Liquid scintillation determination of low level components in complex mixtures of radionuclides. *Applied radiation and isotopes, 53*(1-2), pp. 303–308. doi: 10.1016/S0969-8043(00)00145-7.

Kim, C.K., Al-Hamwi, A., Törvényi, A., Kis.Benedek, G. and Sansone, U. (2009) Validation of rapid methods for the determination of radiostrontium in milk. *Applied radiation and isotopes, 67*(5), pp.786–793. doi: 10.1016/j.apradiso.2009.01.036.

Kim, Y.J., Kim, C.S., Kang, S.H., Row, J.W., Lee, D.M. and Kim, C.K. (2006). Determination ^{129}I using liquid scintillation counting. *In S. Chalupnik, F. Schönhofer, and J. Koakes, eds. LSC 2005. "Advances in Liquid Scintillation Spectrometry."* Tucson: Radiocarbon, University of Arizona, pp. 273–276.

Kouru, H. and Rundt, K., 1991. Multilabel counting using digital overlay technique. *In H. Ross, J. E. Noakes, and J. Spaulding, eds. Liquid Scintillation Counting and Organic Scintillators*. Chelsea: Lewis Publishers, pp. 239–246.

L'Annunziata, M.F. and Kessler, M.J. (2012) Liquid scintillation analysis: principles and practice. In: L'Anninziata, M.F. (ed.) *Handbook of radioactivity analysis*. San Diego. Academic Press.

Llauradó, M., Vallès, I., Abelairas, A., Alonso, A., Díaz, M.F., García, R., Robador, L., Ruiz, P. and Suárez, J.A. (2004) Procedimientos para la determinación de los incices de actividad beta total y beta resto en aguas mediante contador proporcional. Madrid, CSN.

Llauradó, M., Vallès, I., Abelairas, A., Alonso, A., Díaz, M.F., García, R., de Lucas, M.J. and Suárez, J.A. (2005) Procedimiento para la determinación del índice de actividad alfa total en muestras de agua. Métodos de coprecipitación y evaporación. Madrid, CSN.

Mahani, M., Ghomi, S.H., Mazloomifar, A. and Salimi, B. (2012) Application of multi-way partial least squares calibration for simultaneous determination of radioisotopes by liquid scintillation technique. *Nuclear Technology and Radiation Protection, 27*(2) pp. 125–130.

Malinovsky, S.V., Kashirin, I.A., Ermakov, A.I., Tikhomirov, V.A., Belanov, V.A. and Sobolev, A.I. (2002) Mathematical aspects of decoding complex spectra applied to liquid scintillation counting. *In S. Möbius, J. E. Noakes, and F. Schönhofer, eds. LSC 2001. "Advances in Liquid Scintillation Spectrometry."* Tucson: Radiocarbon, University of Arizona, pp. 127–135.

McDowell, W.J. and McDowell, B.L. (1989) Liquid scintillation α spectrometry: a method for today and tomorrow. *In: Noakes JE, Schdnhofer F, Polach HA, editors.* Liquid Scintillation Counting and Organic Scintillators*.* Gatlinburg, Tenn, USA: RadioCarbon; 1989. pp. 105–122.

Montaña, M., Camacho, A., Serrano, I. and Vallés, I. (2012) Experimental analysis of the mass efficiency curve for gross alpha activity and morphological study of the residue obtained by the co-precipitation method. *Applied Radiation and Isotopes 70*, pp. 1541–1548.

Muresan, V., Danthine, S., Muresan, A.E., Racota, E., Blecker, C., Muste, S., Socaciu, C. and Baeten, V. (2016) In situ analysis of lipid oxidation in oilseed-based food products using near-infrared spectroscopy and chemometrics: The sunflower kernel paste (Tahini) example. *Talanta*, *155*, pp. 336–346. doi: 10.1016/j.talanta.2016.04.019.

Nakanishi, T., Kusakabe, M., Aono, T. and Yamada, M. (2009) Simultaneous measurements of cosmogenic radionuclides ^{32}P, ^{33}P and ^{7}Be in dissolved and particulate forms in the upper ocean. *Journal of Radioanalytical and Nuclear Chemistry, 279*(3), pp. 769–776. doi: 10.1007/s10967-008-7374-5.

Natake, T., Takiue, M. and Fujii, H., 1996. Nuclide identification for pure beta-emitting radionuclides with very similar beta end-point energies using a liquid scintillation spectrometer. *Nuclear Instruments and Methods in Physics Research Section A,* 378, pp. 506-510. doi: 10.1016/0168-9002(96)00520-7.

Nebelung, C. and Baraniak, L. (2007) Simultaneous determination of ^{226}Ra, ^{233}U and ^{237}Np by liquid scintillation spectrometry. *Applied Radiation and Isotopes, 65*(2), pp. 209–217. doi: 10.1016/j.apradiso.2006.06.002.

Nebelung, C., Jähnigen, P. and Bernhard, G. (2009) Simultaneous determination of beta nuclides by liquid scintillation spectrometry. *In J. Eikenberg et al., eds. LSC 2008. "Advances in Liquid Scintillation Spectrometry."* Tucson: Radiocarbon, University of Arizona, pp. 193–201.

Noor, A., Kasim, N. and L'Annunziata, M.F. (1995) Application of Pulse Height Spectral Analysis to Double-Label Counting of ^{35}S-^{32}P. *Applied Radiation and Isotopes, 44*(8), pp.791–797. doi: 10.1016/0969-8043(95)00027-B.

Noor, A., Zakir, M., Rasyid, B., Kasim, N., A Nurr, L., Anthony, Maming and Agung, M. (1996) Pulse Height Spectral Analysis of ^{3}H:^{14}C Ratios. *Applied Radiation and Isotopes, 47*(8), pp.767–775. doi: 10.1016/0969-8043(96)00046-2.

Okita, G.T., Kabara, J.J., Richardson, F. and LeRoy, G.V. (1957) Assaying compounds containing tritium and carbon-14. *Nucleonics, 15*(6), pp.111–114.

Pates, J.M., Cook, G.T., McKenzie, A.B., Passo, C.J. (1994) Quenching and its effect on alpha/beta separation liquid scintillation spectrometry. *Radiocarbon 1996* 75-85.

Pujol, Ll. and Sanchez-Cabeza, J.A. (1997) Role of quenching on alpha/beta separation in liquid scintillation counting for several high capacity cocktails. *The Analyst 122*, 383-385.

Remetti, R. and Franci, D. (2012) ABCD-Tool, a software suite for the analysis of α/β spectra from liquid scintillation counting. *Journal of Radioanalytical and Nuclear Chemistry*, *292*(3), pp.1115–1122. doi: 10.1007/s10967-012-1664-7.

Remetti, R. and Sessa, A. (2011) Beta spectra deconvolution for liquid scintillation counting. *Journal of Radioanalytical and Nuclear Chemistry, 287*(1), pp.107–111. doi: 10.1007/s10967-010-0882-0.

Roig, M., De Juan, A., García, J.F. and Rauret, G. (1999) Determination of a mixture of gamma-emitting radionuclides using solid scintillation detectors and multivariate calibration. Analytica Chimica Acta, 379(1), pp. 121-133. doi: 10.1016/S0003-2670(98)00620-5.

Royal Decree 314/16 of 29 July, that amends Royal Decree 140/2003 of 7 February, laying down sanitary criteria for the quality of water for human consumption, Royal Decree 1798/2010 of 30 December, which regulates the exploitation and commercialization of natural mineral waters and spring bottled waters for human consumption, and Royal Decree 1799/2010 of 30 December, regulating the process of elaboration and

commercialization of prepared bottled waters for human consumption. BOE-A-2016-7340.

Royal Decree 783/2001 of 6 July, by which it is approved the Regulation on the sanitary protection against ionizing radiations BOE-A-2001-14555.

Rundt, K. and Kouru, H. (1992) Apparatus and a method for measuring the activity of radioactive samples containing a multiple of radioactive isotopes. Patent US 5120962 A.

Salonen, L. (2006) Alpha spillover depends on alpha energy: a new finding in alpha/beta liquid scintillation spectrometry. *In S. Chalupnik, et al., (Eds.) LSC 2005. "Advances in Liquid Scintillation Spectrometry."* Tucson: Radiocarbon, University of Arizona. 135-148.

Shaffer, C.L. and Langer, C.S., 2007. Metabolism of a $^{14}C/^{3}H$-labeled GABAA receptor partial agonist in rat, dog and human liver microsomes: evaluation of a dual-radiolabel strategy. *Journal of pharmaceutical and biomedical analysis, 43*(4), pp. 1195–1205. doi: 10.1016/j.jpba.2006.11.022.

Stamoulis, K.C., Ioannides, K.G. and Karamanis, D., 2010. Deconvolution of liquid scintillation alpha spectra of mixtures of uranium and radium isotopes. *Analytica Chimica Acta, 657*(2), pp. 108–115. doi: 10.1016/j.aca.2009.10.034.

Stojkovic, I., Tenjovic, B., Nikov, J., Todorovic, N. (2015). Radionuclide, scintillation cocktail, and chemical/color quench influence on discrimination setting in gross alpha/beta measurements by LSC. *Journal of Environmental Radioactivity, 144*, 41-46.

Takiue, M., Fujii, H., Natake, T. and Matsui Y. (1991) Analytical measurements of multiples beta-emitter mixtures with liquid scintillation spectrometry. *Journal of Radioanalytical and Nuclear Chemistry, 155*(3), pp. 183-193. doi: 10.1007/BF02166643.

UNSCEAR, United Nations Scientific Comitee on the Effects of Atomic Radiation, Sources and effects of ionizing radiation. Annex B. Exposures of the public and workers from various sources of radiation, New York. United Nations 2000.

UNSCEAR, United Nations Scientific Comitee on the Effects of Atomic Radiation, Sources, effects and risk of ionizing radiation. New York. United Nations 2012.

UNSCEAR, United Nations Scientific Comitee on the Effects of Atomic Radiation, Sources and effects of ionizing radiation. New York. United Nations 2008.

UNSCEAR, United Nations Scientific Comitee on the Effects of Atomic Radiation Developments since the 2013 UNCEAR report on the levels and effects of radiation exposure due to the nuclear accident following the great east-Japan earthquake and tsunami. New York. United Nations 2016.

USEPA, United States Environmental Protection Agency (1980) Method 900.0 Gross alpha and gross beta Radioactivity in drinking water. United States.

Viteri, F.E. and Kohaut, B. (1997). Improvement of the Eakins and Brown method for measuring ^{59}Fe and ^{55}Fe in blood and other iron-containing materials by liquid scintillation counting and sample preparation using microwave digestion and ion-exchange column purification of iron. *Analytical biochemistry, 244*(1), pp. 116–123. doi: 10.1006/abio.1996.9882.

Warner, F. and Harrison, R.M. (eds.) (1993) Radioecology after Chernobyl: Biogeochemical pathways of artificial radionuclides (scope 50), John Wiley & Sons. Chichester.

Weakley, A.T., Takahama, S. and Dillner, A.M. (2016) Ambient aerosol composition by infrared spectroscopy and partial least-squares in the chemical speciation network: Organic carbon with functional group identification. Aerosol Science and Technology, 50(10), pp. 1096–1114. doi: 10.1080/02786826.2016.1217389.

ANNEX I: SUMMARY IN CATALAN

Estructura de la tesi

Aquesta tesi s'estructura en 8 capítols. En el primer es descriu la estructura de la tesis i s'esmenten els articles científics que inclou. En el segon capítol s'introdueix la radioactivitat en el medi ambient, així com la Directiva per a les aigües de consum 2013/51/EURATOM, que recull els radionúclids objecte d'estudi en aquesta tesi. En el tercer capítol, es resumeixen els objectius de la present tesi.

Els resultats de la tesi es presenten com a compendi d'articles en els següents tres capítols. En el quart capítol es presenten dos articles en relació amb la optimització y validació del procediment per a la determinació dels índex d'activitat alfa i beta per espectrometria d'escintil·lació líquida. En el cinquè, es recullen dos articles més en relació al desenvolupament i validació de la determinació de ^{226}Ra, ^{228}Ra i ^{210}Pb en aigua de beguda mitjançant extracció en fase sòlida amb 3M Empore Radium RAD disk. Després en el capítol 6, s'inclouen dos articles més, un relacionat amb l'estudi de viabilitat d'aplicació de models PLS a la deconvolució d'espectres de LSS, i el segon un estudi dels efectes sobre el desplaçament dels espectres, la eficiència i la separació alfa-beta de l'esmorteïment químic i el de color.

En el capítol set, es discuteixen de forma global els resultats recollits en tota la tesi. A més, es descriu una estratègia per a l'aplicació de les metodologies desenvolupades en el transcurs de la tesi per a la determinació de múltiples emissors alfa i beta. Finalment, el vuitè capítol conté les principals conclusions extretes de la present tesi.

Llistat d'articles científics presentats en aquesta tesi:

1- ***Simultaneous determination of gross alpha, gross beta and ^{226}Ra in natural water by liquid scintillation counting.***

   Autors: J. Fons, D. Zapata-García, J. Tent, M. Llauradó

   Revista: Journal of Environmental Radioactivity 125 (2013). pp. 56-60

2- ***A comparative experimental study of gross alpha methods on natural waters.***

   Autors: Montaña, M.; Fons, J.; Corbacho, J.A.; Camacho, A.; Zapata-García, D.; Guillén, J.; Serrano, I.; Tent, J.; Baeza, A.; Llauradó, M.; Vallés, I.

   Revista: Journal of Environmental Radioactivity 118 (2013). pp. 1-8

3- ***On the direct measurement of ^{226}Ra and ^{228}Ra using 3M Empore™ RAD disk by liquids scintillation spectrometry.***

Autors: J. Fons-Castells, M. Vasile, H. Loots, M. Bruggeman, M. Llauradó, F. Verrezen

Revista: Journal of Radioanalytical and Nuclear Chemistry 309 (2016). pp. 1123-1131.

4- ***Simultaneous determination of ^{226}Ra, ^{228}Ra and ^{210}Pb in drinking water using 3M Empore™ RAD disk by LSC-PLS.***

Autors: J. Fons-Castells, J. Oliva, J. Tent-Petrus, M. Llauradó

Revista: Applied Radiation and Isotopes 124 (2017). pp. 83-89

5- ***Simultaneous determination of specific alpha and beta emitters by LSC-PLS in water samples.***

Autors: J. Fons-Castells, J. Tent-Petrus, M. Llauradó

Revista: Journal of Environmental Radioactivity 166 (2017). pp. 195-201

6- ***Effect quenching on efficiency, spectra shape and alpha-beta discrimination in liquid scintillation spectrometry.***

Autors: J. Fons-Castells, V. Díaz, A. Badía, J. Tent-Petrus, M. Llauradó

Acceptat per publicació a *Applied Radiation and Isotopes.*

Introducció

La radioactivitat es un fenomen espontani mitjançant el qual, nuclis inestables decauen a nuclis de major estabilitat emetent radiació. Aquesta radiació comporta un alliberament d'energia, causat per la reorganització interna del nucli per tal d'assolir una relació entre neutrons i protons estable. Les radiacions poden esser classificades com a alfa, beta, gamma o neutrons. En el context d'aquesta tesi s'estudiaran les emissions alfa i beta, i s'emprarà espectrometria gamma per a la determinació d'alguns radionúclids.

Les partícules alfa son, nuclis d'heli que son generalment, alliberats per nuclis amb un nombre de protons massa elevat respecte els neutrons. L'energia de les partícules alfa es característica de l'emissor. Atesa la seva gran massa i càrrega, les partícules alfa interaccionen fortament amb la matèria fet que comporta un important perill per a la salut si son incorporades a l'organisme.

Com a partícula beta s'entenen tant electrons com la seva antipartícula, els positrons, En el procés d'emissió a part d'un electró s'emet alhora, un antineutrí. Com l'energia alliberada en la reorganització nuclear es comparteix entre l'electró i l'antineutrí, l'energia de l'electró pot anar des de 0, quan total l'energia es depositada sobre l'antineutrí, fins a una energia màxima (característica de l'emissor) quan tota es depositada sobre l'electró. De forma anàloga succeeix amb l'emissió de les antipartícules (positrons i neutrins). Les partícules beta tenen un major poder de penetració que els alfa.

Respecte a les emissions gamma, es tracta de radiació electromagnètica d'alta energia emesa per el nucli inestable. Aquest radiació es característica del radionúclid emissor. Ates el seu comportament com a radiació, les emissions gamma tenen un alt poder de penetració.

La magnitud per a la mesura de la radioactivitat es la activitat i en el sistema internacional s'expressa en Becquerels (Bq) que són equivalents a desintegracions per segon (s^{-1}). L'activitat d'una font radioactiva depèn del nombre de nuclis i de la constat de desintegració del nucli en qüestió (λ), que és característica d'aquest i fa referencia a la probabilitat de desintegració en un període determinat de temps.

No sempre els radionúclids decauen a nuclis estables, i en ocasions aquest donen com a producte de desintegració altres radionúclids. Quan això succeeix es parla d'una cadena radioactiva. La relació que pot haver-hi entre RN pares i els seus descendents depèn de la relació entre les seves constant de desintegració. Quan la del pare es molt inferior a la del descendent (superior a quatre ordres de magnitud), es pot assolir el que s'anomena equilibri secular. Quan aquest s'assoleix, l'activitat del fill s'iguala amb la del pare, Si la constant de desintegració del pare es inferior a la del fill però en menys de quatre ordres de

magnitud s'assoleix equilibri transitori, on l'activitat del pare i la de fill decauen amb la constant del pare. Quan la constant del pare es superior a la del fill s'arriba a una situació de no equilibri.

Radioactivitat en l'ambient

Les fonts de radioactivitat poden classificar-se com a naturals i artificials. Existeixen diversos tipus de radioactivitat natural, els raigs còsmics, els radionúclids cosmogènics i els radionúclids primordials.

Els raigs còsmics es composen de partícules carregades d'alta energia. Aquest en entrar en contacte amb l'atmosfera terrestre poden donar a lloc reaccions nuclears amb els àtoms constituents de les capes altes de l'atmosfera produint el que s'anomena radionúclids cosmogènics.

Els radionúclids primordials son aquells que han estat a la terra des de els seus orígens. Alguns d'aquest radionúclids formen part de les cadenes de desintegració naturals, les mes importants de les quals son les que s'inicien amb ^{232}Th, ^{238}U i ^{235}U. L'altra seria natural, que s'inicia amb ^{241}Pu ha decaigut totalment des de la formació de la terra i actualment només se'n poden trobar els últims dos isòtops.

Es important senyalar que les industries que empren com a matèries primes materials que contenen radionúclids naturals (anomenades industries NORM), son susceptibles de generar productes on aquests han quedat en major concentració.

Quan es parla de radioactivitat artificial es fa referència aquella produïda per l'activitat humana. Em algunes ocasions els radionúclids poden esser l'objectiu que es busca, com quan es sintetitzen radionúclids amb finalitats mèdiques. En altres, la radioactivitat es un subproducte d'allò que realment es busca com es el cas de les centrals nuclear, on l'energia alliberada per la reacció de fissió de l'urani o el plutoni s'aprofita per a generar energia elèctrica.

Per tal d'assegurar que l'impacte de les centrals nuclears no te efectes sobre l'esser humà i el medi ambient, es realitzen plans de vigilància al voltant de les centrals nuclears, que solen consistir en mesures gamma així com la presa de mostra de diferents tipus de matriu per el posterior anàlisis al laboratori. A nivell espanyol el CSN (*Consejo de Seguridad Nuclear*) s'encarrega d'establir els requisits del plans de vigilància radiològica ambiental.

A banda dels usos civils també cal afegir els usos militars que han tingut i tenen cert impacte sobre la dosis rebuda per la població.

A l'octubre de 2013 el consell de la Unió Europea va publicar la directiva 2013/51/EURATOM en la que s'estableixen els requisits per a la protecció de la salut del públic en general en relació a les substàncies radioactives en aigües de consum humà. Aquesta directiva, que substitueix la directiva 98/83/CE del Consell, estableix valors paramètrics, freqüències y característiques del mètodes per al seguiment de les substancies radioactives.

Els paràmetres regulats son la concentració d'activitat de ^{3}H, de ^{222}Rn i la dosis indicativa (ID). Els valors paramètrics són 100 Bq L^{-1} tant per ^{3}H com per ^{222}Rn i 0,1 mSv any^{-1} per a la ID. La dosi indicativa s'ha de calcular segons la directiva 96/29/EURATOM per a un consum de 730 L per any.

La directiva permet avaluar paràmetres e garbellat per tal d'assegurar que la ID es compleix, un d'aquest mètodes consisteix en la determinació dels índex d'activitat alfa i beta total, que han de trobar-se per sota de 0.1 Bq L^{-1} i 1.0 Bq L^{-1}, respectivament.

Aquest paràmetres es poden determinar per espectrometria d'escintil·lació líquida, que va ser una de les primeres tècniques emprades per a la determinació de radioactivitat. L'espectrometria d'escintil·lació líquida (LSS) es basa en la mescla de la mostra amb una mescla de substancies orgàniques (còctel escintil·lador) capaç de captar l'energia d'una partícula emesa en el si d'aquesta solució i emetre-la de nou com a pols lumínic. Aquest pols lumínic es detectat pels fotomultiplicadors i classificat segons la seva intensitat (nombre de fotons). La intensitat dels polsos es relaciona amb la energia de la partícula que els ha produït i el seu nombre amb el nombre de desintegracions que s'han produït en l'interior del vial de comptatge. D'aquesta forma, es pot obtenir un espectre on es representen els canals (energia) respecte el nombre de comptes enregistrats.

Paràmetres que cal tenir en compte a l'hora de realitzar mesures de mescles d'0emissors α i emissors β per LSS són l'esmorteïment i el paràmetre instrumental per a la separació α/β.

L'esmorteïment lumínic es un terme on s'engloben els fenòmens que interfereixen en la transferència d'energia de la partícula a mesurar, des de que es emesa fins que el pols lumínic es detectat per el fotomultiplicador.

Els tipus d'esmorteïment que més afecten a LSS i que s'estudien en aquest atesi son l'esmorteïment químic i el causat pel color. L'esmorteïment químic interfereix en la transferència d'energia entre el solvent excitat i els diferents soluts que componen el còctel, de forma que part de l'energia no arriba a ser emesa en forma de llum i per tant no es detecta en el fotomultiplicador. L'esmorteïment de color es aquell que, a causa d'una coloració en la

solució de comptatge, interfereix absorbint fotons emesos i d'aquesta forma atenuant la intensitat dels polsos produïts.

Respecte a la separació α/β, aquesta es realitza mitjançant un paràmetre instrumental (SQP[E]) per a l'equip que s'utilitza en aquesta tesi (Quantulus 1220) que permet diferencia entre polsos produïts per partícules α i els produïts per partícules β, gràcies a la diferencia en la seva durada.

La determinació dels índex d'activitat alfa i beta total per escintil·lació líquida mitjançant LSS proporciona espectres que son integrats en unes finestres determinades per quantificar els esmentats índex. Tot i això, la informació espectroscòpia obtinguda permetria en alguns casos determinar radionúclids individuals en comptes de paràmetres globals. Amb aquest objectiu des dels orígens de la LSS s'han desenvolupat mètodes per a la separació dels senyals de diferents radionúclids en el mateix espectre d'escintil·lació líquida. Aquest mètodes es poden separar entre els clàssics i els avançant, que es diferencien bàsicament per la potència computacional necessària per portar-los a terme.

Dintre dels mètodes clàssics englobem els mètodes de exclusió, inclusió, inclusió amb creixement de descendents i espectre complert. Els tres primers en basen en definir tantes finestres com radionúclids conté la mostra (màxim tres) i determinar-ne la eficiència de cadascun dels radionúclids implicats. En la tècnica de l'espectre complert (només útil per a mescles de dos radionúclids), s'utilitza el centre de masses de l'espectre per tal de determinar la proporció de cada radionúclid en la mescla.

Dintre del que anomenem mètodes avançats englobem el mètode del valor mes probable, mètodes de desconvolució mitjançant espectres patró, funcions gaussianes o series de Fourier i mètodes de calibratge multivariant. El mètode del valor més probables es basa en definir múltiples finestres (fins a una finestra per canal) i igualar les comptes de cadascuna amb la contribució de cadascun dels radionúclids, obtenint-se múltiples equacions (tantes com finestres) amb tantes incògnites com radionúclids. Es defineix una funció error que empresa la diferencia entre la suma de contribucions individuals i el valor mesurat a cada finestra i es defineix el valor més probable com el corresponent a aquell que proporciona el mínim en aquesta funció. La desconvolució d'espectres tracta de comparar sumes espectres individuals, o funcions teòriques d'espectres individuals—com gaussianes per emissors alfa, gaussianes modificades per emissors beta, o series de Fourier—a l'espectre mesurat. Finalment el calibratge multivariant es vasa en l'aplicació de models quimiometrics, bàsicament PLS, per a la determinació de mescles de radionúclids.

Els regressió PLS es un mètode de estadístic que es basa en construir un nou sistema de variables, anomenades variables latents (LV) que contenen la major part de la informació espectroscòpica en un nombre molt inferior de variables. L'objectiu serà en el nostre cas, predir una matriu Y que conté les activitats dels diferents radionúclids d'interès, a partir d'una matriu X que conte la informació dels espectres de les mostres a analitzar. Per poder fer això, anteriorment s'ha d'haver creat un model PLS mitjançant un conjunt d'espectres patró (o de calibratge) obtinguts a partir de la mesura de mostres de concentració coneguda.

En aquesta tesi s'estudia la viabilitat de l'ús dels models PLS per a la determinació simultània de diversos emissors alfa i beta a partir d'espectres d'escintil·lació líquida.

Objectius

L'objectiu principal d'aquesta tesi és desenvolupar i aplicar una estratègia per a la determinació ràpida i simultània d'emissors alfa i beta en mostres d'aigua. Els radionúclids en els que es centrarà l'estudi en aquesta tesi són els inclosos en la Directiva Europea 2013/51/EURATOM.

Aquest objectiu general s'ha dividit en objectius específics que es detallen a continuació:

- Desenvolupament i validació de metodologies ràpides, no només per a la determinació del contingut total d'emissors alfa i beta, sinó també radionúclids específics basats principalment en mesures per LSS (Espectrometria d'escintil·lació líquida).
- Estudi de viabilitat i implementació d'eines quimiomètriques per a la deconvolució i quantificació d'emissors alfa i beta específics a partir dels espectres obtinguts mitjançant metodologies ràpides per LSS.
- Descripció d'una estratègia per determinar de forma seqüencial diversos emissors alfa i beta i aplicació de l'estratègia proposada en mostres d'aigua susceptibles de esser considerades aigües de beguda i mostres d'aigua del pla de vigilància al voltant de la central nuclear de Vandellós.

Desenvolupament i validació de metodologies ràpides

Les metodologies analítiques estudiades foren la determinació simultània dels índex d'activitat alfa i beta total pel mètode de concentració i la mesura per espectrometria d'escintil·lació líquida ($LSS_{conc.}$), la mesura directa de les activitats alfa y beta mitjançant espectrometria d'escintil·lació líquida ($LSS_{dir.}$). Aquest procediment es una modificació del

primer mètode en el que s'elimina l'etapa de concentració per tal de mesurar ^{14}C i ^{3}H que son volàtils en les condicions del primer mètode. Finalment la determinació de ^{226}Ra, ^{228}Ra i ^{210}Pb per extracció amb disc 3M Radium RAD i posterior mesura per LSS. D'altra banda, també es va incloure en l'estratègia de quantificació la mesura per espectrometria gamma d'alta resolució com a mètode de cribratge.

La determinació de ^{222}Rn, que també esta inclòs en la Directiva Europea, no s'ha considerat en la present tesi per dues raons. D'una banda, existeixen diversos mètodes ràpids per a la determinació de ^{222}Rn, i per altra, la interferència que podria causar el ^{222}Rn en la determinació d'altres radionúclids es pot eliminar fàcilment eliminant el radó de la mostra mitjançant agitació o escalfament, ja que es un gas.

Estudi de viabilitat de mètodes quimiomètric per a la deconvolució d'espectrs LS

Per tal de comprovar la viabilitat dels models de PLS per predir l'activitat dels radionúclids esmentats anteriorment, es va construir una base de dades amb els espectres de obtinguts mitjançant els procediments de $LSS_{conc.}$, $LSS_{dir.}$ i extracció amb RAD disk. S'han considerat diferents radionúclids, nivells d'activitat i el nivell d'esmorteïment.

L'aplicació de l'estratègia proposada

L'estratègia proposada es basa en un conjunt de les metodologies analítiques que proporcionen informació diferent de la mostra que es combina per quantificar diversos emissors alfa i beta. Aquesta estratègia s'ha aplicat a diferents tipus de problemàtiques reals com la determinació de triti en mostres d'aigua naturals dintre del pla de vigilància radiològica ambiental de Vandellós II (PVRA), radionúclids naturals en l'aigua del medi ambient, i les mostres naturals traçades amb radionúclids artificials que simulen una contaminació accidental.

Validació de la determinació dels índex d'activitat alfa i beta

Dels resultats obtinguts en els dos articles científics que componen aquest capítol, cal destacar que s'ha descrit el desenvolupament de la metodologia analítica per a la determinació simultània dels índex d'activitat alfa y beta total així com la determinació de ^{226}Ra mitjançant una segona mesura del vial aprofitant l'augment d'activitat degut al creixement ^{222}Rn i els seus descendents. Aquesta metodologia s'ha validat i comparat amb altres tècniques clàssiques per a la determinació de l'índex d'activitat alfa total com son el

procediment d'evaporació i determinació per comptador proporcional i el de coprecipitació i mesura per escintil·lació solida de ZnS o comptador proporcional.

A més, s'ha desenvolupat un model matemàtic que permet estimar l'activitat de ^{226}Ra realitzant una segona mesura del vial transcorreguts un mínim de sis dies després del tractament de la mostra. Aquest mateix model permet determinar l'índex d'activitat alfa total sense la contribució del ^{222}Rn i els seus descendents de vida curta, tal i com indica la directiva. Les premisses per la correcta aplicació d'aquest model son:

- Tot el ^{222}Rn ha hagut d'esser eliminat de la mostra durant el tractament i cal esperar dues hores perquè els seus descendents emissors alfa de vida curta (^{218}Po, ^{214}Pb i ^{214}Po) decaiguin.
- El vial de comptatge ha de esser un sistema tancat del qual no es pugui escapar el ^{222}Rn
- El procediment descrit nomes pot ser aplicat per a estimació de ^{226}Ra en mostres que no continguin altres radionúclids susceptibles de causar creixement en l'activitat alfa del vial com ^{228}Ra.

Aquest procediment s'ha comparat amb els d'evaporació y mesura per comptador proporcional i el de coprecipitació i mesura per escintil·lació sòlida de ZnS o comptador proporcional.

El procediment de evaporació i mesura per comptador proporcional es basa en la concentració de la mostra fins a sequedat sobre una planxeta d'acer inoxidable. Degut al baix poder de penetració de les partícules alfa respecte a les partícules beta les partícules la quantitat de precipitat en la planxeta ha de ser menor (de l'ordre de mg cm^{-2} quan per a la mesura del beta total pot ser de 25 mg cm^{-2}), per tal de disminuir la autoabsorció.

En el procediment de coprecipitació s'afegeixen a la mostra portadors de bari i ferro i es precipiten com a $BaSO_4$ i $Fe(OH)_3$ afegint medi basic. Els isòtops de radi coprecipiten amb el $BaSO_4$ mentre que altres elements com actínids i poloni s'absorbeixen en les partícules de $Fe(OH)_3$. El precipitat es filtra, s'asseca i posteriorment pot esser mesurat per escintil·lació líquida o comptador proporcional.

La comparació dels tres mètodes s'ha dut a terme a partir de les anàlisis de mostres traçades amb diferents emissors alfa i de mostres naturals de les quals se n'ha determinat el contingut total d'emissors alfa.

S'ha demostrat que no hi ha diferencies significatives entre els tres mètodes i que aquest proporcionen resultats equivalents a la suma d'emissors alfa mesurats per tècniques selectives com la espectrometria alfa.

Validació de la determinació de ^{226}Ra, ^{228}Ra i ^{210}Pb mitjançant RAD disks

A partir dels resultats obtinguts en els dos articles científics que componen aquest capítol, es destaca que s'ha pogut validar un mètode per a la determinació simultània de ^{226}Ra, ^{228}Ra i ^{210}Pb mitjançant la extracció en fase solida emprant RAD disks i amb la posterior mesura per escintil·lació liquida.

En el primer article s'estudia la viabilitat de mesurar directament el RAD disk a l'interior del vial d'escintil·lació líquida i s'observa que aquet fet comporta certs problemes. Per una banda, quan es mesura de forma seqüencial el RAD disk al llarg del temps, s'observa que l'espectre de ^{226}Ra es va desplaçant cap a canals de major energia. D'altra banda les comptes corresponents al ^{226}Ra (emissor alfa) es classifiquen majoritàriament com a beta just després del tractament de mostra i no es classifiquen correctament fins passades 8 hores de la preparació del vial. Aquest fet es deu a que el RAD disk no està completament impregnat amb el còctel escintil·lador fins passat aquets temps, i per tant la variació en la impregnació interfereix en la detecció de la radiació emesa per el radi retingut en el RAD disk i el còctel.

S'ha observat que per tal de evitar aquest problema es pot, per una banda esperar les 8 hores necessàries per assolir una correcta impregnació del RAD disk amb còctel o per l'altra, forçar la impregnació filtrant el còctel escintil·lador.

Es va comprovar que l'elució complerta dels isòtops del radi del RAD disk es possible amb solucions d'EDTA en medi basic, però el volum necessari per assolir la elució complerta i la concentració d'EDTA necessària no son compatibles amb el còctel. Per aquet motiu, per poder obtenir una solució de comptatge estable i sense separació de fases calia prendre només una alíquota del volum emprat per a la elució, de forma que s'augmenta el límit de detecció.

A mes, com els isòtops de plom també es retenen en el RAD disk, la determinació de ^{228}Ra es veu afectada per la presencia de ^{210}Pb, ja que ambdós son emissors beta amb una energia pròxima.

D'altra banda, si la elució es realitza amb DHC, es poden eluir selectivament els isòtops de plom del RAD disk, fet que permet la determinació de ^{210}Pb i evita la interferència d'aquest sobre el ^{228}Ra.

A més, quan s'empra el calibratge multivariant amb models PLS per a la quantificació dels espectres obtinguts de la mesura del RAD disk i el vial preparat amb la solució d'elució s'aconsegueixen resultats sense interferència entre els radionúclids. Aquest procediment ha estat validat en front a materials de referencia i s'ha emprat per a la quantificació de mostres d'aigua de beguda amb resultats satisfactoris.

Regressió per mínims quadrats parcials (PLS) aplicada al tractament d'espectres d'escintil·lació líquida

Dels resultats obtinguts en els dos articles científics que componen aquesta capítol, cal destacar que la determinació de radionúclids específics a partir d'espectres obtinguts amb el procediment de determinació dels índex d'activitat alfa total i beta total mitjançant models PLS proporciona resultats satisfactoris.

Malgrat això, s'ha observat que, quan s'intenta quantificat mostres que contenen un radionúclid que no esta inclòs en el set de calibratge, la predicció realitzada per els models pot no ser correcta per a tots els radionúclids. Es per això que cal, en la mesura del possible, incloure en el set de calibratge tots els radionúclids que s'espera trobar en la mostra.

A més, aspectes de vital importància en la determinació de radionúclids específics a partir d'espectres d'escintil·lació líquida mitjançant l'ús de models PLS són, la eficiència, la forma de l'espectre (característics del radionúclid a determinar) així com la separació α/β.

Com s'ha vist en l'estudi de l'efecte de l'esmorteïment en l'eficiència, la forma de l'espectre i la separació α/β, aquest presenta diferent comportament depenent del tipus d'agent, químic o de color. S'han considerat $FeCl_3$ i nitrometà per estudiar l'esmorteïment de color i químic respectivament. Per una banda s'ha observat que la eficiència dels emissors beta de baixa energia disminueix de forma intensa amb l'esmorteïment, mestres que els d'alta energia ho fa de forma més gradual. Per als emissors alfa no s'observa un clar efecte de l'esmorteïment sobre la eficiència. Per aquells radionúclids afectats, l'esmorteïment de color redueix mes la eficiència que el químic per a un mateix valor d'SQP[E].

Respecte a la forma de l'espectre, s'ha observat que tant emissors alfa com beta es veuen afectats, desplaçant-se el seu espectre a menors energies tant per l'esmorteïment químic com pel de color.

Finalment, respecte a la separació α/β s'ha observat que al incrementar el nivell d'esmorteïment, el PSA òptim disminueix i que la interferència total en aquest valor de PSA augmenta. Aquests efectes son més acusats per a l'esmorteïment de color que per al químic.

Per totes aquestes raons, quan es pretengui determinar radionúclids específics en mescles de radionúclids en matrius que puguin presentar un nivell elevat d'esmorteïment, caldrà disposar de llibreries que continguin espectres patró dels radionúclids que s'esperen en la mostra a diferents nivells d'esmorteïment emprant agents químics i de color.

D'aquesta forma es crearan sets de calibratge amb els radionúclids esperats i amb els nivells de SQP[E] més pròxims als observats per a la mostra. Pot esser també interesant incloure els espectres de SQP[E] en els espectres emprats per a la construcció de models PLS.

Resultats i discussió. Validació de l'estratègia per a la determinació d'emissors alfa i beta

A partir de les metodologies validades en aquesta tesi d'altres, s'ha proposat una estratègia per a la determinació dels radionúclids que es contemplen a l'annex III de la directiva 2013/51/EURATOM.

Entre les metodologies emprades hi ha la determinació dels índex d'activitat alfa i beta total per LSS (descrit en el Capítol 4), la determinació de ^{226}Ra, ^{228}Ra i ^{210}Pb mitjançant extracció amb RAD disk (descrit en el Capítol 5). Els espectres obtinguts per aquestes metodologies es quantifiquen per calibratge multivariant explicat al Capítol 6.

Les metodologies emprades son;

- *Espectrometria gamma d'alta resolució:* en la nostra estratègia s'empra com a mètode de garbellat der identificar la presencia de ^{241}Am, ^{134}Cs i ^{137}Cs. El procediment es bases en mesurar directament la mostra en una geometria de 500 mL.
- *Mètode de concentració i mesura per LSS ($LSS_{conc.}$):* Aquest procediment s'empra per a la determinació dels índex d'activitat alfa total i beta total. A més l'espectre obtingut s'empra per a la quantificació de radionúclids específics mitjançant models PLS. El procediment es basa en evaporar una alíquota de 100 mL a

sequedat. Aquest precipitat es dissol en 10 mL d'aigua acidificada amb HCl a pH=1,5. Una alíquota de 8 mL de la mostra així preparada es mescla amb 12 Ml de còctel (Ultima Gold AB) i es mesura en un Quantulus 1220 surant 400 min.

- *Mètode directe de mesura per LSS ($LSS_{dir.}$):* Aquest procediment es basa en la mesura directa per LSS del vial preparat amb 8 mL de la mostra sense tractar amb 12 mL de Ultima Gold AB. Aquest vial es mesura en un Quantulus 1220 surant 400 min.
- *Extracció mitjançant RAD disk amb mesura per LSS:* En aquest procediment cal condicionar el RAD disk amb 20mL de HNO3 2 mol L-1 . Després, una alíquota des de 1 fins a 5 L de mostra acidificada es filtra a través del RAD disk. Els isòtops de plom s'elueixen del Rad disk mitjançant 7 mL de DHC 0,05 mols L-1 a pH 5,75. Una alíquota de 5 mL d'aquest eluat es mescla amb 15 mL de Optifase Hisafe III i es mesura en un Quantulus 1220 durant 100 minuts. D'altra banda, el RAD disk es transfereix en un altre vial de comptatge al que s'afegeixen 20 mL de Optifase Hisafe III que es mesura en un Quatulus durant 100 min.

En l'estratègia proposada es mesura primerament els índex d'activitat alfa i beta total per $LSS_{conc.}$. Si els valors obtinguts son inferiors a 0,1 i 1,0 per a l'índex alfa i l'índex beta respectivament, es consideres que la ID esta per sota de 0,1 mSv any^{-1} tal i com recomana la directiva 2013/51/EURATOM. En cas contrari es passa a mesurar per espectrometria gamma, $LSS_{dir.}$ i emprant l'extracció amb RAD disk. A partir dels resultats obtinguts amb aquestes metodologies es pot determinar la presència de ^{60}Co, ^{134}Cs, ^{137}Cs i ^{241}Am (espectrometria γ), ^{3}H i ^{14}C ($LSS_{dir.}$) i ^{226}Ra, ^{228}Ra i ^{210}Pb (RAD disk).

A partir d'aquesta informació i de l'espectre $LSSc_{onc.}$, es construieix un model PLS amb els radionúclids identificats més aquells que no es poden identificar amb els mètodes emprats com ^{40}K, ^{90}Sr/^{90}Y i $^{239+240}$Pu.

Emprant de forma total o parcial aquesta estratègia s'ha determinat el ^{3}H en mostres d'aigua del PVRA al voltant de la central nuclear de Vandellòs, radionúclids naturals en mostres d'aigües susceptibles d'esser emprades com a aigua de beguda i radionúclids naturals i artificials en mostres d'interlaboratoris i materials de referència, amb resultats satisfactoris.

Conclusions

De la recerca realitzada en aquesta tesi doctoral se'n poden extreure les següents conclusions:

En relació amb la determinació dels índex d'activitat alfa i beta total per LSS,

1. S'ha optimitzat i validat el procediment per a la determinació dels índex d'activitat alfa i beta total per a mostres d'aigua.

2. L'activitat de ^{226}Ra es pot determinar de forma simultània mitjançant una segona mesura del vial de comptatge transcorreguts sis dies del tractament de mostra.

3. El procediment validat proporciona resultats comparables amb mètodes clàssics—com els mètodes d'evaporació i coprecipitació—per a la determinació de l'índex alfa total així com amb el sumatori d'emissors alfa determinats per tècniques especifiques.

En relació amb la determinació dels índex d'activitat alfa i beta total per LSS,

4. S'ha desenvolupat i validat un procediment per a la determinació ràpida de ^{226}Ra, ^{228}Ra i ^{210}Pb mitjançant extracció amb RAD disk i mesura per LSS.

5. La mesura directa del RAD disk pot portar-se a terme tenint en compte certes consideracions. La mes important es assegurar una correcta impregnació del RAD disk per tal evitar la interferència α/β i el desplaçament de l'espectre.

6. Per assolir una correcta determinació de ^{228}Ra, evitant interferències de ^{210}Pb, es pot emprar DHC per eluir els isòtops de ^{210}Pb del RAD disk i així mesurar de forma separada els isòtops de radi i els de plom.

En relació a els models PLS per a la deconvolució d'espectres d'escintil·lació líquida,

7. Els estudis realitzats per comprovar la viabilitat dels models PLS per a la desconvolució d'espectres d'escintil·lació líquida han confirmat que aquest es un mètode vàlid per a la determinació de diversos radionúclids a partir d'un espectre LS.

8. Els models PLS son vàlids per a la determinació de mescles de radionúclids no només a partir d'espectres obtinguts per mètodes que determinen paràmetres d'activitat globals, sinó que també ho son per a aquells que comporten una separació radioquímica com l'extracció mitjançant RAD disk.

9. La quantificació de LSS mitjançant PLS en matrius diferents a l'aigua ha de ser avaluada per poder donar resposta a situacions que requereixen mètodes ràpids com una situació accidental.

En relació amb els efectes de l'esmorteïment sobre la eficiència, la forma de l'espectre i la separació α/β,

10. La eficiència dels emissors beta de baixa energia es veu molt afectada metres que la dels d'alta energia només moderadament. Pel que fa a els emissors alfa, no s'observa un clar efecte sobre la eficiència.

11. L'esmorteïment degut al color afecta a la separació α/β en major grau que l'esmorteïment químic.

12. Cal estudiar adequadament la naturalesa de l'esmorteïment en mostres reals per tal de poder seleccionar el millor agent esmorteïdor per realitzar corbes d'esmorteïment i per tant poder optimitzar el PSD, corregir la eficiència i, en cas necessari, corregir el desplaçament de l'espectre.

En relació a l'estratègia d'aplicació dels mètodes desenvolupats,

13. S'ha proposat una estratègia per a la determinació seqüencial de els radionúclids inclosos a l'Annex III de la Directiva 2013/51/EURATOM, que combina els procediments desenvolupats en aqueta tesi i d'altres com la espectrometria γ.

14. S'ha emprat aquesta estratègia tant de forma total com parcial, per a la determinació de radionúclids específics en mostres del PVRA, mostres d'aigua amb un us potencial com a aigua de beguda i materials de control de qualitat traçats.

15. L'estratègia proposada permet la determinació de fins a 13 radionúclids en una mostra de 1,5 L amb menys de 24 hores. El fet de minimitzar les separacions radioquímiques permet reduir l'ús de reactius.